Mechanical Properties Improvement of Ground Tire Rubber/Thermoplastic Composites Produced by Rotational Molding

Thèse

Yao Dou

Doctorat en génie chimique
Philosophiæ doctor (Ph. D.)

Québec, Canada

Mechanical Properties Improvement of Ground Tire Rubber/Thermoplastic Composites Produced by Rotational Molding

Thèse

Yao Dou

Sous la direction de :

Denis Rodrigue, directeur de recherche

Résumé

Dans ce travail, des composites à base de caoutchouc de pneus moulus (GTR)/résines thermoplastiques ont été produits avec succès en combinant une technique de mélange à sec avec un procédé de rotomoulage. Afin d'améliorer les propriétés mécaniques des composites résultants, certaines méthodes de modification ont été utilisées. À partir des composites rotomoulés, un ensemble complet de caractérisation comprenant les propriétés morphologiques, physiques (masse volumique et dureté) et mécaniques (traction, flexion et impact) a été réalisé. La première partie du travail a étudié l'effet de l'incorporation d'agents gonflants chimiques, de fibres de bois d'érable et de deux traitements de surface du GTR (modifié par le polyéthylène maléaté (MAPE) en solution et traité par irradiation micro-ondes) sur les propriétés mécaniques des composites GTR/polyéthylène linéaire de basse densité (LLDPE) produits par rotomoulage. La deuxième partie du travail a étudié l'effet du GTR traité au MAPE sur les propriétés mécaniques des composites GTR/polypropylène (PP) préparés par rotomoulage. Les propriétés mécaniques ont indiqué que le GTR traité par MAPE, parmi ces méthodes de modification, était une approche efficace pour améliorer la compatibilité et l'adhésion interfaciale des composites GTR/thermoplastiques. Par exemple, la résistance à l'impact du LLDPE/GTR (85/15) a montré une amélioration de 30% avec l'addition de 0.3% en poids de MAPE comparé au composite avec la même concentration de GTR sans traitement au MAPE. Aussi, e une augmentation de 52% de la résistance en impact pour le composite PP/GTR (50/50) a été obtenu avec l'introduction de 2% en poids de MAPE en comparaison avec une teneur similaire de GTR sans traitement au MAPE.

Abstract

In this work, ground tire rubber (GTR)/thermoplastic composites were successfully produced by combining a dry-blending technique with a rotational molding process. In order to improve the mechanical properties of the resulting composites, different modification methods were used. From the rotomolded composites produced, a complete set of characterization including morphological, physical (density and hardness) and mechanical properties (tensile, flexural and impact) was performed. The first part of the work investigated the effect of chemical blowing agent and maple wood fibers concentration, as well as two GTR surface treatments (maleated polyethylene (MAPE) in solution and microwave irradiation) on the mechanical properties of GTR/linear low density polyethene (LLDPE) composites. The second part of the work studied the effect of MAPE treated GTR on the mechanical properties of GTR/polypropylene (PP) composites. Overall, the results showed that MAPE treated GTR was an effective approach for improving the compatibility and interfacial adhesion between GTR and thermoplastic composites. For example, the impact strength of LLDPE/GTR (85/15) composite reached a 30% improvement by adding 0.3 wt.% MAPE above that of the same GTR content without MAPE treatment. A 52% improvement of impact strength for PP/GTR (50/50) by introducing 2 wt.% MAPE was obtained compared to the composite with the same content of untreated GTR.

Table of Contents

List of Figures

List of Tables

List of Abbreviations and Acronyms

3M-GTR	Microwave treatment for 3 min
5M-GTR	Microwave treatment for 5 min
APTMS	Aminopropyl trimethoxysilane
ATR-FTIR	Attenuated total reflection Fourier transform infrared spectroscopy
BR	Butadiene rubber
CB	Carbon black
CBA	Chemical blowing agent
CO_2	Carbon dioxide
DSC	Differential scanning calorimetry
DTG	Derivative thermogravimetric
EAA	Ethylene-acrylic acid copolymer
ENR	Epoxidized natural rubber
EPDM	Ethylene propylene diene monomer
EVA	Ethylene-vinyl acetate
FTIR	Fourier transform infrared spectroscopy
GTR	Ground tire rubber
GTR-g-MA	Maleic anhydride grafted ground tire rubber
GTR-MAPE	Ground tire rubber treated by maleated polyethylene
HDPE	High density polyethylene
IIR	Isobutylene isopropylene rubber
LDPE	Low density polyethylene
LLDPE	Linear low density polyethylene
LMDPE	Linear medium density polyethylene
MA	Maleic anhydride
MAPE	Maleated polyethylene
MAPP	Maleated polypropylene
MFI	Melt flow index
MWF	Maple wood fibers
N_2	Nitrogen
N_f	Cell density
NR	Natural rubber
OICA	Organisation Internationale des Constructeurs d'Automobiles
PAH	Polynuclear aromatic hydrocarbon
PB	Polybutadiene
PE	Polyethylene
PE-g-MA	Polyethylene grafted maleic anhydride
PIB	Polyisobutylene
PP	Polypropylene
PP-g-MA	Polypropylene grafted maleic anhydride
PS	Polystyrene
PVC	Polyvinyl chloride
SBR	Styrene-butadiene rubber
SBS	Styrene-butadiene-styrene block copolymer
SEM	Scanning electron microscopy
SO_2	Sulfur dioxide
Tg	Glass transition temperature
TGA	Thermogravimetric analysis
TPE	Thermoplastic elastomers

TMWF	Treated maple wood fibers
UHMWPE	Ultra-high-molecular-weight polyethylene
UMWF	Untreated maple wood fibers
WFC	Wood fibers composites
XLPE	Cross-linked polyethylene
XPS	X-ray photoelectron spectroscopy

Behind every

successful man

there's a lot of

unsuccessful years

--Bob Brown

Acknowledgements

I would like to express my gratitude to all those who helped me and encouraged me during my Ph.D. studies.

My deepest gratitude goes first and foremost to Prof. Denis Rodrigue, my supervisor, for his immense knowledge, invaluable guidance and unfailing assistance throughout every stage of my doctoral program. I am extremely thankful and indebted to him for sharing his expertise to increase my knowledge about the project from zero to excellent understanding, and then arouse my great interest in exploring this research.

I am grateful to my beloved family who has provided me with moral and emotional support in my life. To my parents, thank you for your unconditional love and support throughout the past 32 years. To my two-and-a-half-year-old son, Zihang Dou, you are my inspiration to achieve greatness. A special gratitude goes out to my wife, Lei Yang, not just because she has seen me through the ups and downs of my life since 7 February 2012, but because she has given up so much for me. Without her love and support, I would be lost.

I really appreciate the technical assistance of Mr. Yann Giroux, who is not only a capable technician, but also a very nice man. Also, I would like to thank all my friends at Université Laval for your encouragements and support.

Finally, I wish to acknowledge the financial support of the Natural Science and Engineering Research Council of Canada (NSERC) and the technical support for the Research center on advanced materials (CERMA). As well, I benefitted from a scholarship for the China Scholarship Council (CSC) and thankfully acknowledge this support.

Foreword

This Ph.D. dissertation is mainly based on four conference papers and four journal papers. In total, it is composed of a general introduction and nine chapters. The general introduction section simply presents the importance of recycling waste tires and the necessity of introducing rotational molding to produce ground tire rubber/thermoplastic composites. Following this, the objectives of this thesis are established.

In the literature survey, a detailed introduction on the importance and challenges of recycling waste tires is presented. Modification of ground tire rubber and ground tire rubber/thermoplastic composites produced by injection molding or compression molding combining with a melt mixing process are discussed by reviewing the literature. Then, a brief introduction on the advantages of rotational molding is performed. Rotationally molded products manufactured by different ways along with selected literature review are also presented.

In the following eight chapters, the collected data and characterized properties of the samples based on experimental work are presented in the form of conference and journal articles, published or submitted. My contributions in these research works included carrying out the experimental work, collecting and analyzing the data, and writing the original draft of the manuscripts.

In chapter two, different concentrations of ground tire rubber (0 to 50 wt.%) were dry-blended with linear low density polyethylene (LLDPE) to produce thermoplastic elastomer parts by rotational molding. The morphological and mechanical properties (tensile, flexural and impact) of these composites were investigated. Compared with neat LLDPE, the compounds can have up to 35% higher impact strength and still above 100% elongation at break even if the tensile strength and modulus, as well as flexural modulus decreased with increasing GTR content. The conference paper was published as:

Dou Y, Rodrigue D. Rotational molding of linear low density polyethylene with different concentrations of ground tire rubber. 75th Annual Technical Conference and Exhibition of the Society of Plastics Engineers, SPE ANTEC, Anaheim 2017: 2252-2256.

In chapter three, different ground tire rubber concentrations (0 to 50 wt.%) were dry-blended with different chemical blowing agent contents (0 to 1 wt.%), and then GTR/LLDPE composites and foams were produced by rotational molding. A complete set of characterization was performed in terms of mechanical properties (tensile, flexural and impact), density and morphological properties. The

results showed that increasing the GTR content or CBA content not only decreased both the tensile and flexural moduli, but decreased the ultimate strength and elongation at break. The journal paper was published as:

Dou Y, Rodrigue D. Rotomolding of foamed and unfoamed GTR-LLDPE blends: mechanical, morphological and physical properties. Cellular Polymers, 2018, 37(2): 55-68.

In chapter four, GTR and maple wood fibers (MWF) were dry-blended with LLDPE to produce hybrid composites by rotational molding. The effect of maleated polyethylene as a coupling agent was also investigated. As expected, the addition of GTR led to limited impact strength improvement of the wood fibers composites, but the addition of maleated polyethylene (MAPE) improved the interfacial adhesion resulting in better hybrid composites properties. The conference paper was published as:

Dou Y, Rodrigue D. Rotational molding of hybrid composites based on linear low density polyethylene/ground tire rubber/maple wood fibers. 76th Annual Technical Conference of the Society of Plastics Engineers, SPE ANTEC, Orlando 2018.

In chapter five, the efficiency of two ground tire rubber surface treatments (maleated polyethylene as a coupling agent and microwave devulcanization process) was compared. The treated and untreated GTR were dry-blended with LLDPE to produce the samples via rotational molding. The results showed that both GTR treatments led to limited increase of tensile strength and impact strength, while the tensile modulus, elongation at break, flexural modulus and density were almost unchanged for a fixed GTR content. The conference paper was published as:

Dou Y, Rodrigue D. A comparison between two ground tire rubber surface treatments to produce compounds based on linear low density polyethylene via rotational molding. 77th Annual Technical Conference of the Society of Plastics Engineers, SPE ANTEC, Detroit 2019.

In chapter six, polypropylene (PP) was dry-blended with GTR to produce composites by rotational molding. In particular, the effect of GTR content was investigated to modify the mechanical properties of the PP matrix. Each compound was characterized via morphology, density and mechanical properties (tensile, flexural and impact). As expected, the results showed that all the mechanical properties decreased with increasing GTR concentration due to its low modulus and strength. Also, the crosslinked structure of the GTR particles is believed to limit the interfacial PP-

GTR interaction, thus also limiting mechanical stress transfer. The conference paper was published as:

Dou Y, Rodrigue D. Polypropylene/ground tire rubber (PP/GTR) composites produced via rotational molding. SPE ANTEC 2020: The Annual Technical Conference for Plastic Professionals, 2020: 364-368.

In chapter seven, untreated GTR and MAPE-treated GTR were dry-blended with polypropylene (PP) to produce composites via rotational molding. From the rotomolded samples produced (0-50 wt.%), a complete characterization including morphological, physical (density and hardness) and mechanical properties (tensile, flexural and impact) was performed. The results showed that MAPE-treated GTR can significantly improve the mechanical properties of the resulting composites. The journal paper was submitted as:

Dou Y, Rodrigue D. Rotational molding of polypropylene with ground tire rubber. Plastics, Rubber and Composites, 2020. submitted.

In chapter eight, PP was foamed via rotational molding using a CBA based on azodicarbonamide over a range of concentration (0 to 0.5% wt.). The samples were then analyzed in terms of morphological, thermal and mechanical properties. The morphological analysis showed a continuous increase in the average cell size and cell density with increasing CBA content. Increasing the CBA content also led to lower foam density and thermal conductivity. Similarly, all the mechanical properties (tension, flexion and impact) were found to decrease with increasing CBA content. Finally, the efficiency of the rotomolding process was assessed by producing neat PP samples via compression molding. The results showed negligible differences between the rotomolded and compression molded properties at low deformation and rate of deformation indicating that optimal rotomolding conditions were selected. The journal paper was published as:

Dou Y, Rodrigue D. Morphological, thermal and mechanical properties of polypropylene foams via rotational molding. Cellular Polymers, 2021, DOI: 10.1177/02624893211018825.

In chapter nine, foamed recycled high density polyethylene (rHDPE) parts were produced by rotational molding using different concentration (0 to 1% wt.) of a CBA based on azodicarbonamide. From the samples produced, a complete morphological, thermal and mechanical characterization was performed. The morphological analysis showed a gradual increase in the average cell size, while the cell density firstly increased and then decreased with increasing CBA content. As expected,

increasing the CBA content decreased the foam density as well as the thermal conductivity. Although increasing the CBA content decreased both tensile and flexural properties, the impact strength showed a similar trend as the cell density with an optimum CBA content around 0.1% wt. Finally, neat rHDPE samples were also produced by compression molding. The results showed negligible differences between the rotomolded and compression molded properties indicating that optimal rotomolding conditions were selected. These results confirm the possibility of using 100% recycled polymers to produce rotomolded foam parts. The journal paper was published as:

Dou Y, Rodrigue D. Morphological, thermal and mechanical properties of recycled HDPE foams via rotational molding. Journal of Cellular Plastics, 2021, DOI: 10.1177/0021955X211013793.

General introduction

Nowadays, with a growing number of cars sold, increasing tire production results in a massive stockpile of waste tires [1]. Waste tires are rich materials because of their composition and properties. Vulcanized rubbers are their main components, but are thermoset materials having high resistance to biodegradation, chemical reagents, high temperatures, photochemical decomposition and shear stress [2]. Although landfilling was the earliest approach for waste tires disposal, it can cause health and environmental concerns: accidental fires and pollution of the underground water resources [3]. Thus, finding methods at a suitable cost for recycling waste tires has become a serious challenge worldwide.

So far, several works have been reported on recycling waste tires such as retreading [4], incineration for energy recovery [5] and pyrolysis [6]. Despite tire retreading offering the most resource-efficient strategy for waste tires disposal, it still has some safety risks at high speeds. Waste tires can be used as fuel for several productions such as steam, electricity, pulp, paper, lime and steel [7]. However, incineration of tires releases hazardous gases. Pyrolysis of waste tires could produce several beneficial products such as pyrolysis oil, gas, carbon black, steel, etc. [6]. Nevertheless, the high cost for the construction and operation of pyrolysis plants limits the wide application of this approach. Although it is a challenging task to recycle vulcanized rubbers because they are durable, strong and flexible thermoset materials, these properties are advantages when the material is used as fillers to produce composites.

Therefore, it is an interesting recycling way to blend waste tires with thermoplastics for not only decreasing the final costs of the products, but also reducing environmental concerns. In order to be easily incorporated into thermoplastic matrices, waste tires need to be shredded into GTR [8]. However, poor bonding between GTR and most thermoplastics leads to low mechanical properties of the resulting composites, and it is necessary to modify the GTR [9]. Generally, two modification strategies have been used for improving the interfacial interactions: rubber devulcanization/reclamation [10], as well as physical and chemical methods [11, 12].

Injection molding and compression molding have been used to produce GTR/thermoplastics composites. However, these molding techniques involve melt mixing processes in a batch mixer or a twin-screw extruder, which increase the processing costs and induce thermo-oxidative degradation of the polymers [13, 14]. Compared with some hollow plastic molding techniques like blow molding, thermoforming and injection molding, rotational molding has several advantages such as lower costs,

greater flexibility and lower design limitations [15]. Consequently, rotational molding combined with a simple dry-blending process is a potential substitute method for producing GTR/thermoplastic composites.

Thesis objectives

According to the general introduction, the thesis objectives can be described as follows:

1) For environmental and economic concerns, develop an effective recycling method for waste tires by producing ground tire rubber/thermoplastic resin composites.
2) To reduce the processing costs and limit thermo-oxidative degradation of the polymers by melt mixing processes, use rotational molding and dry-blending to produce the composites over a wide range of concentration.
3) To improve the mechanical properties of GTR-based composites by using some surface treatments and/or compatibilizers.
4) To reduce the parts weight by foaming the composites using a range of chemical blowing agent concentrations.

Chapter 1. Literature survey

1.1 Waste Tires

Today, with a steady increase in the quality of life and the general development in countries, there is a growing number of automotive vehicles used. According to the vehicle's consumer survey studies [16,17], the top two affecting factors contributing to the vehicle annual growth are convenience and flexibility of use. In 2019, the International Organization of Motor Vehicle Manufacturer or Organisation Internationale des Constructeurs d'Automobiles (OICA) showed an increase of 15.5% in the total number of global vehicle sales from the year 2010, amounting to 91,786,861 units [18]. However, such substantial consumption of vehicles makes it a major contributor to the environmental pollution resulting in the stockpiling and disposal of end-of-life tires [19]. Globally, about 5 million tons of tires are discarded every year and about 4 billion waste tires are still piled up in landfills [20,21]. These large volumes of waste tires are persistent and do not degrade by themselves (biodegradation) causing a very serious "black pollution" [1].

1.1.1 Tire composition

Tires are highly engineered and complex assemblage of components, which have a wide range of properties. Figure 1 presents a typical composition of the materials used in the production of a regular tire [22]. The exterior tread, in direct contact with the road, is composed of a high content of natural and synthetic rubbers. The belts consist of several materials like rubber, steel and textile depending on the tire application (passenger car, truck, off-the-road, etc.). To keep the integrity of the tire structure, the sidewalls contain rubber having good resistance to crack propagation. The carcass can be composed of twisted metal or textile cords coated with natural rubber, offering the internal structure of the tire. The inner liner is made of (halo)butyl rubber with a low air permeability to maintain the air pressure and provide good rolling resistance. The beads are composed of metal alloy coated steel wires to ensure a connection between the tire and the wheel rim [12,22].

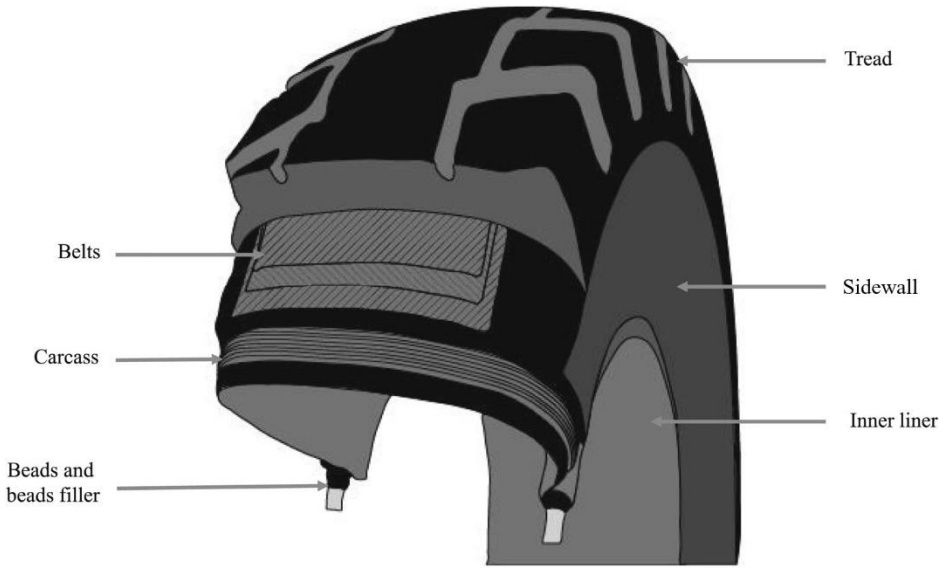

Figure 1. Typical tire structure [22].

The composition of a tire may differ depending on the use (long distances, plane braking) and environment (road quality, temperature) because the tires need to have extremely high resistance to severe outdoor conditions during their lifetime. Table 1 presents typical compositions (materials and concentrations) used in the production of passenger car tire, truck tire and off-the-road tire [23-25].

Table 1. Composition of different tires [23-25].

Components	Passenger car tire (w/w %)	Truck tire (w/w %)	Off-the-road tire (w/w %)
Rubbers/Elastomers (natural)	16	30	31
Rubbers/Elastomers (synthetic)	31	15	16
Carbon black and silica	21.5	22	22
Metal	16.5	25	12
Textile	5.5	-	10
Zinc oxide	1	2	2
Sulfur	1	1	1
Additives	7.5	5	6

Generally, the main component of the tire is a mixture of different natural rubbers (NR), such as polyisoprene, and synthetic rubbers, such as polybutadiene (PB), styrene-butadiene rubber (SBR) and (halo)butyl rubber. Figure 2 illustrates the chemical structure of rubber components [22]. As the

second major components of tires, carbon black and silica contribute to the tire mechanical reinforcement and abrasion resistance. Based on the different positions of these two compounds in the structure, their sizes, structures and shapes may be different. Small particles are used in the tread while the inner liner contains larger particles. Nowadays, silica compounds are gradually replacing carbon black to produce more ecofriendly tires. Metals, such as steel and alloys, are used as reinforcing materials in tires. However, textiles, such as natural rayon, nylon and polyester, are less commonly used in truck tires because of their more limited reinforcement levels [2,25].

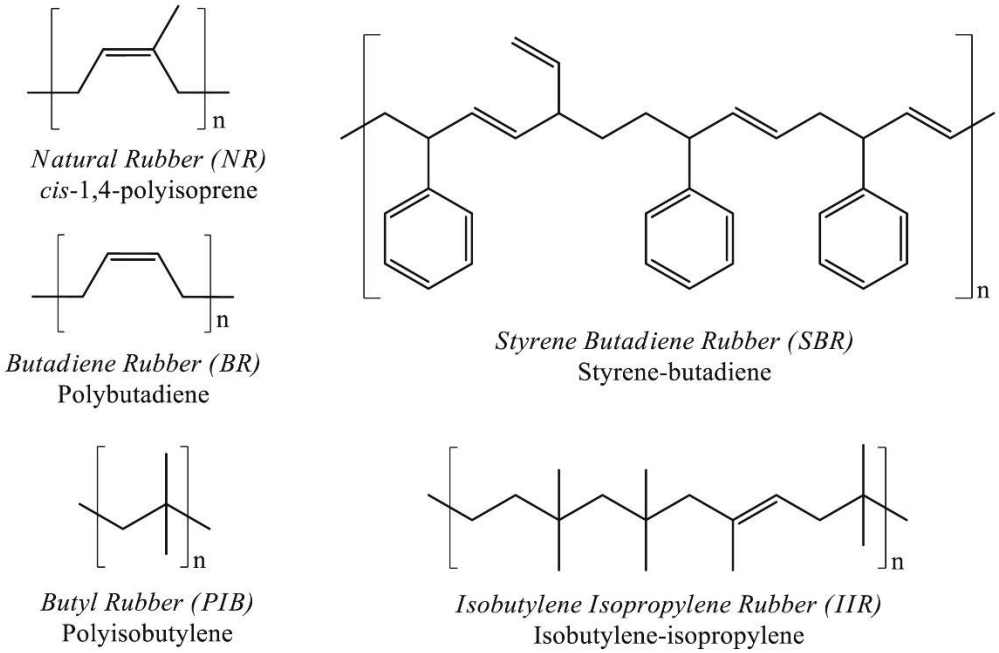

Figure 2. Chemical structure of the different rubber components used in tires [22].

The last components are vulcanization agents (sulfur groups, zinc oxide and stearic acids) and different additives (antioxidants, antiozonants, extender oils and waxes). These compounds are used to generate and speed up the formation of three-dimensional networks. This process, called vulcanization or curing, involves the crosslink formation between rubber or polymer molecules with unsaturated polymeric bonds, such as double or triple bonds, so as to achieve improved elasticity, resilience, tensile strength, hardness and weather resistance [2,25-27]. Figure 3 presents some typical changes in the molecular structure of polymers [27].

Although the desired or enhanced properties of tires can be achieved by vulcanization, its other major impact must not be ignored in the current technological and industrial areas, which is the management of end-of-life tires. The large volume of non-biodegradable waste tires has continuously been

observed to cause environmental pollution that limited the global strategy for sustainable development. Thus, recycling of waste tires has become a serious challenge worldwide.

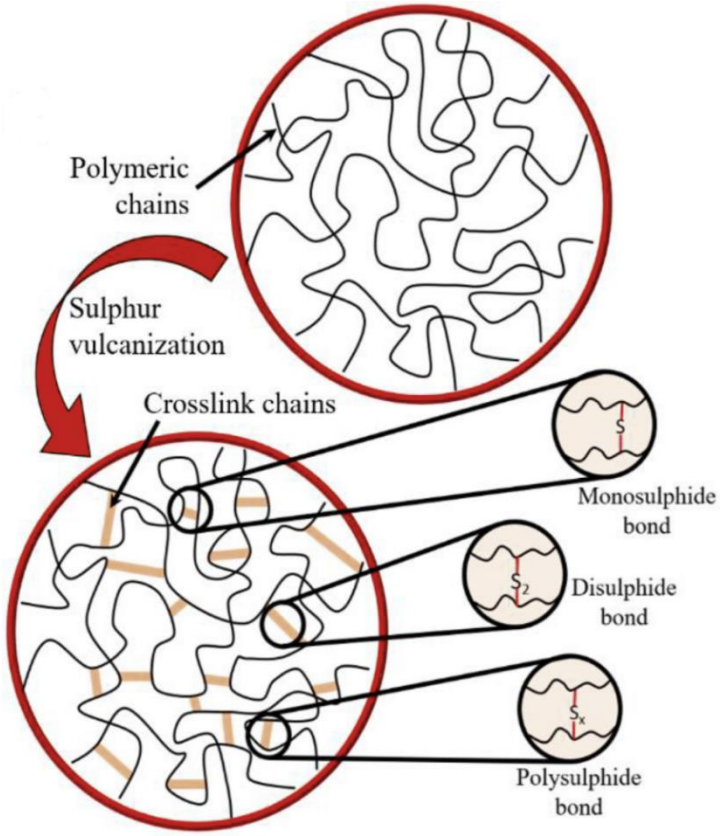

Figure 3. Vulcanization changes in the molecular structure of polymers [27].

1.1.2 Waste tire recycling

Historically, landfilling was the easiest way to dispose of end-of-life tires in the world. However, as landfilling leads to severe environmental problems and has no promising future, it is regarded now as one of the most undesirable strategies of waste tires disposal. For example, the resistance towards biodegradation, photochemical decomposition and chemical reagents make waste tires persistent in the environment, as well as their shape (large empty cavity) holding water for a long time offering sites for mosquito larva breeding that are vectors of deadly diseases such as dengue, chikungunya and malaria [3]. Additionally, tire fires often lead to the production of pyrolytic oils, which can contaminate surface and subsurface water and soils. Furthermore, dense black smoke and toxic gas can be released from these fires. For example, a tire fire took place at the Tire King Recycling, Hagersville, Ontario, Canada in February 1990, lasted for 17 days before it was extinguished [28].

Because of these risks, a Waste Landfill Directive of the European Union legally prohibited tire stockpiling in landfills by the Directive 1999/31/EC [29].

During the past 20 years, different tire recycling methods have been established to reduce the amount of disposable scrap tires as non-degradable waste materials in the environment. It is highly important to analyze the recovery rates of waste tires since it represents the possibility of waste tire use. According to the European Tire & Rubber Manufacturers' Association and the Global End-of-Life Tire Management, there is a recovery rate over 90% for tires in Europe and about 85% for other countries like Japan and USA [22]. These higher recovery rates allow the waste tires to be converted to resources. The main tire recycling methods are: retreading, incineration for energy recovery, pyrolysis to obtain gas and carbon black, as well as granulating into smaller particles used as fillers in various matrices such as concrete, asphalt and polymers [12]. These recycling methods not only help to eliminate the environmental threat on public health and safety, but also contribute to the economic development of several markets such as artificial reef, erosion control, breakwaters, athletic tracks, playground surface, rubberized composites and many more [30].

1.1.2.1 Retreading

Tire retreading is an economically attractive and environmentally beneficial process to extend the lifetime of a used tire by stripping off its tread and applying a new one through cold or hot methods. The total service lifetime of a tire can be extended by 1-2 times via repeated retreading. Because of both material and energy savings, tire retreading provides the most resource-efficient strategy for the management of used tires [4]. The value of rubber and other resources consumed for retreading a waste tire is equivalent to 15-30% that is required to produce a new tire, and the sale price is 20-50% that of new tires [31]. Nevertheless, this method is only suitable for tires that have no damage to the carcass, which can successfully pass a wear and tear inspection [32,33]. Nevertheless, the quality of retreaded tires is always lower than that of new tires. No matter how well the work was done, some safety concerns at high speed are limiting the promotion and application of this solution.

1.1.2.2 Incineration for energy recovery

A tire contains energy which can be released through incineration or combustion. In general, a tire has a heat value of 32.6 MJ/kg compared to that of coal which is 18.6-27.9 MJ/kg [5]. One of the greatest consumers of waste tires is the cement industry, where whole and shredded tires are used as a fuel source in cement kilns. The operation temperature is above 1200 °C, which ensures that all the tire components are completely combusted. Waste tires are also treated as fuel for preparing other

productions such as steam, electrical energy, pulp, paper, lime and steel [7]. However, tire-derived fuel is not the most environmentally beneficial method for handling waste tires because it will discharge large amounts of environmental pollutants when performed incorrectly, such as sulfur dioxide (SO_2) and polynuclear aromatic hydrocarbon (PAH) [34].

1.1.2.3 Pyrolysis

Pyrolysis for recycling waste tires is a thermal degradation process heating whole or shredded tires in a reactor vessel under the exclusion of ambient oxygen to avoid oxidation. When whole waste tires are processed, four output products are produced: liquid (oil), gas, solid (char) and steel. Figure 4 shows the beneficial products obtained from the pyrolysis process [6]. The main product is pyrolysis oil having a high calorific value (38-45 MJ/kg), which encourages the researchers to explore its potential for substituting fossil oil as a liquid fuel [35]. Rombaldo and co-workers investigated different operating conditions for pyrolyzing shredded tires to produce fuel oil and activated carbon [36]. They reported that the properties of the activated carbon obtained were similar to that of commercial products with surface areas above 200 m^2/g. They further found that larger surface area was obtained at higher temperature. Therefore, pyrolysis is a good way to eliminate waste tires by the production of potentially valuable products. However, because the construction and operation (high temperature with low pressure) of pyrolysis plants are very costly, the effort is hampered [6].

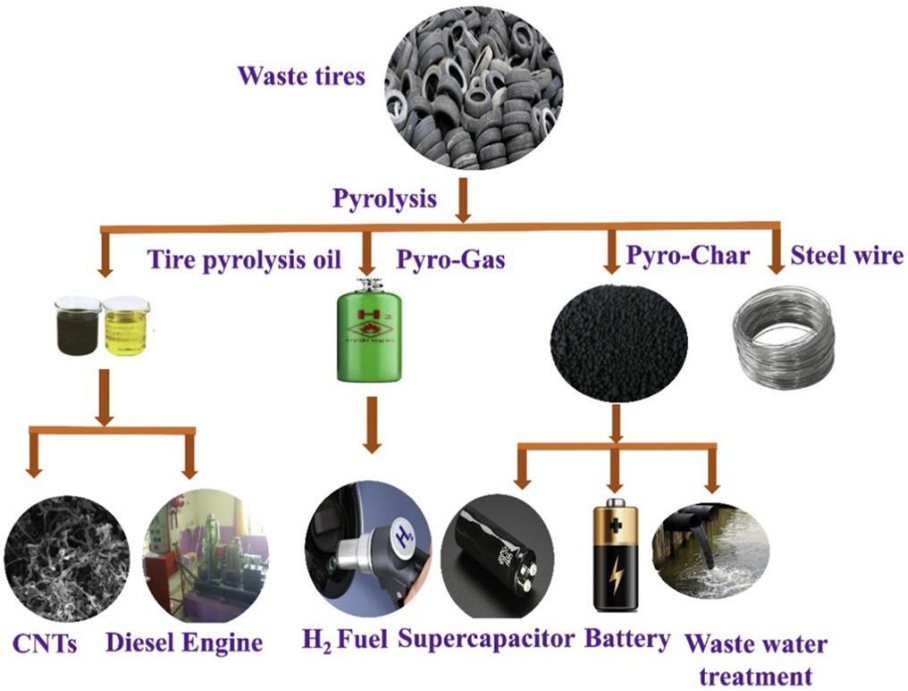

Figure 4. Schematic diagram for the waste tire pyrolysis product and their applications [6].

1.1.2.4 Ground tire rubber (GTR)

As mentioned above, waste tires contain NR and synthetic rubbers, which can be used as reinforcement in virgin matrices for producing composites. In order to improve the filler distribution and increase the probability of better contact with rubber chains, waste tire rubbers should be shredded into ground tire rubber (GTR) with small particle sizes and high specific surface areas. This process can be considered as downsizing or down-cycling [8]. Downsizing waste tires, a technologically complex process, requires special equipment capable of shredding and grinding waste tires, which have complex structures and high mechanical properties [37]. The main methods of waste tire downsizing along with their advantages and disadvantages are listed in Table 2. Furthermore, Figure 5 reports the surface characteristics of GTR obtained from different downsizing processes [8]. The figure clearly shows that, based on different downsizing processes, different types of surfaces and sizes are produced.

The GTR particles produced by ambient processes have rough and irregular surfaces, while cryogenic processes offer smooth and edgy surfaces. In general, the incorporation of GTR into polymeric matrices (thermoplastics, thermosets and rubbers) is one of the most promising technique for an effective recycling of waste tire rubbers. The resulting polymer composites not only decrease the cost of the final products, but also reduce the use of virgin polymers and simultaneously decrease the environmental footprints of the final products [38].

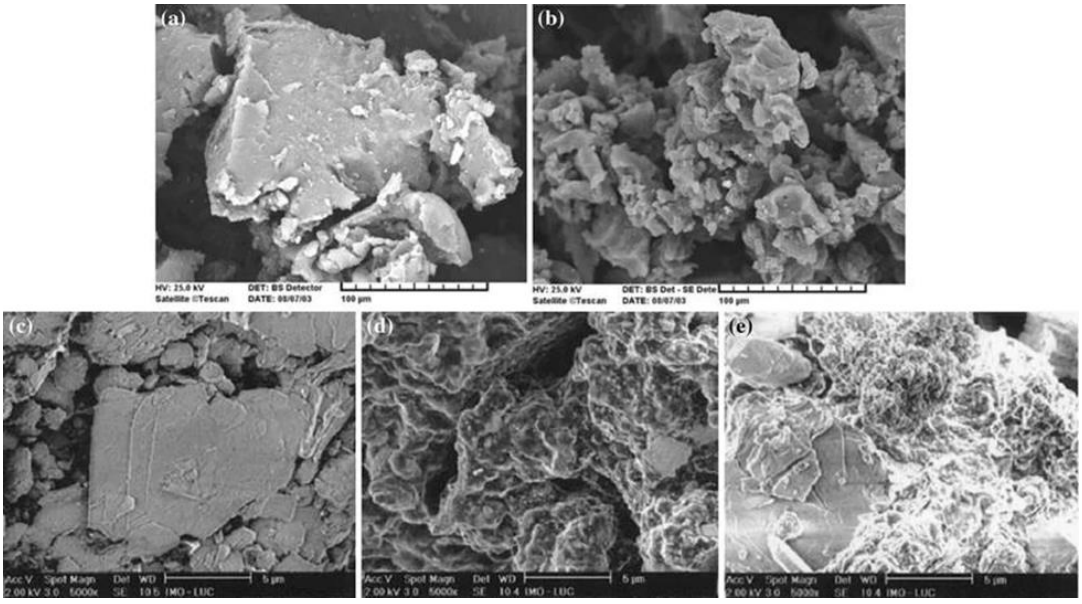

Figure 5. The surface of GTR produced by different downsizing processes: (a) ambient-mechanical; (b) water jet; (c) cryogenic-pin mill; (d) ambient-rotary mill; (e) cryogenic-rotary mill [8].

Table 2. General methods of waste tire downsizing [6,8].

Methods	Description	Advantages	Disadvantages
Ambient (rough, irregular)	Repeated grinding using shredder, mills, knife, granulators and rolling mills	High surface area and volume ratio	1. Temperature can rise up to 130°C 2. Oxidation on the surface of granulates 3. Cooling needed to prevent combustion
Wet ambient (rough, irregular)	1. Grinding a suspension of shredded rubber using grindstone 2. Water cooled granulates and grindstone	1. Lower level of degradation on granulates 2. High surface area and volume	Requires a drying step and shredding of tires before grinding
Water jet (rough, irregular)	1. Used for large size tires (trucks and tractors) 2. Water jet of >2000 bar pressure and high velocity used to strip rubber	Environmentally safe, energy saving, low level of noise and no pollutants	Requires high pressure and trained personnel
Cryogenic (sharp edge flat/smooth)	Rubber cooled in liquid nitrogen and shattered using impact type mills	No surface oxidation of granulates and cleaner granulates	1. High cost of liquid nitrogen 2. High humidity of granulates

1.2 Ground Tire Rubber/Thermoplastic Composites

Nowadays, we are heavily dependent on thermoplastic products, which have already replaced a large number of products produced by conventional materials such as wood and metal in a wide range of applications. Economically speaking, incorporating GTR into thermoplastics can reduce the cost of the products created. Environmentally speaking, blending GTR with thermoplastics also reduces environmental problems corresponding to the world's 3R (reduce, reuse and recycle) notion. Therefore, these factors have encouraged scientists and researchers in the world to fabricate and evaluate thermoplastic blends and composites containing GTR.

1.2.1 Modification of GTR

Incorporation of GTR, containing high quality natural and synthetic rubbers, into thermoplastic materials can be regarded as an upcycling process. Nevertheless, a significant issue is always focused on the compatibility between the GTR and thermoplastic matrices [39]. Due to insufficient bonding

between GTR and virgin matrices coming from completely different groups of macromolecular compounds with different physicochemical properties, the blends containing GTR have lower mechanical properties. To improve the interfacial bonding and promote smooth stress transfer between GTR and the matrix, the GTR surface should be modified [9]. This modification makes the interfaces similar to each other or provides specific interaction sites between the phases, leading to higher mechanical properties and longer-term stability of the composites [40]. Normally, two modification strategies are dedicated to GTR: rubber devulcanization/reclamation/regeneration, as well as physical and chemical methods.

1.2.1.1 GTR devulcanization or reclamation

GTR devulcanization or reclamation is used for converting a three-dimensional crosslinked, infusible and insoluble vulcanized rubber (100% gel content) into partially soluble materials with lower crosslink density having more chain mobility, which could generate molecular entanglement between the polymer matrix and curable rubber. Success of devulcanization or reclamation can be determined by how much of the regenerated tire rubber has become soluble after treatment, and this parameter is called the sol content [41]. By definition, devulcanization and reclamation are different processes. Devulcanization is defined as the scission of C–S and S–S bonds to break down the three-dimensional structure to obtain plasticity [42]. On the other hand, reclamation is the cleavage of C–C bonds on the rubber backbone to reduce the molecular weight and produce plasticity [43]. The outcome of both processes is the same: improvement of chain mobility/interaction (easier compounding) and obtention of a rubber compound which can be revulcanized similar to fresh/virgin rubber.

Regardless of the distinction between reclaiming and devulcanization, the processes can hardly be separated into devulcanization or reclamation since the required energies to cleave the S-S and C-S bonds (227 kJ/mol and 273 kJ/mol, respectively) are very close to the energy to break the C-C bonds (348 kJ/mol) [44,45]. Reclamation is usually coupled with devulcanization as shown in Figure 6 [10]. In general, the processes can be classified as follows: thermomechanical, thermochemical, ultrasonic, microwave and microbiological processes.

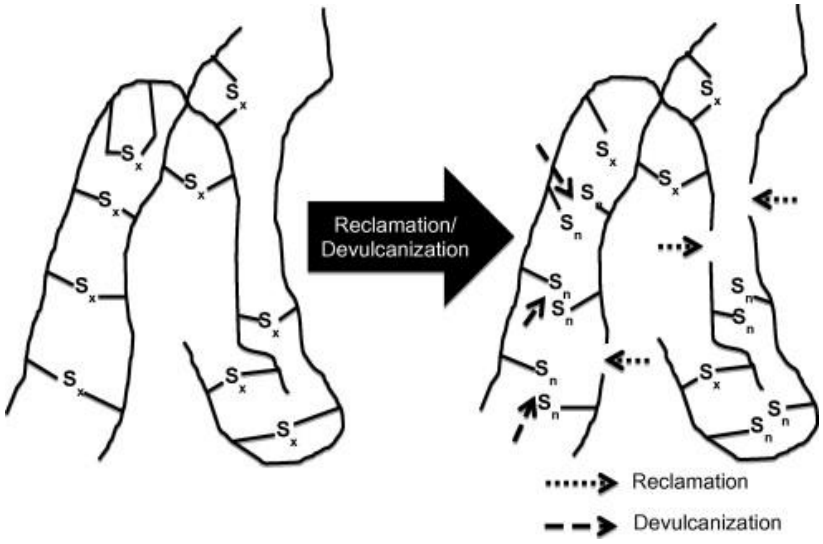

Figure 6. Schematic representation of devulcanization and reclamation [10].

Thermomechanical processes

In this process, crumb rubber undergoes shear stress and/or elongational stress on suitable equipment such as mills, twin-screw extruders, etc. Milling and extrusion are usually operated at high temperatures around 200°C. This process may lead to a significant decrease in the molecular weight due to mechanical shearing at high temperatures. The characteristics of the products are considerably influenced by the processing equipment, such as its flow characteristics (local shear rate) and processing parameters (residence time). To obtain the optimum processing parameters, different methods of experimental design are used, such as the response surface method [46]. Furthermore, one topic of ongoing research is to design and construct effective devulcanization extruders [47]. Figure 7 presents the schematics of a generally used twin-screw extruder [44].

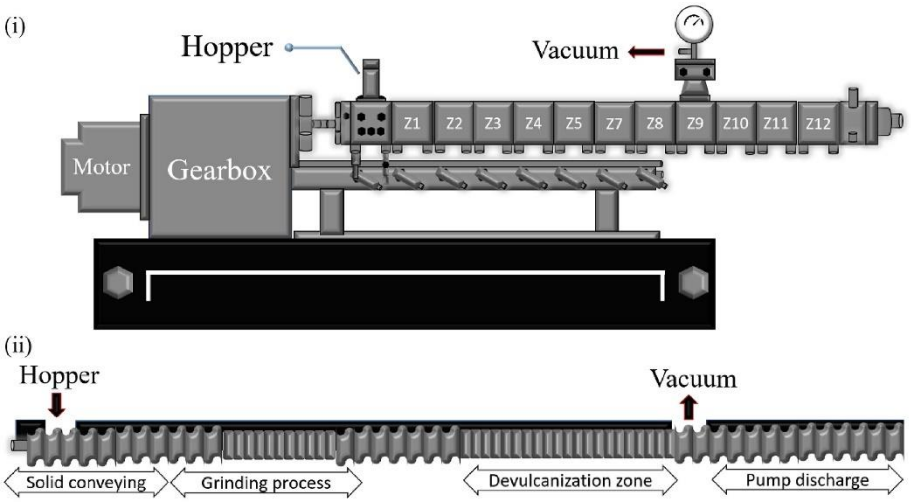

Figure 7. The typical external and internal screw configuration of a twin-screw extruder [44].

Yazdani et al. [48] reported that the barrel temperature and screw rotational speed were the main determining factors of a twin-screw extruder for the GTR devulcanization rate. They concluded that increasing the operating temperature from 220 to 280℃ at constant screw speed (120 rpm) resulted in a slightly lower devulcanization rate from 88% to 85%. This phenomenon might be associated with the degradation of the rubber backbone instead of the crosslinked network. Similar results were obtained by Edwards et al. [49], where selectivity of crosslink cleavage decreased with increasing barrel temperature.

Thermochemical processes

Nowadays, many thermomechanical processes are classified into thermochemical processes because they are often carried out with reclaiming agents. The majority of the current industries are using chemical reclaiming agents for manufacturing reclaimed rubbers. These reclaiming agents are used in the range of 0.5-10 wt.% for natural and synthetic rubbers, aiming to break the sulfur crosslinks between the rubber chains and stabilize the free radicals generated [50]. There is a large number of chemical reclaiming agents used in thermochemical processes, such as diphenyl disulfide [51], tetrabenzylthiuram disulfide [52], benzoyl peroxide [53], etc. Figure 8 illustrates the chemical structure of some disulfides and mercaptans developed to reclaim rubber from waste tires [50]. Generally, these chemical agents are used at elevated temperature and the related processes usually require mechanical mixing or kneading.

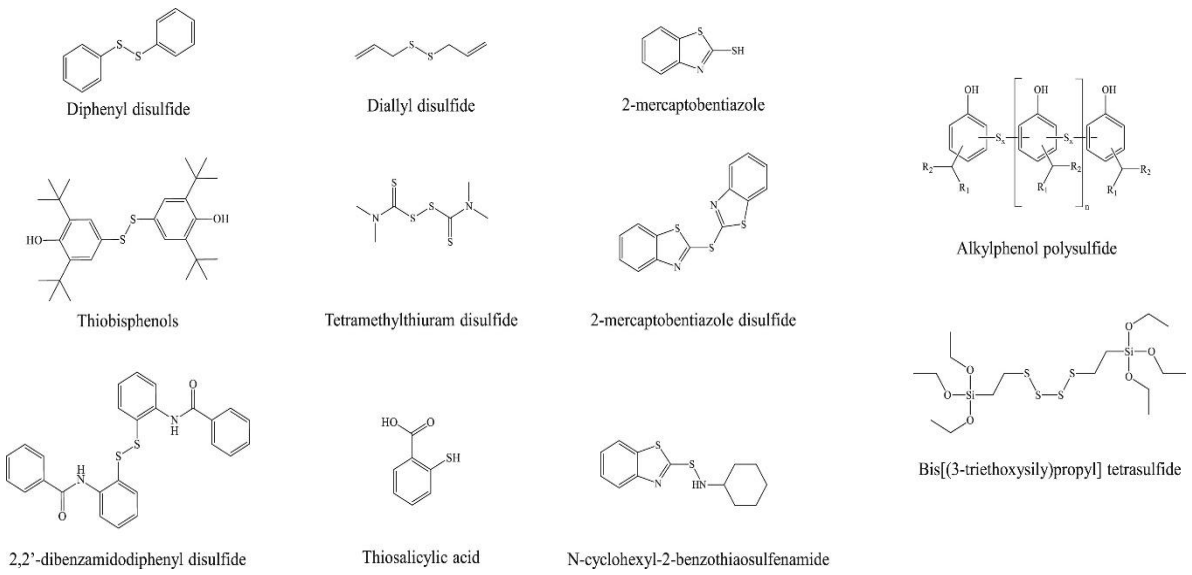

Figure 8. Typical sulfides and mercaptans used in tire reclaiming [50].

Cook et al. [54] prepared and evaluated alkyl phenol sulfides as reclaiming agents for SBR. The reclaiming was carried out at 188°C for 4 h using 5 mesh vulcanized rubber powder. Finally, they determined both the total and combined sulfur in the reclaimed materials, but they did not report their method of sulfur estimation.

Zhang et al. [55] synthesized a new reclaiming agent, 4,4′-dithiobis(2,6-di-t-butylphenol), used in an internal (batch) mixer at 180 and 200°C for the thermochemical devulcanization of GTR. They found that the crosslink density of the reclaimed rubber decreased as both the reclaiming agent content and temperature increased due to the simultaneous breakdown of both crosslinked bonds and polymer backbone chains.

Furthermore, as for GTR reclaiming, "softeners" (processing oils, reclaim oils) are usually used to stretch the bonds between the rubber chains (swelling of the crosslinked structure) to reduce the mechanical energy required for mixing or kneading. Asphalts [56] and bitumens [57] can also be used as softeners.

Lievana and Karger-Kocsis [57] produced thermoplastic elastomers (TPE) containing GTR. They found that bitumen not only acted as a reclaiming agent for GTR devulcanization, but also acted as a plasticizer and compatibilizer in the blends based on low-density polyethylene (LDPE) with ethylene propylene diene monomer (EPDM) and GTR. Furthermore, they pinpointed that the reclaiming activity of bitumen on GTR depended on the temperature and storage time, as well as the compounding conditions.

Ultrasonic method

A viable alternative method for devulcanization of crosslinked rubber is to use ultrasonic energy (low-frequency range of the ultrasound defined by the interval between 20 kHz and 500 MHz) as this process is simple, fast and efficient. This devulcanization process demands a high energy level to break C-S and S-S bonds. An ultrasonic wave can provide high-frequency extension-compression stresses in various media [58]. During the negative pressure period of the ultrasound, cavitation of bubbles formed during the treatment can lead to the chemical and mechanical effects of the ultrasound. There are two contrary theories contributing to the cavitation-induced chemical changes: "hot spot" and "electrical theory". The former theory assumes that the formed bubbles may have a temperature of 5000 K and a pressure of 500 bar. The latter postulates that an electrical field gradient that was generated on the surface of the bubble is high enough to break down chemical bonds [59].

Tukachinsky et al. [60] proposed that devulcanized rubber having a crosslink density lower than 0.06 kmol/m^3 can be considered as overtreated, while rubbers with a crosslink density higher than 0.10 kmol/m^3 can be seen as undertreated. Consequently, overtreatment by ultrasound results in main chain backbone breakage and undertreatment gives rise to insufficient devulcanization. Moreover, they found that ultrasonic devulcanization can break not only C-S or S-S bonds, but also C-C bonds in rubber because the molecular weight of the sol fraction decreased.

Isayev et al. [61] investigated the effect of particle size (10 and 30 mesh) on the ultrasonic devulcanization of GTR. Under a devulcanization temperature of 250°C with an ultrasonic amplitude of 10 μm, they found that 30 mesh GTR exhibited a lower crosslink density (0.1 kmol/m^3) and gel content (57%) than that of 10 mesh GTR (crosslink density = 0.2 kmol/m^3 and gel content = 67%). Thus, smaller particles can produce higher devulcanization rate.

Microwave method

The microwave technique can provide a controlled dose of microwave energy at specified frequency and sufficient energy level to cleave S-S bonds in the rubber [62]. This method is a viable as well as very useful approach because it can offer economical and ecological process for reusing waste rubber to return it to the same products where it was originally produced with equivalent physical properties [63]. Figure 9 presents the devulcanization treatment through a microwave irradiation technique [64].

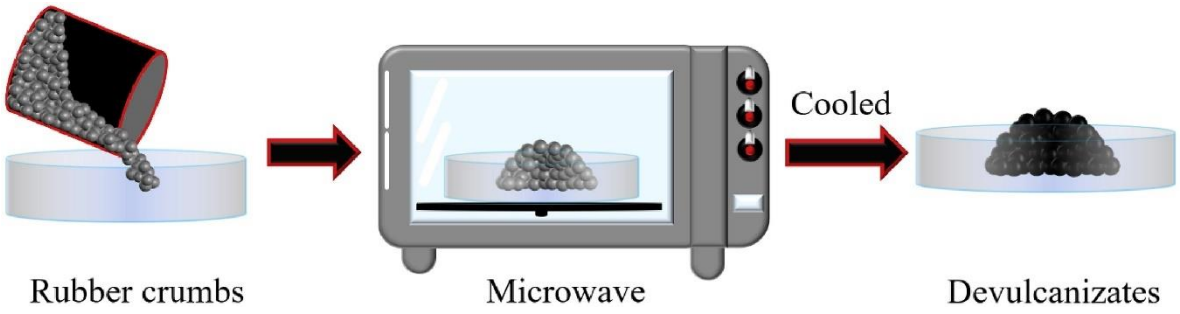

Figure 9. Diagram of typical microwave devulcanization treatment [64].

In the microwave technique, the waste rubber must be polar so the microwave energy will generate the heat (>250°C) necessary for devulcanization. The high thermal conductivity and heat capacity of carbon black (CB) support the accumulation of internal energy and its uniform distribution in the material [65]. Microwave energy between 915 and 2450 MHz and between 41 and 177 Wh/lb is sufficient to break all the crosslinked bonds, but it is not enough for the degradation of polymer chains [41].

The microwave technique is often coupled with extrusion and mixing. Tyler et al. [66] claimed that the microwave devulcanization process can be regarded as an effective way to control the pollution by reclaiming sulfur vulcanized elastomer containing polar groups. The microwave device produced heat at a temperature (>260°C) to yield a mass effect, and was then fed into an extruder to extrude the rubber at a temperature of 90-125°C.

However, when softeners are apolar, they will have a negative influence on the devulcanization. Pistor et al. [67] used microwave-aided devulcanization for EPDM systems in the absence/presence of paraffinic oil (apolar). They concluded that the devulcanization level was better controlled under the conditions that paraffinic oil was extracted from the rubber and the samples were exposed to microwaves for a short time.

Microbiological processes

According to the fact that NR-latex can be considered as a microbiological attacking target in nature, researchers sought bacteria able to cleave the polysulfide linkages [68]. Many reports have found that several bacteria are capable of breaking the sulfide linkages and the extent of reaction can be adjusted through temperature, pH, etc. [69-71]. For example, Li et al. [71] studied the microbial devulcanization of GTR by *Thiobacillus ferrooxidans*, which was selected from the soil of an iron mine having strong sulfur oxidizing capacity. GTR was also devulcanized in the modified Silverman

medium during the culture of *T. ferrooxidans* for 30 days. The increasing amount of SO_4^{2-} in the medium revealed that the sulfur on the GTR surface was oxidized. Attenuated total reflection Fourier transform infrared spectroscopy (ATR-FTIR) and X-ray photoelectron spectroscopy (XPS) indicated that a cleavage of C-C bonds and a reduction of sulfur content on the GTR surface took place during the devulcanization step. Finally, they found that compared with untreated GTR, the devulcanized GTR had much smoother surfaces, better physical properties and higher swelling values.

In the microbiological processes, the devulcanization can only partially occur because the bacteria only have access to the rubber surface. Another problem is the toxicity of the different rubber additives, limiting the function of bacteria.

1.2.1.2 GTR surface activation

For the surface activation of GTR, physical and chemical methods can also be used.

Physical methods

For the physical modification of GTR, treatments in different environments (dry or wet) are used, leading to chemical changes on the GTR surface. Consequently, the name "physical methods" may be ambiguous. In order to modify the GTR surface, reactive gas (a mixture of oxygen and chlorine) [72], ozone, plasma, corona and electron beam irradiation processes were explored. These approaches can oxidize the GTR surface to produce polar groups such as peroxy, hydroperoxy, hydroxyl and carbonyl group [11]. These groups on the GTR surface can not only enhance the interaction with polar polymers, but also be mediated to interact with reactive compatibilizers to improve the interaction between GTR and polymer matrices.

Li et al. [73] conducted the surface modification of GTR by cold plasma to introduce oxygen-containing functional groups. As shown in Figure 10, the high-speed plasma particles firstly attack C-C and C-H bonds on the GTR main chains or branched chains. Then, these broken chains react with the oxygen and hydrogen species. Finally, XPS analysis confirmed the formation of functional groups such as -COOH, C-OH and -CHO on the GTR surfaces.

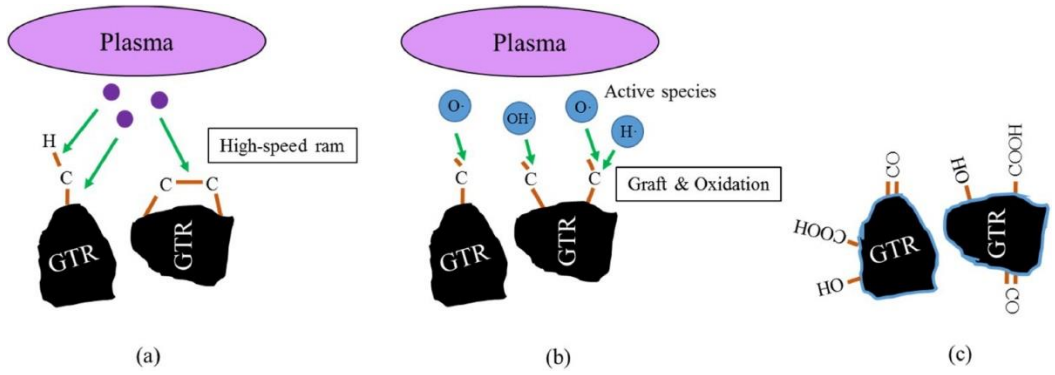

Figure 10. Mechanism of surface modification of GTR by cold plasma: (a) attack on weak bonds, (b) chain scission and (c) hydrophilic groups formation [73].

GTR oxidation can also be carried out in H_2O_2, HNO_3, $HClO_4$ and H_2SO_4 solutions to improve the adhesion at the interface between GTR and polymer matrices [74,75]. Elenien et al. [76] enhanced the compatibility between GTR and polypropylene (PP) by the treatment of GTR using H_2SO_4. The H_2SO_4 treatment could produce microcracks on the GTR surface, which allows better PP matrix penetration and coverage on the GTR. This finding is in agreement with the results obtained by Cepeda-Jiménez et al. [77], where surface treated GTR with H_2SO_4 contributed to a better adhesion between the rubber and polyurethane matrix.

Chemical methods

Chemical methods focus on different kinds of grafting process including non-reactive methods and reactive methods [12]. As for non-reactive methods, block or graft copolymers are incorporated into polymer blends to reduce the interfacial tension and improve the interaction between phases. Some copolymers are preferred, such as polyethylene-grafted-maleic anhydride (PE-g-MA) [78], ethylene-vinyl acetate (EVA) [79], ethylene-acrylic acid copolymer (EAA) [80], styrene-butadiene-styrene block copolymer (SBS) [81], etc.

Ahmad et al. [82] worked on the binary blends of 70/30 high density polyethylene/epoxidized natural rubber (HDPE/ENR) and studied the effect of PE-g-MA as a compatibilizer on the morphological and mechanical properties. They reported that the tensile strength, elongation at break and impact strength of HDPE/ENR blend increased with increasing PE-g-MA content. The optimum values were achieved when 6% PE-g-MA was used in the blend. Furthermore, scanning electron microscopy (SEM) analysis showed that the size of voids between phases became smaller, while the blends were more homogeneous when using PE-g-MA as a compatibilizer.

Wang et al. [83] investigated the effects of SBS on the morphological and mechanical properties of high density polyethylene (HDPE)/GTR composites. They found that no tearing strips were observed on the fractured surface of HDPE/GTR composites after the addition of SBS, revealing better elastic recovery ability and better interaction between phases. Compared with HDPE/GTR composites, the tensile strength and elongation at break were maximum with 12 phr SBS.

For the reactive methods, the in situ formation of block or graft copolymers serves as a bridge to improve bonding by covalent reactions between the functionalized components in polymers [12]. For example, maleic anhydride (MA) is widely used for the surface modification of rubbers to improve compatibility and interfacial adhesion between immiscible phases [84-86]. Naskar et al. [85] prepared maleic anhydride (MA) grafted GTR (GTR-g-MA) via free radical-induced process in an internal mixer at a temperature of 160°C. They concluded that the properties of GTR-g-MA were much better than that of the reference sample with the same GTR content. Abou-Helal et al. [86] functionalized the EPDM surface with MA by free radical-induced grafting and γ-irradiation. The grafted EPDM was then used in EPDM/NR compounds. The results showed that the tensile strength and elongation at break of compatibilized EPDM/NR compounds increased with higher MA content.

Coiai et al. [87] functionalized the GTR surface with styrene by in situ free radical polymerization. They proposed that reactive double bonds located on the GTR surface can act as “anchoring” sites for styrene grafting. Under the function of dibenzoyl-peroxide (initiator), the percentage of grafted styrene over the total weight of formed polymer could reach 40%.

Lee et al. [88] modified the GTR with allylamine via UV-induced photo-grafting. After the successful GTR grafting with allylamine, the mechanical properties of PP/PP-g-MA/GTR blends were superior compared to blends without GTR treatment. This phenomenon is associated to the reaction between $–NH_2$ and the anhydride groups of the graft and PP-g-MA compatibilizer.

1.2.2 GTR in thermoplastics

One often preferred way of recycling GTR is to use it as a component for composites based on thermoplastics, such as PE, PP, polystyrene (PS) and polyvinyl chloride (PVC). Injection molding or compression molding is now used to produce the majority of GTR/thermoplastics composites. Several reasons for these composites achieving growing attention in polymer material markets are as follows:

- Due to the large market share of thermoplastics, a small percentage of GTR in thermoplastics (<10 wt.%) can result in a huge consumption of GTR.

- Like rubbers, thermoplastics can also act as filler and GTR is a major component in the related products.
- Recycled thermoplastics can also be modified by GTR, which further reduces the cost.
- Based on the fact that the majority of toughened thermoplastics are rubber modified, the incorporation of GTR can improve the toughness of the corresponding blends.

In order to enhance the toughness and overall properties of polymer composites, a suitable compatibilization strategy must be adopted. The mechanical properties of these composites significantly rely on the type of thermoplastic matrix, the amount of GTR and the dispersion level (homogeneity) in the matrix, as well as the interactions between each component.

In a study by Mészáros et al. [13], LDPE as the matrix, GTR as the filler and EVA as the compatibilizer were melt-blended in a twin-screw extruder and then granulated. The LDPE/GTR/EVA composites were produced by injection molding. Based on tensile tests, the tensile modulus and tensile strength decreased, while the elongation at break increased with increasing GTR and EVA content.

Qin et al. [89] used SBS as a compatibilizer to prepare linear low density polyethylene (LLDPE)/GTR composites. They firstly blended these components on a kneading mixer, and then compressed them at 180°C. Through mechanical performance evaluation, the results showed that the tensile strength, tear strength and the elongation at break increased with SBS addition up to 6 wt.%, and then decreased with further increasing SBS content.

Shanmugharaj et al. [90] produced PP/GTR composites compatibilized by allylamine grafted GTR along with PP-g-MA. All the components were blended at 200°C in a kneading mixer and the composites were manufactured via compression molding. They concluded that all the improved mechanical properties obtained by the modified PP/GTR composites was related to the enhanced compatibility through a chemical reaction between PP-g-MA with the allylamine grafted GTR.

Fuhrmann et al. [91] blended GTR into PS in a twin-screw extruder. The GTR particles were swollen in a paraffinic plasticizing oil so as to modify their surface properties. The PS/GTR composites were produced by injection molding. The mechanical properties indicated that the tensile strength and tensile modulus decreased with increasing GTR content. However, the notched Charpy impact strength remained at the same level for all the PP/GTR composites.

Orrit-Prat et al. [14] used PVC mixed with different GTR contents and particle sizes, then fed them into a batch mixer to manufacture PVC/GTR composites via compression molding. As expected, the mechanical properties of the PVC/GTR composites decreased with increasing both parameters.

In order to limit the loss of mechanical properties in blends with increasing GTR content, it is mandatory to use some surface treatment of the GTR and/or compatibilizers. Furthermore, before producing the composites by injection molding or compression molding, all untreated or treated GTR and thermoplastics should be melt-mixed in a batch mixer or a twin-screw extruder. This mixing process not only increases the cost, but also induces polymer degradation. It should be interesting to use a plastic molding technique for GTR without a melt-blending step. This is possible by using dry-blending and rotational molding.

1.3 Rotational molding

1.3.1 Introduction

Rotational molding is a low residual stress level, high-temperature manufacturing technique for producing hollow, one-piece plastic parts. It is also known as rotomolding or rotocasting [92]. The earliest commercial application of rotational molding for plastics was using vinyl plastisols for coating the inside surface of a hollow metal mold. Typical products were play balls and toy dolls. With the introduction of powdered polyethylene grades, rotational molding expanded more quickly since the 1950s. Compared with other techniques in the plastics industries, rotomolding is one of the fastest-growing polymer processes, expanding at an annual rate of 10% to 25% [93]. Nowadays, different types of polyethylene, such as LDPE, HDPE, linear medium density polyethylene (LMDPE), LLDPE, cross-linked polyethylene (XLPE) and ultra-high-molecular-weight polyethylene (UHMWPE), are the most widely used polymer in the rotomolding, accounting for about 85 to 90% of the total plastics consumed [94]. This is mainly because the powder flows, melt flow rates, thermal stability and relatively low cost of polyethylene are ideally fit for the process of rotomolding [94].

Rotational molding can also provide designers with the opportunity to produce economic stress-free articles with uniform wall thickness and potentially complex shapes. Therefore, as for producing hollow plastic products, rotational molding is currently a very competitive alternative to blow molding, thermoforming and injection molding [15]. The major limitation of rotational molding is that the cycle times are relatively long, resulting in possible thermal degradation of the polymer compared to other plastic molding techniques. Table 3 lists the main differences between rotational molding and competitive molding techniques, such as blow molding, thermoforming and injection molding [15,96,97].

Table 3. The major differences between rotational molding and competitive molding methods, such as blow molding, thermoforming and injection molding [15,96,97].

Factor	Blow molding	Thermoforming	Injection molding	Rotational molding
Plastics available	limited	broad	broad	limited
Feedstock	pellets	sheet	pellets	powder/liquid
Mould materials	steel/aluminium	aluminium	steel/aluminium	steel/aluminium
Mould pressure	<1 MPa	<0.3 MPa	20-150 MPa	<0.1 MPa
Mould cost	high	moderate	high	moderate
Wall thickness uniformity	Tends to be nonuniform	Tends to be nonuniform	Tends to be nonuniform	Uniformity possible
Residual stress	moderate	high	high	low
Cycle time	fast	fast	fast	slow

1.3.2 The process of rotational molding

There are four basic processing stages devoted to rotational molding which are shown in Figure 11 [98]. In the first step, a predetermined quantity of powdered (or liquid) plastic is loaded into a hollow metal mold at room temperature. The amount of material depends on the surface area of the mold, the required thickness and density of the final plastic product [92]. An important benefit of rotomolding is that there is no material waste because all the plastic in the mold is entirely used for manufacturing the part.

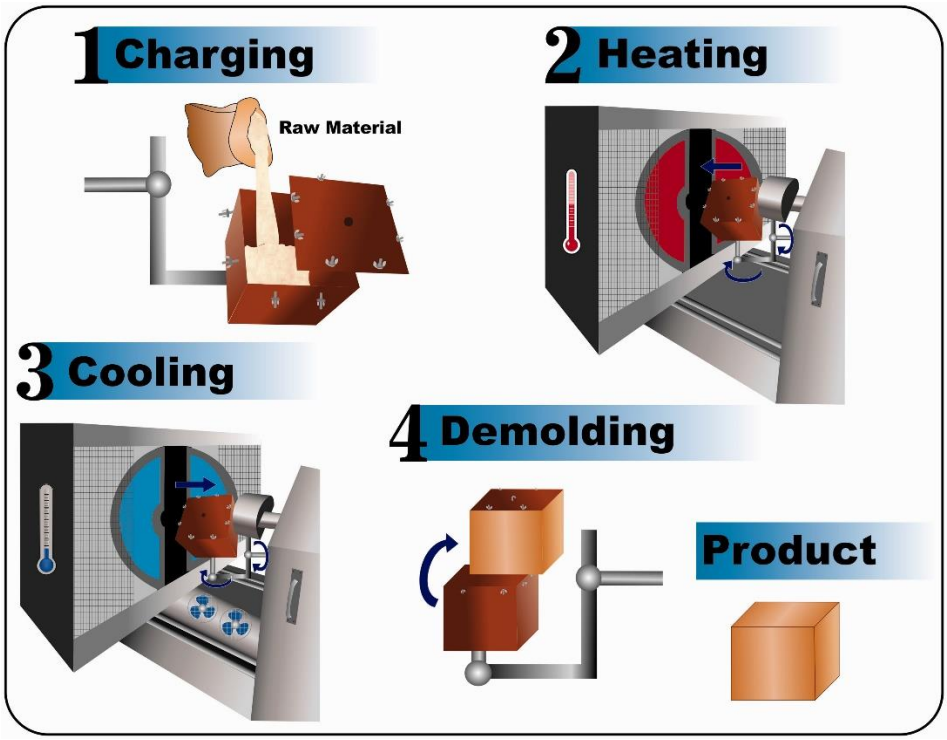

Figure 11. The four main steps of the rotational molding process [98].

In the second step, the mold is rotated biaxially through two mutually perpendicular axes and then moved into an oven. More importantly, the mold rotation is relatively slow (<12 rpm). Thus, this process does not rely on the centrifugal force. Although it might be helpful to increase productivity under the conditions of rotating the mold at high speeds, the complex shape and size of molds do not permit this [99]. During the rotomolding process, the plastic particles are sintered, forming a dense layer coating the mold walls. Bubble removal and melt densification can be controlled based on the particles geometry and melt rheology of the plastic [100,101]. It is also possible to control the wall thickness of the final product by changing the speeds of rotation about the perpendicular axes of rotation. In addition, according to the different shapes of the plastic part required, the ratio of the speeds for both axes can be set to different values. Different speed ratios can be used depending on the parts geometry to ensure that the mold surface is adequately coated. In rotational molding, the speed ratio (arm/plate) is defined as [94]:

$$\text{Speed ratio}=\frac{\text{Major axis (rpm)}}{\text{Minor axis (rpm)-Major axis (rpm)}} \quad (1)$$

In the third step, the hot mold is moved to a cool station to perform the cooling cycle. During this stage, the mold continues to rotate and cooling is commonly assisted by forced air, water spray or a

combination of both methods. Because cooling is normally only from the outside of the mold, the cooling method has a significant influence on the quality of the molded part. Unsymmetrical cooling can lead to warpage and distortion of the end product. Slow cooling allows the plastic to crystallize, resulting in high strength and stiffness of the final part, but lowers its resistance to impact loading. Fast cooling leads to a tougher molded part, but reduces its stiffness [102,103].

Finally, once the part has sufficiently solidified, the mold is opened and the final product is removed. The mold is then prepared for the next processing cycle [100,101].

1.3.3 Rotationally molded products

As mentioned above, rotational molding has several advantages over other plastic molding processes such as lower costs, great flexibility and lower design limitations. Because of the low melting point, low cost and good thermal stability of polyethylene, it is the main polymer material used for rotational molding. However, polyethylene has lower mechanical properties compared to high performance polymers, limiting its applications for high mechanical needs [104]. Nowadays, two ways have been proposed to modify the properties of rotomolded parts. The first one is to add reinforcements to produce polymer composites or add blowing agents to produce polymer foams [105]. Another way is to modify the part design. In the latter case, multi-layer rotomolded parts can be manufactured where each layer has its own function.

1.3.3.1 Rotomolded composites

Like other polymer molding technologies, reinforcements have also been incorporated into rotomolded parts to increase their mechanical properties. Wisley [106] produced glass fiber reinforced polyethylene composites by rotational molding. They found that compared with virgin polyethylene parts, the tensile strength and flexural modulus of the composites with a glass loading of 25 wt.%, can be increased by 54% and 40%, respectively.

López-Bañuelos et al. [107] incorporated agave fibers into LMDPE to manufacture rotomolded composites. They investigated the effect of fiber content on the morphological and mechanical properties of rotomolded parts. In particular, two sizes of agave fibers (0.165 mm and 0.368 mm) were used alone or together to determine their effect on the tensile, flexural and impact properties. Because all the materials used were in a powder state, they simply mixed them by a dry-blending technique (high speed mixer). Finally, they found that the addition of agave fibers in LMDPE can increase both flexural and tensile moduli, but the flexural and tensile strengths, as well as the impact

strength, decreased due to poor interfacial adhesion. A mixture of different fiber sizes (auto-hybrid composite) generated better tensile properties than using each size alone for a fixed total content.

Torres and Aragon [108] developed the process of rotational molding for natural fibers (cabuya and sisal) reinforced HDPE composites. To characterize unreinforced and reinforced natural fiber composites, they carried out several mechanical tests such as tensile, compression, impact, deep drawing and recovery. They finally concluded that there is an optimal fiber content (2.5 wt.% for cabuya fiber and 5 wt.% for sisal fiber) for the best tensile properties of fiber reinforced composites. The impact strength of cabuya-reinforced composites was higher than that of sisal-reinforced composites. The shrinkage level of the natural fiber reinforced HDPE composites decreased with increasing fiber content.

Although glass fibers and different types of natural fibers have been incorporated into rotomolded parts, only a few research studies have been reported in this field mainly because of poor adhesion between the fibers and the matrix. But to solve this problem, some efforts have been made.

Hanana and Rodrigue [109] produced self-hybrid composites based on LLDPE and maple fibers by rotational molding. They also investigated the effect of fiber surface treatment with maleic anhydride modified polyethylene (MAPE), fiber loading (10, 20 and 30 wt.%), fiber sizes (short, medium and long), as well as fiber ratio (100/0, 75/25, 50/50, 25/75 and 0/100) on the physical, morphological and mechanical properties. They found that MAPE as a coupling agent enhanced the interfacial compatibility between the phases leading to fewer defects (holes, voids and interfacial gaps) in rotomolded composites with treated maple fibers, while their mechanical properties (tensile modulus, tensile strength, flexural modulus and impact strength) improved. For example, the addition of MAPE to the composite increased the tensile and flexural moduli by 60% compared with the neat LLDPE.

Yuan et al. [110] studied the incorporation of aminosilane treated wollastonite fiber/sisal fiber into LMDPE and used MAPE as a coupling agent. They firstly premixed wollastonite, sisal fiber, MAPE and LMDPE by blending and compounding with a single screw extruder, and then ground the materials to get particles with diameters of about 0.5 mm prior to rotational molding. According to the SEM analysis, adding MAPE to the composites highly improved the adhesion between wollastonite fibers and LMDPE, especially for wollastonite fibers coated with aminopropyl trimethoxysilane (APTMS). Moreover, the impact strength rose by 20% for the composite containing 5 wt.% wollastonite fibers and 5 wt.% sisal fibers compared to the neat LMDPE, and further improvement was obtained by adding 5 wt.% MAPE where the impact strength was increased by 46%.

1.3.3.2 Rotomolded foams

Polymer foams, also known as cellular polymers, produce light parts with a good strength to weight ratio. Since insulating properties, impact strength, buoyancy and low sound transfer properties are also enhanced, the applications of polymer foams are very extensive such as construction, automotive, packaging and protection, biotechnology, etc. [111]. Rotational molding of foamed polymers has been attracting more and more attention because it can be used for manufacturing innovative and high added value parts with simple equipment [112]. Polymer foams manufactured by rotational molding is conditioned via the special nature of this molding process. Due to the requirement for high pressure, physical blowing agents (PBA) are not suitable for rotational molding. Thus, chemical blowing agents (CBA) are normally used to produce rotomolded polymer foams, releasing gasses through thermal decomposition at a specific temperature [113].

Liu et al. [114] conducted a study on the mechanisms of cell nucleation and growth during foaming of polyethylene and polypropylene melts in rotational molding. In order to form a foam structure in rotational molding from a chemical blowing agent, the polymer matrix needs to be a continuous melt phase and the CBA should be uniformly dispersed and wetted in the molten polymer. With increasing temperature, the CBA undergoes thermal decomposition and generates gases in the polymer matrix (cell nucleation). These gas bubbles will continue growing and neighboring bubbles will share one common polymer wall leading to a decreased wall thickness of the polymer. In addition, with increasing the polymer melt temperature during the process, the melt viscosity and melt strength decreases, leading to possible coalescence among adjacent cells. So an optimum between time and temperature must be determined.

Emami et al. [115] studied the effect of three chemical blowing agents (azodicarbonamide [exothermic], 4,4′-oxy-bis(benzenesulfonyl hydrazide) [exothermic] and sodium bicarbonate [endothermic]) on rotational molding of foamed metallocene polyethylene. During the decomposition process, exothermic blowing agents generate heat and evolve mainly nitrogen (N_2), while endothermic blowing agents absorb heat and generate mainly carbon dioxide (CO_2). They concluded that density reduction was higher while using exothermic blowing agents compared with endothermic blowing agent. This phenomenon was related to the better heat flow parameters, lower permeability and diffusing property of N_2 with respect to CO_2.

Raymond and Rodrigue [116] produced LLDPE foams and wood fiber/LLDPE composite foams by rotational molding. They also studied the effect of chemical blowing agent (0-0.6 wt.%) and wood (0-20 wt.%) contents on the rotomolded foam parts. The results showed that both tensile property and

flexural property of LLDPE foams decreased with increasing CBA content. Moreover, the tensile and flexural moduli of the composite foams (0.1 wt.% CBA) increased with increasing amount of wood fibers, while the tensile strength and elongation at break dropped.

1.3.3.3 Multi-layer rotomolded parts

Compared with single material formed products, multi-layer products offer a wide range of advantages. For example, by combining two materials, the advantages of both materials can be used in specific part areas. For example, by using recycled material for the inner structure and virgin material for the surface components, cost reduction can be achieved while keeping good aesthetics and surface quality [117].

Multi-layer rotomolded parts can be produced by sequential addition of different polymers to the mold, while the thickness of each layer is controlled by the amount of each material [129]. In particular, after spreading and melting of a first material, a second material is introduced into this process. By adhering powder particles, the second layer forms on the first layer. Thus, multi-layer rotomolded parts can be prepared by sequential addition of further materials.

Liu and Yang [118] used LLDPE and CBA to produce two-layer polyethylene foamed parts. They used a LDPE bag (with a melt point of 110°C) filled with a LLDPE/CBA mixture as the inner layer. This kind of bag is designed in such a way that it will only melt after the material of the outer layer already stuck to the mold wall, leading to the material of inner layer to be released and adhere to the first layer.

Archer et al. [119] proposed another possibility to build multi-layer structures by using a “drop box” in rotational molding. The drop box (a thermally insulated container) is placed inside the mold, and then opened at a specific point of time during the process. Therefore, the material in the container can be introduced into the mold and forms the inner layer.

Vázquez-Fletes et al. [120] prepared three-layer rotomolded parts by combining different concentration of agave fibers (0-15 wt.%) in the outer layer, CBA content (0-0.75 wt.%) in the middle layer and LMDPE in the internal layer. The results of the morphological analysis showed that due to gas migration, the three layers were not well defined. They also found that the impact strength was directly associated with the overall density of the rotomolded parts.

Chapter 2

Rotational molding of linear low density polyethylene with different concentrations of ground tire rubber

Dou Y, Rodrigue D. Rotational molding of linear low density polyethylene with different concentrations of ground tire rubber. 75th Annual Technical Conference and Exhibition of the Society of Plastics Engineers, SPE ANTEC, Anaheim 2017: 2252-2256.

2.1 Résumé

Dans ce travail, du caoutchouc de pneu broyé (GTR) a été mélangé à sec avec du polyéthylène linéaire de basse densité (LLDPE) pour produire des pièces en élastomère thermoplastique par rotomoulage. En particulier, différentes concentrations de GTR (0, 5, 10, 15, 20, 25, 30, 35, 40, 45 et 50% en poids) ont été incorporées pour déterminer l'effet de la phase de caoutchouc sur la facilité de moulage et les propriétés globales des pièces. Chaque composition a été caractérisée en termes de morphologie et de propriétés mécaniques (traction, flexion et impact). Les résultats ont montré que l'ajout de la phase de caoutchouc diminuait les modules et le résistances à la traction et à la flexion, mais l'allongement à la rupture était toujours supérieure à 100%. Fait intéressant, le composé optimum (30/70 GTR/LLDPE) a obtenu une résistance aux chocs supérieure de 35% à celle de la matrice pure.

2.2 Abstract

In this work, ground tire rubber (GTR) was dry-blended with linear low density polyethylene (LLDPE) to produce thermoplastic elastomer parts by rotational molding. In particular, different GTR concentrations (0, 5, 10, 15, 20, 25, 30, 35, 40, 45 and 50 wt.%) were incorporated to determine the effect of the rubber phase on the processability and overall properties of the parts. Each composition was characterized in terms of morphology and mechanical properties (tensile, flexural and impact). The results showed that the addition of the rubber phase decreased the tensile and flexural moduli and strengths, but the tensile elongation at break was always above 100%. Interestingly, the GTR/LLDPE compound had 35% higher impact strength than the neat matrix with an optimum GTR content around 30 wt.%.

2.3 Introduction

In recent years, along with the continuous development of the rubber industry, the problem of waste rubber disposal became more and more critical for environmental and economic reasons. For example, about 800 million of tires are rejected every year and this amount is increasing by 2% annually [121,122]. Consequently, the recycling of rubber waste is of high importance for the society and the rubber industry. Due to the crosslinked nature (thermoset material) of rubber waste, its management requires special techniques to revalorize/recycle the materials. To this end, size reduction to produce ground tire rubber (GRT) is an interesting technique for an effective recycling of rubber waste [123]. One important GTR application is to introduce the material into thermoplastic resins and composites to improve their impact strength [124]. This is usually done by a preliminary extrusion step to improve dispersion and adhesion. Nevertheless, other processes can be developed.

Rotational molding is a polymer processing technology used to produce hollow seamless products such as tanks, automotive parts, toys and several other items [107]. Unlike most other plastic processes, there is no pressure involved in rotational molding, which means that the molds can be very thin and generally inexpensive. Additionally, rotomolding can more easily handle complex shapes with a very wide range of part sizes and variable thicknesses [120,125,126,]. However, a very limited number of polymers are industrially rotomolded since the materials need specific requirements, limiting their use. This is generally related to viscosity and thermal degradation [127]. This is why still today, most rotomolded parts are based on the different grades of polyethylene. Because of its broad processing window, excellent chemical/thermal resistance and low cost, linear low density polyethylene (LLDPE) is one of the most commonly used grade of polyethylene [128-130].

In this study, up to 50 wt.% of GTR was introduced in LLDPE. To reduce the processing cost, time and material degradation, the dry-blending technique was used to mix the materials (powder state). After processing conditions optimization, the morphological, mechanical and thermal properties of the compounds were investigated, including density and hardness.

2.4 Materials

The matrix was linear low density polyethylene grade 8460 from Exxon Mobil (Canada). This polymer has a melt flow index of 5 g/10 min (2.16 kg/190°C) and a density of 0.93 g/cm^3. The ground tire rubber (GTR) was supplied by Phoenix Innovation Technologies (Montreal, Canada). This material has a density of 1.16 g/cm^3 and the particle size distribution is presented in Figure 12.

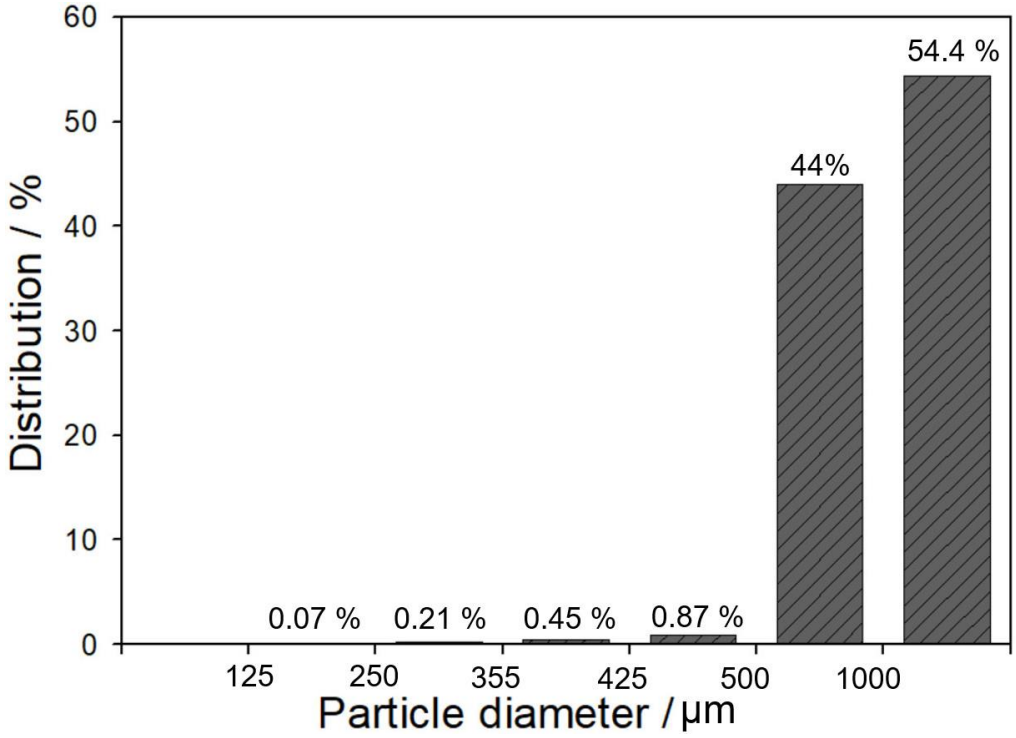

Figure 12. The particle size distribution of GTR.

2.5 Experimental

2.5.1 Material Mixing

For each composition, a total of 650 g of material was used based on LLDPE with 0, 5, 10, 15, 20, 25, 30, 35, 40, 45 and 50 wt.% of GTR. Mixing (dry-blending) was carried out in a high speed mixer (LAR-15LMB (Skyfood, USA) at 3320 rpm) for a total of 4-5 min.

2.5.2 Rotational Molding: Process and Equipment

A laboratory-scale rotational molding machine was used for processing. Rotationally molded parts were manufactured with an aluminum cubic mold of 3.6 mm wall thickness and a side length of 19 cm. Before loading the material, a demolding agent (Trasys 420, DuPont) was applied to the internal surface of the mold. The powder blends were then loaded into the mold to produce parts with an approximate wall thickness of 3 mm. Then, the charged mold was closed and mounted on the rotating arm. Preliminary trials were performed to determine the optimum conditions leading to homogeneous and uniform wall thickness. Finally, an oven at 275°C and a speed ratio of 1:4 with a major axis speed of 1 rpm was chosen. The heating was fixed at 25 min. Afterwards, the mold was removed from the oven and cooled by forced air for 35 min. Finally, the mold was opened to retrieve the part.

2.5.3 Morphological Characterization

The rotomolded samples were cryogenically fractured (liquid nitrogen) and micrographs of the exposed cross-sections were taken using a JOEL JSM-840A scanning electron microscope (SEM) and Olympus SZ6 stereomicroscope coupled with a Spot Insight (Diagnostic Instrument) high resolution (1600×1200 pixels) camera.

2.5.4 Density and Hardness Measurements

Density was determined by a Quantachrome Ultrapyc 1200e gas pycnometer. Nitrogen was used as the gas phase. Hardness (shore A and shore D) were also determined by a PTC Instruments Model 306L and Model 307L (ASTM D2240). The data reported are the average and standard deviation of a minimum of five repetitions.

2.5.5 Differential Scanning Calorimetry (DSC)

DSC analysis was performed on a DSC7 (Perkin Elmer) equipped with a thermal analysis controller TAC7/DX. For each test, around 15 mg of sample was placed in a sealed aluminum pan. The measurements were carried out with a scanning rate of 10°C/min between 50 and 200°C under a flow of dry nitrogen (20 mL/min).

2.5.6 Thermogravimetric Analysis (TGA)

TGA was carried out on a Q5000IR TGA analyzer (TA Instruments). The scans were performed from 50 to 800°C at a rate of 10°C/min with a gas flow rate of 25 mL/min. The tests were performed in nitrogen and air to evaluate the thermal and oxidative resistance.

2.5.7 Mechanical Properties

The tensile properties at room temperature were measured on an Instron model 5565 universal testing machine with a 500 N load cell. Type V samples were cut in the rotomolded parts according to ASTM D638. The crosshead speed was set at 10 mm/min. The reported values for the tensile modulus, strength and elongation at break are based on the average of at least six samples.

Flexural 3-point bending tests were performed (room temperature) at a crosshead speed of 2 mm/min on an Instron universal tester model 5565 (50 N load cell) (ASTM D790). The span was 60 mm. At least 5 samples (60×12.7 mm^2) were used to report the average and standard deviation (modulus and strength).

Charpy impact strength was determined by a Tinius Olsen (USA) testing machine model Impact 104. At least ten rectangular specimens (60×12.7 mm^2) were prepared according to ASTM D6110. The samples were V-notched by an automatic sample notcher model ASN (Dynisco, USA) at least 24 hours before testing.

2.6 Results and Discussion

2.6.1 Structure, Appearance and Color

The appearance of the samples is related to rubber content, processing temperature and processing time. Figure 13 shows rotomolded parts, where it can be observed that their appearance changes from white (neat LLPDE) to strong dark (50 wt.% GTR). Furthermore, it is difficult to distinguish the parts with 25 wt.% to 50 wt.% GTR by the naked eye, indicating that the GTR has already saturated the external surface of the parts.

Figure 13. Pictures of the rotomolded parts with different GTR contents: (a) 0, (b) 5, (c) 10, (d) 15, (e) 20, (f) 25, (g) 30, (h) 35, (i) 40, (j) 45 and (k) 50 wt.%.

2.6.2 Morphology

Figure 14 shows SEM of the cross-section of the rotomolded parts containing different GTR contents. Figures 14b and 14c reveal that homogeneous distribution of the GTR in the matrix was achieved, indicating that good processing conditions were used and low GTR content (0-10%) produced the best morphology. Nevertheless, with increasing GTR content (Figures 14d-14k), some bubbles and defects took place. This is due to the fact that at higher GTR content, the total rubber surface to be wetted by the polymer increases and the matrix is not able to cover all the particles, leading to GTR agglomeration [107].

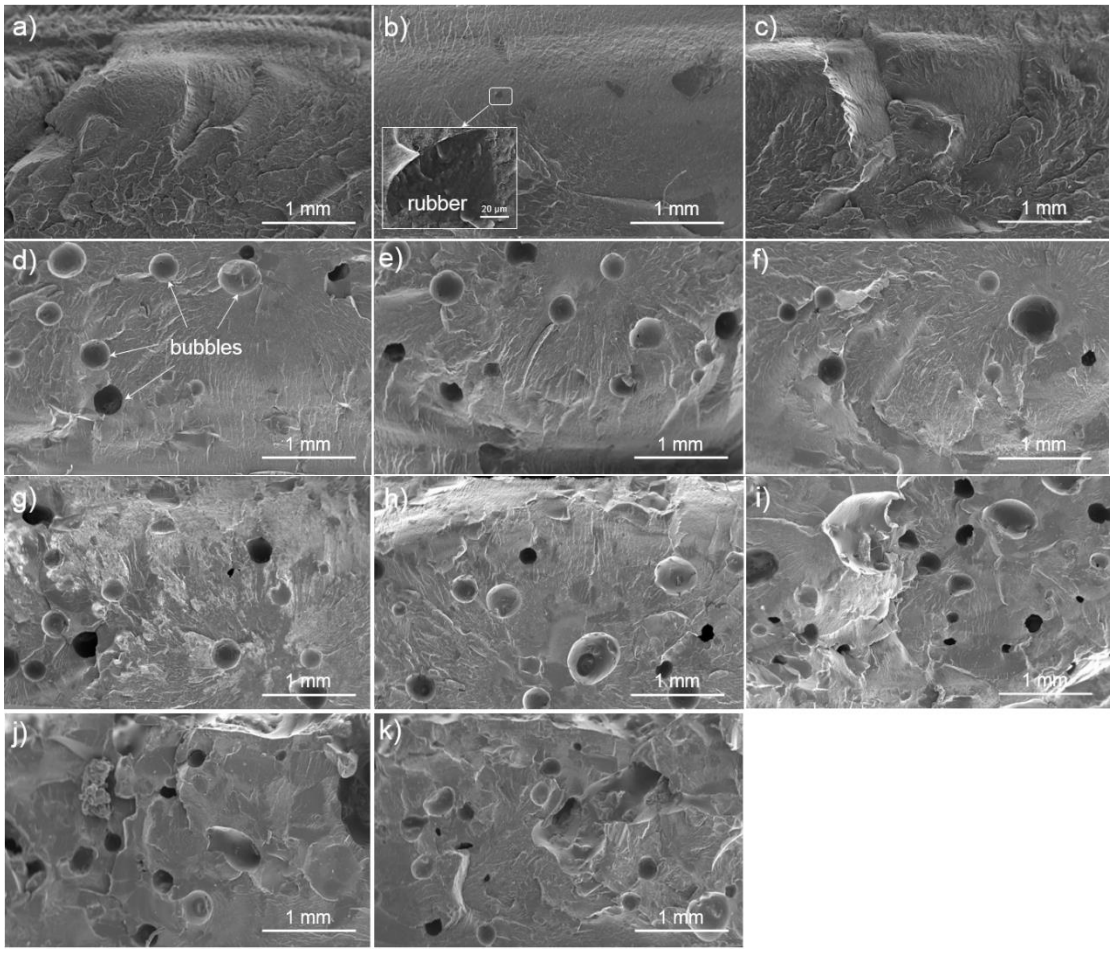

Figure 14. SEM of the cross-section of rotomolded specimens with different GTR concentration: (a) 0, (b) 5, (c) 10, (d) 15, (e) 20, (f) 25, (g) 30, (h) 35, (i) 40, (j) 45 and (k) 50 wt.%.

2.6.3 Density and Hardness Measurements

The density of the composites is reported in Figure 15 together with LLDPE powder and GTR particles. It can be observed that density firstly increases with increasing GTR content up to 10%. This might be related to the good physical adhesion between LLDPE and GTR, and absence of bubbles corresponding to Figures 14b and 14c. Subsequently, because of bubbles and defects, the density decreases with GTR addition up to 35%. However, the density finally increases with increasing GTR content up to 50%. This might be due to GTR content gradually taking over as the quantity and size of the voids do not increase according to Figures 14i-14k and GTR density is much higher.

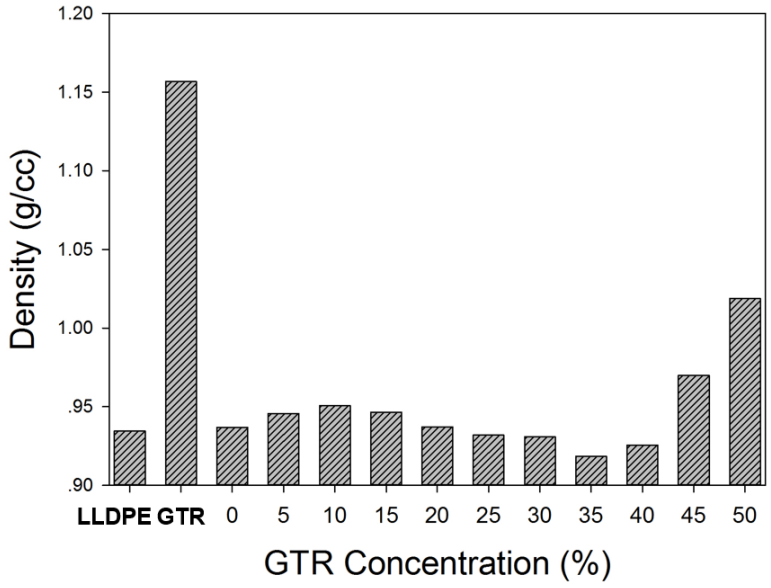

Figure 15. Density of the different materials used and samples produced.

Finally, hardness (shore A and shore D) data are presented in Figure 16. It is observed that hardness decreases with increasing GTR content. In this case, the Shore A decreased from 98 to 68 (30 points difference), while the Shore D decreased from 65 to 37 (28 points difference). This was expected due to the elastic nature of the rubber.

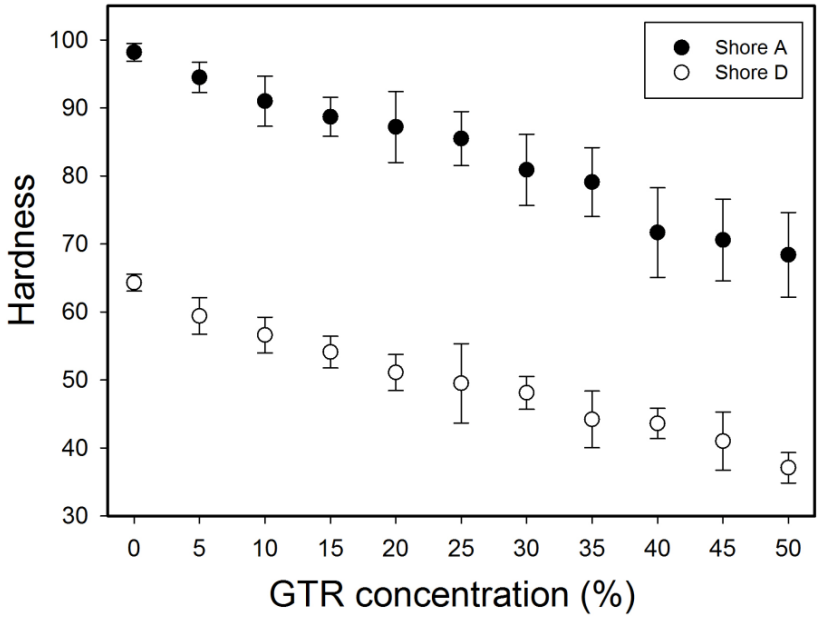

Figure 16. Hardness (Shore A and Shore D) as a function of GTR concentration.

2.6.4 Differential Scanning Calorimetry

The DSC thermographs of LLDPE, GTR, and the compounds are shown in Figure 17. The peak melting temperature and crystallization peak temperature for LLDPE are 126.9°C and 113°C, respectively. With increasing GTR content, there is no significant change towards the melting temperature and crystallization temperature.

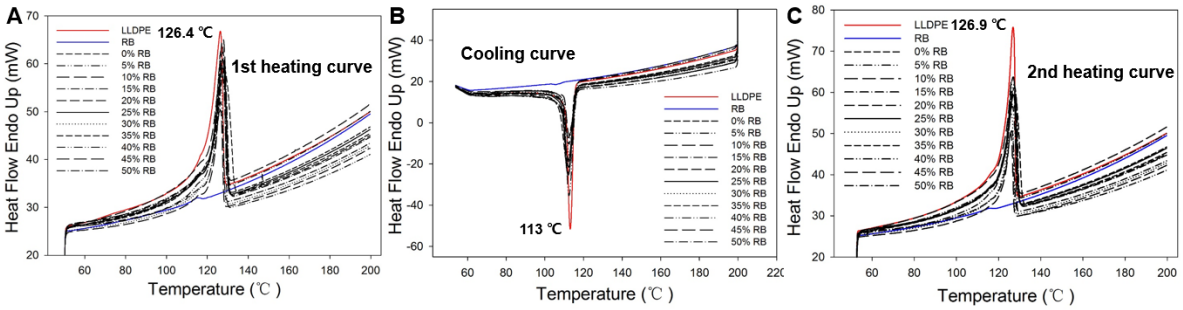

Figure 17. DSC traces of LLDPE, GTR and rotomolded parts with different GTR concentrations.

2.6.5 Thermogravimetric Analysis

The weight loss of a polymer as a function of time or temperature is commonly determined by TGA [131,132]. Figure 18 reports the TGA and DTG curves of LLDPE, GTR and their blends in air. Figure 18A reveals that the weight loss of neat LLDPE begins around 250°C, and then a gradual weight loss occurs up to complete degradation around 500°C. On the other hand, the weight loss of neat GTR begins around 220°C, and degradation is completed around 570°C. One important observation is that GTR addition to LLDPE shifts the thermal degradation of the compounds to higher temperature. Therefore, the compounds have higher thermal stability due to GTR. The DTG curves of Figure 18B illustrates that neat LLDPE has a sharp peak with a maximum at 441°C, while neat GTR presents several wide peaks between 358 and 534°C.

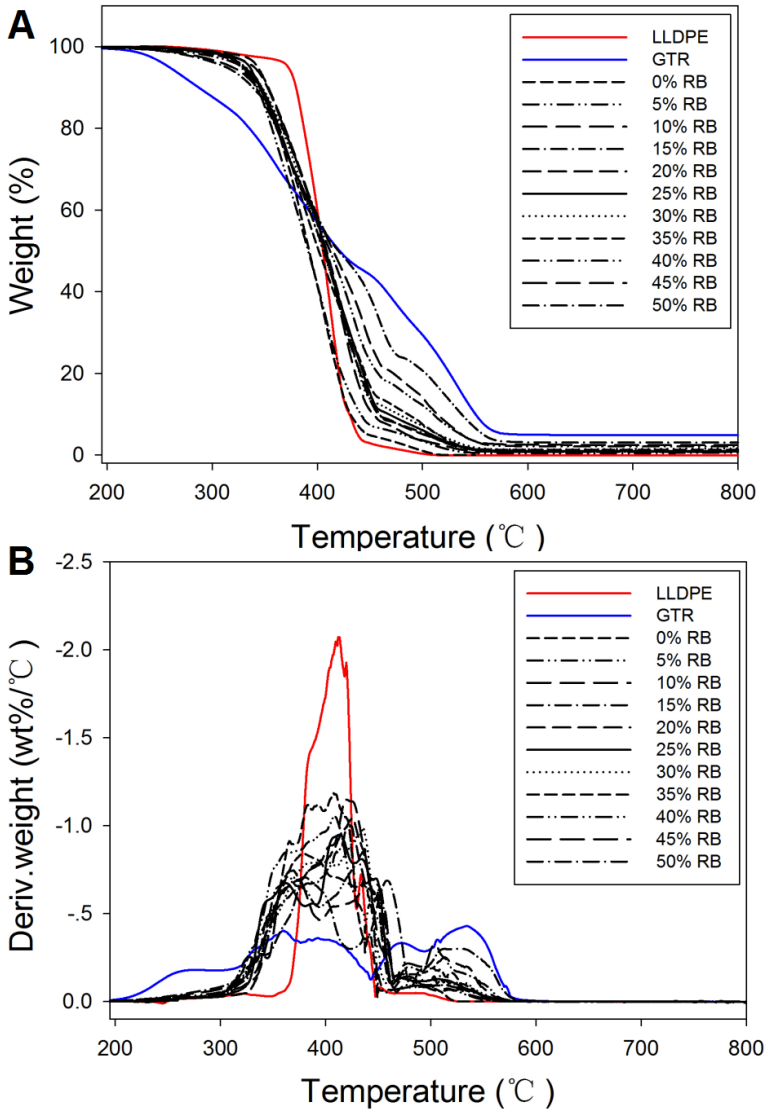

Figure 18. TGA (A) and DTG (B) curves of LLDPE, GTR and rotomolded parts with different GTR content in air.

Figure 19 presents the TGA and derivative of thermogravimetry (DTG) curves of neat LLDPE, neat GTR and their composites under nitrogen. The TGA curve of neat GTR shows 35% of minerals (such as carbon black and vulcanization formulation). These minerals increase with GTR content as shown in Figure 19A. The DTG curve in nitrogen also indicates that LLDPE still has a sharp peak with a maximum at 445°C, while GTR degrades incompletely with a single peak having a maximum at 358°C.

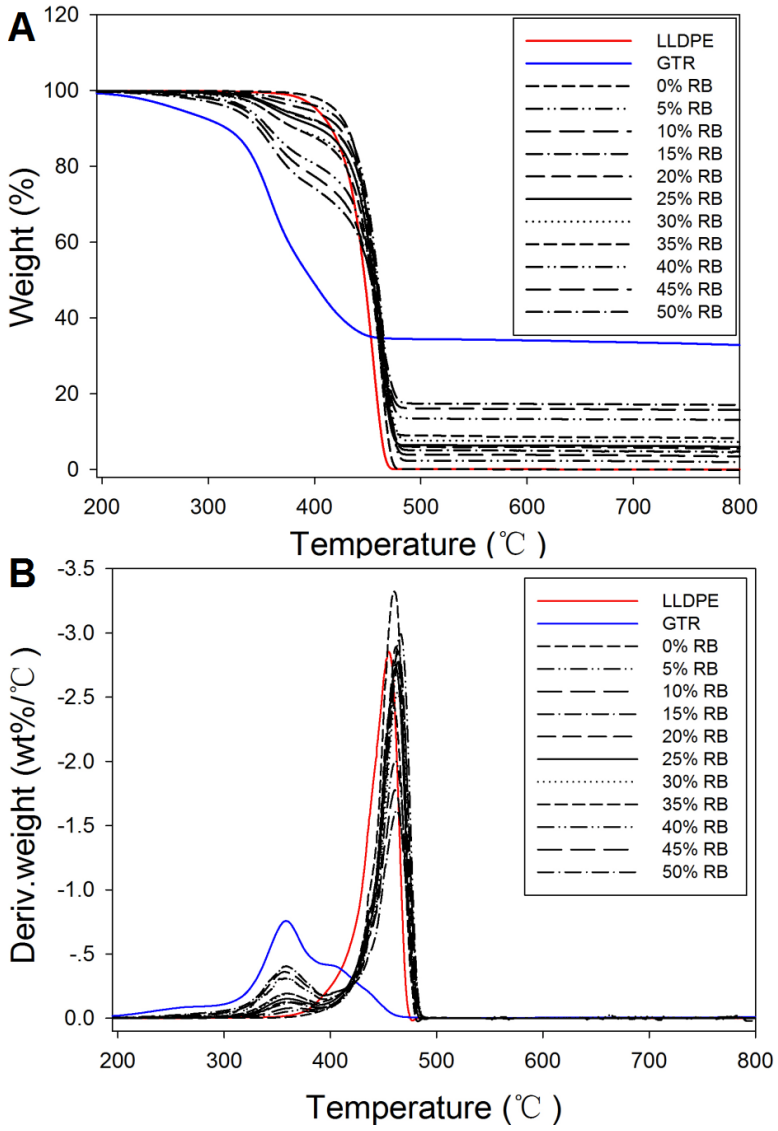

Figure 19. TGA (A) and DTG (B) curves of LLDPE, GTR and rotomolded parts with different GTR content in N_2.

2.6.6 Tensile Properties

Tensile moduli are presented in Figure 20. As expected, the value decreases with increasing GTR content. Similarly, as shown in Figure 21, tensile strength has a similar tendency. Finally, the strain at break also decreases with GTR content in Figure 22. All these findings are consistent with other studies [133,134]. But in all case, the elongation at break is higher than 100% indicating the good elasticity of the materials produced.

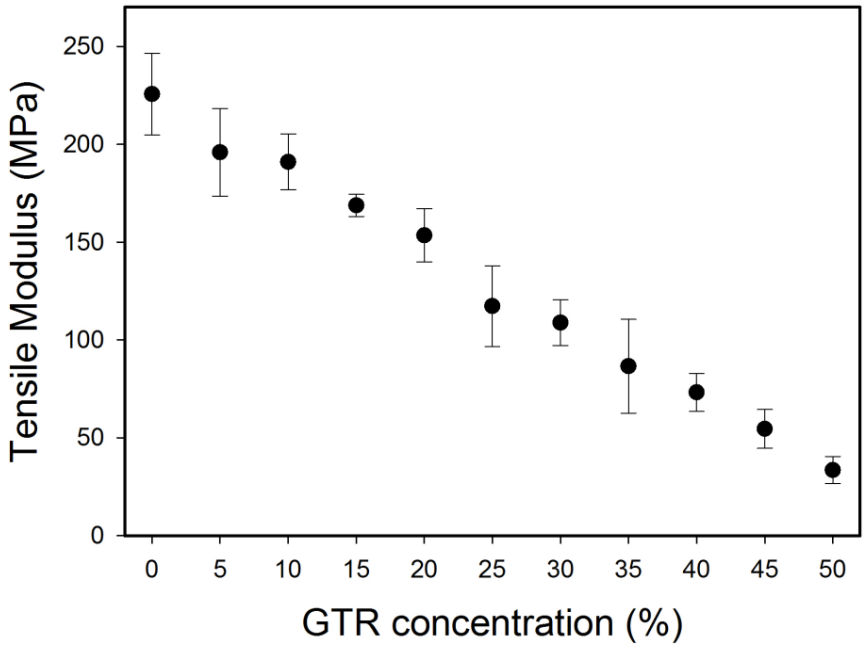

Figure 20. Tensile modulus as a function of GTR concentration.

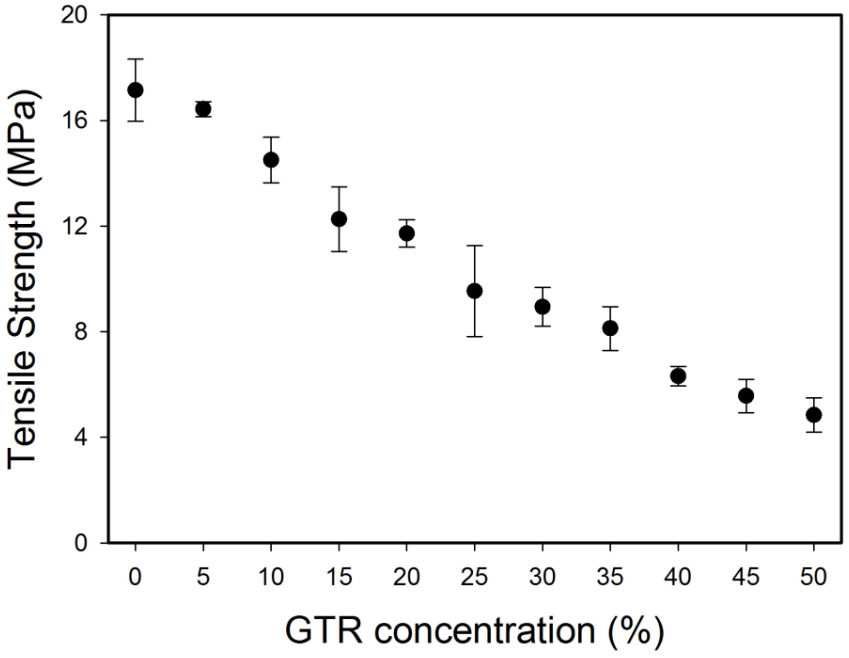

Figure 21. Tensile strength as a function of GTR concentration.

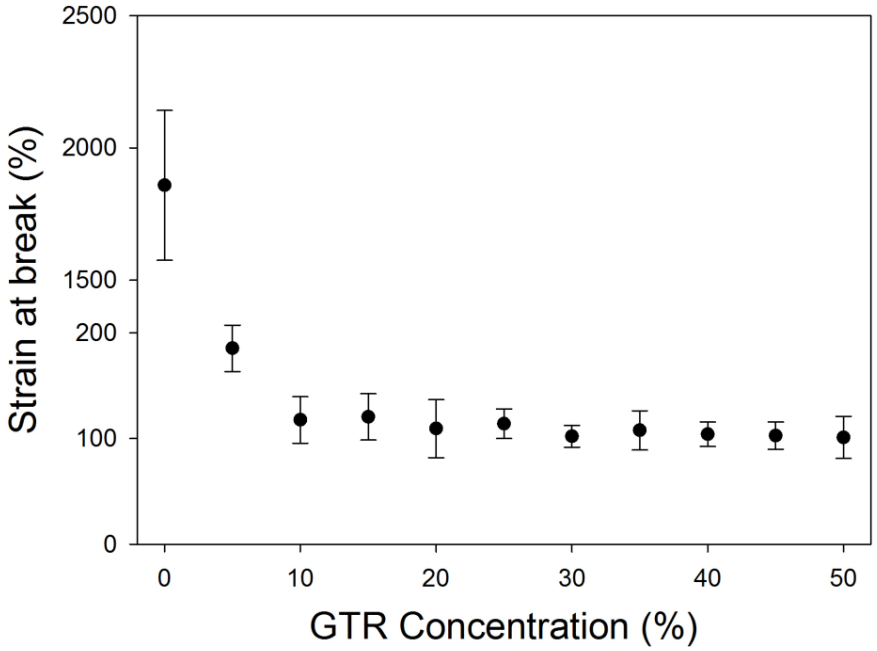

Figure 22. Strain at break as a function of GTR concentration.

2.6.7 Flexural Properties

Figure 23 presents the flexural modulus of the compounds. A similar trend as for the tensile modulus is observed.

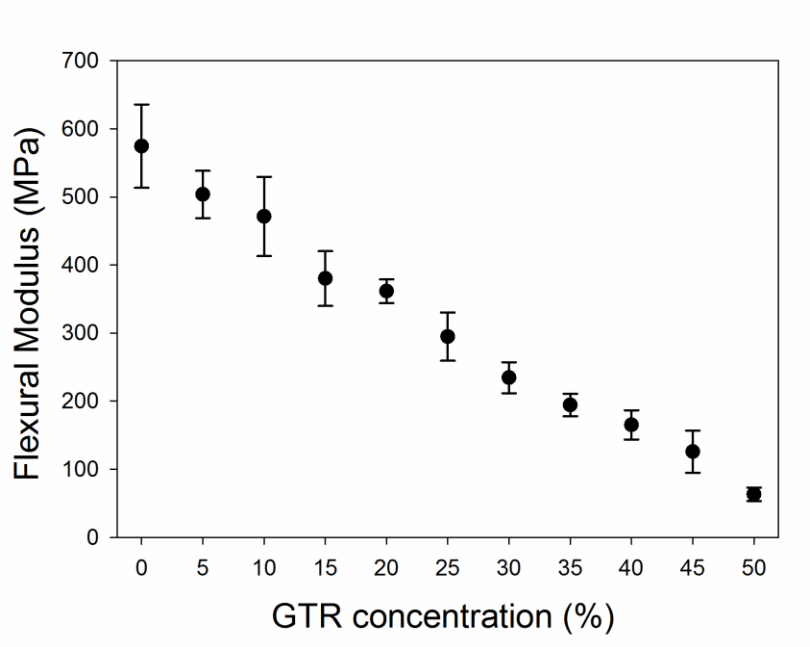

Figure 23. Flexural modulus as a function of GTR concentration.

2.6.8 Impact Strength

Impact strength results are shown in Figure 24. Compared with neat LLDPE, impact strength of GTR/LLDPE compound firstly decreases until GTR content at 10 wt.% (168.3 J/m to 156.3 J/m), and increases up to 226.5 J/m at 30 wt.% of GTR, and then decreases gradually to 131.2 J/m at 50 wt.% of GTR. Thus, the compound can have up to 35% higher impact strength compared to neat LLDPE. The primary decrease in impact strength may result from microvoids inside the parts caused by the poor compatibility between GTR and LLDPE. However, when the GTR concentration increases to some extent, the crosslinked structure of GTR makes the parts more deformable and able to absorb more energy before crack initiation [135]. Finally, as the GTR concentration further increases, GTR agglomeration occurs, leading to a gradual decrease in the impact strength of the GTR/LLDPE compound.

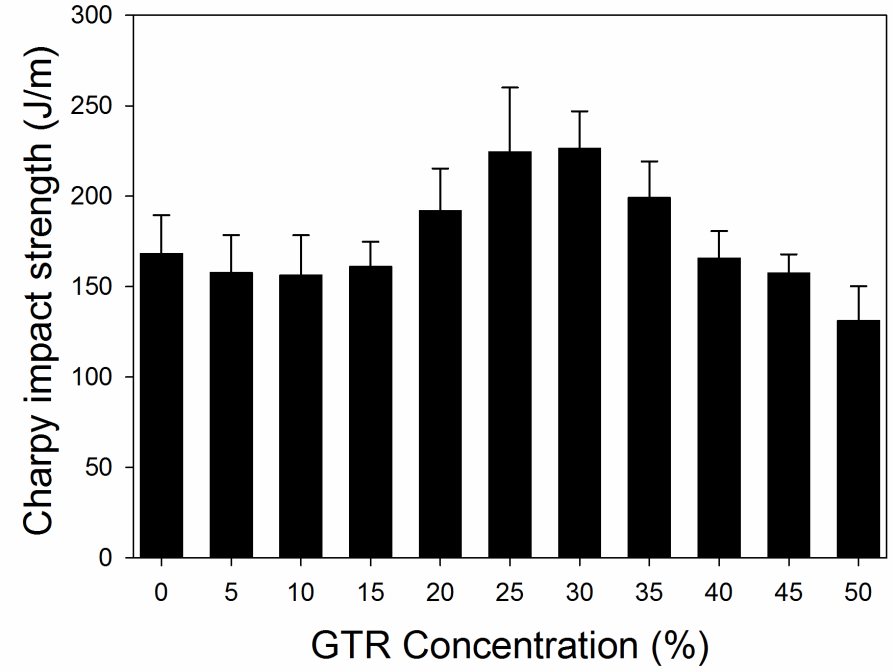

Figure 24. Impact strength as a function of GTR concentration.

2.7 Conclusions

In this work, ground tire rubber (GTR)/linear low density polyethylene (LLDPE) compounds were produced by dry-blending followed by rotomolding. From the samples produced (up to 50 wt.%), a

complete morphological and mechanical (tension, flexion and impact) characterization was done, including density and hardness.

The results showed that a homogeneous distribution of the rubber phase in LLDPE can be achieved at low GTR content (0-10 wt.%). However, with further GTR addition, a number of bubbles and defects was observed. In general, compared with neat LLDPE, the compounds can have up to 35% higher impact strength and still above 100% elongation at break even if tensile strength and modulus, as well as flexural modulus decreased with increasing GTR content.

2.8 Acknowledgements

The authors acknowledge the financial support of the National Science and Engineering Research Council of Canada (NSERC) and the Chinese Scholarship Council (CSC).

Chapter 3

Rotomolding of foamed and unfoamed GTR-LLDPE blends: Mechanical, morphological and physical properties

Dou Y, Rodrigue D. Rotomolding of foamed and unfoamed GTR-LLDPE blends: mechanical, morphological and physical properties. Cellular Polymers, 2018, 37(2): 55-68.

3.1 Résumé

Dans ce travail, une méthode simple est présentée pour produire des composites et des mousses en caoutchouc de pneu broyé (GTR) - polyéthylène linéaire de basse densité (LLDPE) par rotomoulage. En particulier, différentes concentrations de GTR (0 à 50% en poids) ont été mélangées à sec avec différentes teneurs en agent gonflant chimique (CBA) (0 à 1% en poids). À partir des échantillons produits, un ensemble complet de caractérisation a été réalisé en termes de propriétés mécaniques (traction, flexion et impact), de densité et de propriétés morphologiques. Les résultats ont montré que l'augmentation de la teneur en GTR ou en CBA non seulement diminuait les modules de traction et de flexion, mais diminuait la résistance ultime et la déformation à la rupture. Comme prévu, l'augmentation de l'agent gonflant a diminué la densité. En ce qui concerne la résistance aux chocs, la valeur de tous les échantillons a diminué avec l'ajout de GTR ou de CBA à l'exception de 0,2% en poids de CBA, qui est resté similaire à la matrice.

3.2 Abstract

In this work, a simple method is presented to produce ground tire rubber (GTR) - linear low density polyethylene (LLDPE) compounds and foams via rotational molding. In particular, different GTR concentrations (0 to 50 wt.%) were dry-blended with different chemical blowing agent (CBA) content (0 to 1 wt.%). From the samples produced, a complete set of characterization was performed in terms of mechanical properties (tensile, flexural and impact), density and morphological properties. The results showed that increasing GTR content or CBA content not only decreased both tensile and flexural moduli, but decreased the ultimate strength and strain at break. As expected, increasing blowing agent decreased density. With respect to impact strength, the value of all samples decreased with the addition of GTR or CBA except for 0.2 wt.% CBA of GTR-LLDPE composite foams, which nearly remain at the same level.

3.3 Introduction

Rotational molding, also known as rotomolding or rotocasting, is considered as a low shear processing technology to produce one-piece hollow seamless products such as tanks, automotive parts, toys and several other items [107]. Unlike most plastic processing methods, such as injection and blow molding, there is no pressure involved, meaning that the molds can be very thin and generally inexpensive. Furthermore, rotomolding can more easily handle complex shapes with a very wide range of part sizes and variable thickness, as well as easy color changes [125,126]. These features make rotomolding to be one of the fastest growing process of the plastic industry over the last few years [120,136]. However, some disadvantages of this process are high operating temperatures and long cycle times [137-139]. Additionally, a very limited number of polymers are industrially rotomolded since the materials need specific requirements, limiting their use. This is generally related to particle size, melting point, viscosity, and thermal degradation [127]. This is why, still today, most rotomolded parts are based on different polyethylene grades because of their broad processing window, excellent chemical/thermal resistance and low cost. Today, linear low density polyethylene (LLDPE) is one of the most commonly used grade of polyethylene for rotomolding [128-130].

Nevertheless, LLDPE has limited mechanical properties and ways to improve mechanical and thermal properties through structural modifications are being investigated. Adding reinforcement to produce a composite is one method to improve the mechanical properties of a rotomolded part [107,140,141]. Another well-known modification is to add a blowing agent to foam a rotomolded part for lower density and higher insulation [115,142-144].

With the continuous development of products, an important amount of waste is produced around the world when the materials reach their end of life. This is especially the case for rubber tires, and their disposal becomes more and more critical for environmental and economic reasons. Consequently, due to high thermal and chemical stability, as well as availability and low cost, ground tire rubber (GTR), which can be made into different sizes, is now used in a variety of industrial applications to recycle waste tires [145]. More interestingly, one important application of GTR is to introduce into thermoplastic resins and composites to improve their impact strength [124,146,147].

In this work, the main objective is to prepare foamed and unfoamed GTR-LLDPE compounds via rotational molding. In particular, since all the materials are in a powder/particle state (LLDPE, GTR, CBA), a simple dry-blending technique is proposed to reduce processing costs and limit thermo-oxidative degradation related to melt mixing (twin-screw extrusion). This initial physical mixing also

reduces processing time and post-processing cost/degradation (extrusion + pelletizing/pulverizing). After rotomolding optimization, the mechanical, morphological and physical properties of the compounds are investigated.

3.4 Materials and Methods

3.4.1 Materials

The polymer used was linear low density polyethylene grade 8460 from Exxon Mobil (Canada). This polymer has a melt flow index of 5 g/10 min (2.16 kg/190°C) and a density of 0.935 g/cm^3. The recycled rubber was from ground tire rubber and provided by Royal Mat (Canada). This material has a density of 1.206 g/cm^3. The material was sieved to keep only particle size less than 500 μm (similar to the LLDPE powder). For foaming, the chemical blowing agent (CBA) used was Celogen 754A (Chempoint, USA) which has a decomposition temperature range between 165 and 180°C.

3.4.2 Processing

To achieve proper mixing, all the materials were dry-blended in a high speed mixer (LAR-15LMB (Skyfood, USA) at 3320 rpm) with fixed intervals of 1 min mixing time and 1 min cooling time repeated for 4-5 times. For processing, a laboratory-scale rotational molding machine was used. Rotationally molded parts were manufactured with a cubic aluminum mold of 3.6 mm wall thickness and an internal side length of 19 cm. Before loading the material, a demolding agent (Trasys 420, DuPont) was applied to the internal surface of the mold. Furthermore, the vent (diameter = 10 mm) was filled with glass wool to prevent powder losses. After preliminary runs, the optimum processing conditions for GTR-LLDPE compounds (foamed and unfoamed) were: a 1:4 speed ratio, a heating time of 25 minutes with an oven (electrically heated) temperature of 275°C and a cooling time of 30 minutes with forced air (blowing fans). Finally, the mold was opened and the part was demolded. To perform the characterizations, samples were directly cut in the molded parts.

The first series of samples was performed by changing the GTR content (0, 5, 10, 15, 20, 25, 30, 35, 40, 45 and 50 wt.%) to produce GTR-LLDPE compounds. Then, a second series of samples was produced by changing the CBA content (0, 0.1, 0.2, 0.3, 0.4, 0.5, 0.6, 0.7, 0.8, 0.9, 1 wt.%) to prepare LLDPE foams. Finally, the last series of samples was prepared using two different CBA content (0.1 and 0.2 wt.%) for selected GTR contents (10, 15, 20, 25, 30 and 35 wt.%).

3.4.3 Morphological Characterization

The rotomolded samples were cryogenically fractured (liquid nitrogen) and micrographs of the exposed cross-sections were taken using a JEOL JSM-840A scanning electron microscope (SEM) and Olympus SZ6 stereomicroscope coupled with a Spot Insight (Diagnostic Instrument) high resolution (1600×1200 pixels) camera.

Foam morphology was investigated based on two parameters: cell size (D) and cell density (N_f). The average cell size was measured by the ImageJ software (US National Institutes of Health, USA). A minimum of 45 cells was used to compute the statistics and standard deviation. Cell density, which is defined as the number of cell (n) per cubic centimeter of foam, was calculated by [148]:

$$N_f = \left(\frac{n}{A}\right)^{\frac{3}{2}} \quad (2)$$

where A is the area of the micrograph in cm^2.

3.4.4 Density and Hardness Measurements

Density was determined using a gas (nitrogen) pycnometer Ultrapyc 1200e (Quantachrome Instruments, USA). Hardness (Shore A and Shore D) was determined by a PTC Instruments Model 306L and Model 307L (ASTM D2240). The results reported are the average and standard deviation of a minimum of 5 samples.

3.4.5 Mechanical Properties

The tensile properties at room temperature were measured on an Instron model 5565 universal testing machine with a 500 N load cell. Type V samples were cut in the rotomolded parts according to ASTM D638. The crosshead speed was set at 10 mm/min and the values for tensile modulus, tensile strength and elongation at break are based on the average of at least six samples.

Flexural tests (three-point bending) were performed at room temperature using a crosshead speed of 2 mm/min on an Instron universal tester model 5565 with a 50 N load cell according to ASTM D790. The span length was fixed at 60 mm. At least five rectangular samples (60×12.7 mm^2) were used to report the average and standard deviation for the modulus.

Charpy impact strength was determined by a Tinius Olsen (USA) testing machine model Impact 104. At least ten rectangular specimens (60×12.7 mm^2) were prepared according to ASTM D6110. The

samples were notched ("V" shaped notch) by an automatic sample notcher model ASN 120m (Dynisco, USA) at least 24 h before testing.

3.5 Results and Discussion

3.5.1 Morphological Characterization

Figure 25 presents typical cross-sections (morphologies) for GTR/LLDPE compounds, LLDPE foams, and GTR/LLDPE foams. For GTR/LLDPE composites, the number of cells increases with the increasing GTR content. This can be associated to heterogeneous nucleation effects produced by the presence of particle inside the gas-laden polymer melt [149].

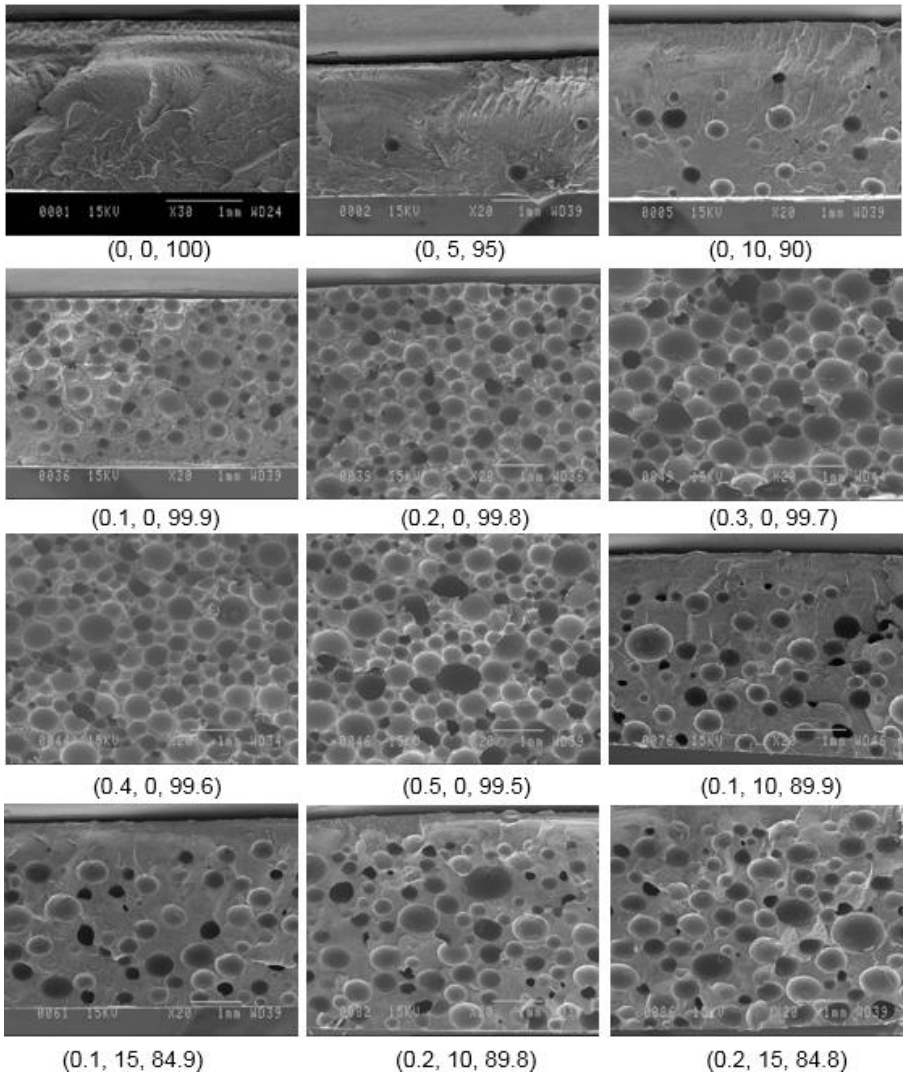

Figure 25. Typical morphologies of the rotomolded parts. The numbers in parenthesis represent (CBA content, GTR content, LLDPE content) in wt.%.

Table 4 presents the results for the average cell size and cell density of the foams. Based on the maximum cell density, 0.2 wt.% CBA seems to be the optimum for the neat foams (LLDPE as the matrix), while for LLDPE-GTR compounds, the optimum depends on the GTR content. Again, this is related to GTR particles acting as nucleating agents [150] as well as limiting gas diffusion [151]. The combined effect can lead to possible gas pockets and cell coalescence in the polymer melt, thus increasing cell size and decreasing cell density. The results show that the optimum foam content is around 15 wt.% GTR at 0.1 wt.% CBA, while it decreases to 10 wt.% GTR at 0.2 wt.% CBA.

Table 4. Average cell size and cell density of LLDPE foams and GTR/LLDPE foams.

Sample	Cell size (μm)	Cell density ($10^3/cm^3$)
(0.1, 0, 99.9)	154±55	21.9
(0.2, 0, 99.8)	258±87	30.2
(0.3, 0, 99.7)	277±98	21.3
(0.4, 0, 99.6)	288±114	17.8
(0.5, 0, 99.5)	273±124	16.9
(0.6, 0, 99.4)	310±136	11.8
(0.7, 0, 99.3)	305±145	11.3
(0.8, 0, 99.2)	280±115	11.1
(0.9, 0, 99.1)	363±167	10.5
(1.0, 0, 99.0)	347±154	10.8
(0.1, 10, 89.9)	369±130	3.69
(0.1, 15, 84.9)	284±89	5.97
(0.1, 20, 79.9)	333±139	3.74
(0.1, 25, 74.9)	362±168	2.41
(0.1, 30, 69.9)	346±157	2.26
(0.1, 35, 64.9)	244±161	4.18
(0.2, 10, 89.8)	296±120	6.49
(0.2, 15, 84.8)	330±131	5.76
(0.2, 20, 79.8)	416±186	4.76
(0.2, 25, 74.8)	371±147	4.28
(0.2, 30, 69.8)	236±121	6.56
(0.2, 35, 64.8)	341±160	6.67

3.5.2 Density and Hardness

The density of all the rotomolded articles is reported in Figure 26. Based on Figure 25 and Figure 26A, because of bubble formation, the density of the GTR/LLDPE compounds firstly slightly decreases with increasing GTR content up to 30 wt.% due to voids and interfacial gaps created between both phase. However, the density finally increases with increasing GTR content up to 50 wt.% GTR density (1.206 g/cm^3) is much higher than LLDPE (0.935 g/cm^3) and gradually dominates the overall compounds. But in Figure 25B, the behavior for the neat foams is more typical. With increasing CBA content, more gas is generated and trapped inside the molten LLDPE matrix and the density gradually decreases from 0.937 to 0.473 g/cm^3 (49.5%) around 0.8 wt.% CBA. However, because of gas loss and cell collapse above this value the foam density increases slightly from 0.473 to 0.537 g/cm^3. For the GTR/LLDPE foams, the density does not change much as it represents a balance between adding GTR (higher density) and CBA (density reduction associated to foaming and nucleating effect). Nevertheless, for the range of conditions studied, the density slightly increase with GTR due to its higher density and this interaction seems to be more important at higher CBA content.

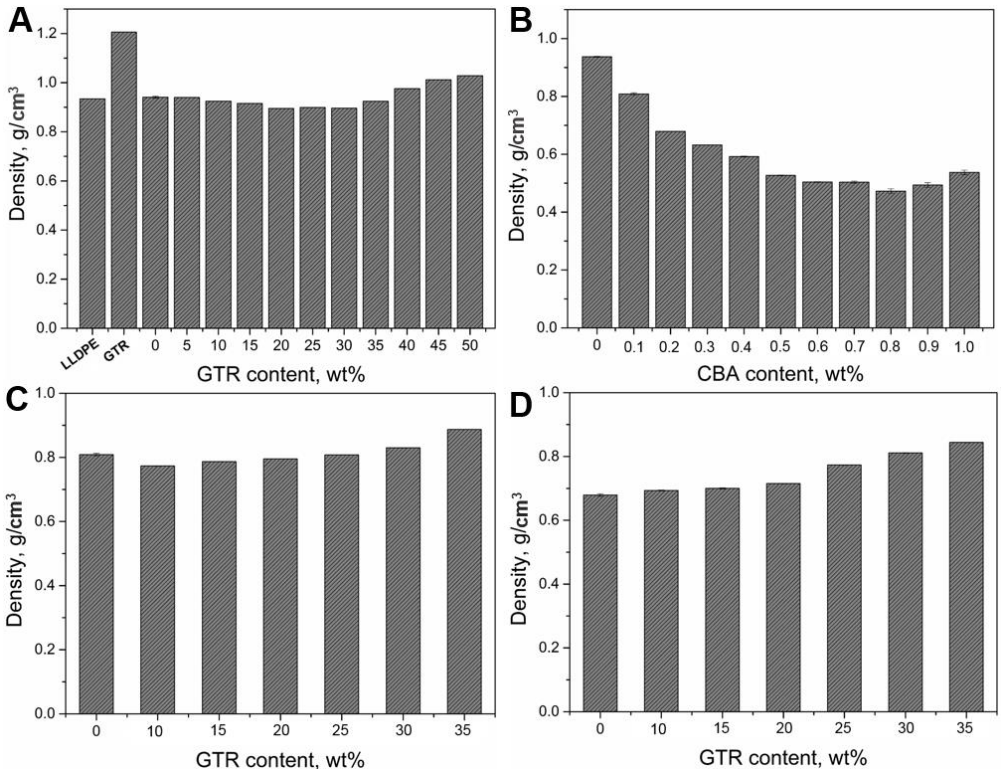

Figure 26. Density of: A) GTR/LLDPE compounds, B) LLDPE foams, C) GTR/LLDPE foams with 0.1 wt.% CBA and D) GTR/LLDPE foams with 0.2 wt.% CBA.

Finally, hardness (Shore A and Shore D) data are presented in Figure 27. For GTR/LLDPE composites and composite foams, there is nearly constant value for Shore A because it is close to the maximum of the scale. But for the Shore D scale, a continuous decrease is observed with GTR content: 48% for GTR/LLDPE compounds, 29% for GTR/LLDPE foams with 0.1 wt.% CBA and 32% for GTR/LLDPE foams with 0.2 wt.% CBA. These trends are expected due to the elastic nature of GTR and soft property of gas cell compared to the neat matrix (LLDPE).

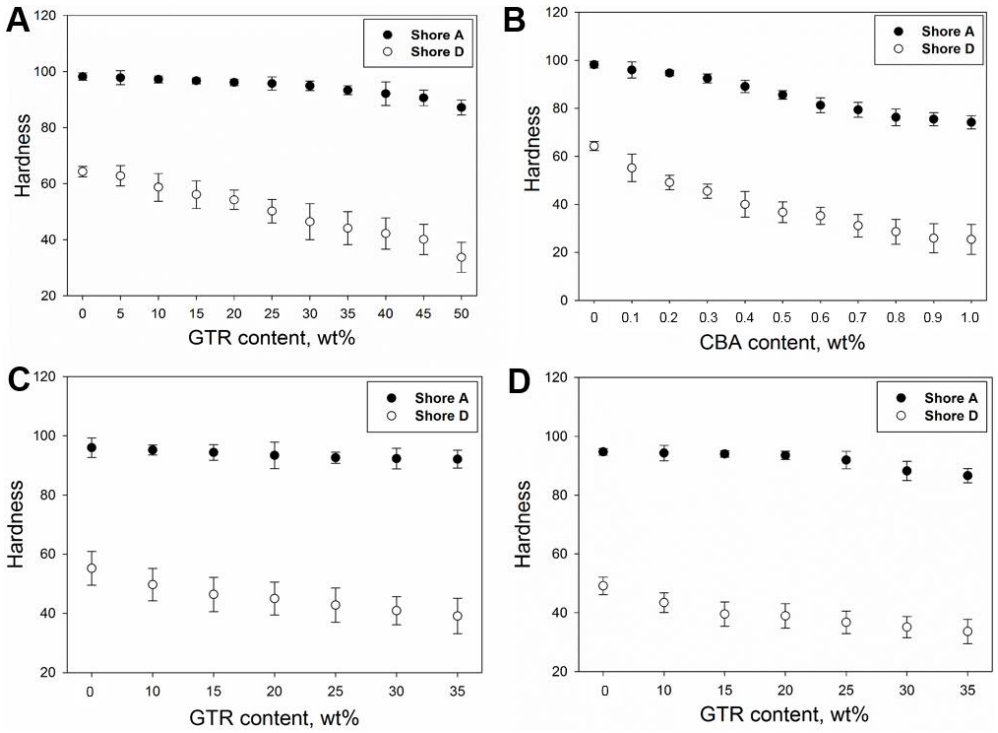

Figure 27. Hardness (Shore A and Shore D) of: A) GTR/LLDPE compounds, B) LLDPE foams, C) GTR/LLDPE foams with 0.1 wt.% CBA and D) GTR/LLDPE foams with 0.2 wt.% CBA.

3.5.3 Flexural Properties

Figure 28 presents the flexural modulus results. It can be seen that the values decrease substantially with both GTR and CBA contents. For example, down by 92% (from 574.4 to 43.6 MPa) for GTR/LLDPE compounds, 93% (from 574.4 to 38.7 MPa) for LLDPE foams, 66% (from 363.6 to 123.6 MPa) for GTR/LLDPE foams with 0.1 wt.% CBA, and 51% (from 221.0 to 108.9 MPa) for GTR/LLDPE foams with 0.2 wt.% CBA. For the GTR/LLDPE compounds, bad interfacial adhesion and the presence of voids in the samples can lead to low flexural modulus. For the LLDPE foams, lower modulus is expected because less material is available to sustain the stresses when density

decreases [116,152,153]. For the GTR/LLDPE foams the addition of CBA and GTR both leads to lower modulus and their combined effect results in even lower flexural modulus.

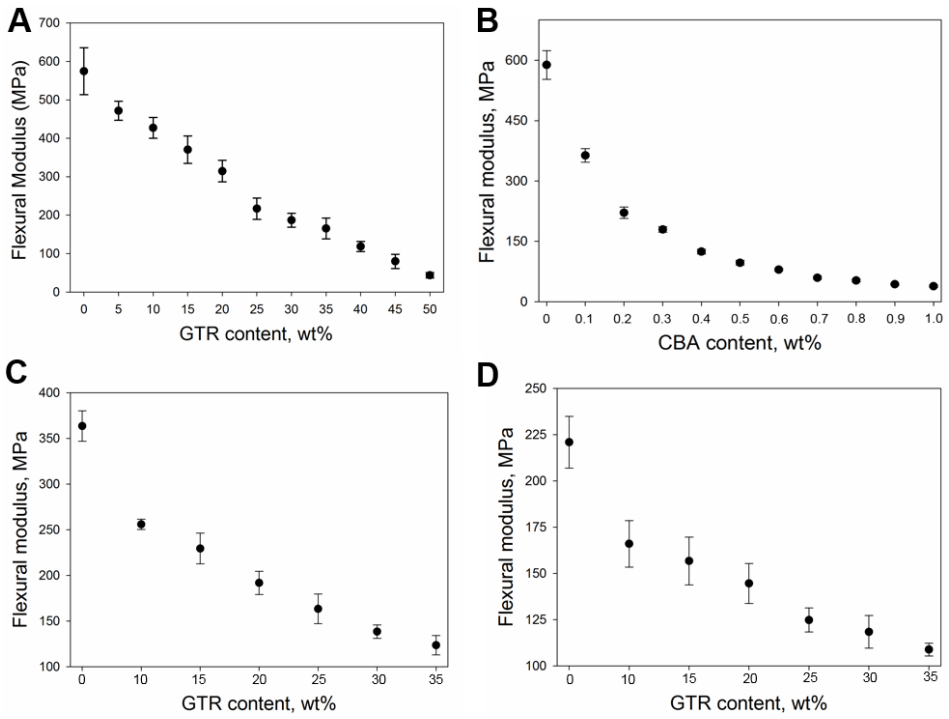

Figure 28. Flexural modulus of: A) GTR/LLDPE compounds, B) LLDPE foams, C) GTR/LLDPE foams with 0.1 wt.% CBA and D) GTR/LLDPE foams with 0.2 wt.% CBA.

3.5.4 Tensile Properties

Figures 29-31 present the tensile properties of the samples produced. As shown in Figure 29, the tensile moduli have the same trend as the flexural moduli (Figure 28). For example, the tensile modulus of GTR/LLDPE compounds decreased down to 92% (from 225.6 to 18.2 MPa) which is similar to the 92% in flexion. As for tensile strength, Figure 30 reveals that the values decrease with increasing GTR or CBA content as a result of poor adhesion between GTR and LLDPE. For the LLDPE foams, the decrease is 85% (from 18.1 to 2.65 MPa) as less material is available to sustain the applied stress when density decreases. Finally, Figure 31 presents the results for the elongation at break. Again, the values are decreasing with increasing GTR and CBA content. In the case of foamed and unfoamed GTR/LLDPE, the values are all below 100% when the GTR content is above 10 wt.% All these findings are consistent with other studies reporting decreasing modulus and strength with rubber and foaming [133]. These results also indicates that more work needs to be done to improve the rubber-matrix adhesion and this work is currently under way.

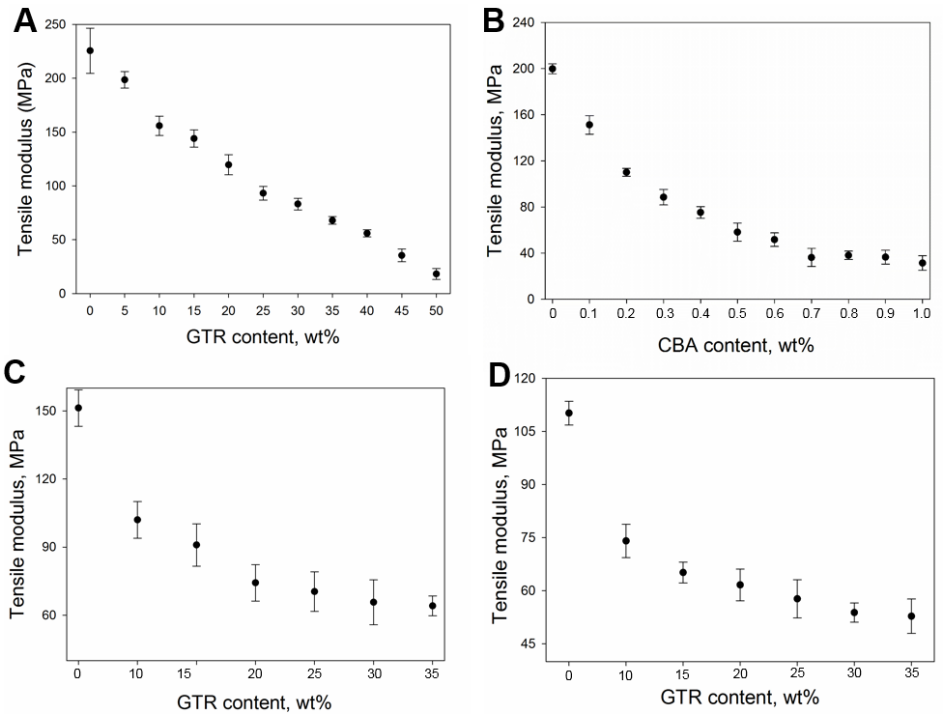

Figure 29. Tensile modulus of: A) GTR/LLDPE compounds, B) LLDPE foams, C) GTR/LLDPE foams with 0.1 wt.% CBA and D) and GTR/LLDPE foams with 0.2 wt.% CBA.

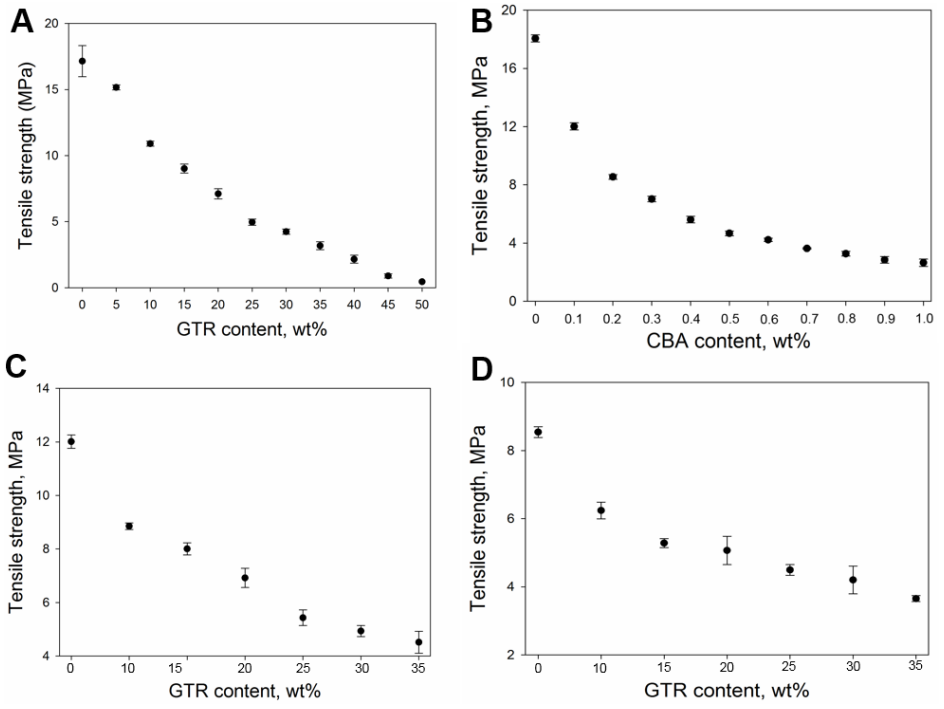

Figure 30. Tensile strength of: A) GTR/LLDPE compounds, B) LLDPE foams, C) GTR/LLDPE foams with 0.1 wt.% CBA and D) GTR/LLDPE foams with 0.2 wt.% CBA.

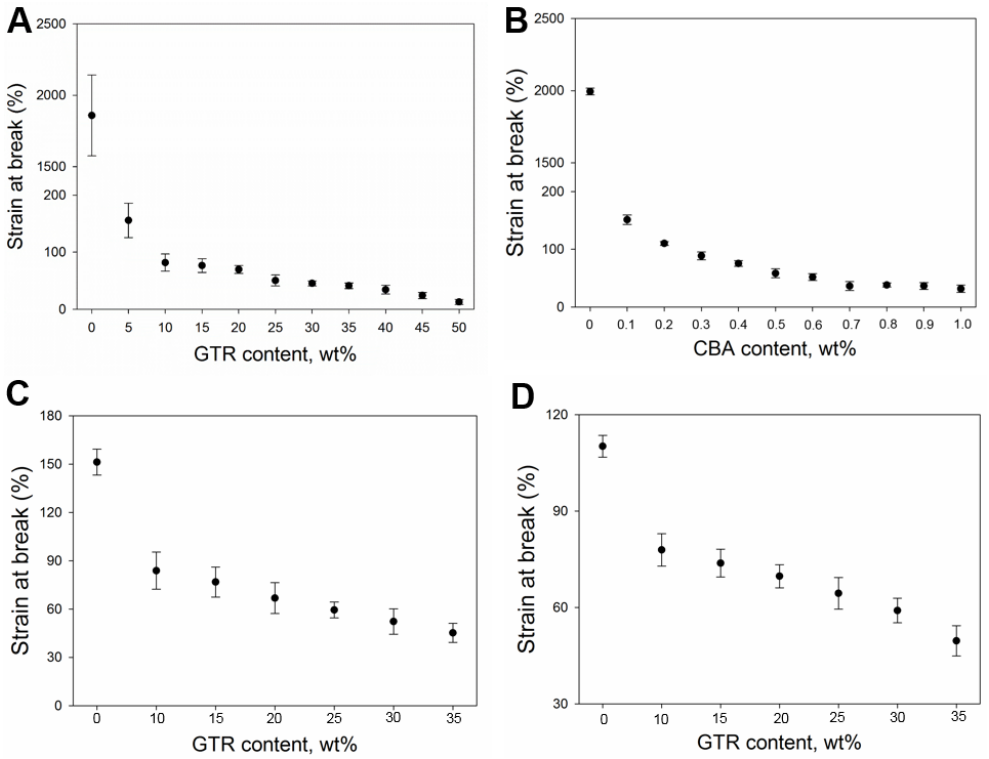

Figure 31. Tensile elongation at break of: A) GTR/LLDPE compounds, B) LLDPE foams, C) GTR/LLDPE foams with 0.1 wt.% CBA and D) GTR/LLDPE foams with 0.2 wt.% CBA.

3.5.5 Impact Strength

Impact strength results are shown in Figure 32. Compared to neat LLDPE, impact strength of GTR/LLDPE composites and LLDPE foams decreases with the increasing GTR or CBA content. In this case, the decrease is 58% (from 219 to 91.7 J/m) for GTR/LLDPE compounds and 78% (from 219 to 48.0 J/m) for LLDPE foams. The former observation may result from the powder nature (particle size and shape) of the original material before melting (creating more gas cavities), the low pressure inside the mold resulting in voids inside the parts, and poor adhesion at the interface between GTR and LLDPE (no coupling agent or GTR surface treatment performed). Furthermore, the significant decreased impact strength for LLDPE foams may be caused by bubbles, which are acting as stress concentration points and propagate the cracks since they are empty spaces within the structure.

As for GTR/LLDPE composite foams with 0.1 wt.% CBA (Figure 32C), the impact strength firstly decreases until GTR content at 25 wt.% (from 160.7 J/m to 121.6 J/m), and then increases slightly (up to 135.9 J/m). As the reason for decreased impact strength in LLDPE foams, the addition of GTR

was not enough to overcome the drawback of foaming technology. However, when GTR content increases (30 to 35 wt.%), there is possible the elastic effect of GTR dominates in the composite foams. Furthermore, there is no significant change for the impact when 0.2 wt.% CBA is used (Figure 32D). This behavior represents a balance between the effect of voids and rubber particles by adding GTR and both effects offset each other.

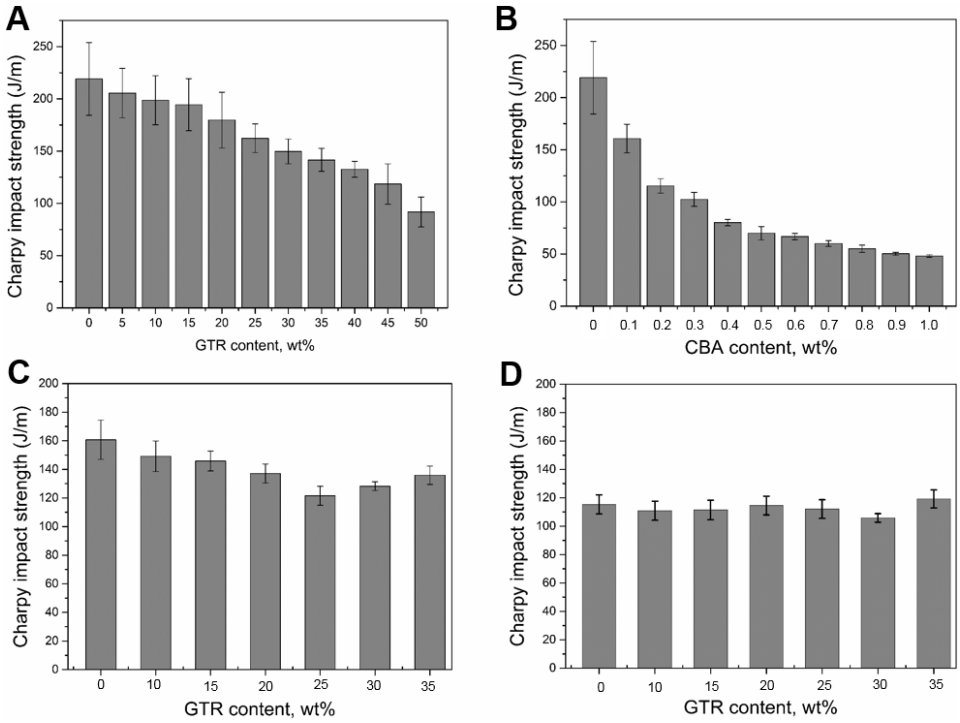

Figure 32. Impact strength of: A) GTR/LLDPE compounds, B) LLDPE foams, C) GTR/LLDPE foams with 0.1 wt.% CBA (C) and D) GTR/LLDPE foams with 0.2 wt.% CBA.

3.6 Conclusion

In the current study, GTR-LLDPE composites, LLDPE foams and GTR-LLDPE composite foams were successfully produced via rotomolding since all the raw materials were in a powder form. The influence of GTR content and CBA content was evaluated. From the samples produced, the characterization including density, morphological and mechanical properties was performed. According to the results obtained, several conclusions can be made:

Firstly, the optimum blowing agent content for the processing conditions used is around 0.2 wt.% as this value gave relative lower cell size, maximum cell density and best foam morphology.

Secondly, due to bad adhesion at the interface between GTR and LLDPE or the decreased density, increasing GTR content or CBA content not only decreased both tensile and flexural moduli, but decreased ultimate strength and strain at break.

Thirdly, as for impact strength, the value of all rotomolded parts decreased with the addition of GTR or CBA apart from GTR-LLDPE composite foams with 0.2 wt.% CBA, which didn't change a lot from 0 wt.% to 35 wt.% GTR concentration.

Finally, although rotomolded parts were produced successfully, mechanical properties were not ideal. In the future, more work still needs to be done in order to improve the adhesion at the GTR-LLDPE interface and then enhance the mechanical properties.

3.7 Acknowledgements

The authors acknowledge the financial support of the National Science and Engineering Research Council of Canada (NSERC) and the Chinese Scholarship Council (CSC).

Chapter 4

Rotational molding of hybrid composites based on linear low density polyethylene/ground tire rubber/maple wood fibers

Dou Y, Rodrigue D. Rotational molding of hybrid composites based on linear low density polyethylene/ground tire rubber/maple wood fibers. 76th Annual Technical Conference and Exhibition of the Society of Plastics Engineers, SPE ANTEC, Orlando 2018.

4.1 Résumé

Dans ce travail, du caoutchouc de pneu broyé (GTR) et des fibres de bois d'érable (MWF) ont été mélangés à sec avec du polyéthylène linéaire de basse densité (LLDPE) pour produire des composites hybrides par rotomoulage. En particulier, l'effet d'un agent de couplage (polyéthylène maléaté, MAPE) a été étudié pour modifier les propriétés mécaniques des composites hybrides. Chaque composé a été caractérisé en termes de morphologie, de densité et de propriétés mécaniques (traction, flexion et impact). Les résultats ont montré que l'ajout de GTR conduisait à une faible amélioration de la résistance aux chocs dans les composites de fibres de bois (WFC), tandis que l'ajout de MAPE améliorait l'adhérence interfaciale, entraînant de meilleures propriétés des composites hybrides.

4.2 Abstract

In this work, ground tire rubber (GTR) and maple wood fibers (MWF) were dry-blended with linear low density polyethylene (LLDPE) to produce hybrid composites by rotational molding. In particular, the effect of a coupling agent (maleated polyethylene, MAPE) was studied to modify the mechanical properties of hybrid composites. Each compound was characterized in terms of morphology, density and mechanical properties (tensile, flexural and impact). The results showed that the addition of GTR led to limited improvement of impact strength in wood fibers composites (WFC), while the addition of MAPE improved the interfacial adhesion further resulting in better hybrid composites properties.

4.3 Introduction

Natural fibers are still attracting much attention over synthetic fibers because of low cost, lightweight, environmental friendliness, availability, etc. [154-157]. Thus, above advantages give rise to a continual development of polymer composites reinforced with natural fibers in automotive, building, and construction industries [158]. However, nature fibers possess some disadvantages such as low thermal stability, low moisture resistance and poor interaction with hydrophobic polymers (thermosets and thermoplastics) [159,160]. To overcome these issues, coupling agents are generally used for interfacial adhesion improvement [161]. Several reports found that, for polyethylene/natural fiber composites, the maleic anhydride-grafted polymers had been proved effective [162]. Therefore, the mechanical properties of nature fiber composites substantially enhanced after maleated polyolefin was added [163]. Unfortunately, a major disadvantage of natural fiber composites is the substantial loss in impact strength [164]. Nevertheless, incorporating a rubber phase can be an effective strategy to recover the impact strength [165]. For example, in a work by Ruksakulpiwat et al., it was reported that introducing more than 20 wt.% of rubber powder (natural and EPDM) to vetiver grass-polypropylene composites caused better impact resistance [166].

Nowadays, the disposal of worn tires is becoming a great challenge because of environmental problems. Consequently, due to high thermal and chemical stability, as well as availability and low cost, ground tire rubber (GTR), which can be grinded into different sizes, is now used in a variety of industrial applications to recycle scrap tires [145]. Some works have already focused on blending GTR with thermoplastics as fillers [167]

In this work, hybrid composites based on linear low density polyethylene/ground tire rubber/maple wood fibers is produced by rotational molding, which is a polymer processing technology used to produce hollow seamless products such as tanks, automotive parts, toys and several other items [107]. Unlike most other plastic processes, there is no pressure involved in rotational molding, which means that the molds can be very thin and generally inexpensive. Additionally, rotomolding can more easily handle complex shapes with a very wide range of part sizes and variable thicknesses [120,126].

To the best of our knowledge, this is the first report in which LLDPE/GTR/MWF is manufactured by rotational molding. The purpose of adding GTR is to control the impact strength of maple wood fiber reinforced composites. To improve the mechanical properties of the hybrid composites, a coupling agent (MAPE) is employed. Finally, all the rotomolded parts are characterized.

4.4 Materials

The matrix was linear low density polyethylene grade 8460 from Exxon Mobil (Canada). This polymer has a melt flow index of 5 g/10 min (2.16 kg/190°C) and a density of 0.93 g/cm^3. The ground tire rubber (GRT) was supplied by Phoenix Innovation Technologies (Montreal, Canada). This material has a density of 1.16 g/cm^3. The maple wood fibers (PWI Industries, Canada) were sieved to retain particles of 250-355 μm. For the surface treatment, xylene (laboratory purity grade) from Fisher Chemicals (USA) was used as the solvent, while the coupling agent was maleated polyethylene (MAPE) (Epolene C26, Westlake Chemicals, USA). This grade has an average molecular mass of 65 kg/mol, a melt flow index (MFI) of 8.0 g/10 min (190°C/2.16 kg), an acid number of 8.0 mg KOH/g, a density of 915 kg/m^3, and a melting point of 121°C.

4.5 Experimental

4.5.1 Maple Surface Treatment with MAPE

The maple wood fiber surface treatment was performed according to the report of Hanana and Rodrigue [109]. Firstly, 1% MAPE was added in xylene at 80-90°C under vigorous stirring until it just dissolved. Next, the wood fibers were added and left stirring in the solution for 30 min. The ratio of fibers: xylene was 1:10 (w/v). Finally, the treated fibers were filtrated and then dried overnight at 60°C in an oven.

4.5.2 Material Mixing

For each composition, a total of 650 g of material was used based on LLDPE with different contents of GTR and untreated maple wood fibers (UMWF) or treated maple wood fibers (TMWF). Mixing (dry-blending) was carried out in a high speed mixer (LAR-15LMB (Skyfood, USA) at 3320 rpm) for a total of 4-5 min.

4.5.3 Rotational Molding: Process and Equipment

A laboratory-scale rotational molding machine was used for processing. Rotationally molded parts were manufactured with an aluminum cubic mold of 3.6 mm wall thickness and a side length of 19 cm. Before loading the material, a demolding agent (Trasys 420, DuPont) was applied to the internal surface of the mold. The powder blends were then loaded into the mold to produce parts with an approximate wall thickness of 3 mm. Then, the charged mold was closed and mounted on the rotating arm. Preliminary trials were performed to determine the optimum conditions leading to homogeneous and uniform wall thickness. Finally, an oven at 275°C and a speed ratio of 1:4 with a major axis speed

of 1 rpm was chosen. The heating was fixed at 25 min. Afterwards, the mold was removed from the oven and cooled by forced air for 35 min. Finally, the mold was opened to retrieve the part.

4.5.4 Fourier Transform Infrared Spectroscopy (FTIR)

Infrared spectra were obtained with a Nicolet FTIR spectrometer (model 730, Nicolet Instruments, USA) equipped with a mercury-cadmium-telluride detector. The sample absorbance was measured in the IR region 4000-750 cm^{-1}. Each spectrum was obtained from 128 scans at a resolution of 4 cm^{-1}. All spectral operations were executed using the GRAMS/AI 8.0 software (Thermo Galactic, USA).

4.5.5 Morphological Characterization

The rotomolded samples were cryogenically fractured (liquid nitrogen) and micrographs of the exposed cross-sections were taken using a JOEL JSM-840A scanning electron microscope (SEM) and Olympus SZ6 stereomicroscope coupled with a Spot Insight (Diagnostic Instrument) high resolution (1600×1200 pixels) camera.

4.5.6 Density Measurements

Density was determined by a Quantachrome Ultrapyc 1200e gas pycnometer. Nitrogen was used as the gas phase. Hardness (shore A and shore D) were also determined by a PTC Instruments Model 306L and Model 307L (ASTM D2240). The data reported are the average and standard deviation of a minimum of five repetitions.

4.5.7 Thermogravimetric Analysis

TGA was carried out on a Q5000IR TGA analyzer (TA Instruments). The scans were performed from 50 to 800°C at a rate of 10°C/min with a gas flow rate of 25 mL/min. The tests were performed in nitrogen to evaluate the thermal resistance.

4.5.8 Mechanical Properties

The tensile properties at room temperature were measured on an Instron model 5565 universal testing machine with a 500 N load cell. Type V samples were cut in the rotomolded parts according to ASTM D638. The crosshead speed was set at 10 mm/min. The reported values for the tensile modulus, strength and elongation at break are based on the average of at least six samples.

Flexural 3-point bending tests were performed (room temperature) at a crosshead speed of 2 mm/min on an Instron universal tester model 5565 (50 N load cell) (ASTM D790). The span was 60 mm. At least 5 samples (60×12.7 mm^2) were used to report the average and standard deviation (modulus and strength).

Charpy impact strength was determined by a Tinius Olsen (USA) testing machine model Impact 104. At least ten rectangular specimens (60×12.7 mm^2) were prepared according to ASTM D6110. The samples were V-notched by an automatic sample notcher model ASN (Dynisco, USA) at least 24 hours before testing.

4.6 Results and Discussion

4.6.1 Confirmation of Maple Surface Modification

To confirm the maple surface modification was successful, TGA and FTIR were employed. The DTG curve (Figure 33) shows the broad peak around 220-280°C associated to the thermal depolymerization of hemicellulose and the break of glycosidic bonds in cellulose [168], whereas the highest peak at 320°C corresponds to cellulose degradation [169]. Importantly, the peak of treated fibers around 430 ℃ is related to the thermal degradation of the MAPE surface layer [170].

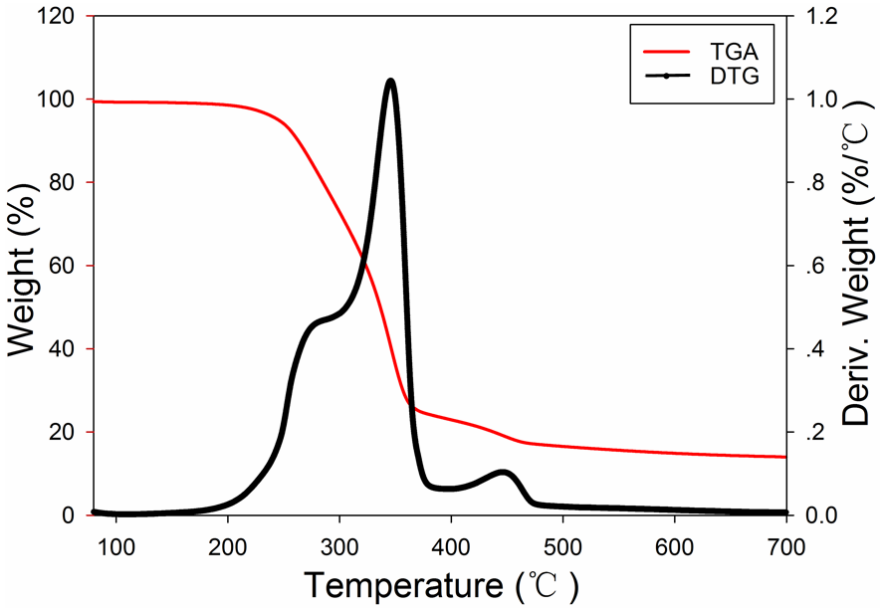

Figure 33. TGA (red) and DTG curves (black) of the treated maple wood fibers (TMWF).

To further confirm the successful surface treated, Figure 34 shows FTIR spectra of various samples, the intensity increases at 2920 and 2850 cm^{-1} related to symmetric and asymmetric aliphatic C–H

vibrations, which confirms the increase of C-H groups at the treated fiber surface due to the presence of PE in MAPE [171]. All these observations reveal the presence of the coupling agent at the maple fiber surface.

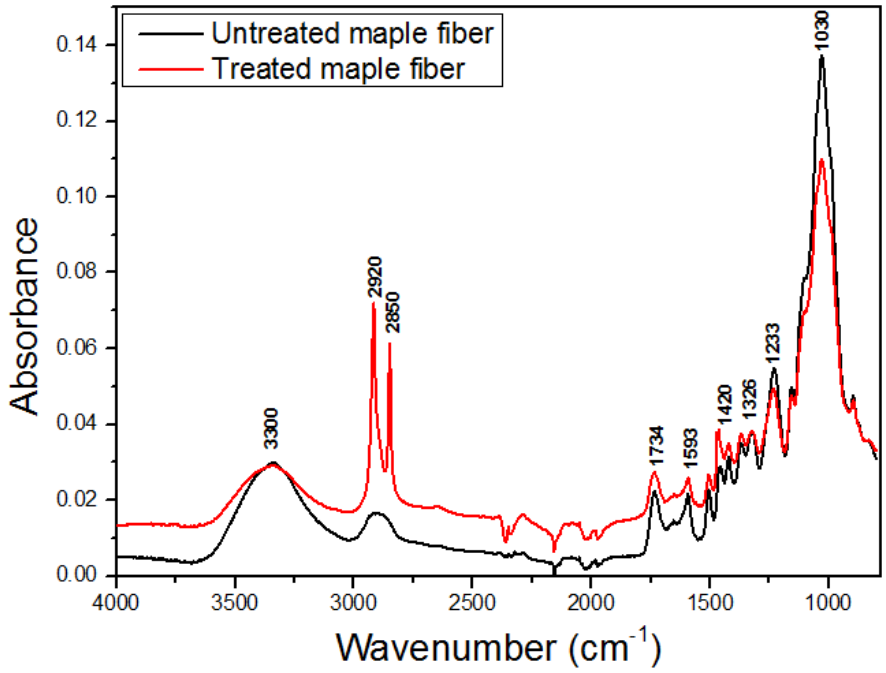

Figure 34. FTIR spectra of TMWF (red) and UMWF (black).

4.6.2 Morphology

To better observe the surface of maple fibers and morphology of hybrid composites, SEM was used and the results are showed in Figure 35. Figure 35a presents the surface of UMWF is rough, conversely, TMWF has a smooth surface due to the presence of a MAPE layer on the fiber surface (Figure 35b). Compared with UMWF and GTR hybrid composites (Figure 35e,g), the number of defects (holes, voids and interfacial gaps) is much lower for TMWF and GTR hybrid composites (Figure 35f,h) which is attributed to the improvement in interfacial compatibility due to presence of MAPE.

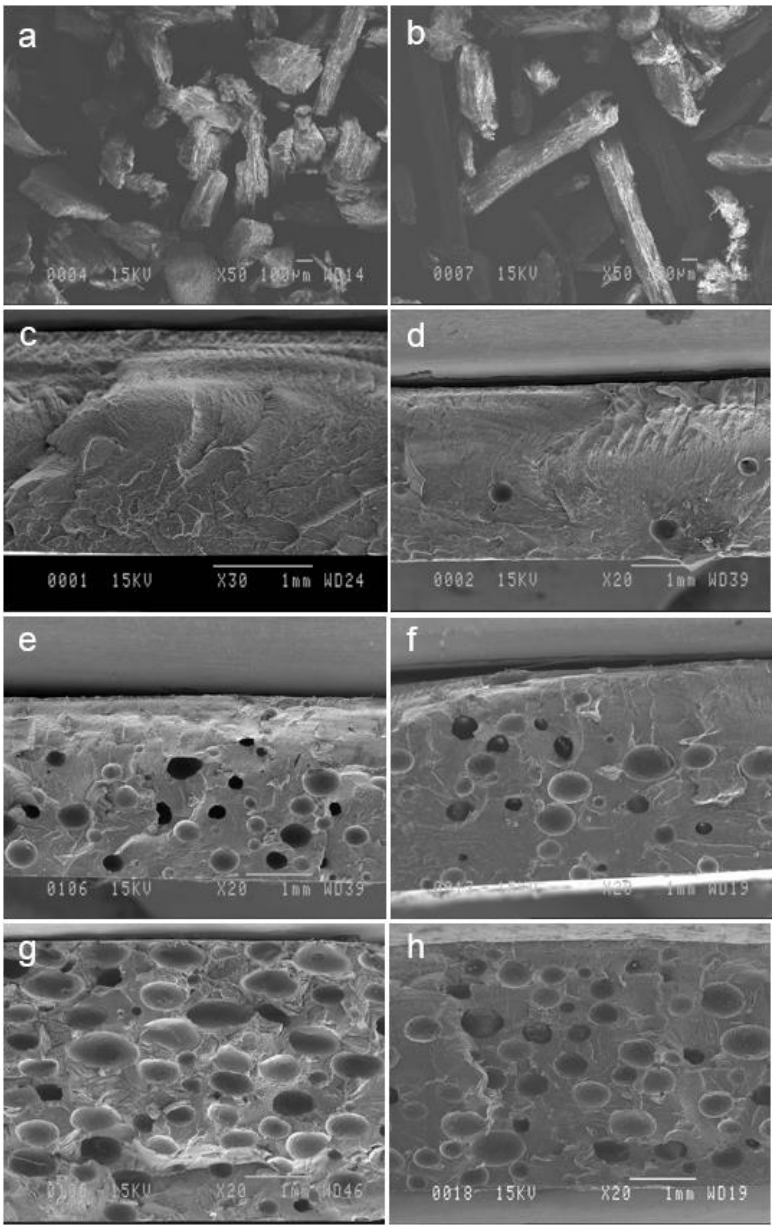

Figure 35. SEM of UMWF (a), TMWF (b) and some typical rotomolded specimens with different percentages of GTR content/UMWF content (e, g) or TMWF content (f, h)/LLDPE content: (c) 0/0/100, (d) 10/0/90, (e) 5/5/90, (f) 5/5/90, (g) 0/10/90, (h) 0/10/90.

4.6.3 Density Measurement

The density of the hybrid composites is reported in Figure 36 together with GTR, UMWF, TMWF and LLDPE powder. It can be observed that density of maple fibers drops by 7.4% after solution modification. This might be related to the density difference between the removed components (lignin and hemicellulose around 1500 kg/m^3) and MAPE addition (915 kg/m^3) [172]. Similarly, the density

of TMWF and GTR hybrid composites is slightly lower than that of UMWF and GTR hybrid composites, which is attributed to the combination of low density of TMWF and less defects in the TMWF and GTR hybrid composites.

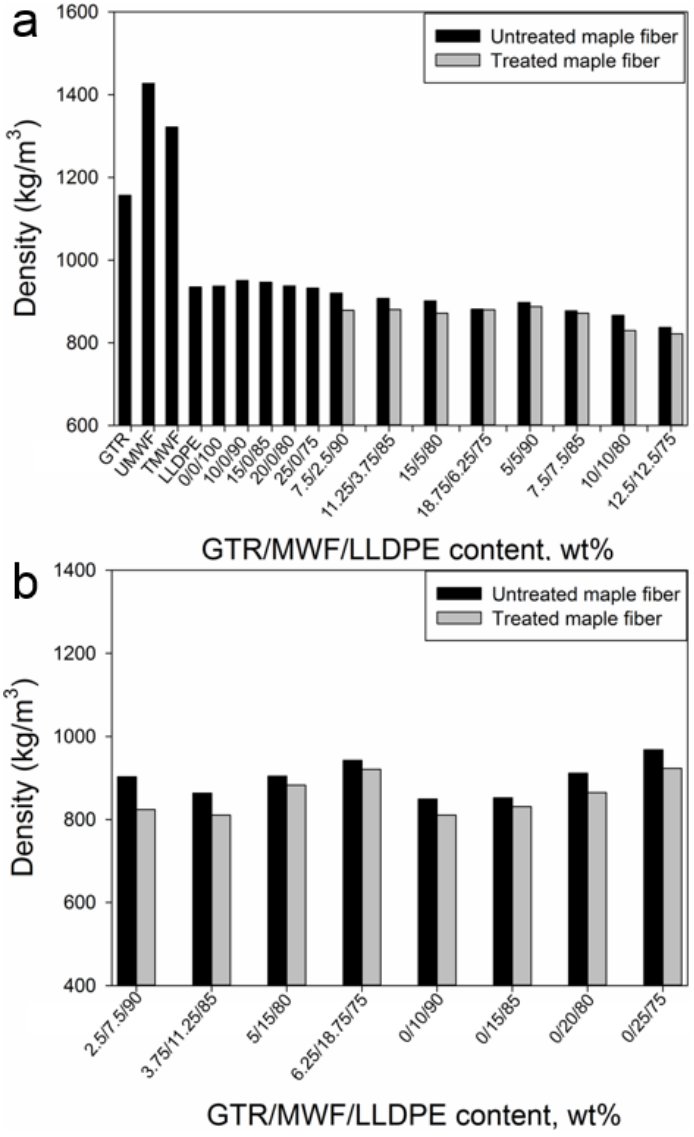

Figure 36. Density of the different materials used and composites produced.

4.6.4 Tensile Properties

Tensile moduli for rotomolded samples with and without coupling agent are presented in Figure 37. Because of defects (holes, voids and interfacial gaps) existing, all the tensile moduli of composites are lower than neat LLDPE (225.6 MPa). Certainly, the tensile moduli of TMWF and GTR hybrid composites slightly increase compare to those of UMWF and GTR hybrid composites due to the

effect of MAPE. For example, the tensile moduli for GTR/UMWF/LLDPE of 5/5/90 and 5/15/80 are 187 MPa and 138 MPa, respectively, compared with 196 MPa and 141 MPa for GTR/TMWF/LLDPE of 5/5/90 and 5/15/80, respectively.

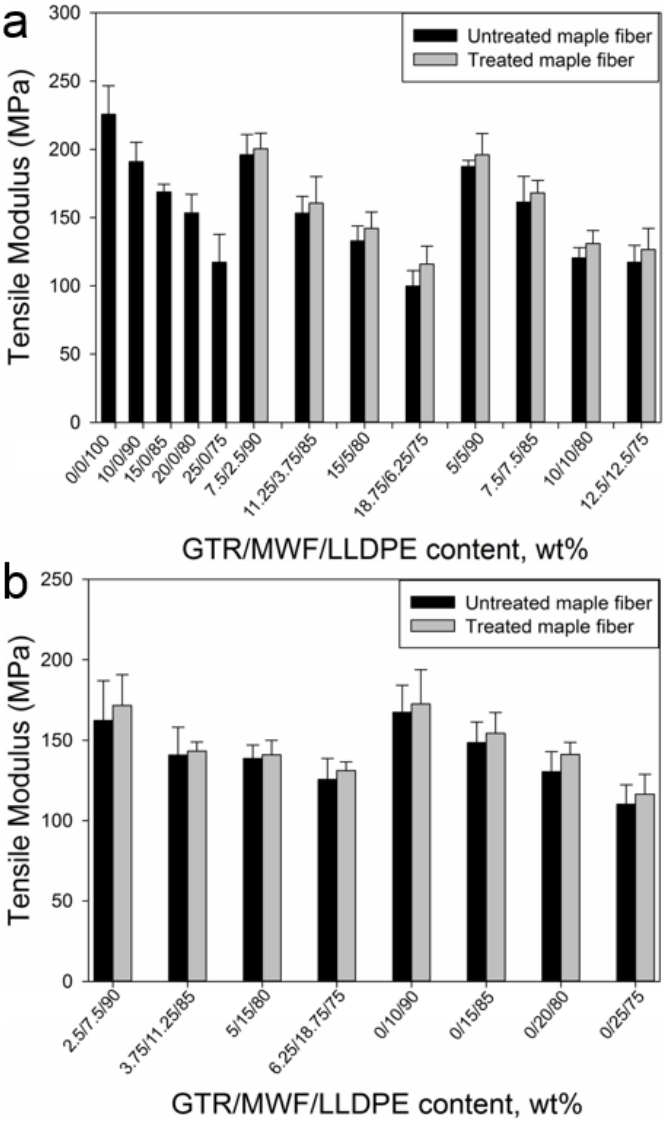

Figure 37. Tensile modulus of all the composites produced.

Figure 38 shows the tensile strength of rotomolded samples produced. The tensile strength for all the composites is lower than neat LLDPE (17.1 MPa). However, the tensile strength is substantially increased after addition of MAPE. This observation is attributed to the fact that the presence of MAPE on the surface of maple fibers can improve the interfacial strength resulting in smoother stress transfer from the matrix to the fibers [173]. For example, the tensile strength increases by 57.6% and 60.9%

for GTR/TMWF/LLDPE of 18.75/6.25/75 and 6.25/18.75/75 compared to GTR/UMWF/LLDPE of 18.75/6.25/75 and 6.25/18.75/75, respectively.

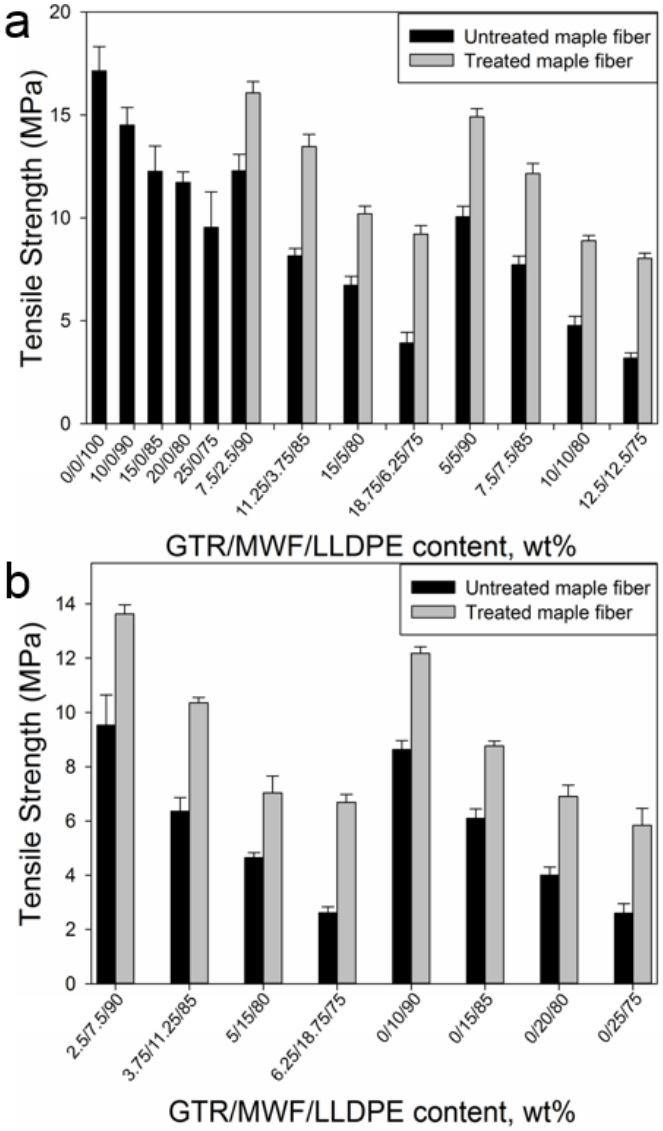

Figure 38. Tensile strength of all the composites produced.

Figure 39 indicates the elongation at break of neat LLDPE and composites with different GTR/fiber ratios with and without MAPE. Due to the low elasticity of maple fibers and defects in the composites, a substantial reduction of the elongation at break occurs for all composites. The addition of GTR and MAPE does not affect this trend for all composites. Similar findings were also found by Verdaguer and Rodrigue [174].

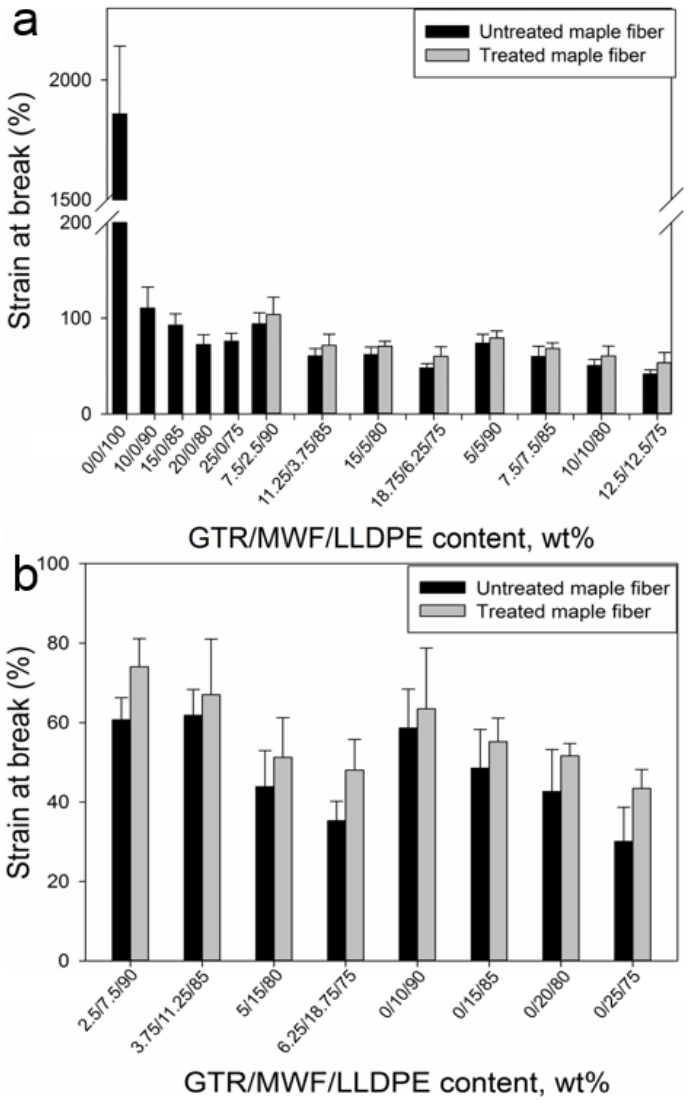

Figure 39. Elongation at break of all the composites produced.

4.6.5 Flexural Properties

Figure 40 presents the flexural modulus of composites with different GTR/fiber ratios with and without MAPE and neat LLDPE. The results reveal that a similar trend as for the tensile modulus (Figure 37) is observed. The addition of MAPE slightly improves the flexural modulus from to 327 MPa to 342 MPa and from 307 MPa to 328 MPa for GTR/TMWF/LLDPE of 10/10/80 and 5/15/80 with respect to their untreated counterparts, respectively.

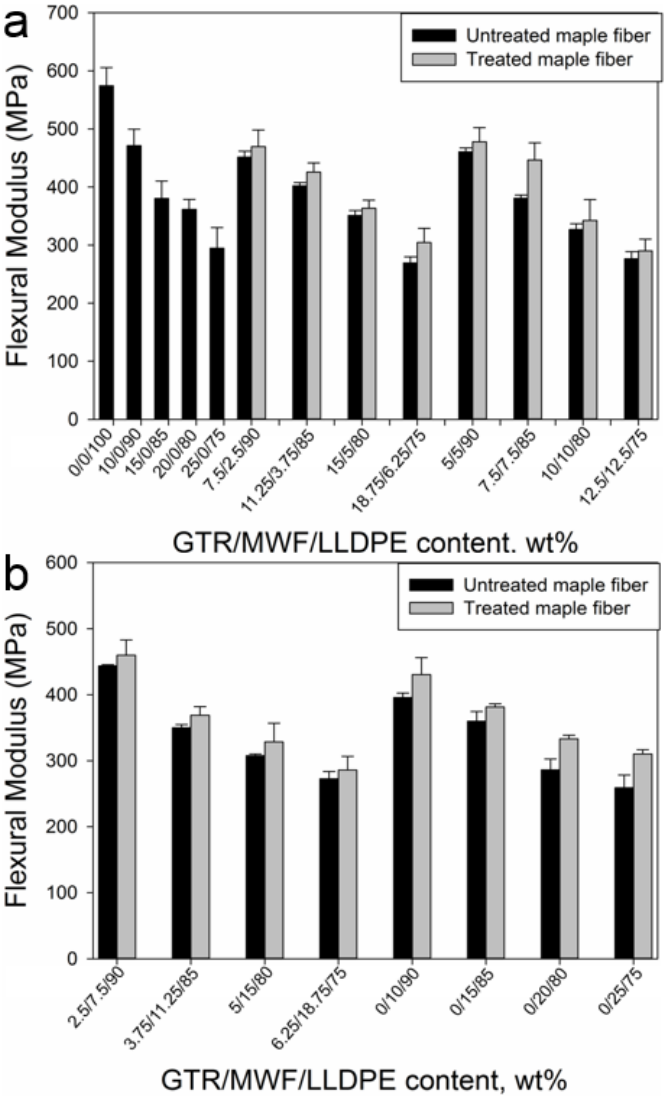

Figure 40. Flexural modulus of all the composites produced.

4.6.6 Impact Strength

Impact strength of all the composites are shown in Figure 41. For GTR/LLDPE composites, the impact strength drops a little due to poor adhesion between matrix and GTR. With the increasing GTR contents to 25%, the crosslinked structure makes GTR more deformable and able to relax more easily in rapid forming stress field before crack initiation [27]. On the other hand, the impact strength of maple fibers reinforced composites is decreasing with fiber loading. This can be related to the rigid fiber property and fiber ends acting as stress concentration zones promoting crack initiation and propagation [135]. Nevertheless, there is a little improvement in UMWF/LLDPE composites impact strength occurred after GTR addition. For example, the impact strength for UMWF/LLDPE of 20/80

increases form 61 J/M to 75.5 J/M for GTR/UMWF/LLDPE of 5/15/80. The addition of a coupling agent further improves the impact strength of UMWF/LLDPE composites as well as GTR/UMWF/LLDPE composites. For example, the impact strength for UMWF/LLDPE of 20/80 increases to 64.2 J/M and GTR/UMWF/LLDPE of 5/15/80 increases to 77 J/M when MAPE was used, respectively.

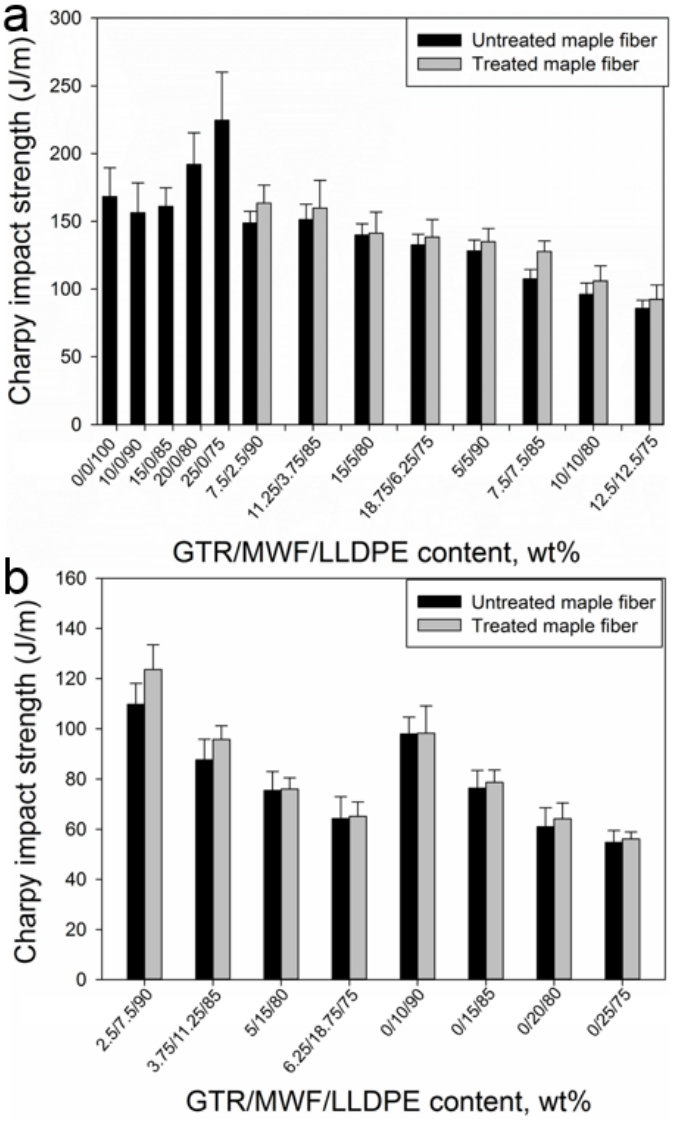

Figure 41. Impact strength of all the composites produced.

4.7 Conclusion

This work presented the mechanical, physical, and morphological properties of hybrid composites based on linear low density polyethylene (LLDPE), ground tire rubber (GTR) and maple wood fibers

(MWF). Additionally, the effect of GTR and MWF surface treatment (MAPE in solution) on the tensile, flexural and impact properties of the composites were studied.

The TGA curves and FTIR spectra obtained indicated that the surface of maple fiber was successfully coated with MAPE. Meanwhile, the morphological analysis of the composites showed that MAPE as a coupling agent improved the interfacial compatibility producing samples with less defects (holes, voids and interfacial gaps). Finally, the addition of GTR lead to little improvement of impact strength in wood fibers composites, and the incorporation of MAPE resulted in better hybrid composites properties.

4.8 Acknowledgements

The authors acknowledge the financial support of the National Science and Engineering Research Council of Canada (NSERC) and the Chinese Scholarship Council (CSC).

Chapter 5

A comparison between two ground tire rubber surface treatments to produce compounds based on linear low density polyethylene via rotational molding

Dou Y, Rodrigue D. A comparison between two ground tire rubber surface treatments to produce compounds based on linear low density polyethylene via rotational molding. 77th Annual Technical Conference of the Society of Plastics Engineers, SPE ANTEC, Detroit 2019.

5.1 Résumé

Ce travail compare l'efficacité de deux traitements de surface de caoutchouc de pneu broyé (GTR): un ajout d'agent de couplage (polyéthylène maléaté, MAPE) via un traitement en solution et un procédé de dévulcanisation par traitement micro-ondes. Les particules de GTR traitées et non-traitées ont été mélangées à sec avec du polyéthylène linéaire de basse densité (LLDPE) pour produire les composés par rotomoulage. En particulier, l'effet des traitements MAPE et micro-ondes a été étudié pour modifier les propriétés physiques (densité) et mécaniques (tension, flexion et impact) des composés résultants à température ambiante. Les résultats ont montré que les deux traitements de GTR conduisaient à une augmentation limitée de la résistance à la traction et de la résistance aux chocs, tandis que le module de traction, l'allongement à la rupture, le module de flexion et la densité demeuraient quasi inchangés pour une teneur fixe en GTR.

5.2 Abstract

This work compares the efficiency of two ground tire rubber (GTR) surface treatments: a coupling agent (maleated polyethylene, MAPE) addition via solution treatment and a devulcanization process using a microwave treatment. The treated and untreated GTR particles were dry-blended with linear low density polyethylene (LLDPE) to produce the compounds via rotational molding. In particular, the effect of MAPE and microwave treatments were investigated to modify the physical (density) and mechanical (tension, flexion and impact) properties of the resulting compounds at room temperature. The results showed that both GTR treatments led to limited increase of tensile strength and impact strength, while the tensile modulus, elongation at break, flexural modulus and density were almost unchanged for a fixed GTR content.

5.3 Introduction

Nowadays, with the increase in life quality and the general development in every country, there is a growing number of elastomeric wastes from the automobile industries, especially used tires. Thus, the disposal of used tire rubbers is becoming a great challenge because of its crosslinked structure (they cannot be melted or dissolved) [175-177]. As a result, a large number of waste tires are ground to reduce their size and to introduce into different applications [178]. Due to the important market share of thermoplastic materials, it is widely accepted that the incorporation of ground tire rubber (GTR) into thermoplastic resins would contribute to a substantial increase in waste tire consumption [179]. However, the highly crosslinked tire rubber is not able to entangle with the polymer molecules of thermoplastic matrices, resulting in low adhesion between both phases and poor mechanical properties of the hybrid composites. To overcome this drawback, various surface modifications and treatments have been proposed to improve the interfacial bonding and to promote the stress transfer between GTR particles and thermoplastic matrices. These methods can be classified as rubber devulcanization [180,181], compatibilizers addition [182], and surface activations [183].

Maleated polyolefins, such as maleated polypropylene (MAPP) or maleated polyethylene (MAPE), are believed to improve the adhesion between tire rubber and polyolefins because of a possible reaction between the maleic anhydride groups with unsaturated C=C bonds of the rubber molecules [184,185]. On the other hand, devulcanization is believed to be the most attractive method of reusing waste tire rubbers by restoring some of the flowing ability of the vulcanized rubber by breaking the crosslinks in the rubber network without degradation of the main polymer backbone [186]. Once the rubber molecules have more mobility, the regenerated material can be incorporated into thermoplastic matrices to produce high toughness materials [187]. Microwave treatment of waste rubbers, as a devulcanization method, is a technique in which microwave energy is provided to break S-S bonds [188]. This method is a viable as well as very useful approach because it can become an economical and ecological process to reuse waste rubber and to return it to the same products where it was originally produced with equivalent physical properties [189].

In this work, blends of linear low density polyethylene (LLDPE) and ground tire rubber (GTR) are produced by rotational molding, which is a polymer processing technology used to produce hollow seamless products such as tanks, automotive parts, toys, etc. [107]. Unlike most other plastic processes, there is no pressure involved in rotational molding, which means that the molds can be very thin and generally inexpensive. Additionally, rotomolding can more easily handle complex shapes with a very wide range of part sizes and variable thicknesses [120,126]. Thus, the main

objective of this work is to produce LLDPE/GTR compounds via rotational molding and to improve the overall properties of the parts by using two GTR surface treatments.

5.4 Materials

The matrix was linear low density polyethylene grade 8460 from Exxon Mobil (Canada). This polymer has a melt flow index of 5 g/10 min (2.16 kg/190°C) and a density of 930 kg/m^3. The ground tire rubber (GRT) was supplied by Phoenix Innovation Technologies (Montreal, Canada). This material has a density of 1.16 g/cm^3. For the GTR surface treatment, xylene (laboratory purity grade) from Fisher Chemicals (USA) was used as the solvent, while the coupling agent was maleated polyethylene (MAPE) (Epolene C26, Westlake Chemicals, USA). This grade has an average molecular mass of 65 kg/mol, a melt flow index (MFI) of 8.0 g/10 min (190°C/2.16 kg), an acid number of 8.0 mg KOH/g, a density of 915 kg/m^3, and a melting point of 121°C.

5.5 Experimental

5.5.1 GTR Surface Treatment with MAPE

GTR surface treatment in solution was performed as follows. Firstly, 3 g of MAPE was dissolved in 900 mL of xylene at 80-90°C under vigorous stirring. Next, 100 g of GTR was added in the solution and left under stirring for 20 min. Finally, the treated GTR was filtrated and dried overnight at 60°C in an oven.

5.5.2 GTR Devulcanization

The microwave devulcanization process was carried out by using a conventional microwave oven, Danby DMW799W at the maximum power output of 700 W. During the devulcanization process, 50 g of GTR was placed inside a glass beaker and exposed to the microwave treatment for 3 or 5 min. The samples were coded as 3M-GTR and 5M-GTR, respectively.

5.5.3 Material Mixing

For each composition, a total of 650 g of material was used based on LLDPE with different GTR contents. Powder mixing via dry-blending was carried out in a high speed mixer (LAR-15LMB, Skyfood, USA) at 3320 rpm for a total of 4-5 min.

5.5.4 Rotational Molding: Process and Equipment

A laboratory-scale rotational molding machine (MedKeff-Nye Roto-Lab model 22) was used for processing. Rotationally molded parts were manufactured with an aluminum cubic mold of 3.6 mm wall thickness and a side length of 19 cm. Before loading the material, a demolding agent (Trasys 420, DuPont, USA) was applied to the internal surface of the mold. The powder blends were then loaded into the mold to produce parts with an approximate wall thickness of 3 mm. Then, the charged mold was closed and mounted on the rotating arm. Preliminary trials were performed to determine the optimum conditions leading to homogeneous and uniform wall thickness. An oven at 275°C and a speed ratio of 1:4 with a major axis speed of 1 rpm were chosen. The heating time was fixed at 25 min. Then, the mold was removed from the oven and cooled by forced air for 35 min. Finally, the mold was opened to retrieve the part.

5.5.5 Density Measurements

Density was determined by a Quantachrome Ultrapyc 1200e gas pycnometer. Nitrogen was used as the gas phase.

5.5.6 Thermogravimetric Analysis

TGA was carried out on a Q5000IR TGA analyzer (TA Instruments, USA). The scans were performed from 50 to 800°C at a rate of 10°C/min with a gas (nitrogen) flow rate of 25 mL/min. The tests were performed to evaluate the thermal stability of the materials.

5.5.7 Mechanical Properties

The tensile properties at room temperature were measured on an Instron model 5565 universal testing machine with a 500 N load cell. Type V samples were cut in the rotomolded parts according to ASTM D638. The crosshead speed was set at 10 mm/min. The reported values for the tensile modulus, strength and elongation at break are based on the average of at least six samples.

Flexural three-point bending tests were performed (room temperature) at a crosshead speed of 2 mm/min on an Instron universal tester model 5565 (50 N load cell) following ASTM D790. The span was 60 mm. At least 5 samples (60×12.7 mm^2) were used to report the average and standard deviation (modulus).

Charpy impact strength was determined by a Tinius Olsen (USA) testing machine model Impact 104. At least ten rectangular specimens (60×12.7 mm^2) were prepared according to ASTM D6110. The samples were V-notched by an automatic sample notcher model ASN (Dynisco, USA) at least 24 h before testing.

5.6 Results and Discussion

5.6.1 Confirmation of GTR Surface Modification

To confirm the GTR surface modification via MAPE in solution, TGA was used. The DTG curves (Figure 42) show a broad peak around 220-280°C associated to the volatilization of processing oils and other low boiling-point components. Then, the main peak around 350°C belongs to the decomposition of natural rubber (NR). But more importantly, the higher peak for GTR-MAPE around 425°C is related to the thermal degradation of the MAPE layer on the GTR surface.

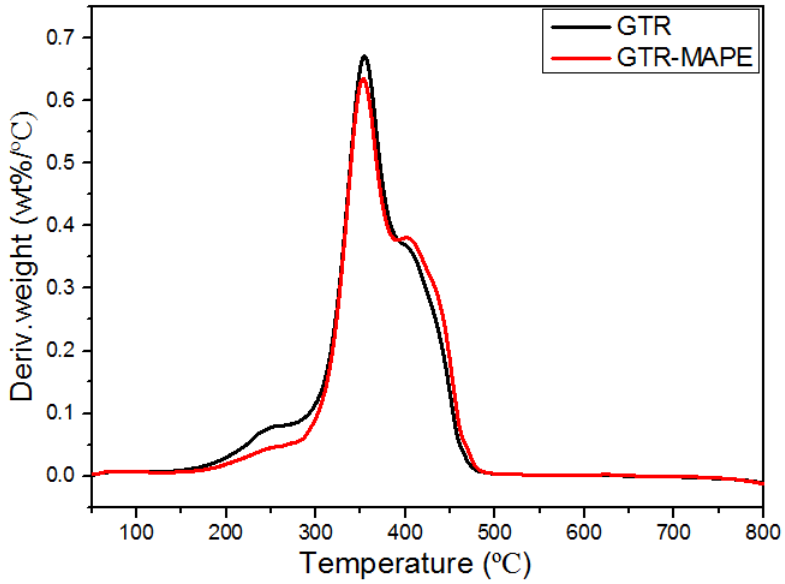

Figure 42. DTG curves of the GTR (black) and GTR-MAPE (red).

5.6.2 Density Measurement

The density of the raw materials and the molded samples is reported in Figure 43. Figure 43a shows that the GTR density increased by 3.5% after the MAPE treatment in solution. This increase is related to some interactions between MAPE and GTR particles and also possible particle shrinkage due to low molecular weight compounds being extracted [179]. This also explains the lower intensity of the shoulder around 250°C for the treated GTR in Figure 1. Accordingly, increasing the GTR content

slightly increased the densities of LLDPE/GTR-MAPE compounds. It is also shown in Figure 43b that the density of GTR increased as a function of the microwave treatment time. This is associated with the process of revulcanization; i.e. too much heat led to the vulcanization of the residual sulphur in the GTR, reforming S-S links and increasing density [190].

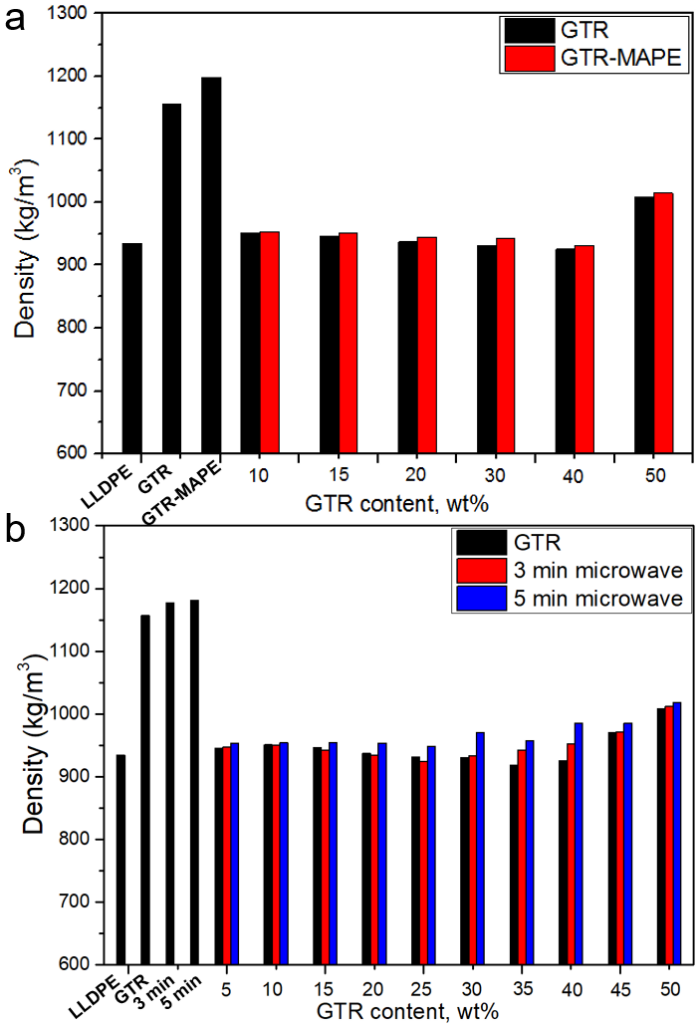

Figure 43. Density of the raw materials and molded samples with different GTR surface treatment: (a) MAPE in solution and (b) microwave devulcanization.

5.6.3 Tensile Properties

The tensile moduli of the rotomolded samples with and without GTR treatment are presented in Figure 44. Because of defects (holes, voids and interfacial gaps), all the tensile moduli of the molded samples are lower than the neat LLDPE (225.6 MPa). Nevertheless, Figure 44a clearly shows that the tensile moduli of LLDPE/GTR-MAPE are slightly higher that LLDPE/GTR due to the effect of

MAPE. For example, the tensile modulus for 85/15 LLDPE/GTR is 169 MPa compared with 186 MPa for LLDPE/GTR-MAPE. On the other hand, microwave treatment can break the crosslinked structure in the rubber network leading to lower GTR stiffness. Therefore, the tensile moduli of LLDPE/3M-GTR and LLDPE/5M-GTR are lower compared to LLDPE/GTR (Figure 44b).

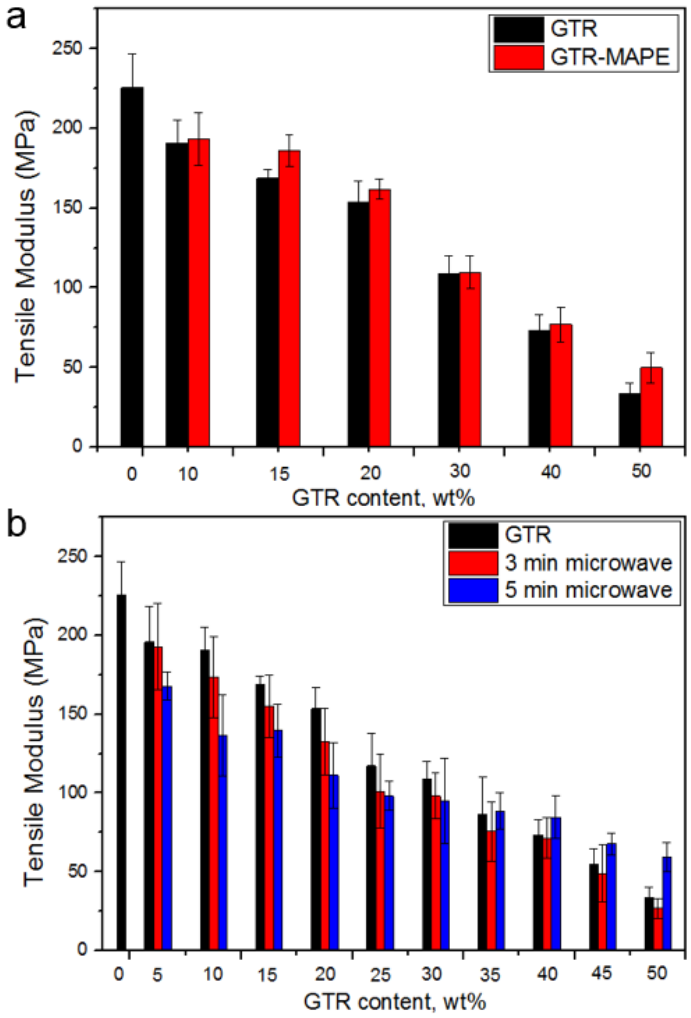

Figure 44. Tensile modulus of all the compounds produced.

Figure 45 shows the tensile strength of the rotomolded samples. It can be seen that for all the compounds, lower values than neat LLDPE (17.1 MPa) are obtained. However, the tensile strength of LLDPE/GTR-MAPE (Figure 45a) are increased after MAPE treatment. This observation is attributed to the presence of MAPE on the GTR surface improving the interfacial strength resulting in better stress transfer from the matrix to the GTR [191]. For example, the tensile strength increases by 17% for 85/15 LLDPE/GTR-MAPE compared to LLDPE/GTR. Furthermore, due to the increased chain mobility of microwave treated GTR, the tensile strength of LLDPE/3M-GTR and LLDPE/5M-

GTR are slightly increased (Figure 45b). For example, the tensile strength increased by 7% for 85/15 LLDPE/3M-GTR compared to LLDPE/GTR.

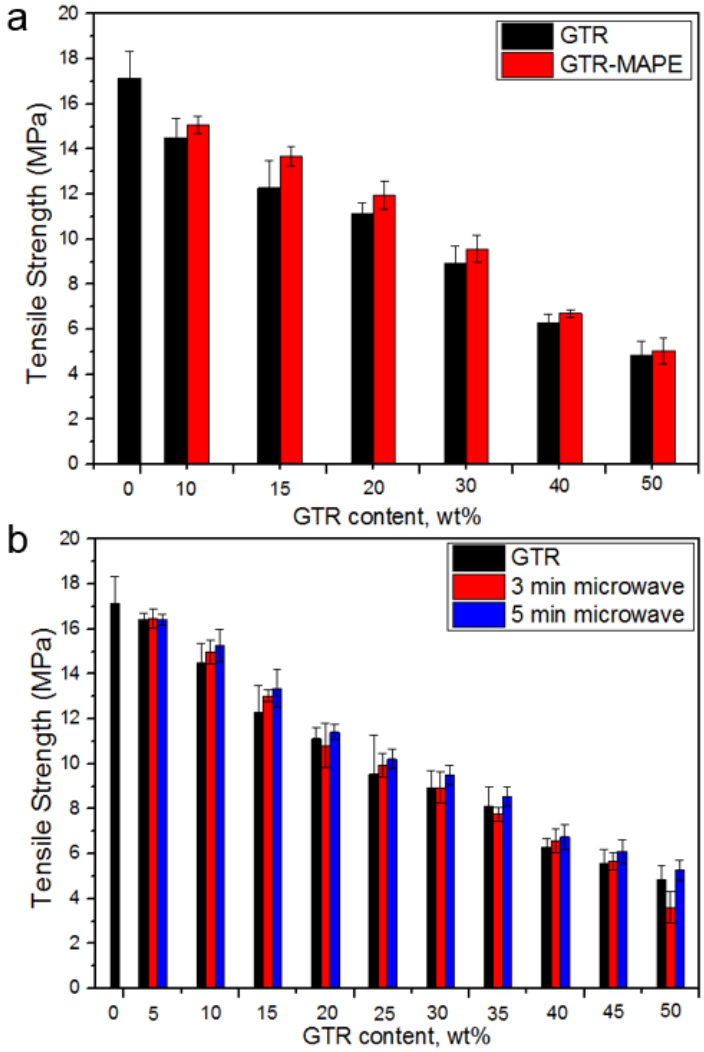

Figure 45. Tensile strength of all the compounds produced.

Figure 46 reports on the elongation at break of neat LLDPE and all the compounds. Since there are some defects in the molded samples with GTR addition, a substantial reduction of the elongation at break occurs. This is also related to the lower elongation of the GTR particles. Nevertheless, compared with the elongation at break of LLDPE/GTR with a GTR content between 10 and 20 wt.%, the elongation at break of LLDPE/GTR-MAPE is slightly higher due to the effect of MAPE. Similarly, the same trend is observed for LLDPE/3M-GTR and LLDPE/5M-GTR with a GTR content between 10 and 15 wt.%.

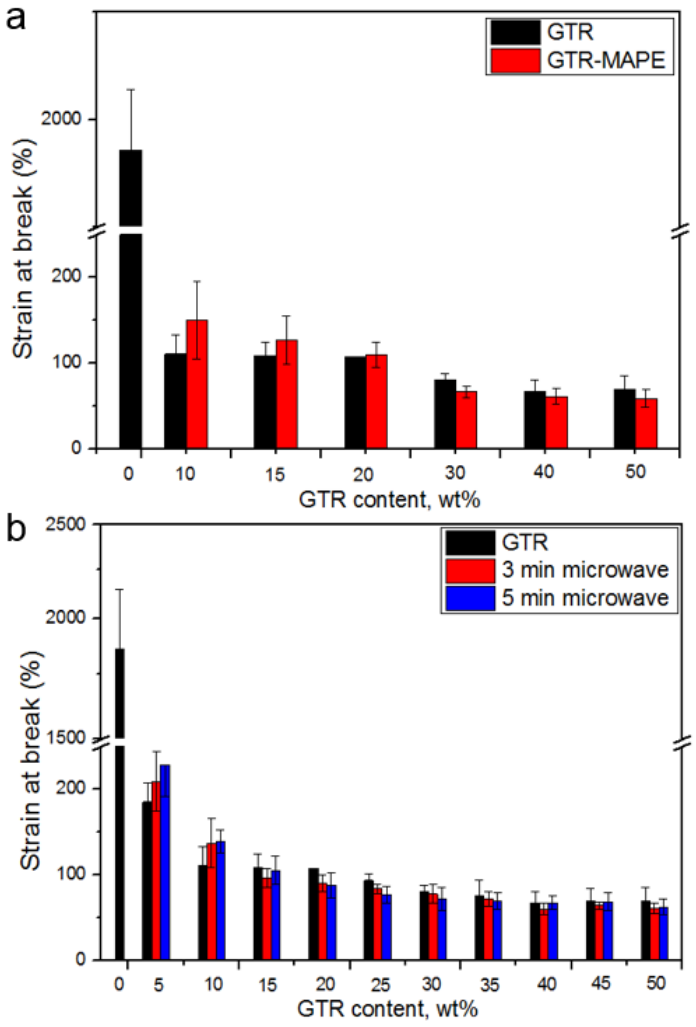

Figure 46. Elongation at break of all the compounds produced.

5.6.4 Flexural Properties

Figure 47 presents the flexural modulus of all the samples produced. The results show that a similar trend as for the tensile modulus (Figure 44) is observed. For example, the MAPE treatment slightly improved the flexural modulus from 380 to 404 MPa and from 234 MPa to 282 MPa for 85/15 and 70/30 LLDPE/GTR-MAPE respectively, compared with their untreated counterparts.

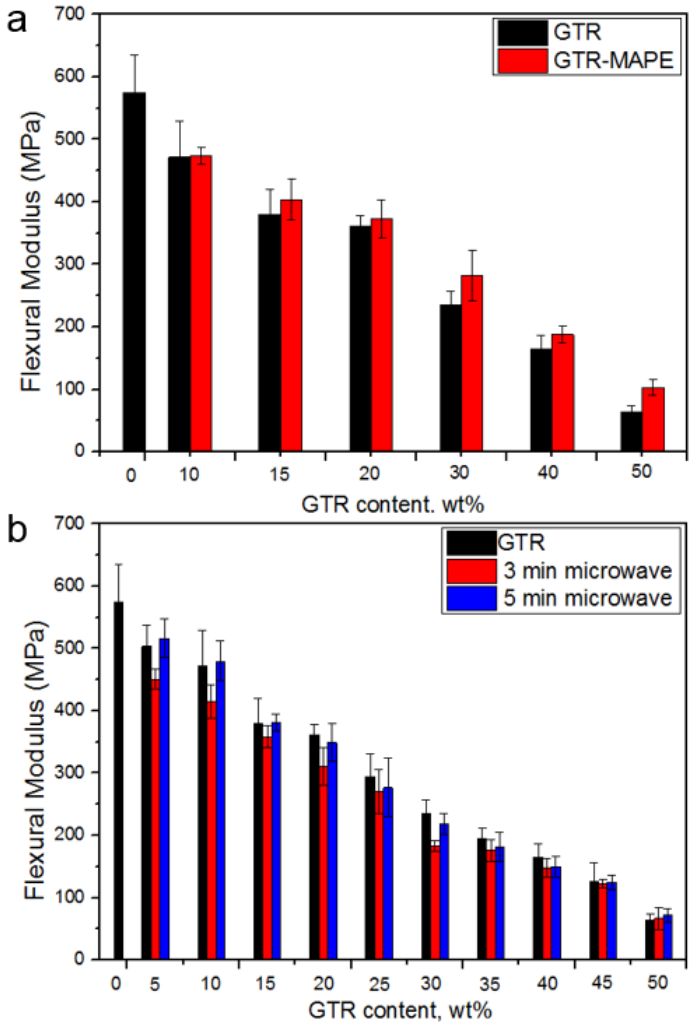

Figure 47. Flexural modulus of all the compounds produced.

5.6.5 Impact Strength

Impact strength results are presented in Figure 48. For LLDPE/GTR composites, the impact strength slightly drops due to poor adhesion between LLDPE and GTR. But increasing the GTR content to 30% makes the GTR crosslinked structure more deformable and able to relax more easily in absorbing the stress before crack initiation [135]. On the contrary, the impact strength of LLDPE/GTR increased after MAPE treatment (Figure 47a), showing again that the MAPE improved the interfacial adhesion between GTR and LLDPE. For example, the impact strength for 85/15 LLDPE/GTR increased from 161 to 210 J/m for LLDPE/GTR-MAPE with the same GTR content, which represents a 30% increase. In addition, the maximum value of impact strength for LLDPE/GTR-MAPE is 234 J/m,

which is 39% higher than the neat LLDPE value. On the other hand, the impact strength of LLDPE/GTR slightly increased after microwave treatment (Figure 48b), especially when longer time is used (5 min). For example, the impact strength of 90/10 LLDPE/GTR increased from 156 to 193 J/m for LLDPE/5M-GTR with same GTR content. However, the maximum impact strength of LLDPE/5M-GTR was similar to LLDPE/GTR.

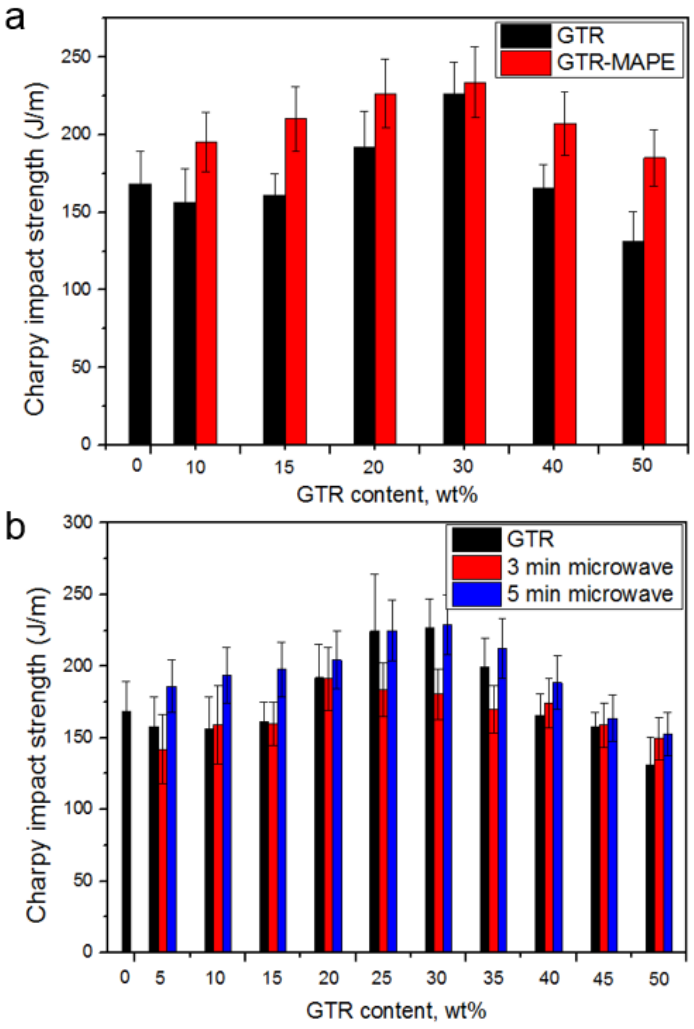

Figure 48. Impact strength of all the compounds produced.

5.7 Conclusions

This work compared two GTR surface treatments: MAPE in solution and microwave devulcanization. The samples were then produced by combining dry-blending and rotomolding using linear low density polyethylene (LLDPE) as the matrix. From the samples produced density and mechanical properties (tension, flexion and impact) were studied and compared.

The results showed that both GTR surface treatments can improve interfacial adhesion between the particles and the matrix, but limited improvement of tensile strength and impact strength were observed. However, the tensile modulus, elongation at break and flexural modulus did not significantly change compared to samples produced without GTR treatments. As a result, the GTR surface treatments have been proven to have limited effect based on the conditions used. So more work is needed to improve the GTR-LLDPE interfacial adhesion and produce rotomolded parts with better mechanical properties.

5.8 Acknowledgements

The authors acknowledge the financial support of the National Science and Engineering Research Council of Canada (NSERC) and the Chinese Scholarship Council (CSC).

Chapter 6

Polypropylene/ground tire rubber (PP/GTR) composites produced via rotational molding

Dou Y, Rodrigue D. Polypropylene/ground tire rubber (PP/GTR) composites produced via rotational molding. SPE ANTEC 2020: The Annual Technical Conference for Plastic Professionals, 2020: 364-368.

6.1 Résumé

Dans ce travail, le polypropylène (PP) a été mélangé à sec avec du caoutchouc de pneu broyé (GTR) pour produire des composites par rotomoulage. En particulier, l'effet de la teneur en GTR a été étudié pour modifier les propriétés mécaniques de la matrice PP. Chaque composé a été caractérisé par sa morphologie, sa densité et ses propriétés mécaniques (traction, flexion et impact). Comme prévu, les résultats ont montré que toutes les propriétés mécaniques diminuaient avec l'augmentation de la concentration de GTR en raison de son faible module et de sa résistance. De plus, on pense que la structure réticulée des particules de GTR limite l'interaction interfaciale PP-GTR, limitant ainsi également le transfert de contraintes mécaniques.

6.2 Abstract

In this work, polypropylene (PP) was dry-blended with ground tire rubber (GTR) to produce composites by rotational molding. In particular, the effect of GTR content was investigated to modify the mechanical properties of the PP matrix. Each compound was characterized via morphology, density and mechanical properties (tensile, flexural and impact). As expected, the results showed that all the mechanical properties decreased with increasing GTR concentration due to its low modulus and strength. Also, the crosslinked structure of the GTR particles is believed to limit the interfacial PP-GTR interaction, thus also limiting mechanical stress transfer.

6.3 Introduction

In the past two decades, the production of waste tires substantially increased with the rapid increase in vehicle use. This is why a large number of countries made efforts to develop some comprehensive use of the tires after their end of life (discarded/waste tires) for environmental and economic reasons [41]. Since traditional landfilling is known to produce hazardous air/water pollution, modern milling techniques (particle size reduction) became a suitable alternative for waste rubbers recycling [5, 192, 193]. Ground tire rubber of different particle sizes, commonly called GTR, can be obtained by several milling techniques and can be used as an active component or inactive filler in various matrices such as thermoplastic resins, thermoset resins or bitumen. But the main idea is to produce "value-added" composites to be used in several applications like civil engineering [194-197].

Nowadays, we are heavily dependent on thermoplastic products which have already replaced a large number of parts produced by more conventional materials such as wood and metal in several areas [198- 200]. Economically speaking, GTR incorporating into thermoplastic resins can decrease the raw material costs of different products. Environmentally speaking, blending GTR with thermoplastic resins also reduces environmental problems corresponding to the 3R concept (reduce, reuse and recycle) [201]. Therefore, these factors encouraged scientists and researchers to evaluate/investigate waste tire rubber containing thermoplastic blends or composites.

As one of the main commodity thermoplastic resins, polypropylene (PP) has shown one of the highest growth rate in the last years [202]. In this work, PP and GTR composites are produced by rotational molding which a low pressure, high-temperature manufacturing technique to produce hollow seamless products such as tanks, automotive parts, toys, etc. [107]. The process is also known as rotomolding or rotocasting. The earliest commercial application of the rotational molding of plastics used vinyl plastisols to coat the inside surface of a hollow metal mold [95]. Typical rotomolded products were play balls and toy dolls. Due to the introduction of powdered polyethylene grades, the rotational molding process expanded more quickly since the 1950s. Compared with other techniques in the plastics industries, rotomolding is one of the fastest-growing polymer processes expanding at an annual rate of 10% to 20% [203]. Furthermore, this molding technique can provide designers the opportunity to obtain at low cost the production of stress-free articles with uniform wall thickness and potentially complex shapes [120, 126, 204]. Therefore, as for producing hollow plastic products, rotational molding is currently a very competitive alternative to blow molding, thermoforming and injection molding [15]. Thus, the main objective of this work is to produce PP/GTR compounds via rotational molding and to measure the properties of the resulting composites.

6.4 Materials and Methods

6.4.1 Materials

The matrix used was polypropylene (RMPP141 NATURAL) from PSD Rotoworx Pty Limited (Australia). This polymer has a melt flow index of 13 g/10 min (2.16 kg/230°C) and a density of 0.90 g/cm^3. The ground tire rubber (GTR) was supplied by Phoenix Innovation Technologies (Montreal, Canada). This material has a density of 1.16 g/cm^3 and an average particle size of around 750 microns.

6.4.2 Material Mixing

For each composition, a total of 650 g of material was used based on blends of PP with different GTR weight contents (5%, 10%, 15%, 20%, 25%, 30%, 35%, 40%, 45% and 50%). Since all the materials are in a powder form, mixing was perform via dry-blending in a high speed mixer (LAR-15LMB, Skyfood, USA) at 3320 rpm for a total of 4-5 min.

6.4.3 Rotational Molding: Process and Equipment

A laboratory-scale rotational molding machine (MedKeff-Nye Roto-Lab model 22) was used to produce the parts via rotational molding. The mold used was made of aluminum with a cubic shape (3.6 mm wall thickness and a side length of 19 cm). Before loading the material, a demolding agent (Trasys 420, DuPont, USA) was applied to the internal surface of the mold. The powder blends were then loaded into the mold to produce parts with an approximate wall thickness of 3 mm. Then, the charged mold was closed and mounted on the rotating arm. Preliminary trials were performed to determine the optimum conditions leading to homogeneous and uniform wall thickness with good surface quality. An oven at 270°C and a speed ratio of 1:4 with a major axis speed of 1 rpm were chosen. The heating time was fixed at 36 min. Then, the mold was removed from the oven and cooled by forced air for 25 min. Finally, the mold was opened to retrieve the part.

6.4.4 Morphological Characterization

The rotomolded samples were cryogenically fractured using liquid nitrogen. To obtain micrographs of the specimens' cross-section, scanning electron microscopy (SEM) (US FEI Inspect F50) was used. The instrument was operated with a voltage of 15 kV at different magnifications.

6.4.5 Density Measurement

Density was determined by a Quantachrome Ultrapyc 1200e gas pycnometer. Nitrogen was used as the gas phase.

6.4.6 Mechanical Properties

The tensile properties at room temperature were measured on an Instron model 5565 universal testing machine with a 500 N load cell. Type V samples were cut in the rotomolded parts according to ASTM D638. The crosshead speed was set at 10 mm/min and the values for tensile modulus, tensile strength and elongation at break are based on the average of at least six samples.

Flexural tests (three-point bending) were performed at room temperature using a crosshead speed of 2 mm/min on an Instron universal tester model 5565 with a 50 N load cell according to ASTM D790. The span length was fixed at 60 mm. At least five rectangular samples with dimensions of 60×12.7 mm^2 were used to report the average and standard deviation for the modulus.

Charpy impact strength was determined by a Tinius Olsen (USA) testing machine model Impact 104. At least ten rectangular specimens (60×12.7 mm^2) were prepared according to ASTM D6110. The samples were notched ("V" shape) by an automatic sample notcher model ASN 120m (Dynisco, USA) at least 24 h before testing.

6.5 Results and Discussion

6.5.1 Morphological Characterization

The cross-section morphologies of the rotomolded parts containing different GTR contents are shown in Figure 49. Figure 49a reveals that no defects can be seen in neat PP specimen indicating that good rotomolding conditions were used to successfully produce the parts. However, with increasing GTR content (Figure 49b-49f), a number of bubbles and defects can be seen in the PP/GTR composites. This phenomenon is caused by the low compatibility between the GTR particles and the PP matrix leading to interfacial voids and particle pull-out. The origin of this poor GTR-PP interaction is related to the crosslinked structure of GTR limiting the molecular chain mobility and the possibility to entangle with the PP matrix [205]. Furthermore, with increasing GTR content, the total number of rubber particle increases thus a larger surface area to be wetted by the PP is created, but the relative amount of PP decreases which is no longer able to cover (embed) all the particles leading to possible

GTR agglomeration and particle-particle contact. These effects leads the way to a higher number or larger bubbles being produced [107].

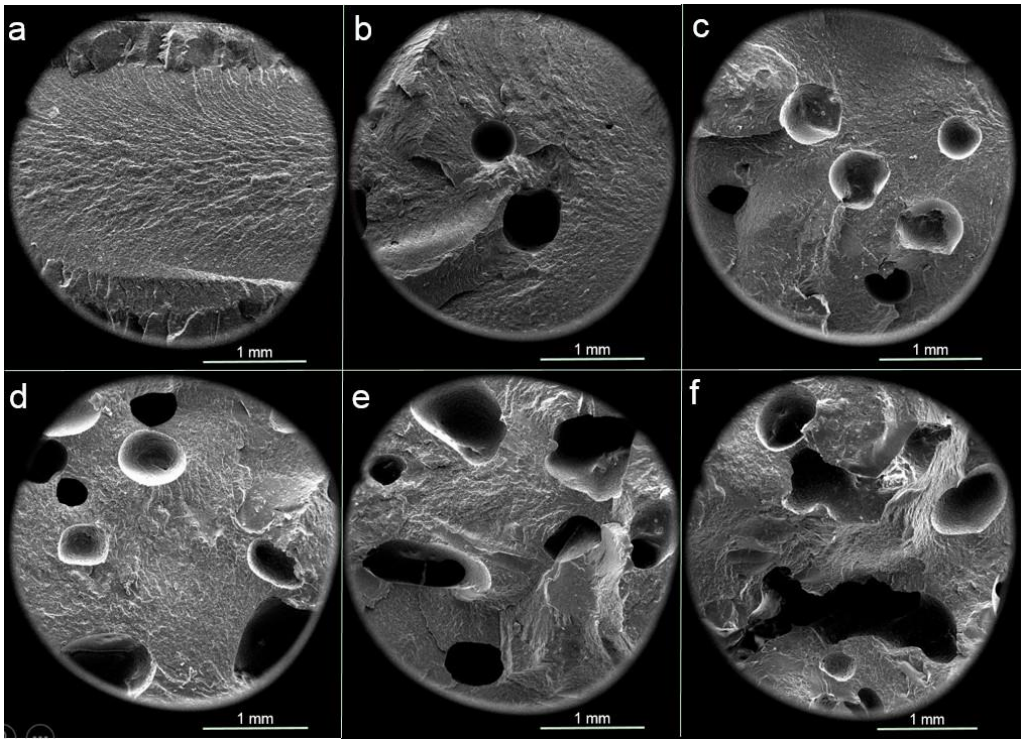

Figure 49. Typical SEM images of the rotomolded specimens' cross-section with different GTR concentrations: (a) 0%, (b) 10%, (c) 20%, (d) 30%, (e) 40% and (f) 50%.

6.5.2 Density Measurement

The density of GTR particles and the rotomolded samples is reported in Figure 50. It can be seen that the PP/GTR composites density does not significantly change with increasing GTR content. The behavior can be associated to two opposing effects: the density should increase with GTR content because of the higher density of the particles (1.16 g/cm^3) compared to the neat PP matrix (0.90 g/cm^3). On the other hand, density decreases as more defects (bubbles and voids) inside the composites are created as reported in Figure 49a, b. But as the GTR content increases (Figure 49c-f), more voids are created lowering the composites density. Nevertheless, the density slightly increases at higher GTR content (above 30%) indicating that the former is more important.

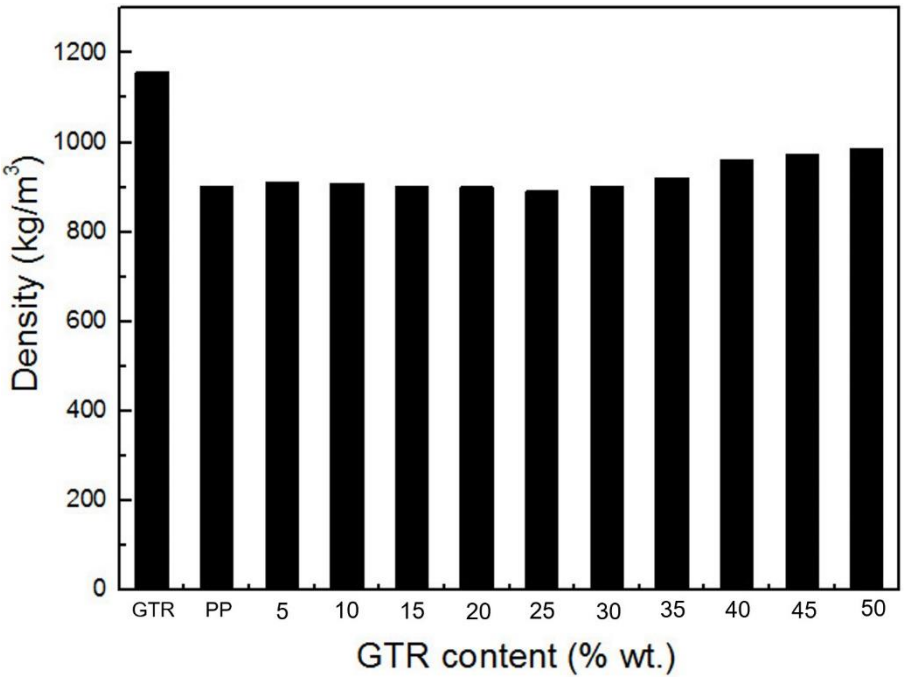

Figure 50. Density of GTR particles and the rotomolded samples as a function of GTR content.

6.5.3 Tensile Properties

The tensile moduli of the rotomolded PP/GTR composites are presented in Figure 51 to compare with the neat PP values (285 MPa). As expected, the tensile moduli decrease with increasing GTR content due to two phenomena: the lower modulus of the GTR compared to PP and the low compatibility between both components leading to internal defects (bubbles and interfacial gaps) resulting in poor stress transfer. A similar trend is observed in Figure 52 for the tensile strength of the composites compared to the neat PP value of 20.2 MPa. The same explanation also applies in this case.

Figure 53 reports on the elongation at break of the neat PP (74.5%) and all the PP/GTR composites. In this case, an important decrease is observed with only 5% GTR which is consistent with values reported from the literature [133, 134]. Again, two phenomena are involved here: the limited elasticity of the crosslinked rubber particles and the internal defects weakening the composites structure in terms of stress transfer and disturbing the polymer macromolecular network.

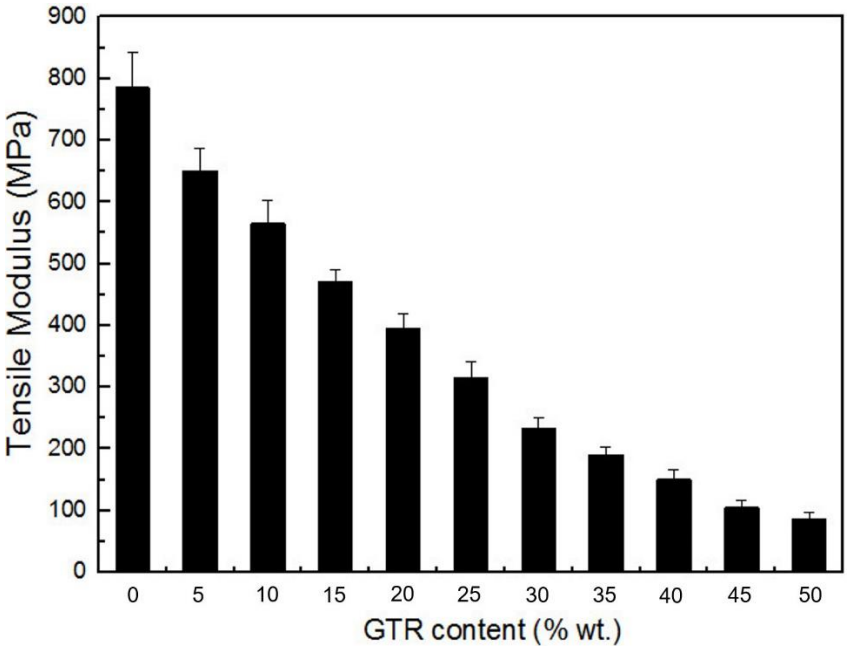

Figure 51. Tensile modulus of the composites as a function of GTR content.

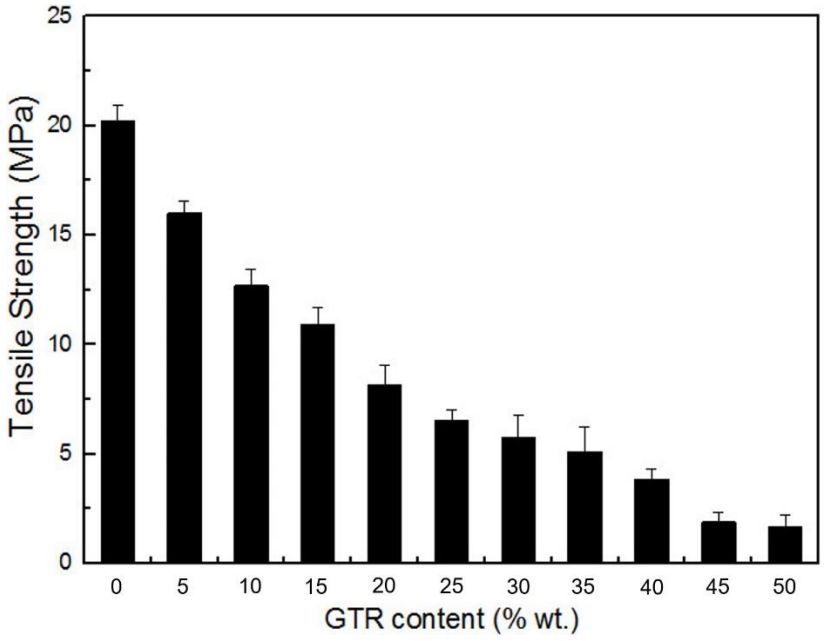

Figure 52. Tensile strength of the composites as a function of GTR content.

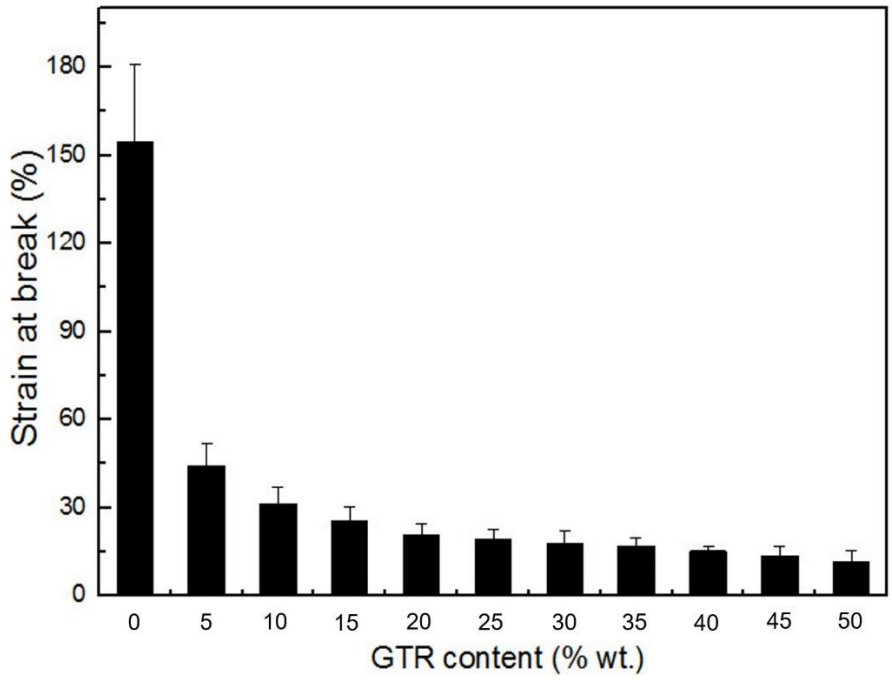

Figure 53. Strain at break of the composites as a function of GTR content.

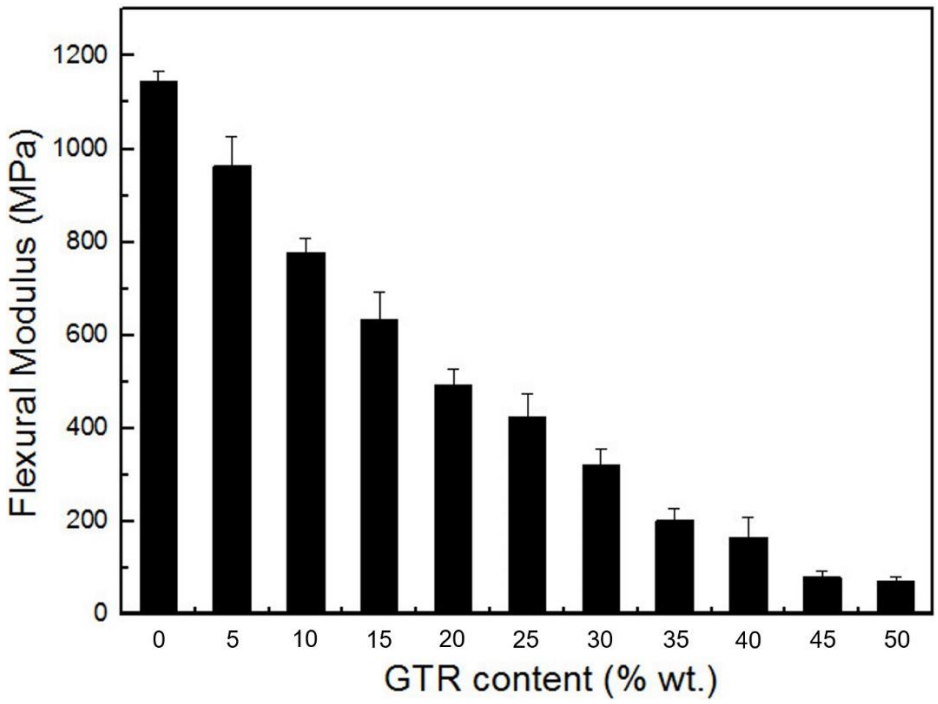

Figure 54. Flexural modulus of the composites as a function of GTR content.

6.5.4 Flexural Properties

Figure 54 presents the flexural modulus of all the composites produced. The results show that a similar trend as for the tensile modulus (Figure 51) is obtained. The highest value is observed for the neat PP matrix (1145 MPa) decreasing down to 71.4 MPa for the composite with 50% wt. GTR. This behavior can also be explained by the same phenomena as for the tensile modulus. Nevertheless, no flexural strength and break-up was measured as the samples deformed and fell between the supports due to high elasticity/toughness.

6.5.5 Impact Strength

The impact strength results of the neat PP and PP/GTR composites is presented in Figure 55. As mentioned above, because of the crosslinked structure of GTR, the poor adhesion between GTR and PP matrix induced the formation of defects (holes, voids and interfacial gaps), resulting in lower composites impact strength with increasing GTR content. For example, the impact strength decreased from 152 J/m for the neat PP down to 50.2 J/m for the 50% wt. PP/GTR composites. Although this represents an overall 67% decrease, it is less than for the other mechanical properties: 89% for tensile modulus, 82% for tensile strength, 92% for tensile elongation at break and 94% for flexural modulus.

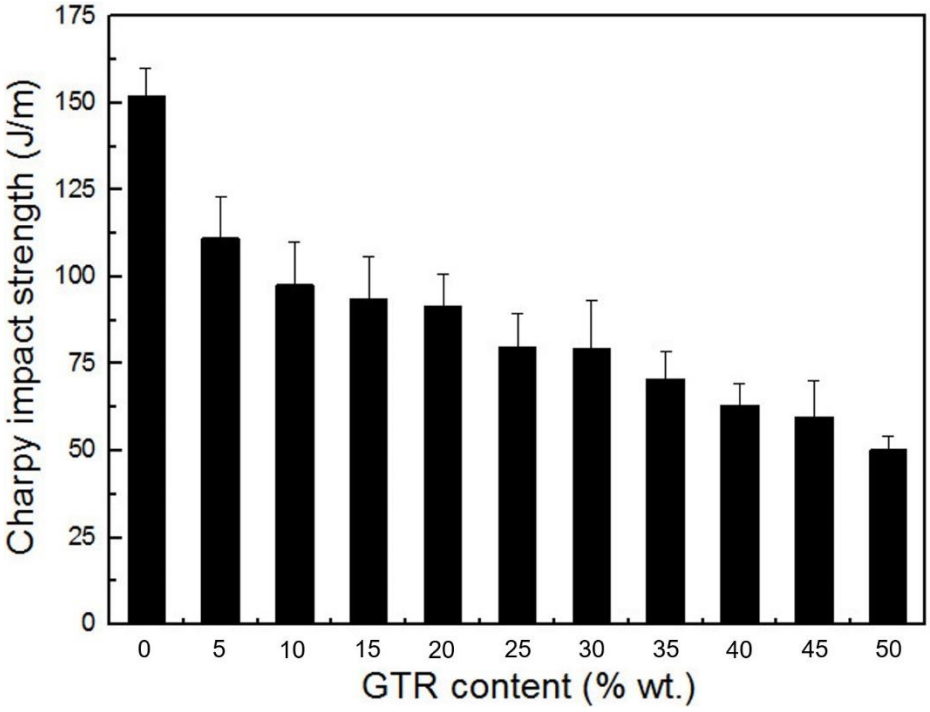

Figure 55. Impact strength of all the composites produced.

6.6 Conclusion

In this work, polypropylene/ground tire rubber (PP/GTR) composites were successfully produced by combining a dry-blending technique and a rotational molding process. After optimization of the mixing and processing conditions, the resulting composites were characterized in terms of morphology, density and mechanical properties (tensile, flexural and impact) for a wide range of GTR content (0-50% wt.).

The results showed that an increasing number and size of bubbles with more defects were generated in PP/GTR composites with increasing GTR content. Consequently, a gradual decrease of all the composites mechanical properties was observed with increasing GTR content. This behavior was directly related to the crosslinked structure of the GTR particles having low compatibility and interaction with the PP molecules due to their low chain mobility (limited entanglement possibility) and possible GTR particles agglomeration/particle-particle contact creating some defects (limited stress transfer and stress concentration points). Based on these preliminary results, potential improvement must go through improving the PP-GTR interfacial adhesion to produce better rotomolded parts with better mechanical properties. There is also the possibility to use smaller rubber particles to increase the specific surface area and improve the interfacial interactions between PP and GTR. These effects are currently being investigated.

6.7 Acknowledgements

The authors acknowledge the financial support of the National Science and Engineering Research Council of Canada (NSERC) and the Chinese Scholarship Council (CSC).

Chapter 7

Rotational molding of polypropylene with ground tire rubber

Dou Y, Rodrigue D. Rotational molding of polypropylene with ground tire rubber. Plastics, Rubber and Composites, 2020. submitted.

7.1 Résumé

Dans ce travail, du caoutchouc de pneu broyé non traité (GTR) et du GTR traité au polyéthylène maléaté (GTR/MAPE) ont été mélangés à sec avec du polypropylène (PP) pour produire des mélanges PP/GTR et PP/MAPE/GTR par rotomoulage. À partir des échantillons produits (0-50% en poids), une caractérisation complète incluant les propriétés morphologiques, physiques et mécaniques (traction, flexion et impact) a été réalisée. Les résultats ont montré que toutes les propriétés mécaniques du PP/MAPE/GTR étaient inférieures aux valeurs du PP pur en raison des propriétés élastomères du GTR. Cependant, les propriétés étaient significativement plus élevées pour le GTR/MAPE que pour le GTR pur. Par exemple, le module de traction et la résistance à la traction ont augmenté jusqu'à 57% et 76%, respectivement. De même, le module de flexion et la résistance aux chocs ont été améliorés jusqu'à 74% et 52%, respectivement. Ces résultats indiquent que le rotomoulage a été possible pour ces mélanges, menant à de bonnes propriétés mécaniques pour la gamme de paramètres étudiés.

7.2 Abstract

In this work, untreated ground tire rubber (GTR) and maleated polyethylene treated GTR (GTR/MAPE) were dry-blended with polypropylene (PP) to produce PP/GTR and PP/MAPE/GTR blends via rotational molding. From the samples produced (0-50 wt.%), a complete characterization including morphological, physical and mechanical properties (tensile, flexural and impact) was performed. The results showed that all the mechanical properties of PP/MAPE/GTR were below the neat PP values due to the elastomeric properties of GTR. However, the properties were significantly higher for GTR/MAPE compared to neat GTR. For example, the tensile modulus and tensile strength increased by up to 57% and 76%, respectively. Similarly, the flexural modulus and impact strength were improved by up to 74% and 52%, respectively. These results indicated that successful rotomolding of these blends was achieved with good mechanical properties for the range of parameters studied.

7.3 Introduction

With the ever-increasing consumption of commercial products, a large number of solid wastes are produced, causing serious environmental issues worldwide. For example, over 10 billion postconsumer tires (after their end of life) are generated annually in the world, resulting in a large amount of waste disposal problem and posing a threat to the environment [206,207]. In recent years, most developed countries released policies and regulations to limit/forbid tire landfilling and require other means to discard them. So the mechanical recycling of used tire is interesting to reuse these high amount of rubbers [208-210]. Nevertheless, waste tire rubber recycling poses important challenges since they are vulcanized; i.e. these materials have a very stable cross-linked structure which prevents their melting and reprocessing [211,212].

Currently, an interesting and efficient method to recycle used tires is to turn them into ground tire rubber (GTR), which could be incorporated into a polymer matrix to produce blends filled with GTR [213]. Several researchers have attempted to use GTR as fillers in various thermoplastics [214,215] and rubber compounds [216]. Typical examples/applications are automotives, cables, constructions and wires. However, the mechanical properties of GTR-filled thermoplastics highly depend on the concentration and nature of the components (GTR and matrix), as well as the extent of interfacial interaction between them [217]. Generally, interfacial compatibility/adhesion is a major concern for good mechanical properties. So the GTR surface should be treated/modified to improve the interfacial bonding and promote good stress transfer between the GTR particles (dispersed phase) and the thermoplastic matrix (continuous phase). This modification makes the interfaces more similar to each phase by providing specific interactions between them [35]. According to several reports [184,185], maleated polyolefins (copolymers), such as maleated polypropylene (MAPP) or maleated polyethylene (MAPE), were shown to improve the adhesion between GTR and thermoplastics because of a possible reaction between the maleic anhydride groups with unsaturated C=C bonds of the rubber molecules.

Nowadays, thermoplastics have already replaced a large number of products produced by conventional materials, such as wood and metal, for several applications like automotive, packaging and housewares [218, 219]. Among the general purpose thermoplastics, polypropylene (PP) is highly used because it combines several good physical and mechanical properties with easy processability and low cost. However, due to its relatively high glass transition temperature (Tg around 0°C) and high crystallinity, it has limited impact strength, especially at low temperature [220]. PP-GTR compounds produced by injection molding [221] or compression molding [222] have been reported

to have improved impact resistance. However, to the best of our knowledge, there is no report on the production of PP/GTR compounds by rotational molding.

Rotomolding is a polymer processing technology used to produce hollow seamless products such as tanks, automotive parts, toys, etc. [223]. Unlike most plastic processes, there is no pressure involved in rotational molding, which means that the molds can be very thin and generally inexpensive. Rotational molding can also more easily handle complex shapes with a very wide range of part sizes and thicknesses [120].

Thus, the main objective of this work is to produce PP/GTR compounds over a wide range of GTR content. In particular, GTR surface modification is performed to improve the interfacial compatibility using MAPE. Furthermore, rotational molding is used to produce the final parts, which were characterized via morphological, physical and mechanical properties.

7.4 Materials and Methods

7.4.1 Materials

The matrix was polypropylene (RMPP141 NATURAL) from PSD Rotoworx Pty Limited (Australia). This polymer has a melt flow index of 13 g/10 min (2.16 kg/230°C) and a density of 900 kg/m^3. The ground tire rubber (GTR) was supplied by Phoenix Innovation Technologies (Montreal, Canada). This material has a density of 1.16 g/cm^3. For the GTR surface treatment, xylene (laboratory purity grade) from Fisher Chemicals (USA) was used as the solvent, while the coupling agent was maleated polyethylene (MAPE) (Epolene C26, Westlake Chemicals, USA). This resin has an average molecular mass of 65 kg/mol, a melt flow index (MFI) of 8.0 g/10 min (190°C/2.16 kg), an acid number of 8.0 mg KOH/g, a density of 915 kg/m^3 and a melting point of 121°C.

7.4.2 GTR Surface Treatment with MAPE

GTR surface treatment in solution was prepared according to our previous work [224]. Firstly, 20 g of MAPE was dissolved in 900 mL of xylene at 80-90 °C under vigorous stirring. Next, 100 g of GTR was added in the solution and left under stirring for 20 min. Finally, the treated GTR (GTR/MAPE) was filtrated and dried overnight at room temperature.

7.4.3 Material Mixing

For each composition, a total of 650 g of material was used based on PP with different GTR or GTR-MAPE contents (0, 10, 20, 30, 40 and 50 wt.%). Powder mixing via dry-blending was carried out in a high speed mixer (LAR-15LMB, Skyfood, USA) at 3320 rpm for a total of 4-5 min.

7.4.4 Rotational Molding: Process and Equipment

A laboratory-scale rotational molding machine (MedKeff-Nye Roto-Lab model 22) was used for rotational molding. The parts were manufactured with an aluminum cubic mold of 3.6 mm in wall thickness and a side length of 19 cm. Before loading the material, a demolding agent (Trasys 420, DuPont, USA) was applied to the internal surface of the mold. The powder blends (PP with GTR or PP with GTR/MAPE) were then loaded into the mold to produce parts with an approximate wall thickness of 3 mm. Then, the charged mold was closed and mounted on the rotating arm. Preliminary trials were performed to determine the optimum conditions leading to homogeneous and uniform wall thickness. An oven at 270°C and a speed ratio of 1:4 with a major axis speed of 1 rpm were chosen. The heating time was fixed at 36 min. Then, the mold was removed from the oven and cooled by forced air for 25 min. Finally, the mold was opened to retrieve the part before starting another cycle.

7.4.5 Thermogravimetric Analysis

Thermogravimetric analysis was carried out on a model Q5000IR TGA analyzer (TA Instruments, USA). The scans were performed from 50 to 800°C at a rate of 10°C/min with a nitrogen flow rate of 25 mL/min.

7.4.6 Fourier Transform Infrared Spectroscopy

Infrared spectra were obtained with a Nicolet FTIR spectrometer (model 730, Nicolet Instruments, USA) equipped with a mercury-cadmium-telluride detector. The sample absorbance was measured in the IR region 4000-750 cm^{-1}. Each spectrum was obtained from 128 scans at a resolution of 4 cm^{-1}.

7.4.7 Morphological Characterization

Untreated and treated GTR particles, as well as the rotomolded composites (subjected to cryogenic fracture in liquid nitrogen) were studied by a scanning electron microscopy (SEM) (US FEI Inspect F50).

7.4.8 Density Measurement

Density data were obtained by an Ultrapyc 1200e (Quantachrome, USA) gas pycnometer. Nitrogen was used as the gas phase. The data reported are the average of five measurements with standard deviations less than 1%.

7.4.9 Mechanical Properties

The tensile properties at room temperature were measured on an Instron model 5565 universal testing machine with a 500 N load cell. Type V samples were cut in the rotomolded parts according to ASTM D638. The crosshead speed was set at 10 mm/min and the values for tensile modulus, tensile strength and elongation at break are based on the average of at least six samples.

Flexural tests (three-point bending) were performed at room temperature using a crosshead speed of 2 mm/min on an Instron universal tester model 5565 with a 50 N load cell according to ASTM D790. The span length was fixed at 60 mm. At least five rectangular samples with dimensions of 60×12.7 mm^2 were used to report the average and standard deviation for the modulus.

Charpy impact strength was determined by a Tinius Olsen (USA) testing machine model Impact 104. At least ten rectangular specimens (60×12.7 mm^2) were prepared according to ASTM D6110. The samples were notched ("V" shape) by an automatic sample notcher model ASN 120m (Dynisco, USA) at least 24 h before testing.

7.5 Results and Discussion

7.5.1 Confirmation of GTR Surface Modification

To determine if the GTR surface modification by MAPE was successfully, several characterization methods were used, such as TGA, FTIR and SEM. The thermal degradation of GTR and GTR/MAPE particles is shown in Figure 56. The main thermal decomposition of GTR (60 wt.%) under nitrogen atmosphere occurs in a temperature region between 240°C and 470°C (Figure 56a). By contrast, 70 wt.% loss of GTR/MAPE particles occurs in the temperature region between 240°C and 500°C, among which 10 wt.% loss between 480°C and 500°C is associated with the thermal degradation of the MAPE layer on the GTR surface (Figure 56a) [172].

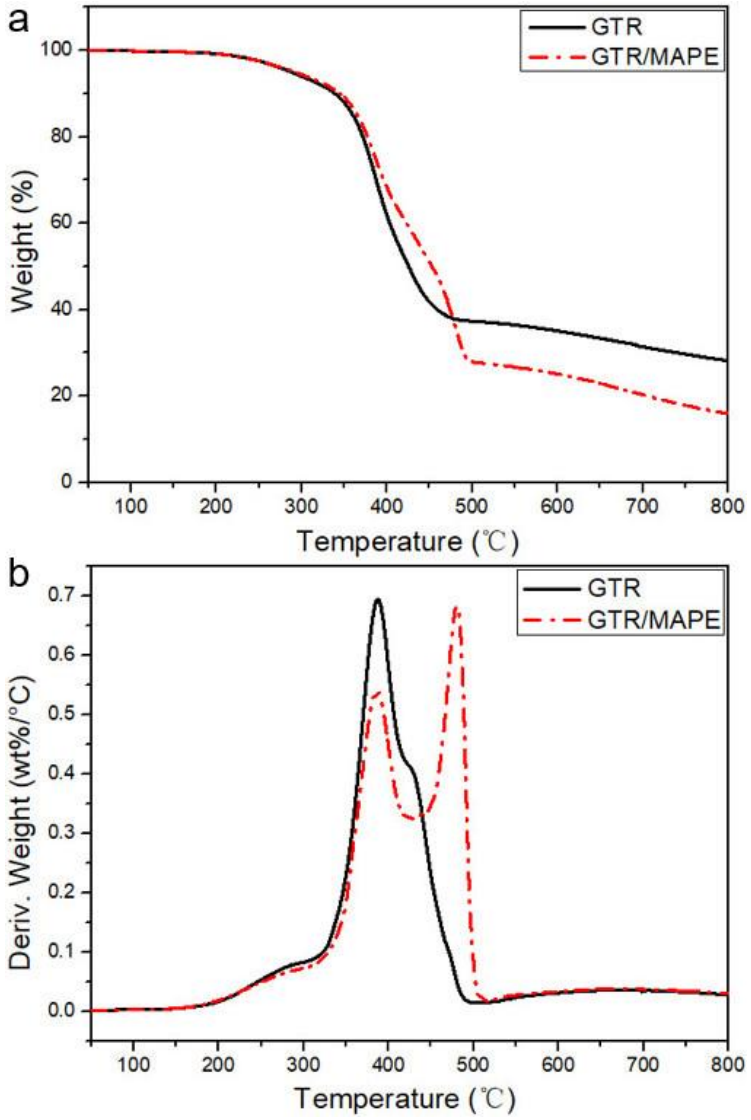

Figure 56. TGA (a) and DTG (b) curves of the GTR and GTR/MAPE particles under a nitrogen atmosphere.

In addition, Figure 56b shows the derivative thermogravimetric curves (DTG) which represent the thermal decomposition rates of the GTR and GTR/MAPE particles. For both curves, the first broad peak around 220-280°C represents the volatilization of processing oils and other low boiling-point components. Then, the main peak around 380°C belongs to the decomposition of natural rubber (NR). For GTR/MAPE particles, an intense peak around 470°C is related to the thermal decomposition of the MAPE layer on the GTR surface.

FTIR is used to further confirm the success of the GTR surface treatment, Figure 57 indicates the comparison of the FTIR spectra of GTR and GTR/MAPE particles. Obviously, the intensity increases at 2915 cm^{-1} and 2848 cm^{-1} in relation to symmetric and asymmetric aliphatic v(C–H) vibration, which confirms the increase of C-H groups at the GTR/MAPE surface due to the presence of PE in MAPE [171].

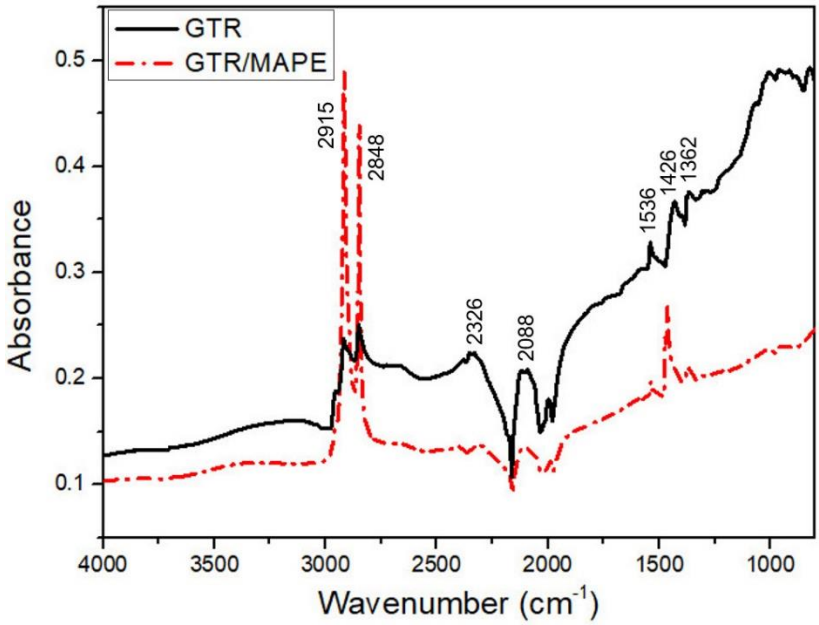

Figure 57. FTIR spectra of the GTR (black) and GTR/MAPE (red) particles.

SEM micrographs of the GTR and GTR/MAPE particles are presented in Figure 58. It can be seen that the surface of neat GTR particles (Figure 58a and 58b) is rough and covered with several smaller GTR particles, which can easily result in air bubbles trapped between these particles during rotomolding. On the other hand, the GTR/MAPE particles have a smooth surface since the smaller particles were removed by the GTR treatment (high mixing in solution and filtration). Also, the MAPE layer coated on the GTR surface (Figure 58c and 58d) eliminates surface roughness/porosity.

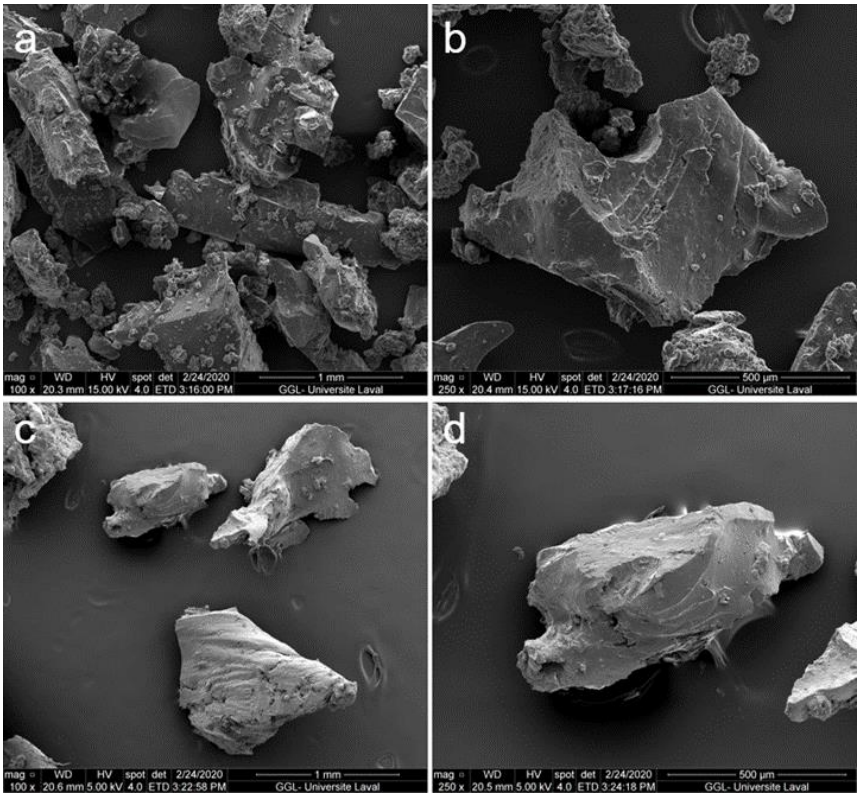

Figure 58. SEM micrographs of the GTR (first column) and GTR/MAPE (second column) particles at different magnifications.

7.5.2 Morphological Characterization

Figure 59 presents the morphologies (cross-section) of the rotomolded PP/GTR and PP/MAPE/GTR. Firstly, there is no defects in the neat PP specimen (Figure 59a), which confirms that the rotomolded parts were successfully produced using optimal processing conditions. Then, the PP-GTR images (Figure 59b, 59c, 59g, 59h and 59i) show that a growing number of bubbles and defects takes place with increasing GTR content. This behavior is associated to the low compatibility between the GTR particles and PP matrix. Interestingly, for the PP/MAPE/GTR samples (Figure 59e, 59f, 59j, 59k and 59l), both the number and the size of bubbles/defects substantially decreased compared with their PP/GTR counterparts. Finally, Figure 59d and 59e illustrate that the rubber phase has a good physical contact with the PP matrix. Accordingly, these observations confirm that the GTR and PP interfacial adhesion/compatibility was improved by the MAPE surface treatment.

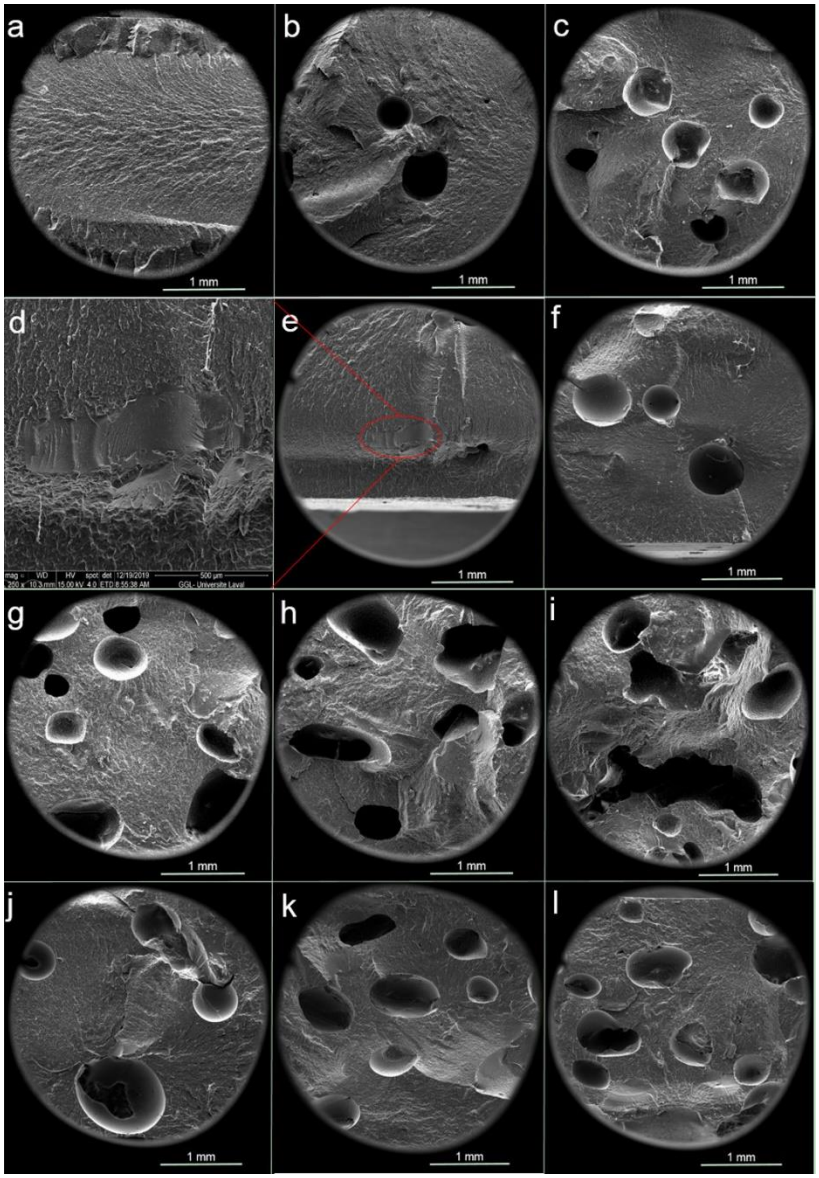

Figure 59. SEM of the rotomolded specimens cross-section with different rubber contents: (a) neat PP, (b) 10% GTR, (c) 20% GTR, (e) 10% GTR/MAPE, (f) 20% GTR/MAPE, (g) 30% GTR, (h) 40% GTR, (i) 50% GTR, (j) 30% GTR/MAPE, (k) 40% GTR/MAPE, (l) 50% GTR/MAPE.

7.5.3 Density Measurement

The density of all the samples is reported in Figure 60 together with the raw material (neat PP, GTR and GTR/MAPE) values. The GTR density increased after being functionalized with MAPE in solution. This increase is associated with some interactions between MAPE and GTR particles and also possible particle shrinkage due to low molecular weight compounds being extracted [179]. Accordingly, compared with the density of PP/GTR composites, the density of PP/MAPE/GTR

composites slightly increases with increasing GTR/MAPE content. This can be explained by the reduced number of bubbles and defects in PP/MAPE/GTR compared to PP/GTR, as shown in Figure 58. Because the number of bubbles and defects increases with filler content, the density of both types of compounds decreased up to 30%. However, the density finally increased with increasing filler content up to 50%. This effect represents a balance between the number of voids generated with increasing GTR content versus the GTR higher density compared to PP (Figure 60).

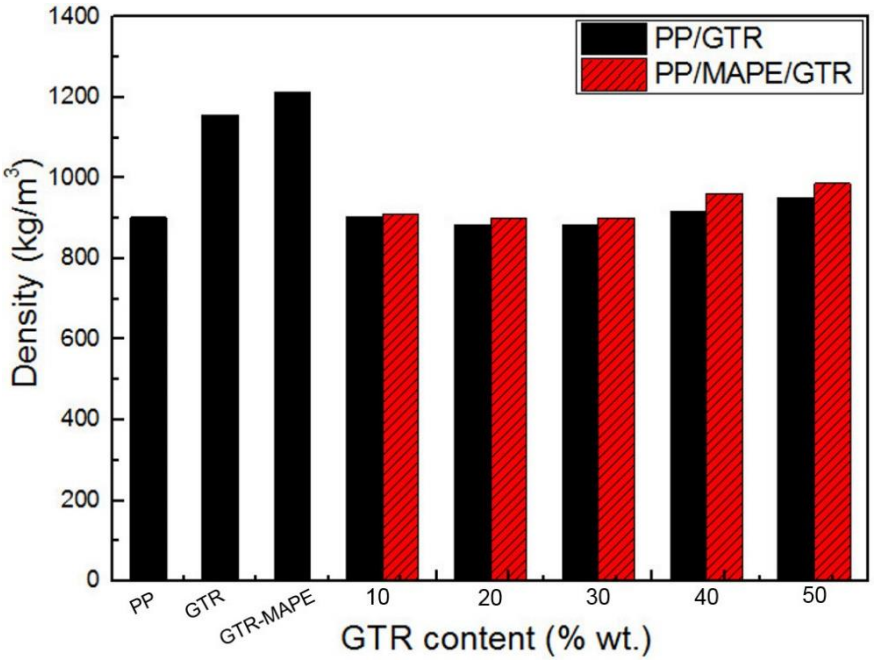

Figure 60. Density of neat PP, GTR and GTR/MAPE particles, as well as the rotomolded samples with different GTR and GTR/MAPE contents.

7.5.4 Tensile Properties

The tensile moduli of PP/GTR and PP/MAPE/GTR composites are presented in Figure 61 to compare with the tensile modulus of neat PP (785.4 MPa). For both types of rotomolded composites, the tensile moduli tend to drop with increasing filler content due to the presence of bubbles and defects (Figure 59), as well as the lower rigidity of the rubber particles (about 2 MPa) compared to the PP matrix [146]. Figure 60 also clearly shows that the tensile moduli of PP/MAPE/GTR composites are higher than those of PP/GTR composites because of the MAPE effect (less defects and voids). For example, the tensile modulus of PP/GTR with 50 wt.% GTR is 85.9 MPa compared with 202.5 MPa for PP/MAPE/GTR at 50 wt.% which represents a 57.6% increase.

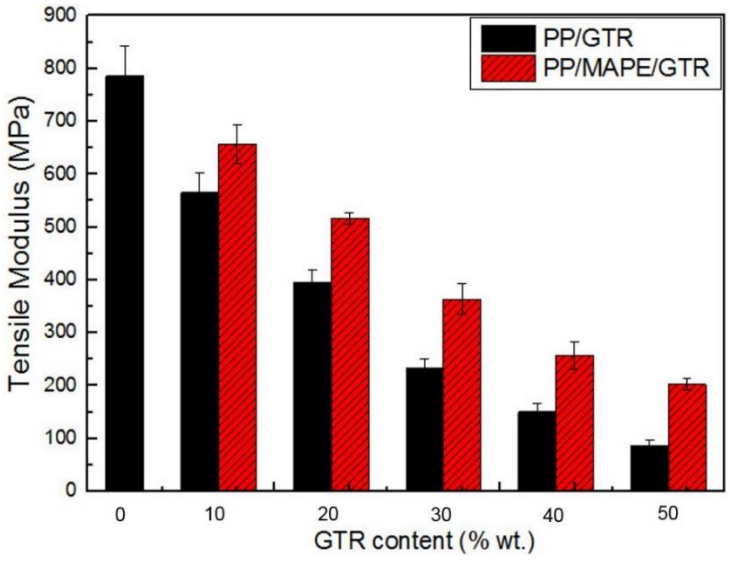

Figure 61. Tensile modulus of neat PP, PP/GTR and PP/MAPE/GTR compounds.

Figure 62 compares the tensile strength of all the samples with respect to the neat PP. For all the compounds, lower tensile strength than the neat PP (20.2 MPa) are obtained. Nevertheless, the tensile strength of PP/MAPE/GTR compounds are significantly higher than for PP/GTR ones having the same filler content. This observation is attributed to the presence of MAPE on the GTR surface enhancing the interfacial strength resulting in better stress transfer from the matrix to the GTR [184]. For example, the tensile strength increases by 76% for PP/MAPE/GTR with 50 wt.% GTR/MAPE compared to PP/GTR with the same GTR content.

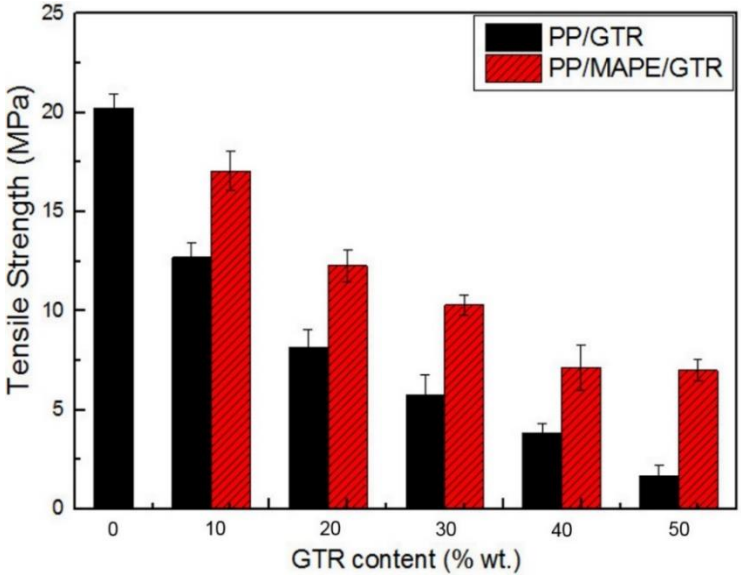

Figure 62. Tensile strength of neat PP, PP/GTR and PP/MAPE/GTR compounds.

The elongation at break of PP/GTR and PP/MAPE/GTR samples is reported Figure 63 and compared to the neat PP values (154.5%). Since some defects are observed in rotomolded parts with GTR or GTR/MAPE addition, a substantial reduction of the elongation at break occurs for all the compounds. This is also related to the lower elongation of the GTR particles being highly crosslinked. However, the values for PP/MAPE/GTR are slightly higher than for PP/GTR due to the effect of MAPE. For example, at 50 wt.%, the elongation at break of PP/MAPE/GTR is 22% while being only 14% for PP/GTR.

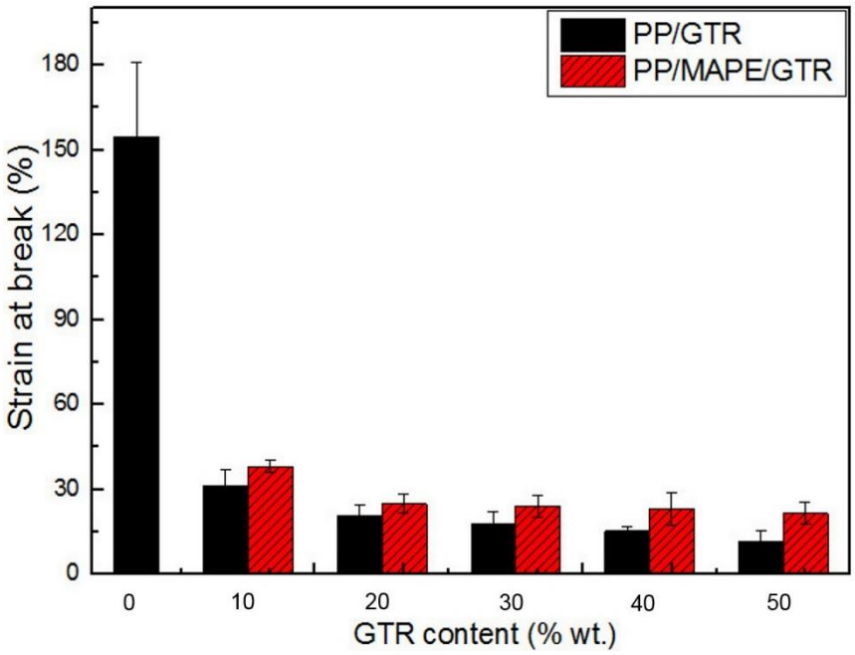

Figure 63. Elongation at break of neat PP, PP/GTR and PP/MAPE/GTR compounds.

7.5.5 Flexural Properties

Figure 64 reports the flexural modulus of all the samples produced. As expected, the highest flexural modulus was obtained for the neat PP (1145 MPa). The results also show that the flexural modulus has a similar decreasing trend as the tensile modulus (Figure 61) with increasing GTR content. Once again, the MAPE treatment improved the values. For example, at 50 wt.%, the flexural modulus increased from 71.4 MPA for GTR to 281.4 MPa for GTR/MAPE, which represents 74.6% increase.

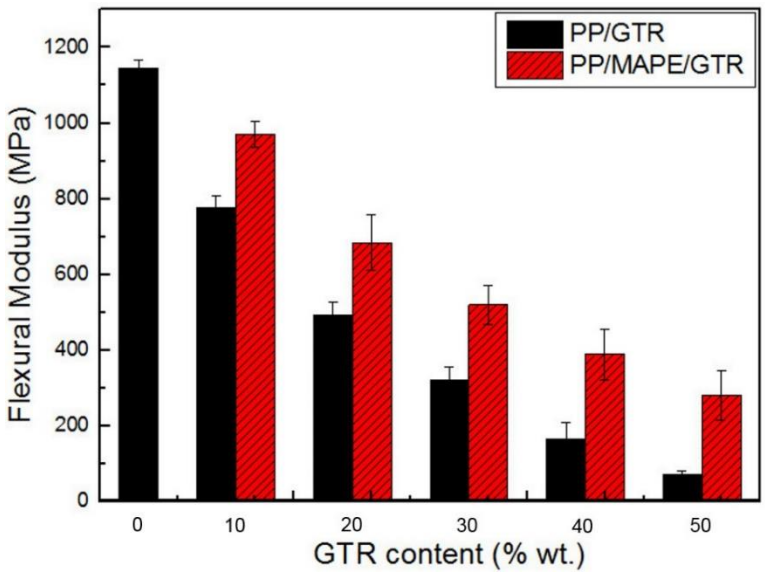

Figure 64. Flexural modulus of neat PP, PP/GTR and PP/MAPE/GTR compounds.

7.5.6 Impact Strength

Impact strength results are presented in Figure 65. Compared to neat PP, the poor adhesion between GTR and PP induces the formation of important defects (holes, voids and interfacial gaps in Figure 59), which finally results in a decrease of impact strength of PP/GTR composites with increasing GTR content. For example, the impact strength decreases from 152.0 J/m for neat PP to 50.2 J/m for PP/GTR at 50 wt.% GTR content, which represents a 67% decrease. Interestingly, the impact strength of PP/MAPE/GTR composites significantly increases after incorporating by GTR/MAPE. For example, a 52% improvement for PP/MAPE/GTR was obtained compared to GTR at the same content (50 wt.%). This observation is attributed to a reduction in interfacial tension and better interfacial adhesion due to the MAPE treatment, allowing the GTR-PP interface to withstand a higher stress level before particle debonding (pull-out) [225]. The highest impact strength (139.3 J/m) was obtained from PP/MAPE/GTR with a 30 wt.% rubber content, which is similar to our previous work on LLDPE/MAPE/GTR composites produced by rotational molding at a 30 wt.% GTR content with the highest impact strength [224]. However, the highest impact strength of PP/MAPE/GTR is still slightly lower than that of the neat PP (151.9 J/m). This shows that the surface modification of GTR with MAPE is not fully effective to significantly improve the impact performances of the neat PP produced by rotational molding and more work is needed to improve on these results. Nevertheless, a high GTR content can be introduced, which improves the carbon footprint of the resulting compounds.

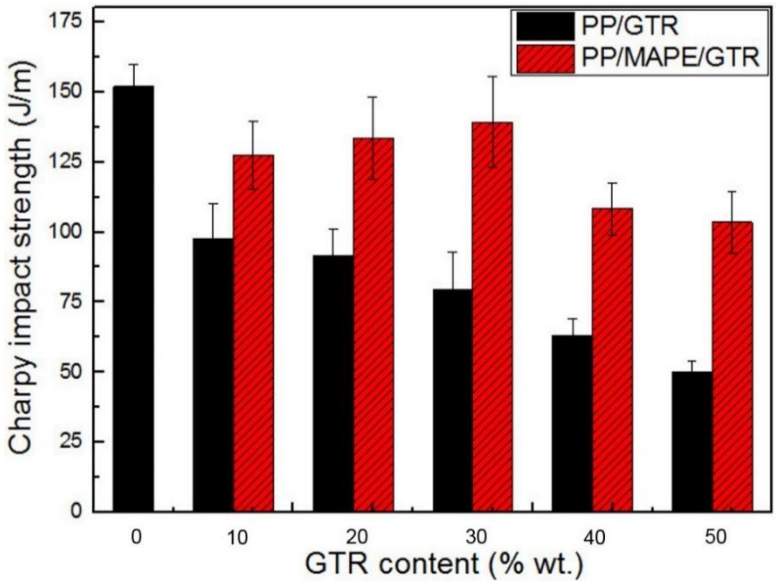

Figure 65. Impact strength of neat PP, PP/GTR and PP/MAPE/GTR compounds.

7.6 Conclusion

In this study, ground tire rubber (GTR) was firstly modified by 2 wt.% maleated polyethylene (MAPE) in solution. Then, different concentrations (0-50 wt.%) were introduced into a rotomolding grade of polypropylene (PP). After some preliminary trials, good samples were successfully produced by combining a simple dry-blending technique and rotational molding procedure. Based on the parts manufactured, their morphology, density and mechanical properties (tensile, flexural and impact) were studied.

The results showed that the GTR surface was successfully modified by MAPE as confirmed by TGA, FTIR and SEM. In addition, SEM micrographs showed that the number and size of defects were substantially reduced in PP/MAPE/GTR compounds comparison with PP/GTR ones. Consequently, the interfacial adhesion between GTR and PP matrix was improved by introducing MAPE.

All the mechanical properties decreased with increasing GTR content due to the low modulus and highly elastic nature of the rubber particles. Nevertheless, the properties of PP/MAPE/GTR compounds were significantly higher than PP/GTR ones. Tensile modulus (57.6%) and tensile strength (76%) improvements were observed, while the flexural modulus (74.6%) and impact strength (52%) showed similar increases. Although good samples were produced with promising properties, future work should focus on further improvement of the PP/GTR interfacial adhesion to produce

rotomolded compounds with better mechanical properties for the development of new rotomolding materials and applications.

7.7 Acknowledgements

The authors acknowledge the financial support of the National Science and Engineering Research Council of Canada (NSERC) and the Chinese Scholarship Council (CSC). Polypropylene samples from 4ROTO LLC (USA) and ground tire rubber from Phoenix Innovation Technologies were highly appreciated for this experimental work.

Chapter 8

Morphological, thermal and mechanical properties of polypropylene foams via rotational molding

Dou Y, Rodrigue D. Morphological, thermal and mechanical properties of polypropylene foams via rotational molding. Cellular Polymers, 2021. DOI: 10.1177/02624893211018825.

8.1 Résumé

Dans ce travail, le polypropylène (PP) a été expansé par moulage par rotation à l'aide d'un agent gonflant chimique (CBA) à base d'azodicarbonamide sur une plage de concentration (0 à 0,5 % en poids). Les échantillons ont ensuite été analysés en termes de propriétés morphologiques, thermiques et mécaniques. L'analyse morphologique a montré une augmentation continue de la taille moyenne des cellules et de la densité cellulaire avec l'augmentation de la teneur en CBA. L'augmentation de la teneur en CBA a également entraîné une diminution de la densité de la mousse et de la conductivité thermique. De même, toutes les propriétés mécaniques (tension, flexion et impact) se sont avérées diminuer avec l'augmentation de la teneur en CBA. Enfin, l'efficacité du processus de rotomoulage a été évaluée en produisant des échantillons de PP purs par moulage par compression. Les résultats ont montré des différences négligeables entre les propriétés rotomoulées et moulées par compression à faible déformation et taux de déformation indiquant que les conditions optimales de rotomoulage ont été sélectionnées.

8.2 Abstract

In this work, polypropylene (PP) was foamed via rotational molding using a chemical blowing agent (CBA) based on azodicarbonamide over a range of concentration (0 to 0.5% wt.). The samples were then analyzed in terms of morphological, thermal and mechanical properties. The morphological analysis showed a continuous increase in the average cell size and cell density with increasing CBA content. Increasing the CBA content also led to lower foam density and thermal conductivity. Similarly, all the mechanical properties (tension, flexion and impact) were found to decrease with increasing CBA content. Finally, the efficiency of the rotomolding process was assessed by producing neat PP samples via compression molding. The results showed negligible differences between the rotomolded and compression molded properties at low deformation and rate of deformation indicating that optimal rotomolding conditions were selected.

8.3 Introduction

Recently, scientific and industrial research increasingly focused on foamed thermoplastic materials, which are composed of a cellular core structure generated by the expansion of a blowing agent inside a thermoplastic matrix. This cellular structure allows the foams to be economically used in a wide variety of applications including automotive parts, protective equipment, building and construction, packaging industry and electromagnetic wave insulators [226-228]. Additionally, foamed plastics present excellent cost to performance and strength to weight ratios compared with their unfoamed analogues because of their tunable weight reduction [229, 230].

Foamed polystyrene (PS) and polyethylene (PE) products have been commercially available for decades. However, their usefulness is limited due to their low heat deflection temperature [231]. When PS foams are heated above their glass transition temperature (Tg) around 100°C, they become soft and deform [232]. Similarly, foamed PE is rarely used above 100°C because of its low melting point (110-130°C) [233]. Consequently, PS and PE foams are not suited for applications requiring elevated service temperature environments like contact with boiling water or sterilization processes. To overcome these PS and PE foams limitations at low cost, polypropylene (PP) foams attracted more and more attention recently. Firstly, the cost of PP has been 15-20% more competitive for the last decade compared to PE [235]. Polypropylene, being a semi-crystalline polymer, enables to provide good flexibility and toughness, while having higher moduli and strengths. Secondly, PP offers better impact resistance than PS because PP is in a rubbery state at room temperature. Thirdly, due to its high melting point (160-175°C), high heat deflection temperature and service temperature is provided [234]. Finally, PP has good chemical resistance (solvents, acids and bases) [235-237]. Therefore, benefiting from these advantages, PP foams have great potential for applications in the food and automotive industries.

So far, some studies have been conducted on PP foams manufactured by injection molding [238-241], compression molding [242-244] and extrusion molding [245, 247]. For example, Ahmadi and Hornsby reported how the structure of PP foams was influenced by the injection molding processing conditions [238]. The effect of injection speed, shot weight, mold temperature and melt temperature were investigated. The results showed that PP foams produced using a high injection rate, a low melt temperature and a high melt pressure exhibited a more uniform and finer cellular core structure. Mechraoui et al. [242] produced PP foams by compression molding using different azodicarbonamide (ADC) concentrations (1.5, 2, 2.5 and 3% wt.) as a chemical blowing agent (CBA). As expected, the cell density, skin thickness and foam density decreased with increasing CBA content. The mechanical properties followed the foam density trend as less materials is available to support the applied loads.

In the last decades, the rotational molding technology gradually became one of the fastest-growing polymer processes in the plastic industries. This technology is a low-stress/shear process aiming at producing stress-free and seamless hollow plastic articles such as containers, tanks, toys, medical equipment and several similar products over a very wide range of dimensions and shapes [100, 114, 224, 247-250]. More recently, rotational molding was developed to process foamed parts. But very few works have been published on PP foams produced by rotational molding [251, 252]. Pop-Iliev and Park selected different PP grades in terms of melt flow rates (5.5 to 35 dg/min) to produce PP foams via rotational molding [251]. It was observed that lower melt flow rates produced better fine-cell morphology and good expansion uniformity. Pop-Iliev et al. [252] investigated how the narrow interval between the melting temperature of PP and the onset decomposition temperature of a CBA influenced the rotomolded PP foam structures. They concluded that desirable PP foam structures can only be achieved when PP sintering took place prior to the CBA decomposition to limit gas losses and the processing temperature kept low to limit cell coalescence. However, to the best of our knowledge, no studies reported the thermal and mechanical properties of PP foams manufactured by rotational molding.

The main objective of this work is to produce foamed and unfoamed rotomolded parts based on polypropylene. In particular, the effect of chemical blowing agent content is investigated to determine its relationship with foam density and cellular structure (cell size and cell density), as well as to determine its effect on the thermal (conductivity) and mechanical (tensile, flexural and impact) properties of PP foams. Finally, to confirm if optimal rotomolding conditions were selected, neat PP samples are also produced by compression molding to compare the properties obtained between both processing methods.

8.4 Materials and Methods

8.4.1 Materials

The matrix selected was polypropylene (RMPP141 NATURAL) from PSD Rotoworx Pty Limited (Australia). This polymer has a melt flow index of 13 g/10 min (2.16 kg/230 °C) and a density of 900 kg/m^3. For foaming, an exothermic chemical blowing agent (CBA) based on activated azodicarbonamide was used: Celogen 754A (powder) from Chempoint (USA). Its peak decomposition temperature is 164 °C as determined via DSC.

8.4.2 Rotational Molding

A series of PP foams were prepared by using different CBA contents (0.1, 0.2, 0.3, 0.4 and 0.5% wt.) to compare with the unfoamed matrix (0% wt.). As the CBA must be thoroughly dispersed in the PP powder prior to charging the mold, all the materials were dry-blended in a high-speed mixer LAR-15LMB (Skyfood, USA) at 3320 rpm with fixed intervals of 1 min mixing time and 1 min cooling time repeated 5 times. A laboratory-scale biaxial rotomolding machine was used (MedKeff-Nye Roto-Lab model 22, Barberton, OH, USA). The parts were produced with a cubic aluminum mold (3.6 mm wall thickness and 19 cm internal side length). A demolding agent (Trasys 420, DuPont, Midland, MI, USA) was applied to the internal mold surface and a circular vent (10 mm diameter) was filled with glass wool to prevent powder losses. After preliminary trials, the optimum processing conditions were: a 3:4 speed ratio (major axis:minor axis), a heating time of 36 min with an electrically heated oven temperature of 270 °C and a cooling time of 30 min with forced air convection. For each characterization, the samples were directly cut in the molded parts (Figure 66). Each sample was based on 660 g leading to final part thickness between 3.0 and 5.4 mm depending on the CBA concentration (expansion ratio).

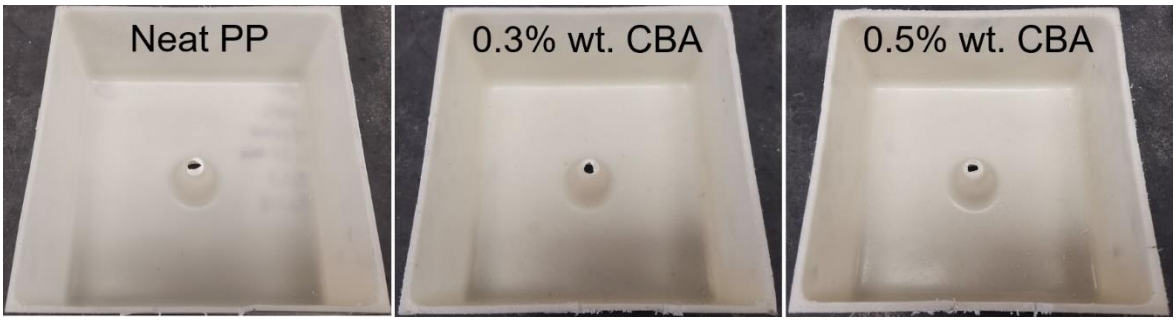

Figure 66. Typical examples of the rotomolded PP parts (cut samples).

8.4.3 Compression molding

Compression molded PP parts were produced using 40 g of powder placed in a rectangular mold (110 × 110 × 3 mm^3). An automatic Carver hydraulic press model Autoseries 3893 (Carver Inc., USA) at 190 °C with a constant force of 2200 kg for 10 min was used before mold cooling to 60 °C via water circulation before removing the pressure and demolding.

8.4.4 Differential scanning calorimetry

Differential scanning calorimetry (DSC) studies were performed on a DSC-7 from Perkin-Elmer (USA) equipped with a thermal analysis controller TAC7/DX. About 15 mg was placed in sealed aluminum pans. The tests were performed between 50 and 220 °C at 10 °C/min under a flow of dry nitrogen (20 mL/min). The first heating cycle for PP was used to erase its thermal history and was not analyzed.

8.4.5 Morphological characterization

The samples were cryogenically fractured (liquid nitrogen) and images of the cross-sections were taken by a scanning electron microscope (SEM) (FEI Inspect F50, USA). The average cell size (D) including standard deviation was determined by the ImageJ software (US National Institutes of Health, USA), while the cell density (N_f), the number of cells per cubic centimeter of foam, was determined as [253]:

$$N_f = \left(\frac{n}{A}\right)^{3/2} \quad (2)$$

where n is the number of cells in a micrograph and *A* is the area of the micrograph in cm^2.

8.4.6 Density and hardness

The density was determined by cutting each sample into cubes. The dimensions were measured with a digital caliper (Mastercraft, Canada) with a resolution of 0.01 mm, while the weight was obtained from a MX-50 moisture analyzer (A&D, Tokyo, Japan), and compared with a gas (nitrogen) pycnometer Ultrapyc 1200e (Quantachrome Instruments, USA). The hardness (Shore A and Shore D) was measured by a PTC Instruments (USA) Model 306L and Model 307L following ASTM D2240, respectively. The results are the average and standard deviation of at least 5 repetitions.

8.4.7 Thermal conductivity

The thermal conductivity (*k*) was determined by a home-made thermal conductivity analyzer based on ASTM E1225. The rotomolded parts were cut (50 × 50 mm^2) and their thickness (L ± 0.01 mm) was measured using a digital caliper (Mastercraft, Canada). Each sample was placed between thin aluminum sheets (low thermal resistance) and the plate temperature (top = T_h) and (bottom = T_c) were fixed at 33 °C and 13 °C respectively to give a 20 °C difference (ΔT) with a 23 °C (room temperature) average. The temperatures were controlled by water cooled Pelletier plates (Model K20, Haake,

Germany) and measured by thermistances (TC-720, TE-Technology, USA), while the equilibrium heat flux (Q) was obtained by a PHFS-01 heat flux sensor (Flux Teq LLC, USA). The data reported represent an average of three repetitions with standard deviations. The thermal conductivity was determined as:

$$k = \frac{Q\,L}{\Delta T} \tag{3}$$

8.4.8 Mechanical properties

Tensile properties were determined according to ASTM D638 (type V) on an Instron (USA) 5565 with a 500 N load cell. The crosshead speed was 10 mm/min and the values (tensile modulus, tensile strength and elongation at break) are the average of six samples (± one standard deviation).

Flexural (three-point bending) tests according to ASTM D790 were done using a crosshead speed of 2 mm/min on an Instron (USA) 5565 with a 50 N load cell and a 60 mm span. Five samples (60 × 12.7 mm^2) were used to report the average and standard deviation of the flexural modulus.

Charpy impact strength was obtained from a Tinius Olsen (USA) Impact 104. Ten specimens (60 × 12.7 mm^2) were prepared according to ASTM D6110. The samples were "V" notched on an automatic sample notcher ASN 120m (Dynisco, USA) at least 24 h before testing.

All the measurements were done at room temperature (23 °C).

8.5 Results and Discussion

8.5.1 Differential scanning calorimetry

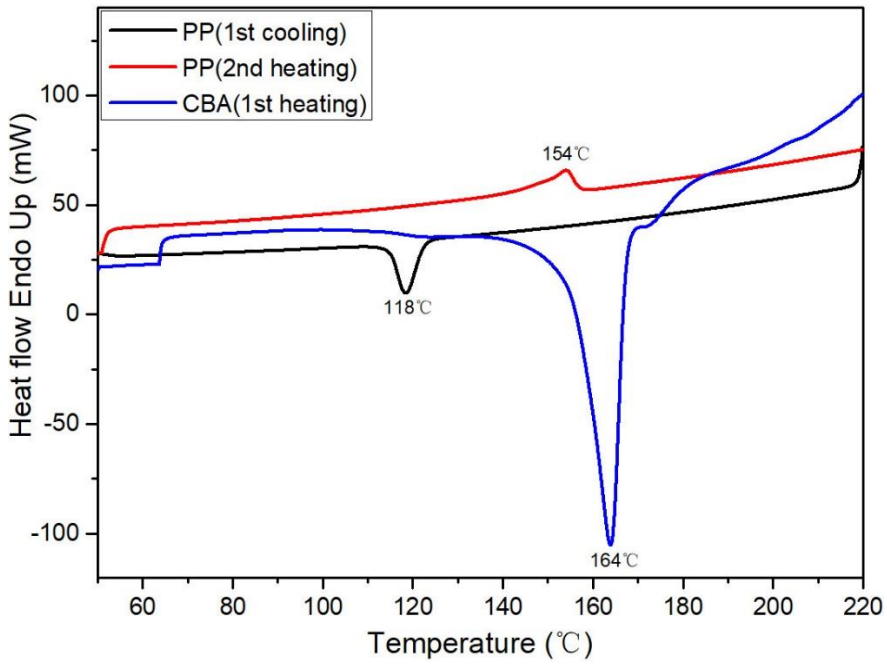

Figure 67. DSC thermograms of the PP and CBA used.

The DSC thermograms of PP and CBA are presented in Figure 67. The cooling and second heating cycle of PP show a peak melting temperature of 154 °C and a crystallization peak temperature of 118 °C. Figure 67 also shows that the CBA onset decomposition temperature is about 140 °C with a peak decomposition temperature of 164 °C. In this case, the onset of PP melting and CBA decomposition occurs at the same time leading to possible loss of gas. However, setting the oven temperature at 270 °C for the rotomolding heating cycle enables a complete PP melt and CBA decomposition.

8.5.2 Morphological characterization

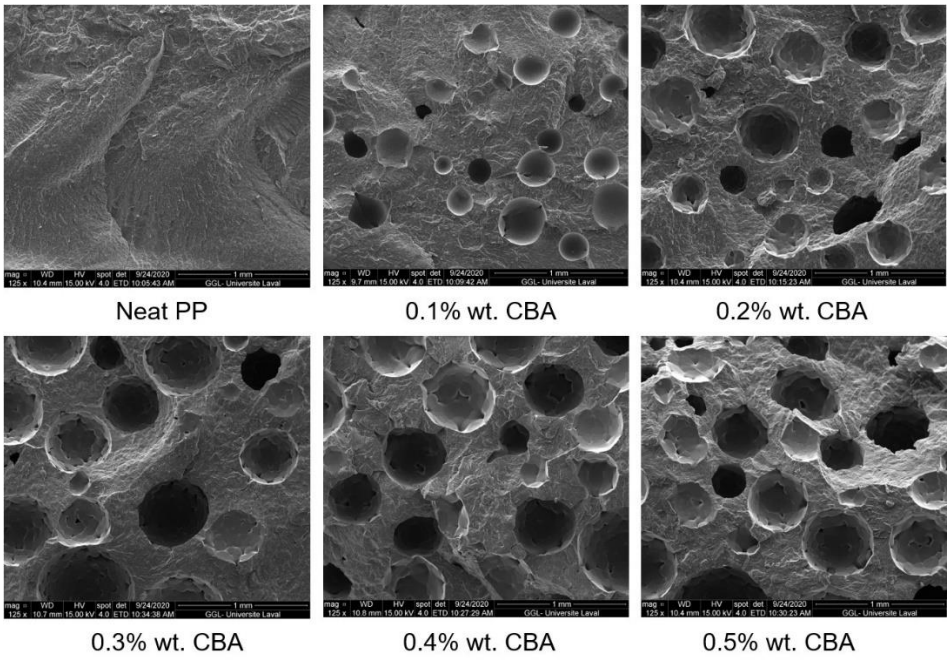

Figure 68. Typical morphologies of the rotomolded PP foams with different CBA contents.

Table 5. Average cell size and cell density of PP foams.

CBA content (% wt.)	Average cell diameter (μm)	Cell density (10^3/cm^3)
0.1	212±95	7.0
0.2	289±117	7.6
0.3	298±118	9.4
0.4	326±74	9.8
0.5	331±123	11.1

SEM images for the foams with different CBA contents at low magnification (125x) are presented in Figure 68. From these images and their quantitative analysis, the average cell size and cell density are compared in Table 5. As expected, both parameters increase with increasing CBA content since more gas is available to blow the nucleated cells. For example, D increases from 0.212 to 0.331 mm, while N_f increases from 7.0x10^3 to 11.1x10^3 cells/cm^3 when the CBA content increases from 0.1% to 0.5% wt.

8.5.3 Density and hardness

Figure 69 presents the density of the neat PP and the PP foams as a function of CBA content. Compared with the density of the rotomolded PP sample (0.908 g/cm^3), the compression molded one has a slightly higher density with 0.912 g/cm^3 resulting from the high pressure generating a more compact structure. With increasing CBA content up to 0.5% wt., the density decreases from 0.908 to 0.631 g/cm^3 (31% reduction). Table 6 and Figure 69 show the hardness (Shore A and Shore D) of the neat PP and the PP foams as a function of CBA content, respectively. Based on the results of Table 6, similar hardness values of neat PP are obtained for the compression molded and the rotomolded samples. For the PP foams produced by rotomolding, an increase in the CBA content decreases the hardness values. For example, the Shore A decreases from 97.0 to 88.5 (8.5 points difference), while the Shore D decreases from 76.4 to 38.0 (38.4 points difference). Lower foam hardness is expected due to decreasing cell wall thickness (increasing cell size and cell density in Table 5) combined with a "softer" nature of the gas cells using more space inside the PP matrix.

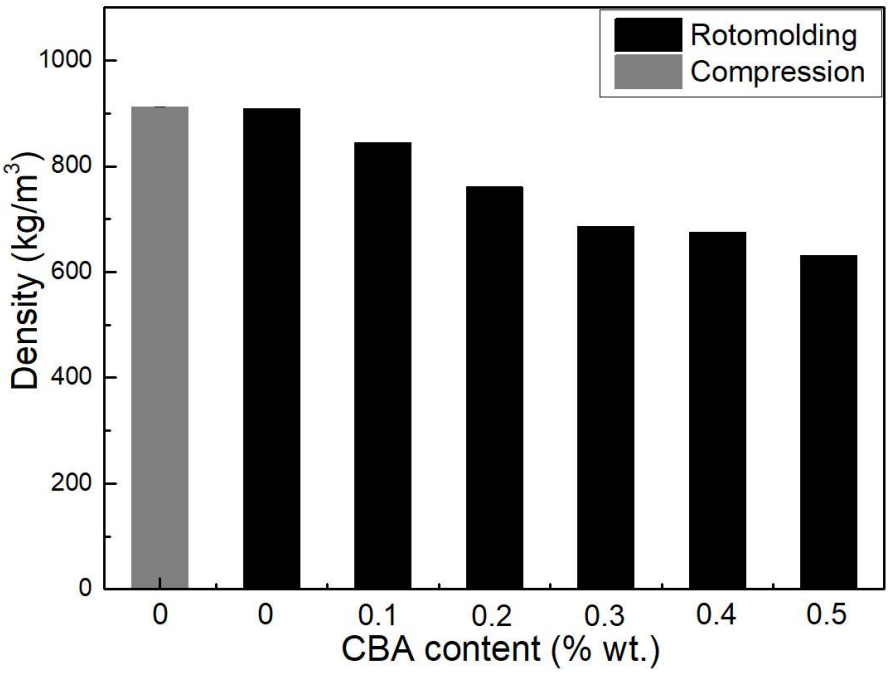

Figure 69. Density of PP and the foams as a function of CBA content.

Table 6. Hardness (Shore A and Shore D) of neat PP samples.

PP sample	Shore A	Shore D
Compression molding	97.5±0.7	77.3±0.9
Rotational molding	97.0±1.3	76.4±1.4

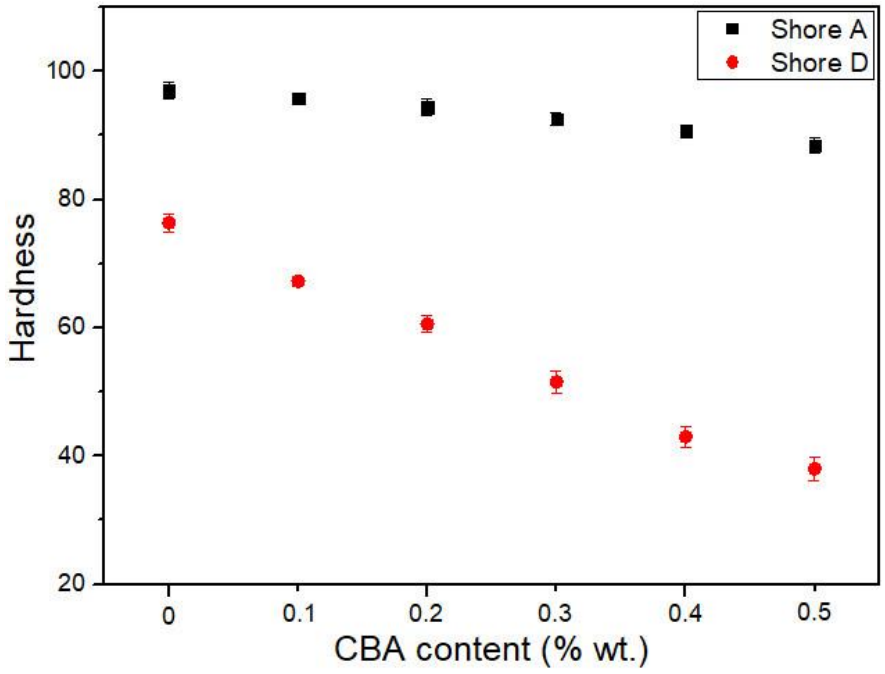

Figure 70. Hardness (Shore A and Shore D) of PP foams as a function of CBA content.

8.5.4 Thermal conductivity

Table 7 presents the thermal conductivity results. The neat PP produced by rotomolding has a value of 145 mW/m·K which is similar to the sample produced by compression molding (149 mW/m·K). This result is in agreement with the reported thermal conductivity for PP (ranging from 0.10 to 0.22 W/m·K) in the literature [254]. As expected, increasing the CBA content slightly decreases the thermal conductivity with the lowest value (104 mW/m·K) at 0.5% wt. CBA. This trend is similar as for foam density in Figure 68 indicating a direct correlation between both parameters.

Table 7. Thickness (*L*) and thermal conductivity (*k*) of the PP samples.

CBA content (% wt.)	*L* (mm)	*k* (mW/m·K)
0[c]	2.31	149±5
0[r]	2.97	145±6
0.1	3.44	143±5
0.2	3.76	132±6
0.3	4.20	118±4
0.4	4.76	110±5
0.5	5.37	104±4

c : compression molded
r : rotational molded

8.5.5 Flexural properties

Figure 71 presents the flexural modulus of the neat PP and the foams. The value for the compression molded sample is 1105±20 MPa which is slightly higher than the rotomolded one (998±28 MPa). This might be related to the high pressure involved in compression molding leading to a better compaction (closer packing) and sintering of the particles leading to higher rigidity. Nevertheless, the values decrease with increasing CBA content. For example, the flexural modulus is 337 MPa at 0.5% wt. CBA which represents a 66% decrease. Lower values for foams are related to less material being available (decreasing density in Figure 69) to sustain the applied stress [255].

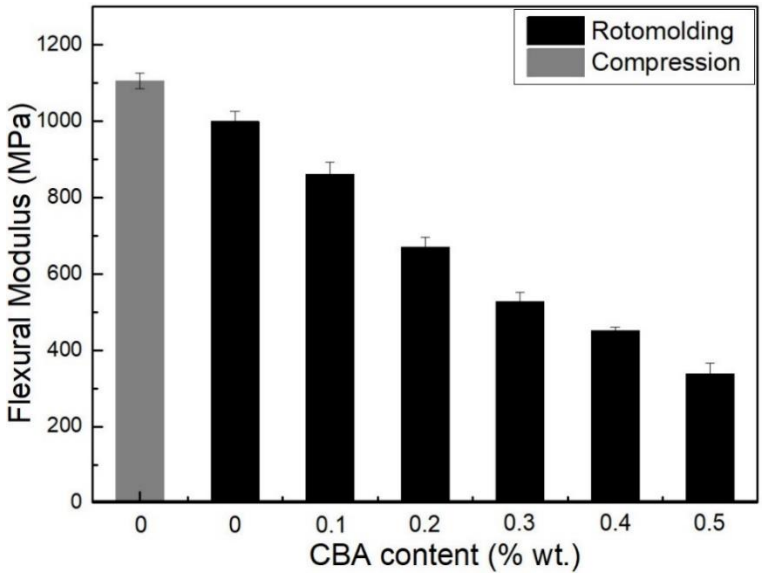

Figure 71. Flexural modulus of PP and the foams as a function of CBA content.

8.5.6 Tensile properties

For the tensile modulus (Figure 72), no significant difference between the compression molded (795±56 MPa) and rotomolded (765±41 MPa) samples was observed, while the same conclusion applies for the tensile strength (Figure 73) with values of 20.9±0.2 MPa and 20.2±0.7 MPa, respectively. However, the elongation at break (Figure 74) of the compression molded PP (1232±113%) is much higher than that of the rotomolded one (155±27%). This difference may be associated with the absence of pressure applied during rotomolding resulting in a looser molecular packing and a higher number of microvoids in the samples, which can be explained by the density difference between compression molding and rotomolding (Figure 69) [256]. These results indicate that differences between both processing methods (compression molding vs. rotomolding) are mainly important at higher deformation (elongation at break) compared to lower deformation (elastic modulus and maximum stress).

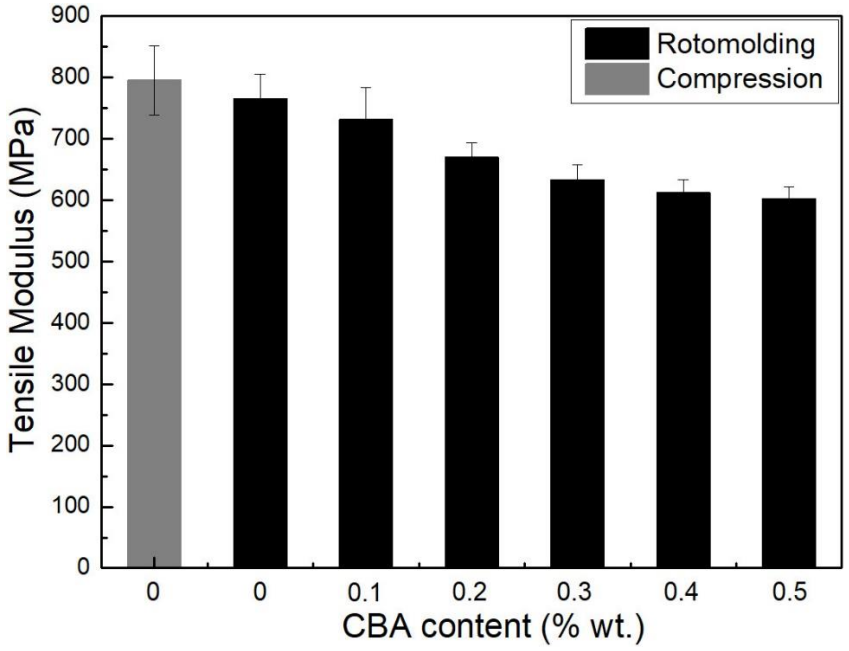

Figure 72. Tensile modulus of PP and the foams as a function of CBA content.

For the rotomolded foams, the tensile modulus (Figure 72) presents a similar trend as for the flexural modulus (Figure 71). The values decrease by 21% (from 765 to 602 MPa) with the addition of 0.5% CBA. Figure 73 also reveals that the tensile strength decreases with increasing CBA content, for the same reasons as for the flexural modulus. The tensile strength of the unfoamed matrix (20.2 MPa) decreased to 7.4 MPa (63% lower) at 0.5% wt. CBA. Finally, Figure 74 compares the elongation at break. Again, the values decrease with increasing CBA content and are all well below 100% (30% to

60%). All these results are in agreement with other studies reporting decreasing moduli, strengths and elongations at break with decreasing density [257].

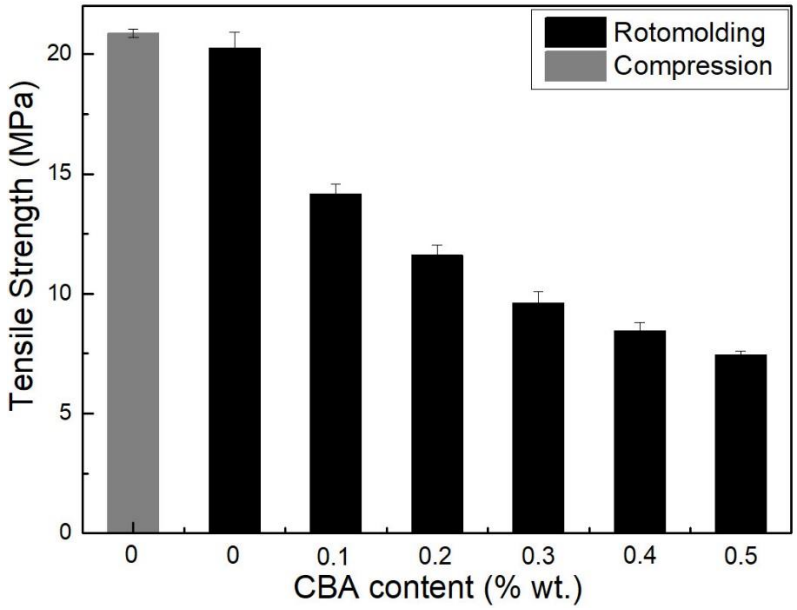

Figure 73. Tensile strength of PP and the foams as a function of CBA content.

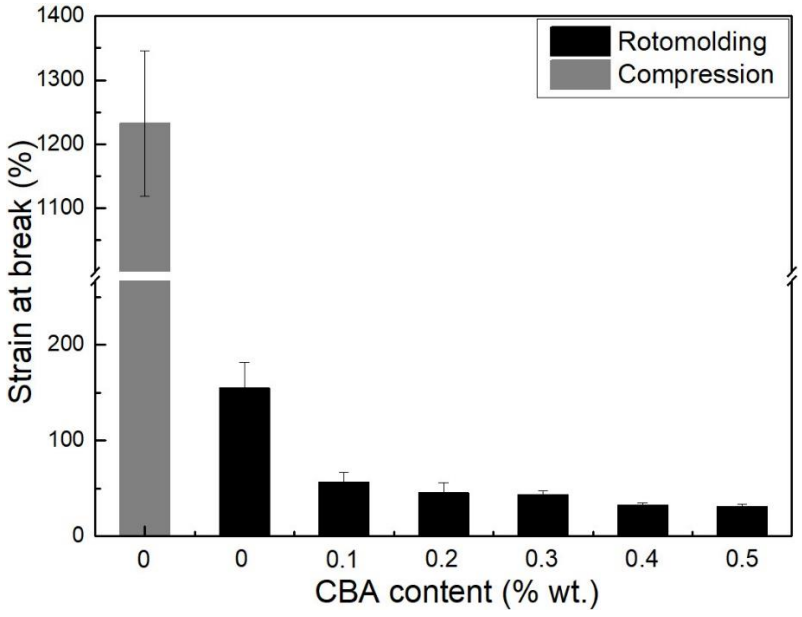

Figure 74. Tensile strain at break of PP and the foams as a function of CBA content.

8.5.7 Impact strength

Impact strength is reported in Figure 75. In this case, a significant difference between the rotomolded (152±8 J/m) and compression molded (493±54 J/m) PP is observed because of a more compact structure of the latter. This indicates that another main difference between both processes occurs at high deformation rate.

The impact strength is also decreasing with higher CBA content. The values decrease from 152 J/m to 37 J/m (76% reduction) by adding 0.5% wt. The main origin of this trend is that the cells act as stress concentration points, and easier crack initiation and propagation occurs when larger cells are produced (Table 5) as the cell wall thickness decreases [258], which confirms our results.

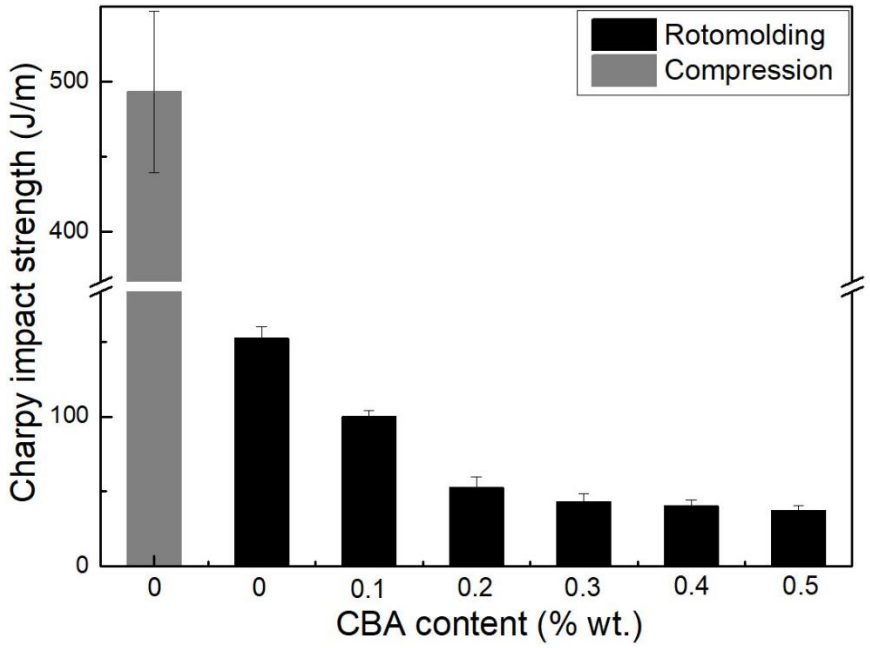

Figure 75. Impact strength of PP and the foams as a function of CBA content.

8.5.8 Final analysis

To finalize our analysis, a comparison between the relative mechanical properties (property of the foam divided by the property of the matrix) and the relative density (density of the foam divided by the density of the matrix) is presented in Figure 76. These curves can be helpful to optimize a specific system (polymer, foaming agent, processing conditions, methods, etc.) since they account for both the mechanical response and density reduction. According to Figure 76, the rotomolded PP foams exhibit a continuously decreasing trend between both relative properties, indicating that no clear

optimum was achieved for the range of conditions studied. Nevertheless, these foams would be better for applications in tension as their relative values are much higher than the other mechanical properties investigated.

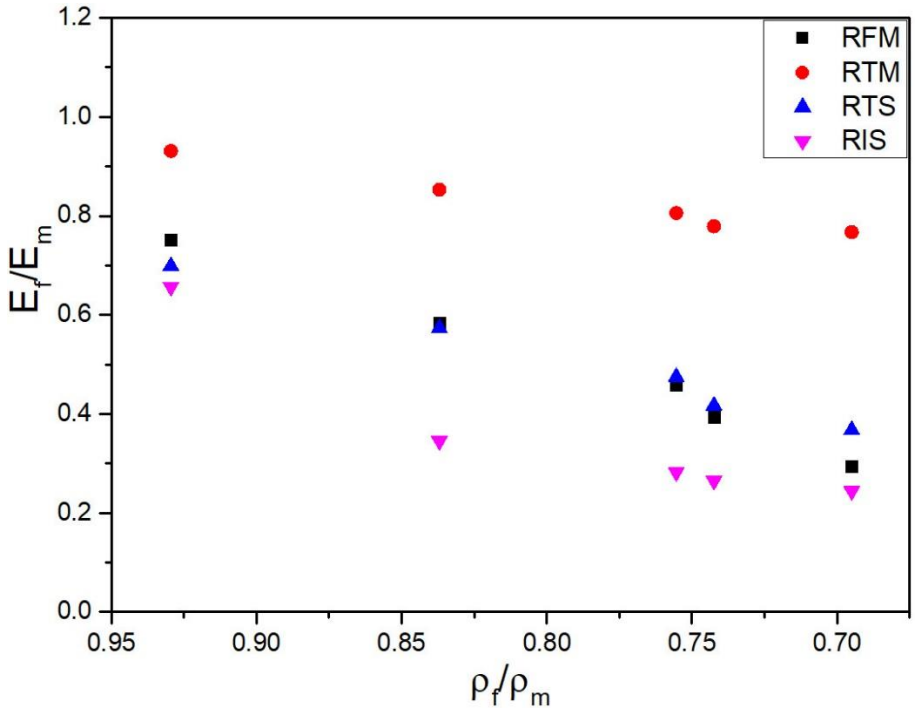

Figure 76. Relative mechanical properties (E_f/E_m) as a function of the relative density (ρ_f/ρ_m). RFM: relative flexural modulus, RTM: relative tensile modulus, RTS: relative tensile strength and RIS: relative impact strength.

8.6 Conclusion

Polypropylene (PP) foams were successfully produced via rotational molding using a simple dry-blending of the chemical blowing agent (CBA) since both materials were in a powder form. The effect of CBA content (0-0.5% wt.) was evaluated on the morphological, mechanical and thermal properties. Finally, a comparison between compression molded and rotomolded neat PP parts was performed.

The results showed that tensile elongation at break and impact strength of compression molded samples were much better than rotomolded ones. Nevertheless, it is assumed that good processing conditions were used as the properties at low deformation and low rate of deformation were similar. This difference can be associated to the high pressure used in compression molding leading to better sintering and compaction of the final parts (slightly higher density).

From the morphological analysis, it was found that the average cell diameter and cell density increased with increasing CBA content. This was expected as more gas is produced improving cell nucleation and growth inside the PP matrix. As expected, a higher amount of porosity (lower density) led to lower hardness with CBA addition. Similarly, more void content improved the thermal insulation properties of PP foams as the thermal conductivity decreased from 149 mW/m.K to 104 mW/m.K (30% reduction) with only 0.5 % wt. azodicarbonamide. Finally, due to the presence of a higher number of larger gas cells in the foams, less material is available to sustain the applied stresses with increasing CBA content leading to lower tensile and flexural moduli, as well as tensile strength and strain at break. A similar trend was observed for the impact strength because of larger cells acting as stress concentrators.

Nevertheless, more work is needed to optimize the processing of polymer foams, especially to completely understand the relations between all the parameters involved and their effect on the final structure and properties of rotomolded parts.

8.7 Acknowledgements

The authors acknowledge the financial support of the National Science and Engineering Research Council of Canada (NSERC) and the Chinese Scholarship Council (CSC).

Chapter 9

Morphological, thermal and mechanical properties of recycled HDPE foams via rotational molding

Dou Y, Rodrigue D. Morphological, thermal and mechanical properties of recycled HDPE foams via rotational molding. Journal of Cellular Plastics, 2021. DOI: 10.1177/0021955X211013793.

9.1 Résumé

Dans cette étude, des pièces en mousse de polyéthylène haute densité recyclé (rHDPE) ont été produites par rotomoulage en utilisant différentes concentrations (0 à 1 % en poids) d'un agent gonflant chimique (CBA) à base d'azodicarbonamide. A partir des échantillons produits, une caractérisation morphologique, thermique et mécanique complète a été réalisée. L'analyse morphologique a montré une augmentation progressive de la taille moyenne des cellules, tandis que la densité cellulaire a d'abord augmenté puis diminué avec l'augmentation de la teneur en CBA. Comme prévu, l'augmentation de la teneur en CBA a diminué la densité de la mousse ainsi que la conductivité thermique. Bien que l'augmentation de la teneur en CBA ait diminué à la fois les propriétés de traction et de flexion, la résistance aux chocs a montré une tendance similaire à celle de la densité cellulaire avec une teneur optimale en CBA d'environ 0,1% en poids. Enfin, des échantillons de rHDPE purs ont également été produits par moulage par compression. Les résultats ont montré des différences négligeables entre les propriétés rotomoulées et moulées par compression indiquant que les conditions optimales de rotomoulage ont été sélectionnées. Ces résultats confirment la possibilité d'utiliser des polymères 100 % recyclés pour produire des pièces en mousse rotomoulée.

9.2 Abstract

In this study, foamed recycled high density polyethylene (rHDPE) parts were produced by rotational molding using different concentration (0 to 1% wt.) of a chemical blowing agent (CBA) based on azodicarbonamide. From the samples produced, a complete morphological, thermal and mechanical characterization was performed. The morphological analysis showed a gradual increase in the average cell size, while the cell density firstly increased and then decreased with increasing CBA content. As expected, increasing the CBA content decreased the foam density as well as the thermal conductivity. Although increasing the CBA content decreased both tensile and flexural properties, the impact strength showed a similar trend as the cell density with an optimum CBA content around 0.1% wt. Finally, neat rHDPE samples were also produced by compression molding. The results showed negligible differences between the rotomolded and compression molded properties indicating that optimal rotomolding conditions were selected. These results confirm the possibility of using 100% recycled polymers to produce rotomolded foam parts.

9.3 Introduction

In the last decades, rotational molding (rotomolding) received a great deal of interest due to its simple processing tools, low machinery cost and limited waste generation [100, 114, 247, 252]. The main reason is the technology allowing to easily produce large one-piece hollow and seamless products such as industrial storage tanks, automotive parts, furniture and several other items. Compared with other plastic processing techniques, like injection and blow molding, there is no pressure involved in rotomolding meaning that the molds can be very thin and generally inexpensive. Furthermore, rotomolding can more easily handle complex shaped articles with uniform wall thicknesses. These features make rotomolding one of the fastest-growing polymer processes in the plastic industries over the last few years [204, 234, 250].

Over the last decades, scientific and industrial research has been increasingly focused on polymeric foams since their cellular structure offers unique physical properties while reducing the weight (amount of materials consumed). Foams have improved insulation properties, cushioning properties and outstanding stiffness-to-weight ratios contributing to several applications, such as thermal insulation, buoyancy, packaging and gaskets [226- 228]. In rotational molding, foams with skin-core morphologies can be used to manufacture creative and high-value articles without specialized equipment. The hollow structure of rotomolded products can also be used to overcome some limitations related to low mechanical and shock mitigation properties [259-261].

Still today, about 90% of all parts produced by rotational molding are based on different grades of polyethylene including low density polyethylene (LDPE), linear low density polyethylene (LLDPE), high density polyethylene (HDPE) and cross-linked low density polyethylene (XLDPE), because they have low melting temperature, low cost and high temperature resistance [125, 262, 263]. Furthermore, several studies have been conducted on the foaming mechanisms of polyethylene [115, 264-266]. As reported in the literature, there is some agreement among researchers regarding the stages of a typical foaming process: cell nucleation, cell growth (cell coalescence and cell coarsening) and cell stabilization. But very few investigations focused on the properties of polyethylene foams produced by rotomolding [248, 258, 267, 268]. For example, Archer et al. reported a linear decrease in both flexural modulus and compressive strength with decreasing metallocene catalyzed LLDPE foam density [268]. In our previous work, we reported that increasing the chemical blowing agent (CBA) content led not only to lower tensile and flexural moduli, but also to lower tensile strength and elongation at break, which can be associated with lower density and larger cell size [258].

With the ever-increasing consumption of polyethylene products in recent decades, a large number of solid wastes are generated causing serious environmental issues worldwide since they do not easily degrade and remain in the environment for a long time [269, 270]. Hence, seeking new ways to reuse recycled polyethylene is essential to minimize the amount of waste. HDPE is a typical example of available recycled polyethylene which can have several potential applications because of its good dimensional, mechanical and thermal stability [270, 271]. Moreover, the average cost of producing plastic products from recycled HDPE (rHDPE) is approximately 31-34% lower than that from virgin HDPE [272]. Consequently, using rHDPE not only decreases waste disposal issues, but also reduces the cost of HDPE based products.

Dvorak [273] studied the applicability of recycled HDPE instead of raw HDPE in rotational molding process. She found that rHDPE initially produced by rotomolding and injection molding possessed enough value of melt flow index to be used in rotomolding again. Chaisrichawla and Dangtungee [274] blended different ratio of virgin LLDPE and recycled HDPE from blowing process to manufacture rotomolded products for application in septic tank. Until now, to our knowledge, none studies have been performed on recycled HDPE foams produced by rotomolding. Consequently, the main objective of this work is to produce foamed and unfoamed rotomolded parts based on recycled high density polyethylene. In particular, the effect of chemical blowing agent content is investigated to determine its relation with foam density and cellular structure (cell size and cell density), and then to further determine its effect on the thermal (conductivity) and mechanical properties (tensile, flexural and impact) of rHDPE foams. Finally, to determine if the optimal rotomolding conditions were selected, neat solid rHDPE samples are also produced by compression molding to compare the properties obtained between both processing methods.

9.4 Materials and Methods

9.4.1 Materials

The recycled HDPE used was provided by Service de Consultation Sinclair (Drummondville, QC, Canada). This material was supplied in flakes coming from recycled solid HDPE bottles. The material was then pulverized using a model PKA18 pulverizer (Powder King, Phoenix, AZ, USA) The powder was then characterized to get its melt flow index (6.7 g/10 min at 2.16 kg/190°C) and its peak melting temperature (123°C) as determined via differential scanning calorimetry (DSC at 10°C/min). The final powder morphology is presented in Figure 77. For foaming, an exothermic chemical blowing agent (CBA) based on activated azodicarbonamide was used: Celogen 754A (powder) from Chempoint (USA). Its peak decomposition temperature is 164°C as determined via DSC.

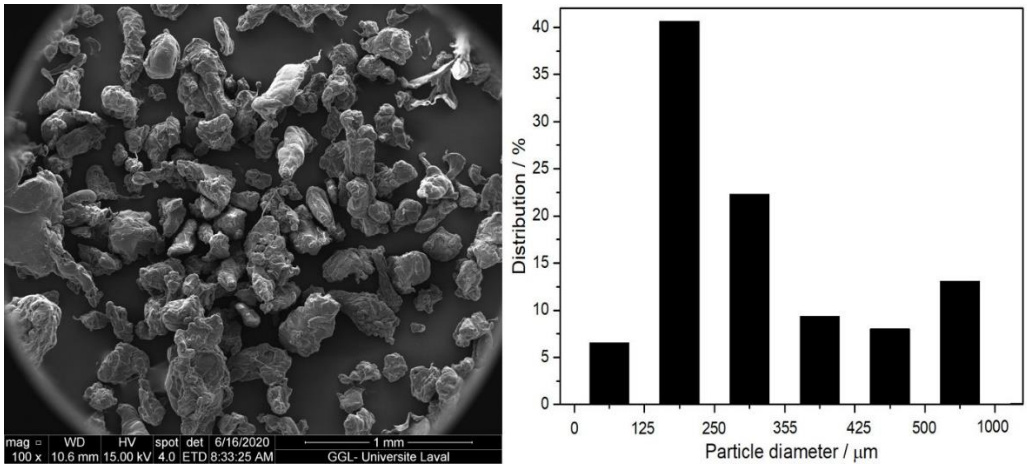

Figure 77. Typical scanning electron microscopy image of the rHDPE powder used (left) with its particle size distribution (right).

9.4.2 Rotational Molding

A series of rHDPE foams were prepared by using different CBA contents (0.1, 0.2, 0.3, 0.4, 0.5, 0.6, 0.7, 0.8, 0.9 and 1% wt.) to compare with the unfoamed matrix (0% wt.). As the CBA must be thoroughly dispersed in the rHDPE powder prior to charging the mold, all the materials were dry-blended in a high-speed mixer LAR-15LMB (Skyfood, USA) at 3320 rpm with fixed intervals of 1 min mixing time and 1 min cooling time repeated 5 times. For processing, a laboratory-scale biaxial rotational molding machine was used (MedKeff-Nye Roto-Lab model 22, Barberton, OH, USA). Rotationally molded parts were manufactured with a cubic aluminum mold of 3.6 mm wall thickness and an internal side length of 19 cm. Before loading the material, a demolding agent (Trasys 420, DuPont, Midland, MI, USA) was applied to the internal mold surface. A circular vent (diameter = 10 mm) was filled with glass wool to prevent powder losses. After several preliminary runs, the optimum processing conditions were: a 3:4 speed ratio (major axis:minor axis), a heating time of 18 min with an oven (electrically heated) temperature of 270°C and a cooling time of 30 min with forced air (blowing fans). Finally, the mold was opened and the part was demolded. To perform the characterizations, samples were directly cut in the molded parts (Figure 78). All the samples were produced using 660 g, so the final part thickness (2.4 to 6.2 mm) depends on the CBA content (final density).

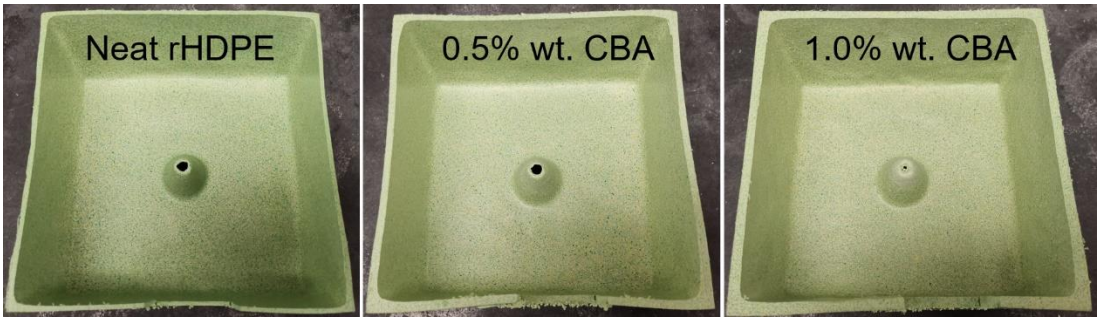

Figure 78. Typical examples of the rotomolded rHDPE parts (cut samples).

9.4.3 Compression molding

To produce the compression molded rHDPE parts, 35 g of the powder was placed in a mold with dimensions of 110 × 110 × 3 mm^3. The material was compression molded in an automatic Carver hydraulic press model Autoseries 3893 (Carver Inc., USA) at 190°C with a constant force of 2200 kg for 10 min, and finally the mold was cooled by water circulation to 60°C before removing the pressure and demolding.

9.4.4 Differential scanning calorimetry

Differential scanning calorimetry (DSC) studies were performed on a DSC-7 from Perkin-Elmer (USA) equipped with a thermal analysis controller TAC7/DX. About 15 mg of rHDPE powder or CBA were weighed and placed in a sealed aluminum pan. The measurements were carried out with a scanning rate of 10°C/min between 50 and 200°C under a flow of dry nitrogen (20 mL/min). The first heating cycle of rHDPE powder was only used to delete its thermal history and was not analyzed.

9.4.5 Thermogravimetric analysis

Thermogravimetric analysis (TGA) was carried out on a Q5000IR TGA analyzer (TA Instruments, USA). The scans were performed from 50 to 800°C at a rate of 10°C/min with a gas (nitrogen) flow rate of 25 mL/min.

9.4.6 Morphological characterization

The foamed rHDPE parts were cryogenically fractured (liquid nitrogen) and micrographs of the exposed cross-sections were taken using a scanning electron microscope (SEM) (FEI Inspect F50, USA). Foam morphology characterization was investigated based on two parameters: cell size (D) and cell density (N_f). The average cell size with standard deviation was measured by the ImageJ

software (US National Institutes of Health, USA). Cell density (N_f), which is defined as the number of cells per cubic centimeter of foam, was calculated according to the method of Kumar and Weller as [148]:

$$N_f = \left(\frac{n}{A}\right)^{3/2} \quad (2)$$

where n is the number of cells in a micrograph and *A* is the area of the micrograph in cm^2.

9.4.7 Density and hardness

To determine the density, each sample was cut into cubes of different dimensions (measured with a caliper having a resolution of ± 0.01 mm), weighed (MX-50 moisture analyzer, A&D, Tokyo, Japan) and determined using a gas (nitrogen) pycnometer Ultrapyc 1200e (Quantachrome Instruments, USA) to compare. Hardness (Shore A and Shore D) was obtained by a PTC Instruments (USA) Model 306L and Model 307L (ASTM D2240), respectively. The results reported are the average and standard deviation of a minimum of 5 samples.

9.4.8 Thermal conductivity

The effective thermal conductivity (k) of the samples was determined by an in-house built thermal conductivity analyzer following ASTM E1225. The rotomolded parts were cut into square samples (50×50 mm^2) and their thickness (d ± 0.01 mm) was measured using a digital caliper (Mastercraft, Canada). The samples were sandwiched between thin aluminum foil sheets to limit the surface thermal resistance during measurement by fixing the hot (top = T_h) and cold (bottom = T_c) plate at 33 ^oC and 13^oC respectively (20^oC of temperature difference giving an average of 23^oC = room temperature) using water cooled Pelletier plates (Model K20, Haake, Germany). These temperatures were measured using thermistances (TC-720, TE-Technology, USA) and the heat flux (*Q*) was determined by a PHFS-01 heat flux sensor (Flux Teq LLC, USA). Each sample was tested three times to measure the average thermal conductivity with their respective standard deviations. For each experiment, equilibrium values were obtained after about 30 min. The thermal conductivity was determined as:

$$k = \frac{QXL}{\Delta T} \quad (4)$$

where Q is the heat flux (BTU/ft^{2}·h), X is the conversion factor (BTU/ft^{2}·h converts to W/m^{2} by multiplying by 3.1546), L is thickness of the specimen (mm) and ΔT is the temperature difference (20^{o}C).

9.4.9 Mechanical properties

All the specimens were cut from the rotomolded parts and measured at room temperature. The tensile properties were conducted on dog bone samples according to ASTM D638 (type V) on an Instron (USA) model 5565 universal testing machine with a 500 N load cell. The crosshead speed was set at 10 mm/min and the values for tensile modulus, tensile strength and elongation at break are based on the average (± one standard deviation) of at least six samples.

Flexural tests (three-point bending) were performed according to ASTM D790 using a crosshead speed of 2 mm/min on an Instron (USA) universal tester model 5565 with a 50 N load cell. The span length was fixed at 60 mm. At least five rectangular samples (60 × 12.7 mm^{2}) were used to report the average and standard deviation for the modulus.

Charpy impact strength was determined by a Tinius Olsen (USA) testing machine model Impact 104. At least ten rectangular specimens (60 × 12.7 mm^{2}) were prepared according to ASTM D6110. The samples were notched ("V" shaped) by an automatic sample notcher model ASN 120m (Dynisco, USA) at least 24 h before testing.

9.5 Results and Discussion

9.5.1 Differential scanning calorimetry

Figure 79 presents the DSC thermographs of the rHDPE powder and CBA. The second heating cycle of rHDPE powder presents a single endothermic peak which confirms that the rHDPE is mainly alone in the resin. The peak melting temperature and crystallization peak temperature for rHDPE are 123°C and 107°C, respectively. Figure 79 also shows that the onset decomposition temperature of CBA is about 140°C, while its peak decomposition temperature is 164°C. Thus, the oven temperature in the heating cycle of rotomolding was set as 270°C to ensure complete rHDPE melt and CBA decomposition.

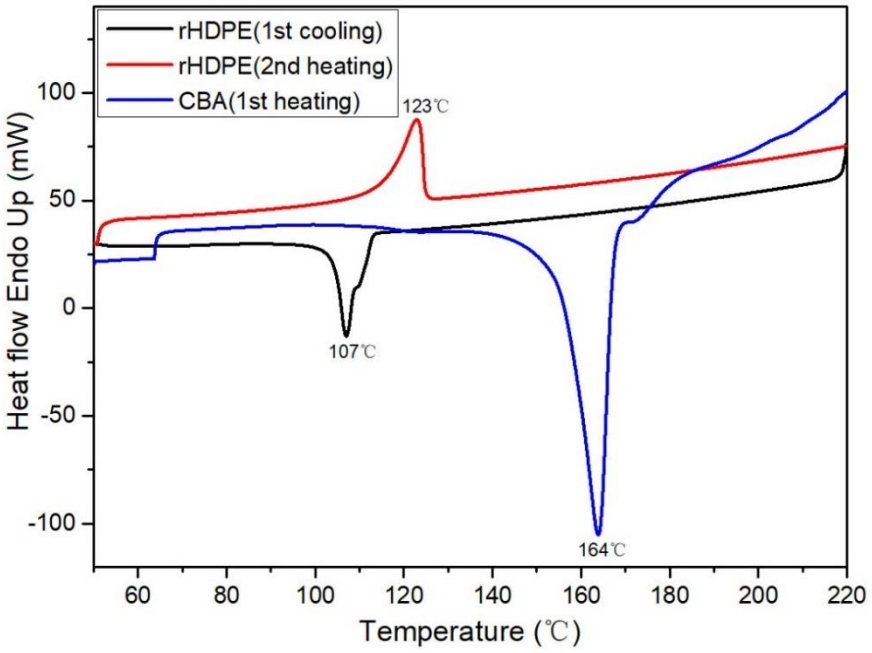

Figure 79. DSC thermograms of the rHDPE powder and CBA used.

9.5.2 Thermogravimetric analysis

The TGA and derivative of thermogravimetry (DTG) curves obtained for the rHDPE powder under a nitrogen atmosphere are depicted in Figure 80. The rHDPE sample remains stable from 50 to 260°C as no weight loss occurs. Above 260°C, the decomposition starts until the sample is completely decomposed at 490°C with a peak temperature at 445°C. A weight loss of 91.3% was recorded in this zone which represents the thermal degradation of rHDPE. Then, around 3.8% weight loss is observed between 628°C and 700°C due to the decomposition of organic fillers. However, there is about 4.9% weight of residues which can be related to the presence of inorganic components in the rHDPE powder (different additives related to the post-consumer origin of the polymer).

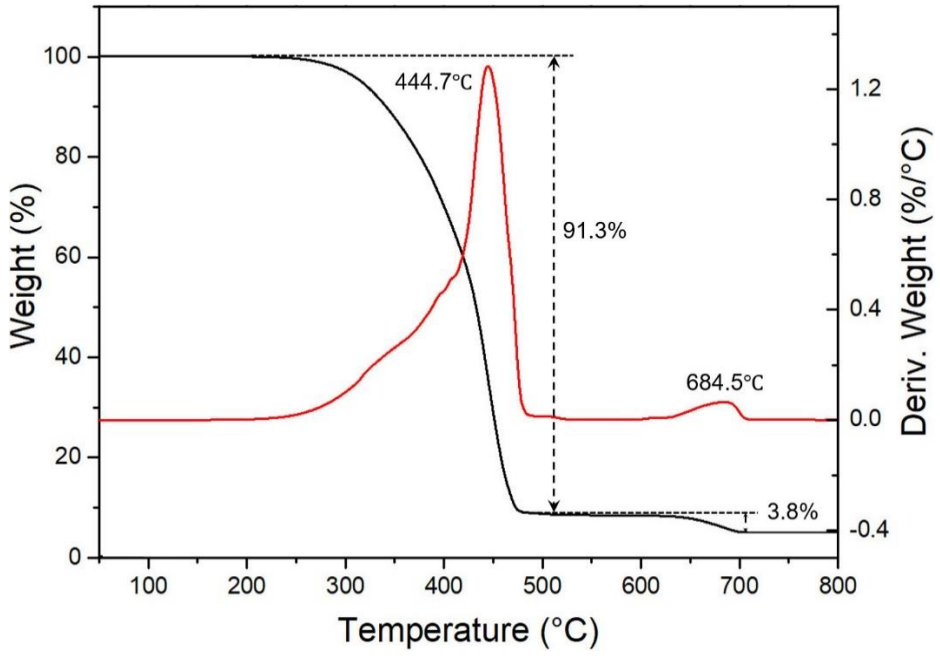

Figure 80. Typical TGA (black) and DTG (red) thermograms of the rHDPE powder used.

9.5.3 Morphological characterization

Table 8. Average cell size and cell density of rHDPE foams.

CBA content (% wt.)	Average cell diameter (μm)	Cell density (10^3/cm^3)
0.1	191±81	14.3
0.2	192±98	24.9
0.3	218±96	28.5
0.4	241±114	26.7
0.5	242±129	24.0
0.6	272±114	24.9
0.7	315±165	21.3
0.8	328±167	18.8
0.9	341±154	15.8
1.0	349±150	15.1

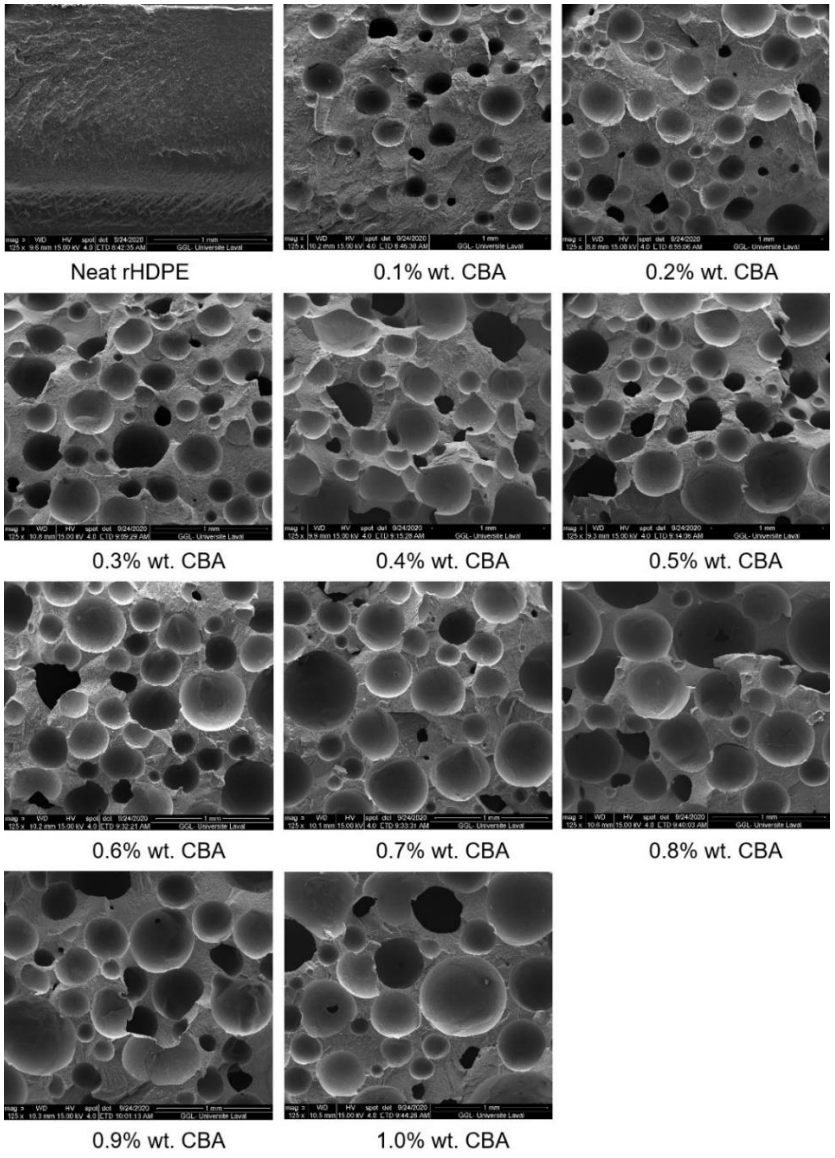

Figure 81. Typical morphologies of the rotomolded rHDPE parts with different CBA contents.

SEM images for the foams with different CBA contents at a low magnification (125x) are shown in Figure 81. Based on these images and their quantitative analysis, the average cell size and cell density are summarized in Table 8. As expected, the average cell size increases with increasing CBA content since more gas is available to blow the nucleated cells. For example, the average cell size increases from 0.191 to 0.349 mm when the CBA content increases from 0.1% to 1.0% wt. On the other hand, the cell density firstly increases at low CBA content (0.1 to 0.3% wt.), but then decreases at higher CBA content (0.3 to 1% wt.). This trend, leading to a maximum *Nf* (optimum CBA content), represents a balance between the amount of gas generated and the thinner cell walls/higher internal cell pressure leading to cell coarsening and coalescence [275]. There is also higher probability of gas

loss with increasing CBA content [116]. This observation is similar with our previous work where the cell density of LLDPE foams firstly increased at low CBA content (0.1 to 0.2% wt.), and then decreased with further CBA content increase from 0.2 to 1% wt. [258].

9.5.4 Density and hardness

Figure 82 presents the density of the rHDPE powder and rHDPE foams with different CBA contents. Increasing the CBA content up to 0.3% wt. decreases (27%) the density from 0.976 to 0.707 g/cm^3. The higher than expected density value (0.93 to 0.96 g/cm^3) for the rHDPE might be coming from the recycled nature of the materials which may contain several additives and/or contamination to give its final color as shown in Figure 77 and the residues in Figure 79 [276, 277]. However, the foam density increases from 0.707 to 0.914 g/cm^3 between 0.3 and 1% wt. CBA. This is attributed to the fact that as CBA content continues to increase, the instability of the cells to coalesce increases leading to possible gas loss and cell collapse (broken cell walls), which can be seen in Figure 81.

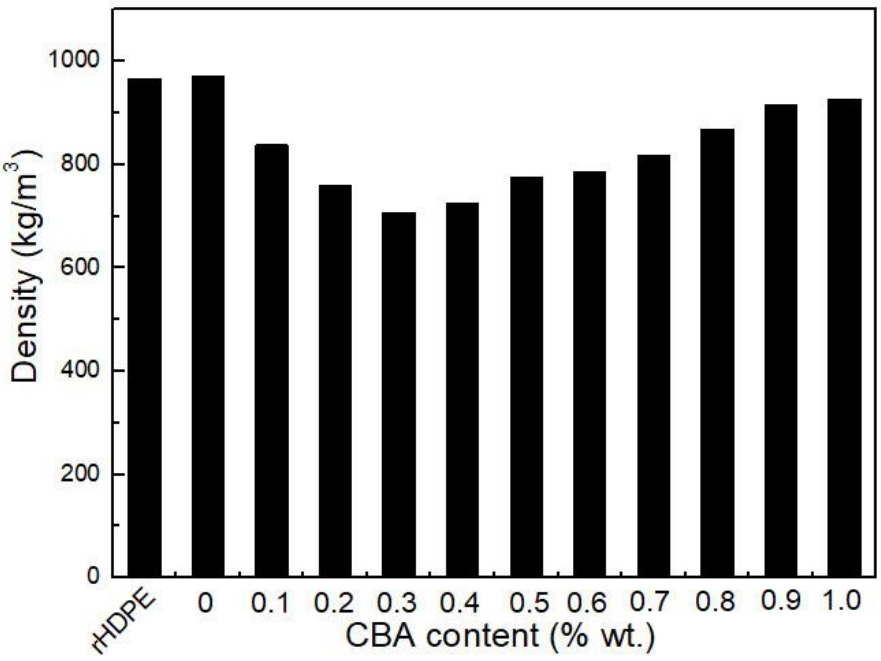

Figure 82. Density of rHDPE powder and rHDPE foams as a function of CBA content.

Figure 83 shows that hardness (Shore A and Shore D) continuously decreases with increasing CBA content from 0% to 1.0% wt. In this case, the Shore A decreased from 97 to 77 (20 points difference), while the Shore D decreased from 69 to 30 (39 points difference). These trends are expected due to decreasing cell wall thickness (increasing cell size in Table 8) inside the foams, and the "soft" nature of gas cells occupying more space compared to the neat matrix (rHDPE).

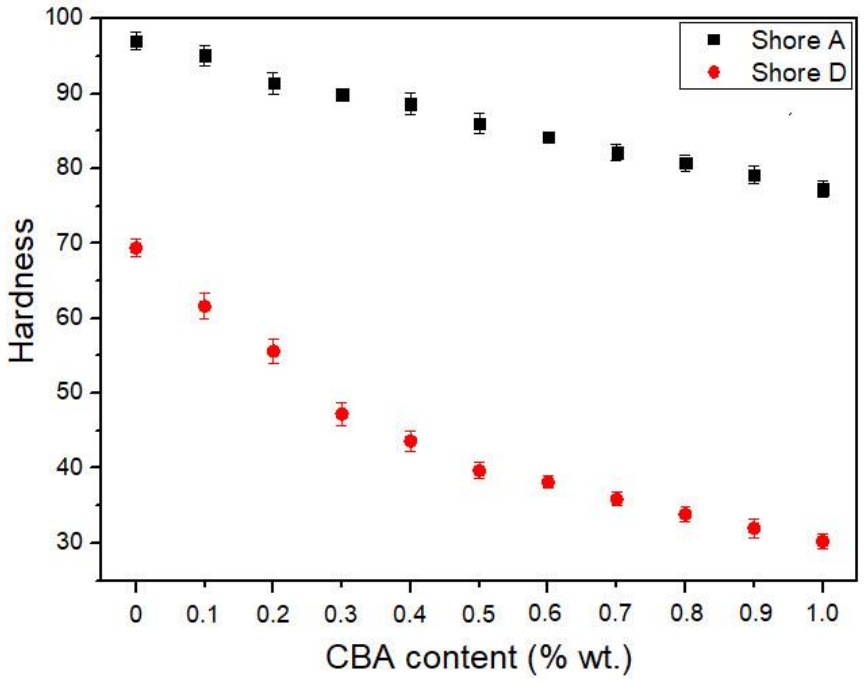

Figure 83. Hardness (Shore A and Shore D) of rHDPE foams as a function of CBA content.

9.5.5 Thermal conductivity

Table 9 reports the effect of CBA content on the thermal conductivity. Both the thermal conductivities of neat rHDPE produced by compression molding and rotomolding are 243 mW/m·K which is lower than reported values of recycled HDPE (300 mW/m·K) in the literature [278]. This might be associated with the rHDPE powder having some non-conductive (inorganic) components as observed via TGA (Figure 80), leading to lower thermal conductivity as it was the case for density (Figure 82). Nevertheless, increasing the CBA content led to lower thermal conductivity with the lowest value (165 mW/m·K) achieved at 1% wt. CBA. This trend is similar as hardness (Figure 83) and inversed to the average cell size (Table 8) indicating that cell size is the most important parameter here (gas contribution compared to the polymer contribution).

Table 9. Thickness (*L*) and thermal conductivity (*k*) of rHDPE samples.

CBA content (% wt.)	*L* (mm)	*k* (mW/m·K)
0^c	2.31	243±11
0^r	2.35	243±12
0.1	2.92	203±18
0.2	3.19	201±12
0.3	3.77	193±4
0.4	4.56	191±5
0.5	4.92	188±4
0.6	5.00	187±14
0.7	5.20	184±6
0.8	5.53	175±9
0.9	5.87	173±7
1.0	6.13	165±10

c : compression molded
r : rotational molded

9.5.6 Flexural properties

Figure 84 presents the flexural modulus of the neat rHDPE parts and the foams. For both neat rHDPE samples, the flexural modulus of the compression molded sample is 1017±41 MPa which is similar to the rotomolded one (996±58 MPa) within experimental uncertainty. It can also be seen that the values substantially decrease with increasing CBA content. For example, the flexural modulus of the sample with 1.0% wt. CBA is 176 MPa, which represents a 82% decrease. Lower values for foams are related to less material being available (decreasing density in Figure 82) to sustain the applied stress and higher amount of cells collapse/larger cells (Table 8 and Figure 81) [152].

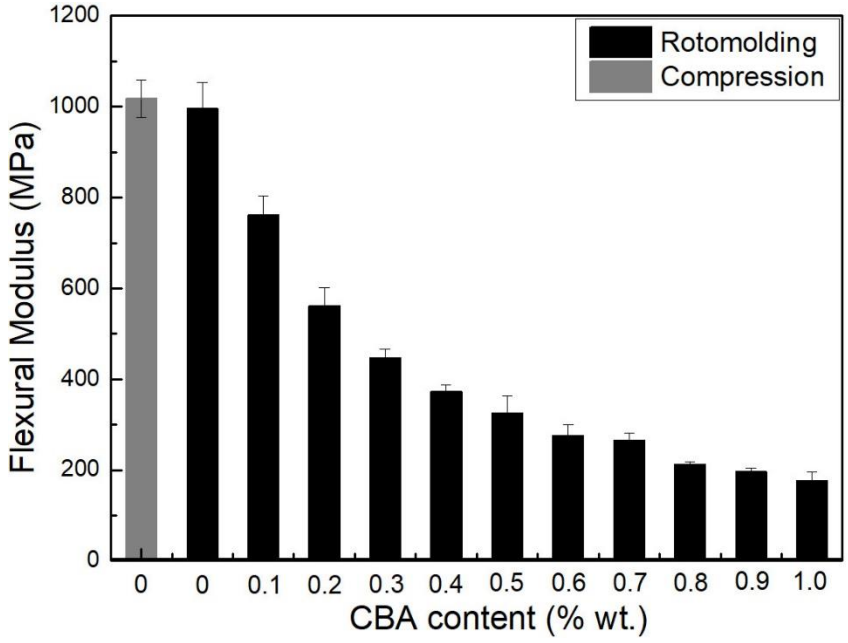

Figure 84. Flexural modulus of rHDPE foams as a function of CBA content.

9.5.7 Tensile properties

Figures 85-87 present the tensile properties of all the rHDPE samples. For the tensile modulus (Figure 85) and tensile strength (Figure 86), there are no statistically significant differences between the compression molded (302±16 MPa) and rotomolded (273±20 MPa) samples as for the flexural modulus (Figure 83), while the values for tensile strength are 23.6±0.4 MPa and 24.3±0.9 MPa, respectively. However, the elongation at break (Figure 87) of the compression molded rHDPE (504±41%) is slightly better than that of rotomolded parts (429±57%), which may be related to high pressure involved in compression molding leading to a better compaction (closer packing) reducing the number of microvoids in the samples [256]. This result indicates that the differences between both processing methods (compression molding vs. rotomolding) are mainly important at higher deformation (elongation at break) compared to lower deformation (elastic modulus and maximum stress).

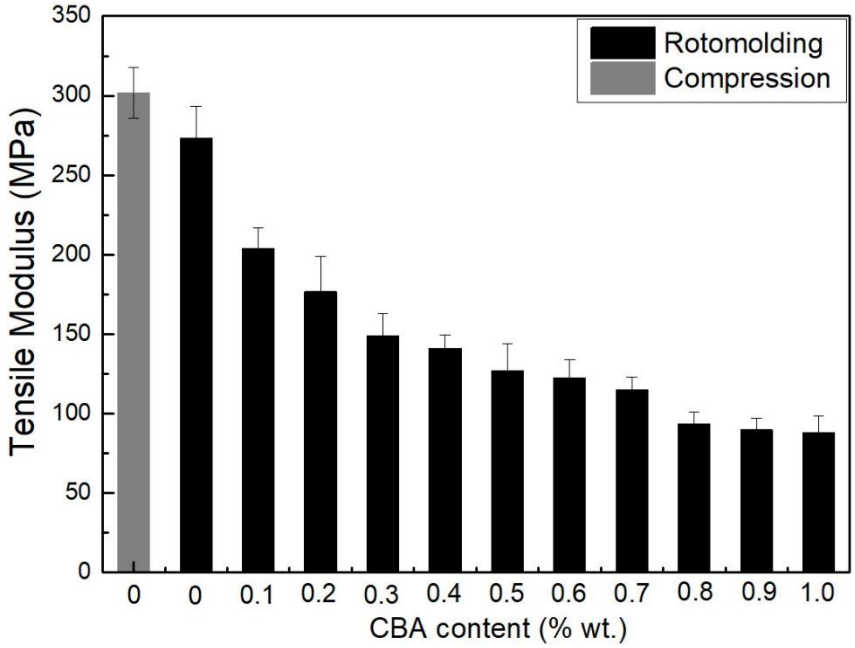

Figure 85. Tensile modulus of rHDPE foams as a function of CBA content.

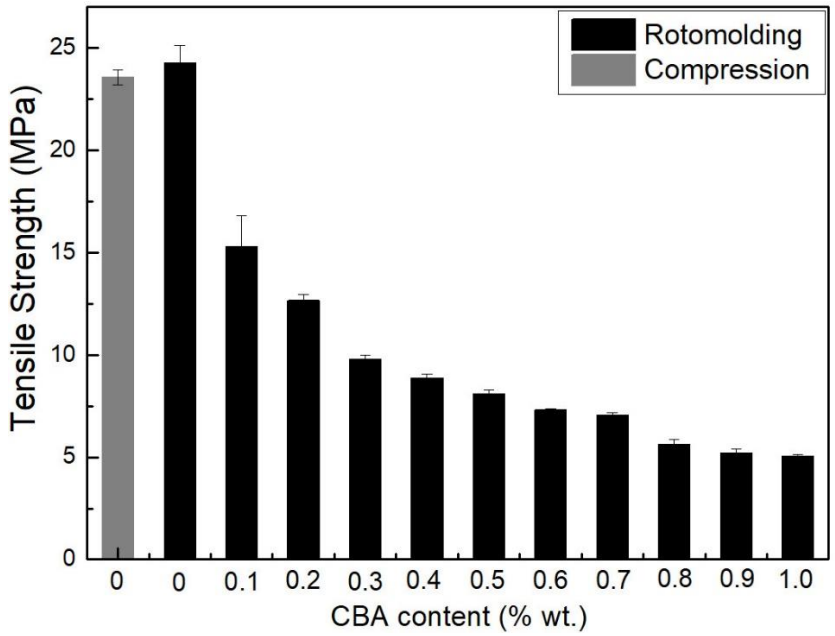

Figure 86. Tensile strength of rHDPE foams as a function of CBA content.

For the rotomolded foams, the tensile modulus (Figure 85) presents the same trend as for the flexural modulus (Figure 84). For example, the tensile modulus decreased by 68% (from 273 to 88 MPa) with increasing CBA content from 0 to 1% wt. Figure 86 reveals that the tensile strength also decreases with increasing CBA content, due to the same reasons as for the flexural modulus. For example, the

tensile strength of the unfoamed matrix (24.3 MPa) decreased to 5.1 MPa (70% lower) at 1% wt. CBA. Finally, Figure 86 presents the results for the elongation at break. Again, the values decrease with increasing CBA content and are all well below 100% (40 to 50%), but do not change much. All these findings are consistent with other studies reporting decreasing mechanical moduli, strengths and deformations at break with increasing foaming level [257].

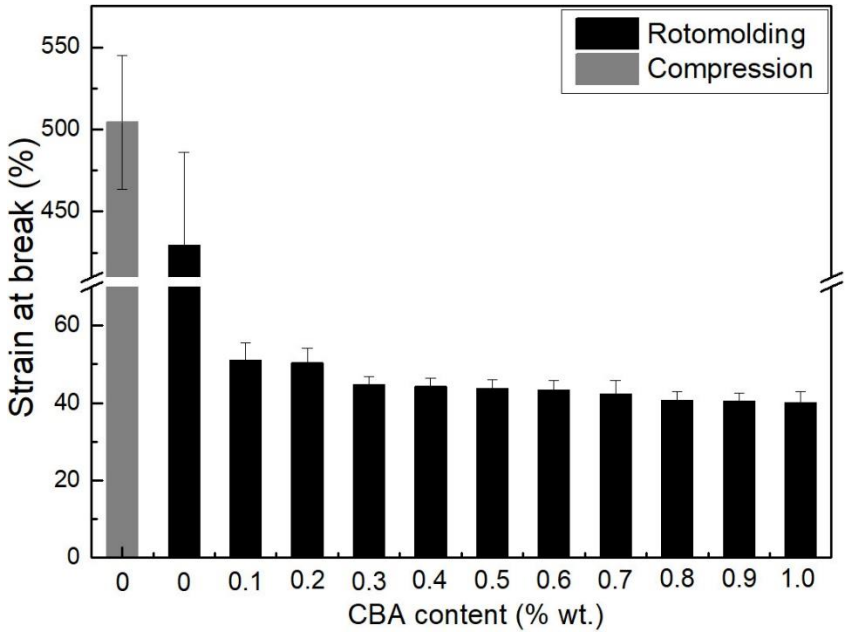

Figure 87. Tensile strain at break of rHDPE foams as a function of CBA content.

9.5.8 Impact strength

Impact strength results are shown in Figure 88. Compared with the neat rHDPE (50.2±4.9 J/m) in rotomolding, the value slightly increases in compression molding (54.2±4.2 J/m) because of a more compact structure. This indicates again that the main difference between both processes is important at higher deformation rate (impact).

Compared with the unfoamed matrix, the impact strength slightly increases at 0.1% wt. (57.2 J/m) and 0.2% (52.0 J/m) CBA. This improvement may result from a finer cellular structure produced at lower CBA content and each (closed) cell acting as energy absorbers leading to higher impact strength [279]. However, as the CBA content further increases (0.3 to 1% wt.), the cell density decreases and cell coalescence occurs (Figure 81 and Table 8). In this case, there is more defects in the samples leading to lower impact strength down to 31.1 J/m at 1.0% wt. CBA. It has been reported that larger

cells are acting as stress concentration points and easier crack propagation occurs with decreasing cell wall thickness (larger cell sizes) [258], which confirms our results.

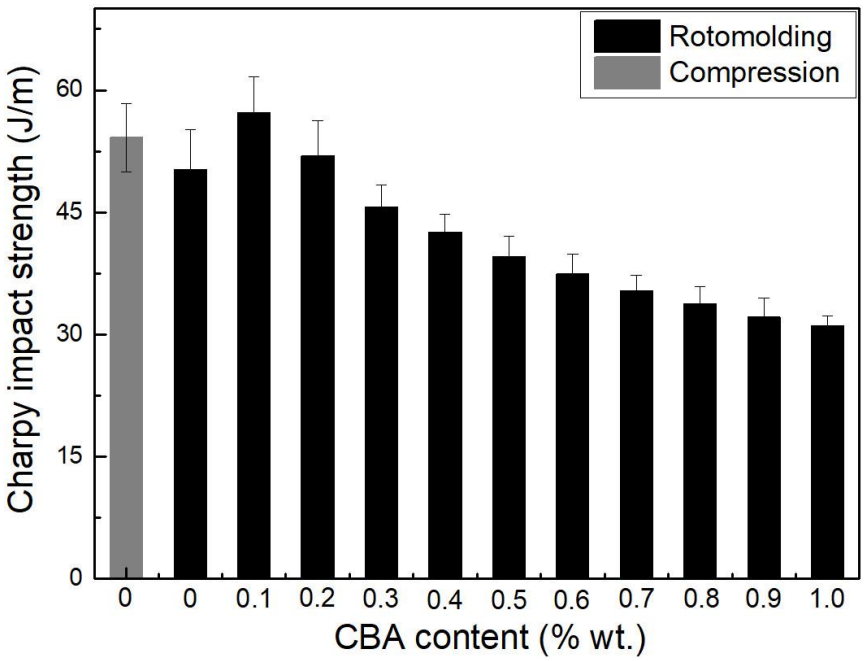

Figure 88. Impact strength of rHDPE foams as a function of CBA content.

9.5.9 Final analysis

To complete our analysis, the relative mechanical properties (property of the foam divided by the property of the matrix) are plotted in Figure 89 as a function of the relative density (density of the foam divided by the density of the matrix) for the rotomolded rHDPE foams. It can be seen that no clear trend can be obtained in our case due to the complex interactions between all the parameters involved. This indicates that more parameters (cell size, cell density, open cell content, etc.) must be included to get a clear picture of these trends. Nevertheless, these plots are helpful to optimize a specific system (polymer, blowing agent, processing methods and conditions, etc.) depending on the final application of the foam. As always, a balance between maximum properties with minimum density must be achieved. Based on the results of Figure 89, it seems that the sample with a relative density of 0.862 g/cm^3 (0.1% wt. CBA) gives the best results.

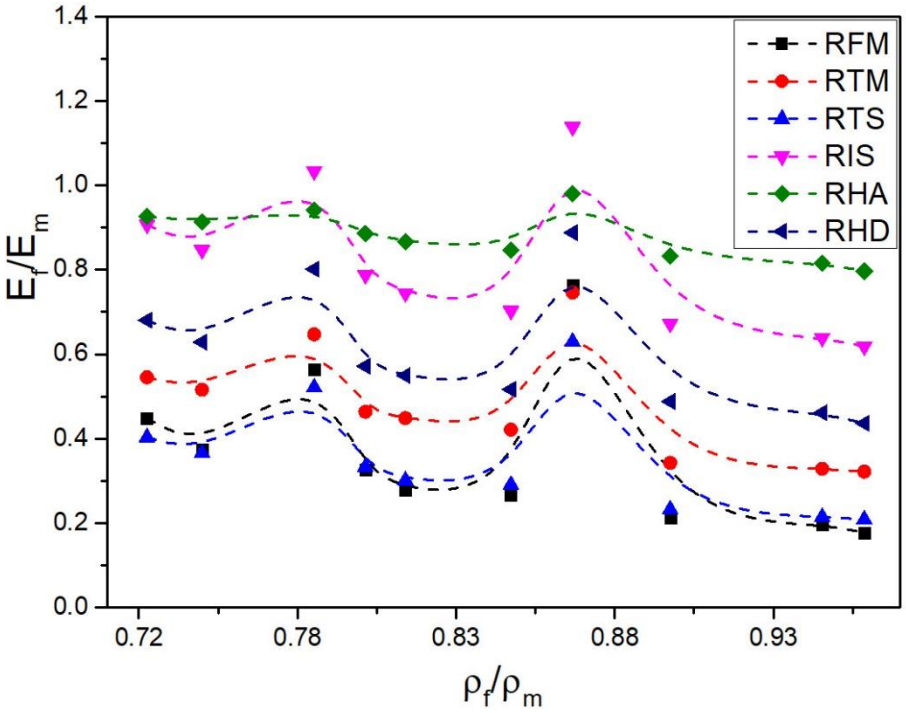

Figure 89. Plots of relative mechanical properties (E_f: mechanical property of the foam divided by E_m: mechanical property of the polymer matrix) as a function of the relative density (ρ_f: density of the foam divided by ρ_m: density of the polymer matrix). RFM: relative flexural modulus, RTM: relative tensile modulus, RTS: relative tensile strength, RIS: relative impact strength, RHA: relative hardness of shore A and RHD: relative hardness of shore D.

9.6 Conclusion

In this study, post-consumer recycled high density polyethylene (rHDPE) foams were successfully produced via rotational molding using an initial dry-blend of a chemical blowing agent (CBA) in a powder form with pulverized rHDPE. Then, the effect of CBA content (0-1% wt.) was evaluated. Furthermore, according to the comparison of thermal and mechanical properties between compression-molded rHDPE parts and rotomolded rHDPE parts, the results showed that good processing conditions were used in rotational molding as the properties at low deformation and/rate of deformation were similar.

As for the rotomolded foam samples produced, a complete set of characterization including morphological, thermal and mechanical properties was performed. According to the results obtained, several conclusions can be made.

Firstly, based on the DSC results, the polymer was completely melted before the CBA started decomposing and the oven temperature selected (270°C) was able to produce good parts over the range of conditions tested after preliminary optimization.

Secondly, the morphological analysis indicated that the average cell diameter of the foamed rHDPE parts increased with increasing CBA content, while cell density initially increased and then decreased due to cell coalescence and possible gas loss. Moreover, the density firstly decreased, and then increased in relation with possible cell collapse and gas loss. As expected, due to the soft nature of the gas cells, the hardness decreased with CBA addition.

Thirdly, the thermal insulation properties of rHDPE foams were improved with increasing CBA content. The lowest thermal conductivity was 0.124 mW/m.K at 1% wt. CBA, which is quite low for this relatively high density foam (0.7 g/cm^3).

Finally, increasing the CBA content not only decreased both the tensile and flexural moduli, but also decreased the tensile strength and strain at break. For the impact strength, the values initially increased due to a fine cellular structure acting as energy absorbers, before decreasing due to larger cells acting as stress concentrators.

Nevertheless, the results obtained clearly indicates that more work is needed to optimize the processing of polymer foams based on recycled resins, especially to completely understand the relations between all the parameters involves on the final structure and properties.

9.7 Acknowledgements

The authors acknowledge the financial support of the National Science and Engineering Research Council of Canada (NSERC) and the Chinese Scholarship Council (CSC).

Conclusion

With a growing number of automotive vehicles used, increasing tire production results in massive stockpile of waste tires. Waste tires pose significant health and environmental concerns if not recycled and/or discarded properly. Thus, waste tires are firstly shredded into ground tire rubber (GTR), and then used to produce ground tire rubber/thermoplastics composites as an effective recycling way for waste tires. This thesis presented a novel strategy to produce GTR/thermoplastic composites via rotational molding combined with a simple dry-blending process. Compared with some hollow plastic molding processes like blow molding, thermoforming and injection molding, rotational molding has several advantages such as lower costs, great flexibility and lower design limitations. In order to enhance compatibility between the GTR and thermoplastic matrix, further improving the mechanical properties of the resulting composites, some modification methods can be used. The following conclusions can be summed up from the results of these studies:

- GTR/LLDPE composites were successfully produced by dry-blending followed by rotational molding. A wide range of GTR content from 0 to 50 wt.% was used. Although weak interfacial adhesion exists between GTR and LLDPE, SEM results revealed a homogeneous distribution of the rubber phase in LLDPE at low GTR content (0-10 wt.%). However, at higher GTR content, some voids and GTR aggregation occurred. Thus, compared with neat LLDPE, the tensile strength and modulus, as well as the flexural modulus decreased with increasing GTR content. Interestingly, due to the good elasticity of GTR, the GTR/LLDPE composites showed up to 35% higher impact strength at 30 wt.% GTR compared to neat LLDPE, and the elongation at break of these composites were all above 100%.
- GTR/LLDPE composites, LLDPE foams and GTR/LLDPE composite foams were successfully produced via rotational molding. Compared to the particle size of GTR (98.4% of particle is above 500 μm) for the first work, smaller GTR particle size (less than 500 μm) was used in this work. The SEM results showed that some voids and defects occurred at 5 wt.% GTR due to higher surface area of the smaller GTR particles and poor adhesion at the interface between GTR and LLDPE. Consequently, as for GTR/LLDPE composites, the mechanical properties (tensile modulus, tensile strength, flexural modulus and impact strength) decreased with increasing GTR content. Likewise, the addition of CBA caused a decreased in density (LLDPE foams) leading to a gradual decrease of the mechanical properties. For GTR/LLDPE composite foams, the density slightly increased with increasing GTR content because of its higher intrinsic density and this effect was more important at 0.2 wt.% CBA. Although increasing the GTR content decreased the tensile properties and

flexural modulus, the impact strength of GTR-LLDPE composite foams with 0.2 wt.% CBA almost stayed unchanged from 0 wt.% to 35 wt.% GTR content. This phenomenon represented a balance between the effect of voids and rubber particles by adding GTR and both effects offset each other.

- GTR/MWF/LLDPE hybrid composites were successfully prepared by dry-blending followed by rotational molding. The effect of GTR and MWF treated by MAPE on the mechanical properties of the hybrid composites were investigated. TGA and FTIR spectra indicated that the surface of maple fibers was successfully modified with MAPE. SEM analysis showed that MAPE, as a coupling agent, was able to improve the interfacial compatibility resulting in hybrid composites with less defects. Compared with untreated maple wood fiber composites, the mechanical properties of the composites based on treated maple fibers were enhanced.
- The effects of two types of GTR treatments, MAPE modification in solution and microwave devulcanization, were studied based on GTR/LLDPE composites produced by rotational molding. Both MAPE treatment (0.3 wt.%) and microwave devulcanization were able to improve the interfacial adhesion between GTR and LLDPE, but limited improvement of tensile strength and impact strength were observed. As a result, these two types of GTR treatments had limited effect based on the conditions used, which could be improved in future works. For example, the amount of MAPE in the solution could be higher. For microwave devulcanization, a more “professional” microwave oven could be used.
- PP/GTR composites were successfully produced by combining a dry-blending technique and a rotational molding process. A gradual decrease of all the composites mechanical properties was observed with increasing GTR content. Thus, potential improvement must go through improving the PP-GTR interfacial adhesion to produce better rotomolded parts with better mechanical properties.
- GTR/MAPE/PP composites were successfully produced by rotational molding. The analyses of TGA, FTIR and SEM confirmed that the GTR surface was successfully modified by MAPE (2 wt.%). Compared with GTR/PP composites, the number and size of defects were substantially reduced in GTR/MAPE/PP composites. The mechanical properties of GTR/MAPE/PP composites were also significantly higher than GTR/PP ones. Tensile modulus (57%), tensile strength (76%) and flexural modulus (74%) improvements were observed, while the impact strength reached a 52% improvement above that of the GTR/PP composites.

- PP foams were successfully produced via rotational molding using a simple dry-blending of CBA. From the morphological analysis, it was found that the average cell diameter and cell density increased with increasing CBA content. This was expected as more gas is produced improving cell nucleation and growth inside the PP matrix. Similarly, more void content improved the thermal insulation properties of PP foams as the thermal conductivity decreased from 149 mW/m·K to 104 mW/m·K (30% reduction) with only 0.5 % wt. azodicarbonamide. Finally, due to the presence of a higher number of larger gas cells in the foams, less material is available to sustain the applied stresses with increasing CBA content leading to lower tensile and flexural moduli, as well as tensile strength and strain at break.
- rHDPE foams were successfully produced by rotational molding using an initial dry-blend of CBA in a powder form with pulverized rHDPE. The morphological analysis indicated that the average cell diameter of the foamed rHDPE parts increased with increasing CBA content, while cell density initially increased and then decreased due to cell coalescence and possible gas loss. The thermal insulation properties of rHDPE foams were improved with increasing CBA content. The lowest thermal conductivity was 0.124 mW/m·K at 1% wt. CBA, which is quite low for this relatively high density foam (0.7 g/cm^3). Besides, increasing the CBA content not only decreased both the tensile and flexural moduli, but also decreased the tensile strength and strain at break. As for the impact strength, the values initially increased due to a fine cellular structure acting as energy absorbers, before decreasing due to larger cells acting as stress concentrators.

According to the findings of this thesis, ground tire rubber/thermoplastic composites and thermoplastic foams can be successfully produced by combining a dry-blending technique with a rotational molding processing, respectively. The mechanical properties of these composites can be improved by GTR modification. So far, among all the modification methods used in this thesis, GTR treated by MAPE in solution is the most effective way to improve the mechanical properties of rotomolded GTR/thermoplastic composites.

Recommendations for future works

Based on the results obtained, the extent of mechanical properties improvement based on treated GTR is not very high. So more work is needed to further enhance the interfacial compatibility and mechanical properties of GTR/thermoplastic composites. Here is a list of recommendations for future works:

1. Maleated polyethylene was shown to be an effective coupling agent to improve the mechanical properties of GTR/LLDPE. Thus, different grades of maleated polyethylene or polypropylene can be incorporated into the composites to investigate their effects.
2. Since several GTR modification methods were reviewed in this thesis, some of them can be studied to improve the interfacial adhesion between GTR particles and thermoplastic matrices. For instance, cold plasma can introduce oxygen containing functional groups on the surface of GTR, so incorporating some reactive compatibilizers may improve the interaction in the composites.
3. In this thesis, GTR/LLDPE composites were reinforced using maple wood fibers. Thus, different types of fibers and sizes (short, medium or long size) can also be investigated to increase the mechanical properties of the composites.
4. In this thesis, only LLDPE and PP were used as matrices to produce rotomolded GTR/thermoplastic composites. In the future, other thermoplastic resins, such as HDPE, LMDPE, polyamide, polycarbonate, acrylonitrile butadiene styrene copolymer, etc., can also be used to prepare products with more diverse characteristics and applications.
5. To reduce the cost of the final products and decrease the environmental issues, recycled thermoplastic resins can also be considered to produce 100% recycled GTR filled thermoplastic composites.
6. So far, only one layer rotomolded GTR/thermoplastic composites were produced in this thesis. In the future, multi-layer rotomolded composites can also be produced for specific applications combining lightweight, strength and other functionalities.

Bibliography

[1] Derakhshan, Z., Ghaneian, M. T., Mahvi, A. H., Conti, G. O., Faramarzian, M., Dehghani, M., Ferrante, M., A new recycling technique for the waste tires reuse, Environ. Res. 158 (2017) 462-469.

[2] Lindenmuth, B. E., An overview of tire technology. In the pneumatic tire 1 (2006) 1-27.

[3] World Health Organization, A global brief on vector-borne diseases (No. WHO/DCO/WHD/2014.1). World Health Organization. 2014.

[4] Simic, V., Dabic-Ostojic, S. Interval-parameter chance-constrained programming model for uncertainty-based decision making in tire retreading industry, J. Clean. Prod. 167 (2017) 1490-1498.

[5] Sienkiewicz, M., Kucinska-Lipka, J., Janik, H., Balas, A., (2012). Progress in used tyres management in the European Union: A review. Waste Manage. 32 (2012) 1742-1751.

[6] Sathiskumar, C., Karthikeyan, S., Recycling of waste tires and its energy storage application of by-products–a review, Sustain Mater. Techno. 22 (2019) e00125.

[7] Fiksel, J., Bakshi, B. R., Baral, A., Guerra, E., DeQuervain, B., Comparative life cycle assessment of beneficial applications for scrap tires, Clean Technol. Envir. 13 (2011) 19-35.

[8] Karger-Kocsis, J., Mészáros, L., Bárány, T., Ground tyre rubber (GTR) in thermoplastics, thermosets, and rubbers, J. Mater. Sci. 48 (2013) 1-38.

[9] Amari, T., Themelis, N. J., Wernick, I. K., Resource recovery from used rubber tires, Resour. Policy 25 (1999) 179-188.

[10] Ramarad, S., Khalid, M., Ratnam, C., Chuah, A.L., Rashmi, W., Waste tire rubber in polymer blends: A review on the evolution, properties and future, Prog. Mater. Sci. 72 (2015) 100-140.

[11] Burillo, G., Clough, R. L., Czvikovszky, T., Guven, O., Le Moel, A., Liu, W., Singh, A., Yang, J., Zaharescu, T., Polymer recycling: potential application of radiation technology, Radiat. Phys. Chem. 64 (2002) 41-51.

[12] Fazli, A., Rodrigue, D. Recycling waste tires into ground tire rubber (GTR)/rubber compounds: A review, J. Compos. Sci. 4 (2020) 103.

[13] Mészáros, L., Tábi, T., Kovács, J. G., Bárány, T., The effect of EVA content on the processing parameters and the mechanical properties of LDPE/ground tire rubber blends, Polym. Eng. Sci. 48 (2008) 868-874.

[14] Orrit-Prat, J., Mujal-Rosas, R., Rahhali, A., Marin-Genesca, M., Colom-Fajula, X., Belana-Punseti, J., Dielectric and mechanical characterization of PVC composites with ground tire rubber, J. Compos. Mater. 45 (2011) 1233-1243.

[15] Crawford, R. J., Practical guide to rotational moulding. Smithers Rapra. 2012.

[16] Tao, S., He, S. Y., Thøgersen, J., The role of car ownership in attitudes towards public transport: A comparative study of Guangzhou and Brisbane, Transport. Res. F-Traf. 60 (2019) 685-699.

[17] Peterson, M., Simkins, T., Consumers' processing of mindful commercial car sharing, Bus. Strat. Environ. 28 (2019) 457-465.

[18] International Organization of Motor Vehicle Manufacturers (OICA). "2019 Production Statistics", OICA, www.oica.net/category/production-statistics/2019-statistics/ (accessed on 2021-03-16)

[19] Kaliyavaradhan, S.K., Ling, T.C., Guo, M.Z., Mo, K.H., Waste resources recycling in controlled low-strength material (CLSM): a critical review on plastic properties, J. Environ. Manag. 241 (2019) 383-396.

[20] Boxiong, S., Chunfei, W., Binbin, G., Rui, W., Pyrolysis of waste tyres with zeolite USY and ZSM-5 catalysts, Appl. Catal. B. 73 (2007) 150-157.

[21] Revelo, C. F., Correa, M., Aguilar, C., Colorado, H. A., Waste tire rubber powders based composite materials, Miner., Met., Mater. Soc. (2019) 437-445.

[22] Bockstal, L., Berchem, T., Schmetz, Q., Richel, A., Devulcanisation and reclaiming of tires and rubber by physical and chemical processes: A review, J. Clean. Prod. 236 (2019) 117574.
[23] Evans, A., Evans, R., The composition of a tyre: typical components, The Waste & Resources Action Programme 5 (2006).
[24] Asaro, L., Gratton, M., Seghar, S., Hocine, N.A., Recycling of rubber wastes by devulcanization, Resour. Conserv. Recycl. 133 (2018) 250-262.
[25] Shulman, V.L., Tire recycling. In: Waste. Elsevier Inc., Brussels (2019) 489-515.
[26] Ghosh, P., Katare, S., Patkar, P., Caruthers, J.M., Venkatasubramanian, V., Sulfur vulcanization of natural rubber for benzothiazole accelerated formulations: from reactions mechanisms to a rational kinetic model, Rubber Chem. Technol. 76 (2003) 592-693.
[27] Saputra, R., Walvekar, R., Khalid, M., Mubarak, N. M., Sillanpää, M., Current Progress in Waste Tire Rubber Devulcanization, Chemosphere 265 (2020) 129033.
[28] Yang, G. C., Recycling of discarded tires in Taiwan, Resour. Conserv. Recycl. 9 (1993) 191-199.
[29] Directive E C W L. Official Journal 182 (1999) 26.
[30] Nuzaimah, M., Sapuan, S. M., Nadlene, R., Jawaid, M., Recycling of waste rubber as fillers: A review, IOP Conf. Ser.: Mater. Sci. Eng. 368 (2018) 012016.
[31] Qiang, W., Jiang, L., Xiaojie, Q. I., Simulation and Experimental Study on Load-bearing Deformation Characteristics of 11R22. 5 Vehicle Retreaded Tire, Mech. Eng. Science 2 (2020) 9-16.
[32] Zebala, J., Ciepka, P., Reza, A., Janczur, R., Influence of rubber compound and tread pattern of retreaded tyres on vehicle active safety, Forensic Sci. Int. 167 (2007) 173-180.
[33] Lebreton, B., Tuma, A., A quantitative approach to assessing the profitability of car and truck tire remanufacturing, Int. J. Prod. Econ. 104 (2006) 639-652.
[34] Danon, B., Van Der Gryp, P., Schwarz, C. E., Görgens, J. F. A review of dipentene (dl-limonene) production from waste tire pyrolysis, J. Anal. Appl. Pyrolysis, 112 (2015) 1-13.
[35] Zhang, G., Chen, F., Zhang, Y., Zhao, L., Chen, J., Cao, L., Gao, J., Xu, C., Properties and utilization of waste tire pyrolysis oil: A mini review, Fuel Process. Technol. 211 (2021) 106582.
[36] Rombaldo, C. F. S., Lisbôa, A. C. L., Méndez, M. O. A., Coutinho, A. D. R., Effect of operating conditions on scrap tire pyrolysis, Mater. Res. 11 (2008) 359-363.
[37] Sunthonpagasit, N., Duffey, M. R., Scrap tires to crumb rubber: feasibility analysis for processing facilities, Resour. Conserv. Recycl. 40 (2004), 281-299.
[38] Korol, J., Hejna, A., Burchart-Korol, D., Wachowicz, J., Comparative Analysis of Carbon, Ecological, and Water Footprints of Polypropylene-Based Composites Filled with Cotton, Jute and Kenaf Fibers, Materials 13 (2020) 3541.
[39] Fan, P., Lu, C., A study on functionalization of waste tire rubber powder through ozonization, J. Polym. Environ. 19 (2011) 943-949.
[40] Mangaraj, D., Role of compatibilization in recycling rubber waste by blending with plastics, Rubber Chem. Technol. 78 (2005) 536-547.
[41] Adhikari, B., De, D., Maiti, S., Reclamation and recycling of waste rubber, Prog. Polym. Sci. 25 (2000) 909-948.
[42] Myhre, M., Saiwari, S., Dierkes, W., Noordermeer, J., Rubber recycling: chemistry, processing, and applications, Rubber Chem. Technol. 85 (2012) 408-449.
[43] Tao, G., He, Q., Xia, Y., Jia, G., Yang, H., Ma, W., The effect of devulcanization level on mechanical properties of reclaimed rubber by thermal‐mechanical shearing devulcanization, J. Appl. Polym. Sci. 129 (2013) 2598-2605.
[44] Seghar, S., Asaro, L., Rolland-Monnet, M., Hocine, N., Thermo-mechanical devulcanization and recycling of rubber industry waste. Resour. Conserv. Recycl. 144 (2019) 180-186.
[45] Markl, E., Lackner, M., Devulcanization Technologies for Recycling of Tire-Derived Rubber: A Review, Materials 13 (2020) 1246.

[46] Maridass, B., Gupta, B. R., Process optimization of devulcanization of waste rubber powder from syringe stoppers by twin screw extruder using response surface methodology, Polym. Compos. 29 (2008) 1350-1357.
[47] Maridass, B., Gupta, B. R., Recycling of waste tire rubber powder-Devulcanization in a counter rotating twin screw extruder, Kaut. Gummi. Kunstst. 56 (2003) 232-236.
[48] Yazdani, H., Karrabi, M., Ghasmi, I., Azizi, H., Bakhshandeh, G. R., Devulcanization of waste tires using a twin-screw extruder: The effects of processing conditions, J. Vinyl Addit. Technol. 17(2011). 64-69.
[49] Edwards, D. W., Danon, B., van der Gryp, P., Görgens, J. F. Quantifying and comparing the selectivity for crosslink scission in mechanical and mechanochemical devulcanization processes, J. Appl. Polym. Sci. 133 (2016) 1-10.
[50] Bockstal, L., Berchem, T., Schmetz, Q., Richel, A., Devulcanisation and reclaiming of tires and rubber by physical and chemical processes: A review, J. Clean. Prod. 236 (2019) 117574.
[51] Kojima, M., Tosaka, M., Ikeda, Y., Chemical recycling of sulfur-cured natural rubber using supercritical carbon dioxide. Green Chem. 6 (2004) 84-89.
[52] Mandal, S. K., Alam, N., Debnath, S. C., Reclaiming of ground rubber tire by safe multifunctional rubber additives: I. tetra benzyl thiuram disulfide, Rubber Chem. Technol. 85 (2012) 629-644.
[53] Rooj, S., Basak, G. C., Maji, P. K., Bhowmick, A. K., New route for devulcanization of natural rubber and the properties of devulcanized rubber, J. Polym. Environ. 19 (2011) 382-390.
[54] Cook, W. S., Albert, H. E., Kilbourne Jr, F. L., Smith Jr, G. E. P., Reclaiming agents for synthetic rubber, Rubber Chem. Technol. 22 (1949) 166-185.
[55] Zhang, X., Saha, P., Cao, L., Li, H., Kim, J., Devulcanization of waste rubber powder using thiobisphenols as novel reclaiming agent, Waste Manag. 78 (2018) 980-991.
[56] Cao, W., Study on properties of recycled tire rubber modified asphalt mixtures using dry process, Constr. Build Mater. 21 (2007) 1011-1015.
[57] Lievana, E., Karger-Kocsis, J., Use of ground tyre rubber (GTR) in thermoplastic polyolefin elastomer compositions, Prog. Rubber Plast. Res. 20 (2004) 1-10.
[58] Warner, W. C., Methods of devulcanization. Rubber Chem. Technol. 67 (1994) 559-566.
[59] Reisse, J., François, H., Vandercammen, J., Fabre, O., Kirsch-de Mesmaeker, A., Maerschalk, C., Delplancke, J. L., Sonoelectrochemistry in aqueous electrolyte: a new type of sonoelectroreactor, Electrochim. Acta, 39 (1994) 37-39.
[60] Tukachinsky, A., Schworm, D., Isayev, A. I., Devulcanization of waste tire rubber by powerful ultrasound, Rubber Chem. Technol. 69 (1996) 92-103.
[61] Isayev, A. I., Liang, T., Lewis, T. M., Effect of particle size on ultrasonic devulcanization of tire rubber in twin-screw extruder. Rubber Chem. Technol. 87 (2014) 86-102.
[62] Makarov, V. M., Drozdovskiĭ, V. F., Reprocessing of tyres and rubber wastes: recycling from the rubber products industry. Ellis Horwood, 1991.
[63] Clifford, M.L., Tubular extrudate. US Patent No. 4,130,616 (1978).
[64] Leary, M., Evaluation of Waste Tire Devulcanization Technologies, CalRecovery Inc.(Ed.) California. EE. UU, (2004) 1-99.
[65] Al-Ghamdi, A. A., Al-Hartomy, O. A., Al-Solamy, F. R., Dishovsky, N., Malinova, P., Atanasova, G., Atanasov, N., Conductive carbon black/magnetite hybrid fillers in microwave absorbing composites based on natural rubber, Compos. B. Eng. 96 (2016) 231-241.
[66] Tyler, K.A., Cerny, G.L., Method of reducing pollution in microwave devulcanization process. US Patent No. 4,459,450 (1984).
[67] Pistor, V., Scuracchio, C. H., Oliveira, P. J., Fiorio, R., Zattera, A. J., Devulcanization of ethylene-propylene-diene polymer residues by microwave-Influence of the presence of paraffinic oil, Polym. Eng. Sci. 51 (2011) 697-703.
[68] Schnecko, H., Rubber recycling. Kaut. Gummi. Kunst. 47 (1994) 885-890.

[69] Jose, J., Satapathy, S., Nag, A., Nando, G. B., Modification of waste polypropylene with waste rubber dust from textile cot industry and its characterization, Proc. Saf. Environ. 85 (2007) 318-326.
[70] Kim, J. K., Park, J. W., The biological and chemical desulfurization of crumb rubber for the rubber compounding. J. Appl. Polym. Sci. 72 (1999) 1543-1549.
[71] Li, Y., Zhao, S., Wang, Y., Microbial desulfurization of ground tire rubber by Thiobacillus ferrooxidans. Polym. Degrad. Stabil. 96 (2011) 1662-1668.
[72] Scheirs, J., Compositional and failure analysis of polymers: a practical approach. John Wiley & Sons. 2000.
[73] Li, J., Yao, S., Xiao, F., Amirkhanian, S. N., Surface modification of ground tire rubber particles by cold plasma to improve compatibility in rubberised asphalt, Int. J. Pavement Eng. (2020) 1-12.
[74] Yehia, A. A., Mull, M. A., Ismail, M. N., Hefny, Y. A., Abdel-Bary, E. M., Effect of chemically modified waste rubber powder as a filler in natural rubber vulcanizates, J. Appl. Polym. Sci. 93 (2004) 30-36.
[75] Colom, X., Carrillo, F., Canavate, J., Composites reinforced with reused tyres: surface oxidant treatment to improve the interfacial compatibility, Compos. Part A Appl. Sci. Manuf. 38 (2007) 44-50.
[76] Elenien, K.F.A., Abdel-Wahab, A., ElGamsy, R., Abdellatif, M.H., Assessment of the properties of PP composite with addition of recycled tire rubber, Ain Shams Eng. J. 9 (2018) 3271-3276.
[77] Cepeda-Jiménez, C.M., Pastor-Blas, M.M., Ferrándiz-Gómez, T.P., Martín-Martínez, J.M., Surface characterization of vulcanized rubber treated with sulfuric acid and its adhesion to polyurethane adhesive, J. Adhes. 73 (2000) 135-160.
[78] Esmizadeh, E., Naderi, G., Bakhshandeh, G. R., Fasaie, M. R., Ahmadi, S., Reactively compatibilized and dynamically vulcanized thermoplastic elastomers based on high-density polyethylene and reclaimed rubber, Polym. Sci. Ser. B 59 (2017) 362-371.
[79] Li, Y., Zhang, Y., Zhang, Y., Morphology and mechanical properties of HDPE/SRP/elastomer composites: effect of elastomer polarity, Polym. Test. 23 (2004) 83-90.
[80] Oliphant, K., Baker, W. E., The use of cryogenically ground rubber tires as a filler in polyolefin blends, Polym. Eng. Sci. 33 (1993) 166-174.
[81] Formela, K., Korol, J., Saeb, M. R., Interfacially modified LDPE/GTR composites with non-polar elastomers: From microstructure to macro-behavior, Polym. Test. 42 (2015) 89-98.
[82] Ahmad, I., Fern, L. P., Effect of PE-g-MA-compatibilizer on the morphology and mechanical properties of 70/30 HDPE/ENR blends, Polym-Plast. Technol. 45 (2006) 735-739.
[83] Wang, L., Lang, F., Li, S., Du, F., Wang, Z., Thermoplastic elastomers based on high-density polyethylene and waste ground rubber tire composites compatibilized by styrene–butadiene block copolymer, J. Thermoplast. Compos. Mater. 27 (2014) 1479-1492.
[84] Aggour, Y. A., Al-Shihri, A. S., Bazzt, M. R., Surface Modification of Waste Tire by Grafting with Styrene and Maleic Anhydride, Open J. Polym. Chem. 2 (2012) 70-76.
[85] Naskar, A. K., De, S. K., Bhowmick, A. K., Thermoplastic elastomeric composition based on maleic anhydride–grafted ground rubber tire, J. Appl. Polym. Sci. 84 (2002) 370-378.
[86] Abou-Helal, M. O., El-Sabbagh, S. H., A study on the compatibility of NR-EPDM blends using electrical and mechanical techniques, J Elastom. Plast. 37 (2005) 319-346.
[87] Coiai, S., Passaglia, E., Ciardelli, F., Tirelli, D., Peruzzotti, F., Resmini, E., Modification of Cross-Linked Rubber Particles by Free Radical Polymerization, Macromol. Symp. 234 (2006) 193-202.
[88] Lee, S. H., Shanmugharaj, A. M., Sridhar, V., Zhang, Z. X., Kim, J. K., Preparation and characterization of polypropylene and waste tire powder modified by allylamine blends, Polym. Adv. Technol. 20 (2009) 620-625.
[89] Qin, J., Ding, H., Wang, X., Xie, M., Yu, Z., Blending LLDPE and ground rubber tires, Polym. Plast. Technol. Eng. 47 (2008) 199-202.

[90] Shanmugharaj, A. M., Kim, J. K., Ryu, S. H., UV surface modification of waste tire powder: characterization and its influence on the properties of polypropylene/waste powder composites, Polym. Test. 24 (2005) 739-745.
[91] Fuhrmann, I., Karger-Kocsis, J., Effects of ground tyre rubber (GTR) on the mechanical properties of thermoplastic blends, Kaut. Gummi. Kunstst. 52 (1999) 836-841.
[92] Martins, J. A., Cramez, M. C., Oliveira, M. J., Crawford, R. J., Prediction of spherulite size in rotationally molded polypropylene, J. Macromol. Sci. Part B 42 (2003) 367-385.
[93] RJ, R. J. C., Throne, J. L., Rotational Molding Technology, Plastics design Library. Norwich: William Andrew, (2002) 2-298.
[94] Hanana, F. E., Chimeni, D. Y., Rodrigue, D., Morphology and mechanical properties of maple reinforced LLDPE produced by rotational moulding: Effect of fibre content and surface treatment, Polym. Polym. Compos. 26 (2018) 299-308.
[95] Crawford, R. J., Throne, J. L., Rotational molding technology. William Andrew. 2001.
[96] Gao, D. M., Nguyen, K. T., Hétu, J. F., Laroche, D., Garcia-Rejon, A., Modeling of industrial polymer processes: injection molding and blow molding, Adv. Perform. Mater. 5 (1998) 43-64.
[97] Throne, J. L., Technology of thermoforming. Munich: Hanser. 882 (1996).
[98] León, L. D. V. E., Escocio, V. A., Visconte, L. L. Y., Junior, J. C. J., Pacheco, E. B. A. V., Rotomolding and polyethylene composites with rotomolded lignocellulosic materials: A review, J. Reinf. Plast. Compos. 39 (2020) 459-472.
[99] Nugent, P., Rotational molding. In Applied plastics engineering handbook. William Andrew Publishing, (2011) 311-332.
[100] Rao, M. A., Throne, J. L., Principles of rotational molding, Polym. Eng. Sci. 12 (1972) 237-264.
[101] Bellehumeur, C. T., Tiang, J. S., Simulation of non-isothermal melt densification of polyethylene in rotational molding. Polym. Eng. Sci. 42 (2002) 215-229.
[102] Asgarpour, M., Bakir, F., Khelladi, S., Khavandi, A., Tcharkhtchi, A., Characterization and modeling of sintering of polymer particles, J. Appl. Polym. Sci. 119 (2011) 2784-2792.
[103] Torres, F. G., Carrillo, M., Cubillas, M. L., Melt densification of polymeric powder beds filled with natural fibres, Polym. Polym. Compos. 14 (2006) 691-700.
[104] Yuan, X., Easteal, A. J., Bhattacharyya, D., Mechanical performance of rotomoulded wollastonite-reinforced polyethylene composites, Int. J. Mod. Phys. B 21 (2007) 1059-1066.
[105] Gupta, N., Ramkumar, P. L., Sangani, V., An approach toward augmenting materials, additives, processability and parameterization in rotational molding: a review, Mater. Manuf. Process. 35 (2020) 1539-1556.
[106] Wisley, B.G., SPE ANTEC Tech. Paper, 1487 (1999) 44.
[107] López-Bañuelos, R. H., Moscoso, F. J., Ortega-Gudiño, P., Mendizabal, E., Rodrigue, D., González-Núñez, R., Rotational molding of polyethylene composites based on agave fibers, Polym. Eng. Sci. 52 (2012) 2489-2497.
[108] Torres, F. G., Aragon, C. L., Final product testing of rotational moulded natural fibre-reinforced polyethylene, Polym. Test. 25 (2006) 568-577.
[109] Hanana, F. E., Rodrigue, D., Rotational molding of self-hybrid composites based on linear low-density polyethylene and maple fibers, Polym. Comp. 39 (2018) 4094-4103.
[110] Yuan, X., Easteal, A. J., Bhattacharyya, D., Influence of surface treatment on hybrid wollastonite-polyethylene composite resins for rotational moulding, J. Mater. Sci. 43 (2008) 6057-6063.
[111] Altan, M., Thermoplastic foams: Processing, manufacturing, and characterization. Polymerization. London: IntechOpen, 6 (2018) 117-137.
[112] González-Núñez, R., Moscoso-Sánchez, F. J., Aguilar, J., López-GonzálezNúñez, R. G., Robledo-Ortíz, J. R., Rodrigue, D., Thermal analysis of foamed polyethylene rotational molding followed by internal air temperature profiles, Polym. Eng. Sci. 58 (2018) E235-E241.

[113] Jin, F. L., Zhao, M., Park, M., Park, S. J., Recent trends of foaming in polymer processing: a review, Polymers. 11 (2019) 953.
[114] Liu, G., Park, C. B., Lefas, J. A., Production of low-density LLDPE foams in rotational molding, Polym. Eng. Sci. 38 (1998) 1997-2009.
[115] Emami, M., Takacs, E., Vlachopoulos, J., Rotational foam molding of metallocene catalyzed polyethylene: CBA screening and process characteristics, J. Cell. Plast. 46 (2010) 333-351.
[116] Raymond, A., Rodrigue, D., Foams and wood composite foams produced by rotomolding, Cell. Polym. 32 (2013) 199-212.
[117] Löhner, M., Drummer, D., Characterization of layer built-up and inter-layer boundaries in rotational molding of multi-material parts in dependency of the filling strategy, J. Polym. Eng. 37 (2017) 411-420.
[118] Liu, S. J., Yang, C. H., Rotational molding of two-layered polyethylene foams, Adv. Polym. Tech. 20 (2001) 108-115.
[119] Archer, E., Harkin-Jones, E., Kearns, M. P., Fatnes, A. M., The rotational molding characteristics of metallocene polyethylene skin/foam structures, J. Cell. Plast. 43 (2007) 491-504.
[120] Vázquez-Fletes, R. C., Rosales-Rivera, L. C., Moscoso-Sánchez, F. J., Mendizabal, E., Ortega-Gudiño, P., González-Núñez, R., Rodrigue, D., Preparation and characterization of multilayer foamed composite by rotational molding, Polym. Eng. Sci. 56 (2016) 278-286.
[121] Lucignano, C., Gugliemotti, A., Quadrini, F., Compression moulding of rubber powder from exhausted tyres, Polym. Plast. Technol. Eng. 51 (2012) 340-344.
[122] Garcia, D., Lopez, J., Balart, R., Ruseckaite, R. A., Stefani, P. M., Composites based on sintering rice husk–waste tire rubber mixtures, Mater. Des. 28 (2007) 2234-2238.
[123] Zhang, S. L., Zhang, Z. X., Pal, K., Xin, Z. X., Suh, J., Kim, J. K., Prediction of mechanical properties of waste polypropylene/waste ground rubber tire powder blends using artificial neural networks, Mater. Des., 31 (2010) 3624-3629.
[124] Hassan, A., Haworth, B., Impact properties of acrylate rubber-modified PVC: Influence of temperature, J. Mater. Process. Tech., 172 (2006) 341-345.
[125] Liu, S. J., Peng, K. M., Rotational molding of polycarbonate reinforced polyethylene composites: processing parameters and properties, Polym. Eng. Sci. 50 (2010) 1457-1465.
[126] Hamidi, A., Khelladi, S., Shirinbayan, M., Bakir, F., Tcharkhtchi, A., Implementation of surface tension force in fluid flow during reactive rotational molding, Int. J. Mater. Form. 9 (2016) 131-148.
[127] Hassan, M., Nour, M., Abdelmonem, Y., Makhlouf, G., Abdelkhalik, A., Synergistic effect of chitosan-based flame retardant and modified clay on the flammability properties of LLDPE, Polym. Degrad. Stab. 133 (2016) 8-15.
[128] Ramkumar, P. L., Kulkarni, D. M., Chaudhari, V. V., Parametric and mechanical characterization of linear low density polyethylene (LLDPE) using rotational moulding technology, Sadhana-Acad. P. ENG. S. 39 (2014) 625-635.
[129] Greco, A., Romano, G., Maffezzoli, A., Selective reinforcement of LLDPE components produced by rotational molding with thermoplastic matrix pultruded profiles, Compos. Part B-Eng. 56 (2014) 157-162.
[130] Chandran V, G., Waigaonkar, S. D., Rheological and dynamic mechanical characteristics of rotationally moldable linear low-density polyethylene fumed silica nanocomposites, Polym. Compos. 37 (2016) 2995-3002.
[131] Wong, A. Y., Lam, F., Study of selected thermal characteristics of polypropylene/polyethylene binary blends using DSC and TGA, Polym. Test. 21 (2002) 691-696.
[132] Prabhu, T. N., Hemalatha, Y. J., Harish, V., Prashantha, K., Iyengar, P., Thermal degradation of epoxy resin reinforced with polypropylene fibers, J. Appl. Polym. Sci. 104 (2007) 500-503.
[133] Jaratrotkamjorn, R., Khaokong, C., Tanrattanakul, V., Toughness enhancement of poly (lactic acid) by melt blending with natural rubber, J. Appl. Polym. Sci. 124 (2012) 5027-5036.

[134] Bitinis, N., Verdejo, R., Cassagnau, P., Lopez-Manchado, M. A., Structure and properties of polylactide/natural rubber blends, Mater. Chem. Phys. 129 (2011) 823-831.
[135] Cigna, G., Matarrese, S., Biglione, G. F., Effect of structure on impact strength of rubber-reinforced polystyrene, J. Appl. Polym. Sci. 20 (1976) 2285-2295.
[136] Chandran, V. G., Waigaonkar, S. D., Rotational Molding of Linear Low Density Polyethylene (LLDPE) Fumed Silica Nanocomposites, Int. Polym. Proc. 32 (2017) 50-57.
[137] Chaudhary, B. I., Takacs, E., Vlachopoulos, J., Processing enhancers for rotational molding of polyethylene, Polym. Eng. Sci. 41 (2001) 1731-1742.
[138] Planes, E., Duchet, J., Maazouz, A., Gerard, J. F., Characterization of new formulations for the rotational molding based on ethylene–propylene copolymer/graphite nanocomposites, Polym. Eng. Sci. 48 (2008) 723-731.
[139] Abdullah, M. Z., Bickerton, S., Bhattacharyya, D., Crawford, R. J., Harkin-Jones, E., Rotational molding cycle time reduction using a combination of physical techniques, Polym. Eng. Sci. 49 (2009) 1846-1854.
[140] Chimeni, D. Y., Dubois, C., Rodrigue, D., Polymerization compounding of hemp fibers to improve the mechanical properties of linear medium density polyethylene composites, Polym. Comp. 39 (2018) 2860-2870.
[141] Cisneros-López, E. O., Anzaldo, J., Fuentes-Talavera, F. J., González-Núñez, R., Robledo-Ortíz, J. R., Rodrigue, D., Effect of agave fiber surface treatment on the properties of polyethylene composites produced by dry-blending and compression molding, Polym. Comp. 38 (2017) 96-104.
[142] Chu, R. K., Naguib, H. E., Atalla, N., Synthesis and characterization of open-cell foams for sound absorption with rotational molding method, Polym. Eng. Sci. 49 (2009) 1744-1754.
[143] Yousefian, H., Rodrigue, D., Morphological, physical and mechanical properties of nanocrystalline cellulose filled Nylon 6 foams, J. Cell. Plast. 53 (2017) 253-271.
[144] Mohebbi, A., Mighri, F., Ajji, A., Rodrigue, D., Polymer ferroelectret based on polypropylene foam: piezoelectric properties prediction using dynamic mechanical analysis, Polym. Adv. Technol. 28 (2017) 476-483.
[145] Shatanawi, K., Biro, S., Thodesen, C., Amirkhanian, S., Effects of water activation of crumb rubber on the properties of crumb rubber-modified binders, Int. J. Pavement Eng. 10 (2009) 289-297.
[146] Ramezani Kakroodi, A., Rodrigue, D., Reinforcement of maleated polyethylene/ground tire rubber thermoplastic elastomers using talc and wood flour, J. Appl. Polym. Sci. 131 (2014) 40195.
[147] Kakroodi, A. R., Rodrigue, D., Impact modification of polypropylene-based composites using surface-coated waste rubber crumbs, Polym. Comp. 35 (2014) 2280-2289.
[148] Kumar, V., Weller, J. E., A model for the unfoamed skin on microcellular foams, Polym. Eng. Sci. 34 (1994) 169-173.
[149] Kuboki, T., Foaming behavior of cellulose fiber-reinforced polypropylene composites in extrusion, J. Cell. Plast. 50 (2014) 113-128.
[150] Rodrigue, D., Souici, S., Twite-Kabamba, E., Effect of wood powder on polymer foam nucleation, J. Vinyl. Addit. Tech. 12 (2006) 19-24.
[151] Mechraoui, A., Riedl, B., Rodrigue, D., Mechanical properties of polypropylene structural foams with fiber-reinforced skins, J. Cell. Plast. 47 (2011) 115-132.
[152] Barzegari, M. R., Kabamba, E. T., Rodrigue, D., Flexural modulus prediction of symmetric structural polymer foams with complex density profiles, J. Porous Mat. 18 (2011) 715-721.
[153] Barzegari, M. R., Rodrigue, D., Flexural behavior of asymmetric structural foams, J. Appl. Polym. Sci. 113 (2009) 3103-3112.
[154] Mohammed, L., Ansari, M. N., Pua, G., Jawaid, M., Islam, M. S., A review on natural fiber reinforced polymer composite and its applications, Int. J. Polym. Sci. 2015 (2015).

[155] Bongarde, U. S., Shinde, V. D., Review on natural fiber reinforcement polymer composites, Int. J. Eng. Sci. Innov. Technol. 3 (2014) 431-436.
[156] Faruk, O., Bledzki, A. K., Fink, H. P., Sain, M., Progress report on natural fiber reinforced composites, Macromol. Mater. Eng. 299 (2014) 9-26.
[157] Sewda, K., Maiti, S. N., Dynamic mechanical properties of high density polyethylene and teak wood flour composites, Polym. Bull. 70 (2013) 2657-2674.
[158] Lu, N., Oza, S., A comparative study of the mechanical properties of hemp fiber with virgin and recycled high density polyethylene matrix, Compos. Part B-Eng. 45 (2013) 1651-1656.
[159] Facca, A. G., Kortschot, M. T., Yan, N., Predicting the elastic modulus of natural fibre reinforced thermoplastics, Compos. Part A-Appl S. 37 (2006) 1660-1671.
[160] Nair, K. M., Diwan, S. M., Thomas, S., Tensile properties of short sisal fiber reinforced polystyrene composites, J. Appl. Polym. Sci. 60 (1996) 1483-1497.
[161] Threepopnatkul, P., Kaerkitcha, N., Athipongarporn, N., Effect of surface treatment on performance of pineapple leaf fiber–polycarbonate composites, Compos. Part B-Eng. 40 (2009) 628-632.
[162] Araújo, J. R., Waldman, W. R., De Paoli, M. A., Thermal properties of high density polyethylene composites with natural fibres: Coupling agent effect, Polym. Degrad. Stab. 93 (2008) 1770-1775.
[163] Kim, S. J., Moon, J. B., Kim, G. H., Ha, C. S., Mechanical properties of polypropylene/natural fiber composites: Comparison of wood fiber and cotton fiber, Polym. Test. 27 (2008) 801-806.
[164] Clemons, C., Elastomer modified polypropylene–polyethylene blends as matrices for wood flour–plastic composites, Compos. Part A Appl. Sci. Manuf. 41 (2010) 1559-1569.
[165] Kuboki, T., Lee, Y. H., Park, C. B., Sain, M., Mechanical properties and foaming behavior of cellulose fiber reinforced high-density polyethylene composites, Polym. Eng. Sci. 49 (2009) 2179-2188.
[166] Ruksakulpiwat, Y., Sridee, J., Suppakarn, N., Sutapun, W., Improvement of impact property of natural fiber–polypropylene composite by using natural rubber and EPDM rubber, Compos. Part B-Eng. 40 (2009) 619-622.
[167] Mahallati, P., Rodrigue, D., Effect of feeding strategy on the properties of PP/recycled EPDM blends, Int. Polym. Process. 30 (2015) 276-283.
[168] Kabir, M. M., Wang, H., Lau, K. T., Cardona, F., Chemical treatments on plant-based natural fibre reinforced polymer composites: An overview, Compos. Part B-Eng. 43 (2012) 2883-2892.
[169] Kabir, M. M., Wang, H., Lau, K. T., Cardona, F., Effects of chemical treatments on hemp fibre structure, Appl. Surf. Sci. 276 (2013) 13-23.
[170] Ouajai, S., Shanks, R. A., Composition, structure and thermal degradation of hemp cellulose after chemical treatments, Polym. Degrad. Stab. 89 (2005) 327-335.
[171] Jannah, M., Mariatti, M., Abu Bakar, A., Abdul Khalil, H. P. S., Effect of chemical surface modifications on the properties of woven banana-reinforced unsaturated polyester composites, J. Reinf. Plast. Compos. 28 (2009) 1519-1532.
[172] Chimeni, D. Y., Toupe, J. L., Dubois, C., Rodrigue, D., Effect of hemp surface modification on the morphological and tensile properties of linear medium density polyethylene (LMDPE) composites, Compos. Interf. 23 (2016) 405-421.
[173] Cisneros-López, E. O., González-López, M. E., Pérez-Fonseca, A. A., González-Núñez, R., Rodrigue, D., Robledo-Ortíz, J. R., Effect of fiber content and surface treatment on the mechanical properties of natural fiber composites produced by rotomolding, Compos. Interf. 24 (2017) 35-53.
[174] Verdaguer A., Rodrigue, D., Effect of surface treatment on the mechanical properties of wood-plastics composites produced by dry-blinding, in Proceedings of the 72nd Annual Technical Conference & Exhibition, (2014) 28-30.

[175] Sonnier, R., Leroy, E., Clerc, L., Bergeret, A., Lopez-Cuesta, J. M., Compatibilisation of polyethylene/ground tyre rubber blends by γ irradiation, Polym. Degrad. Stab. 91 (2006) 2375-2379.
[176] De, D., Das, A., De, D., Dey, B., Debnath, S. C., Roy, B. C., Reclaiming of ground rubber tire (GRT) by a novel reclaiming agent, Eur. Polym. J. 42 (2006) 917-927.
[177] Hürdoğan, E., Ozalp, C., Kara, O., Ozcanli, M., Experimental investigation on performance and emission characteristics of waste tire pyrolysis oil–diesel blends in a diesel engine, Int. J. Hydrogen Ener. 42 (2017) 23373-23378.
[178] Wang, Z., Zhang, Y., Du, F., Wang, X., Thermoplastic elastomer based on high impact polystyrene/ethylene-vinyl acetate copolymer/waste ground rubber tire powder composites compatibilized by styrene-butadiene-styrene block copolymer, Mater. Chem. Phys. 136 (2012) 1124-1129.
[179] Kakroodi, A. R., Rodrigue, D., Degradation behavior of maleated polyethylene/ground tire rubber thermoplastic elastomers with and without stabilizers, Polym. Degrad. Stab. 98 (2013) 2184-2192.
[180] Abraham, E., Cherian, B. M., Elbi, P. A., Pothen, L. A., Thomas, S., Recent advances in the recycling of rubber waste, Recent Developments in Polymer Recycling, 47 (2011) 100.
[181] Lievana, E., Karger-Kocsis, J., Use of ground tyre rubber (GTR) in thermoplastic polyolefin elastomer compositions, Prog. Rubber. Plast. Res. 20 (2004) 1-10.
[182] Colom, X., Canavate, J., Carrillo, F., Velasco, J. I., Pages, P., Mujal, R., Nogués, F., Structural and mechanical studies on modified reused tyres composites, Eur. Polym. J. 42 (2006) 2369-2378.
[183] Naskar, A. K., Bhowmick, A. K., De, S. K., Melt-processable rubber: Chlorinated waste tire rubber-filled polyvinyl chloride, J. Appl. Polym. Sci. 84 (2002) 622-631.
[184] Rezaei Abadchi, M., Jalali Arani, A., Nazockdast, H., Partial replacement of NR by GTR in thermoplastic elastomer based on LLDPE/NR through using reactive blending: Its effects on morphology, rheological, and mechanical properties, J. Appl. Polym. Sci. 115 (2010) 2416-2422.
[185] Saelao, J., Phinyocheep, P., Influence of styrene on grafting efficiency of maleic anhydride onto natural rubber, J. Appl. Polym. Sci. 95 (2005) 28-38.
[186] Sun, X., Isayev, A. I., Continuous ultrasonic devulcanization: Comparison of carbon black filled synthetic isoprene and natural rubbers, Rubber Chem. Technol. 81 (2008) 19-46.
[187] Hassan, M. M., Aly, R. O., Aal, S. A., El-Masry, A. M., Fathy, E. S., Mechanochemical devulcanization and gamma irradiation of devulcanized waste rubber/high density polyethylene thermoplastic elastomer, J. Ind. Eng. Chem. 19 (2013) 1722-1729.
[188] Makarov, V. M., Drozdovskiĭ, V. F., Reprocessing of tyres and rubber wastes: recycling from the rubber products industry. Ellis Horwood, 1991.
[189] Formela, K., Hejna, A., Zedler, L., Colom Fajula, X., Cañavate Ávila, F. J., Microwave treatment in waste rubber recycling–recent advances and limitations, Express Polym. Lett. 13 (2019) 565-588.
[190] Colom, X., Faliq, A., Formela, K., Cañavate, J., FTIR spectroscopic and thermogravimetric characterization of ground tyre rubber devulcanized by microwave treatment, Polym. Test. 52 (2016) 200-208.
[191] Garcia, P. S., De Sousa, F. D. B., De Lima, J. A., Cruz, S. A., Scuracchio, C. H., Devulcanization of ground tire rubber: Physical and chemical changes after different microwave exposure times, Express Polym. Lett. 9 (2015) 1015-1026.
[192] Martınez, J. D., Puy, N., Murillo, R., Garcıa, T., Navarro, M. V., Mastral, A. M., Waste tyre pyrolysis–A review, Renew. Sustain. Energ. Rev. 23 (2013) 179-213.
[193] Yehia, A. A., Recycling of rubber waste, Polym. Plast. Technol. Eng. 43 (2004) 1735-1754.
[194] Wagenknecht, U., Steglich, S., Wiessner, S., Michael, H., Rubber Powder–A Perspective Filler of Thermoplastics, Macromol. Symp. 221 (2005) 237-246.

[195] Navarro, F. J., Partal, P., Martinez-Boza, F. J., Gallegos, C., Novel recycled polyethylene/ground tire rubber/bitumen blends for use in roofing applications: Thermo-mechanical properties, Polym. Test. 29 (2010) 588-595.
[196] Zhang, X., Lu, Z., Tian, D., Li, H., Lu, C., Mechanochemical devulcanization of ground tire rubber and its application in acoustic absorbent polyurethane foamed composites, J. Appl. Polym. Sci. 127 (2013) 4006-4014.
[197] Shi, J., Zou, H., Ding, L., Li, X., Jiang, K., Chen, T., Zhang, X., Zhang, L., Ren, D., Continuous production of liquid reclaimed rubber from ground tire rubber and its application as reactive polymeric plasticizer, Polym. Degrad. Stab. 99 (2014) 166-175.
[198] Stavrov, D., Bersee, H. E. N., Resistance welding of thermoplastic composites-an overview, Compos. Part A-Appl. Sci. 36 (2005) 39-54.
[199] Ghassemieh, E., Materials in automotive application, state of the art and prospects, New trends and developments in automotive industry 20 (2011) 364-394.
[200] Koronis, G., Silva, A., Fontul, M., Green composites: A review of adequate materials for automotive applications, Compos. Part B-Eng. 44 (2013) 120-127.
[201] Gordon, R. G., Legal Incentives for Reduction, Reuse, and Recycling: A New Approach to Hazardous Waste Management, Yale L. J. 95 (1985) 810.
[202] Chan, C. M., Wu, J., Li, J. X., Cheung, Y. K., Polypropylene/calcium carbonate nanocomposites, Polymer 43 (2002) 2981-2992.
[203] Baumer, M. I., Leite, J. L., Becker, D., Influence of calcium carbonate and slip agent addition on linear medium density polyethylene processed by rotational molding, Mat. Res. 17 (2014) 130-137.
[204] Yao, D., Rodrigue, D., Rotational molding of linear low density polyethylene with different concentrations of ground tire rubber, 75th annual technical conference and exhibition of the society of plastics engineers (2017) 2252-2256.
[205] Kakroodi, A. R., Kazemi, Y., Rodrigue, D., Mechanical, rheological, morphological and water absorption properties of maleated polyethylene/hemp composites: Effect of ground tire rubber addition, Compos. Part B-Eng. 51 (2013) 337-344.
[206] Sienkiewicz, M., Borzędowska-Labuda, K., Wojtkiewicz, A., Janik, H., Development of methods improving storage stability of bitumen modified with ground tire rubber: A review, Fuel Process. Technol. 159 (2017) 272-279.
[207] Liang, M., Sun, C., Yao, Z., Jiang, H., Zhang, J., Ren, S., Utilization of wax residue as compatibilizer for asphalt with ground tire rubber/recycled polyethylene blends, Constr. Build. Mater. 230 (2020) 116966.
[208] Wang, L., Chen, M., Policies and perspective on end-of-life vehicles in China, J. Clean. Prod. 44 (2013) 168-176.
[209] Sienkiewicz, M., Janik, H., Borzędowska-Labuda, K., Kucińska-Lipka, J., Environmentally friendly polymer-rubber composites obtained from waste tyres: A review, J. Clean. Prod. 147 (2017) 560-571.
[210] US Tire Manufacturers Association. US scrap tire management summary. US Tire Manufacturers Association, Washington, DC, USA. 2018.
[211] Zanchet, A., Carli, L. N., Giovanela, M., Crespo, J. S., Scuracchio, C. H., Nunes, R. C., Characterization of microwave-devulcanized composites of ground SBR scraps, J. Elastom. Plast. 41 (2009) 497-507.
[212] Shi, Y., Liu, F., Wang, Z., Mullins effect and its reversibility for compatibilised thermoplastic elastomers based on high-density polyethylene/waste ground rubber tyre powder under compression mode. Plast. Rubber Compos. 47 (2018) 373-380.
[213] Lu, X., Wang, W., Yu, L., Waste ground rubber tire powder/thermoplastic vulcanizate blends: Preparation, characterization, and compatibility, J. Appl. Polym. Sci. 131 (2014) 39868.
[214] Fei, Y., Fang, W., Zhong, M., Jin, J., Fan, P., Yang, J., Fei, Z., Chen, F., Kuang, T., Morphological structure, rheological behavior, mechanical properties and sound insulation

performance of thermoplastic rubber composites reinforced by different inorganic fillers, Polymers. 10 (2018) 276.
[215] Mujal-Rosas, R., Marín-Genescà, M., García-Amorós, J., Salueña-Berna, X., Colom-Fajula, X. Influence on the mechanical properties of various polymeric composites reinforced with GTR particles, Afinidad 76 (2019) 241-253.
[216] Agudelo, G., Cifuentes, S., Colorado, H. A., Ground tire rubber and bitumen with wax and its application in a real highway, J. Clean. Prod. 228 (2019) 1048-1061.
[217] Kim, J. I., Ryu, S. H., Chang, Y. W., Mechanical and dynamic mechanical properties of waste rubber powder/HDPE composite, J. Appl. Polym. Sci. 77 (2000) 2595-2602.
[218] Hong, C. K., Isayev, A. I., Plastic/rubber blends of ultrasonically devulcanized GRT with HDPE. J. Elastom. Plast. 33 (2001) 47-71.
[219] Ibeh, C. C., Thermoplastic materials: properties, manufacturing methods, and applications. CRC Press. 2011.
[220] Tantayanon, S., Juikham, S., Enhanced toughening of poly (propylene) with reclaimed-tire rubber, J. Appl. Polym. Sci. 91 (2004) 510-515.
[221] Lima, P. S., Oliveira, J. M., Costa, V. A. F., Partial replacement of EPR by GTR in highly flowable PP/EPR blends: Effects on morphology and mechanical properties, J. Appl. Polym. Sci. 132 (2015) 42011.
[222] Luo, T., Isayev, A. I., Rubber/plastic blends based on devulcanized ground tire rubber, J. Elastom. Plast. 30 (1998) 133-160.
[223] Shaker, R., Rodrigue, D., Rotomolding of thermoplastic elastomers based on low-density polyethylene and recycled natural rubber, Appl. Sci. 9 (2019) 5430.
[224] Dou, Y., Rodrigue, D., Rotational molding of hybrid composites based on linear low density polyethylene/ground tire rubber/maple wood fibers, Proceedings of the 76th Annual Technical Conference & Exhibition, Orlando (FL), Society of Plastics Engineers. (2018) 324-330.
[225] Liang, J. Z., Li, R. K. Y., Rubber toughening in polypropylene: A review, J. Appl. Polym. Sci. 77 (2000) 409-417.
[226] Wang, J. Q., Chow, W. K., A brief review on fire retardants for polymeric foams, J. Appl. Polym. Sci. 97 (2005) 366-376.
[227] Jacobs, L. J., Kemmere, M. F., Keurentjes, J. T., Sustainable polymer foaming using high pressure carbon dioxide: a review on fundamentals, processes and applications, Green Chem. 10 (2008) 731-738.
[228] Marşavina, L., Linul, E., Fracture toughness of rigid polymeric foams: A review, Fatigue Fract. Eng. M. 43 (2020) 2483-2514.
[229] Klempner, D., Frisch, K. C., Handbook of polymeric foams and foam technology, 2nd Ed. New York: Hanser, 1991.
[230] Okoroafor, M. O., Frisch, K. C., Introduction to foams and foam formation, Handbook of Plastic Foams: Types, properties, manufacture and applications (1995) 1-10.
[231] Li, Y. G., Park, C. B., Effects of branching on the pressure− volume− temperature behaviors of PP/CO2 solutions, Ind. Eng. Chem. Res. 48 (2009) 6633-6640.
[232] Rodriguez, F., Cohen, C., Ober, C. K., Archer, L., Principles of polymer systems, 6th ed. CRC Press, 2014.
[233] Lobo, H., Bonilla, J. V., Handbook of plastics analysis, CRC Press, 2003.
[234] Pop-Iliev, R., Liu, F., Liu, G., Park, C. B., Rotational foam molding of polypropylene with control of melt strength, Adv. Polym. Tech. 22 (2003) 280-296.
[235] Park, C. B., Cheung, L. K., A study of cell nucleation in the extrusion of polypropylene foams, Polym. Eng. Sci. 37 (1997) 1-10.
[236] Maddah, H. A., Polypropylene as a promising plastic: A review, Am. J. Polym. Sci. 6 (2016) 1-11.

[237] Jiang, Q., Pei, X., Wu, L., Li, T. T., Lin, J. H., UV resistance and water barrier properties of PP/PLA/MAH/TiO2 functional hybrid biocomposite films for packaging application, Adv. Polym. Tech. 37 (2018) 2971-2980.
[238] Ahmadi, A. A., Hornsby, P. R., Moulding and characterization studies with polypropylene structural foam. I: Structure-property interrelationships, Plast. Rubber Proc. Appl. 5 (1985) 35-49.
[239] Hell, J., Nezbedova, E., Ponesicky, J., Injection-Moulded polypropylene structural foam, Kunstst. Ger. Plast. 77 (1987) 860-863.
[240] Kuboki, T., Mechanical properties and foaming behavior of injection molded cellulose fiber reinforced polypropylene composite foams, J. Cell. Plast. 50 (2014) 129-143.
[241] Wang, L., Hikima, Y., Ohshima, M., Yusa, A., Yamamoto, S., Goto, H., Unusual fabrication of lightweight injection-molded polypropylene foams by using air as the novel foaming agent, Ind. Eng. Chem. Res. 57 (2018) 3800-3804.
[242] Mechraoui, A., Barzegari, M. R., Riedl, B., Rodrigue, D., Compression moulding of polypropylene foams and their properties, Cell. Polym. 27 (2008) 217-233.
[243] Saiz-Arroyo, C., Rodríguez-Pérez, M. A., Tirado, J., López-Gil, A., de Saja, J. A., Structure-property relationships of medium-density polypropylene foams, Polym. Int. 62 (2013) 1324-1333.
[244] Escudero, J., Lopez-Gil, A., Laguna-Gutierrez, E., Rodriguez-Perez, M. A., Low density non-crosslinked closed/open cell polypropylene foams with high mechanical properties, Cell. Polym. 35 (2016) 101-118.
[245] Naguib, H. E., Park, C. B., Reichelt, N., Fundamental foaming mechanisms governing the volume expansion of extruded polypropylene foams, J. Appl. Polym. Sci. 91 (2004) 2661-2668.
[246] Kim, E., Kweon, M. S., Romero-Diez, S., Gupta, A., Yan, X., Spofford, C., Pehlert, G., Lee, P. C., Effects of pressure drop rate and CO2 content on the foaming behavior of newly developed high-melt-strength polypropylene in continuous extrusion, J. Cell. Plast. 2020. DOI:10.1177/0021955X20943110.
[247] Ogila, K. O., Shao, M., Yang, W., Tan, J., Rotational molding: A review of the models and materials, Express Polym. Lett. 11(2017) 778-798.
[248] Vázquez Fletes, R. C., Cisneros López, E. O., Moscoso Sánchez, F. J., Mendizábal, E., González Núñez, R., Rodrigue, D., Ortega Gudiño, P., Morphological and mechanical properties of bilayers wood-plastic composites and foams obtained by rotational molding, Polymers.12 (2020) 503.
[249] León, L. D. V. E., Escocio, V. A., Visconte, L. L. Y., Junior, J. C. J., Pacheco, E. B. A. V., Rotomolding and polyethylene composites with rotomolded lignocellulosic materials: A review, J. Reinf. Plast. Comp. 39 (2020) 459-472.
[250] Hejna, A., Barczewski, M., Andrzejewski, J., Kosmela, P., Piasecki, A., Szostak, M., Kuang, T., Rotational molding of linear low-density polyethylene composites filled with wheat bran, Polymers. 12 (2020) 1004.
[251] Pop-Iliev, R., Park, C. B., Processing of polypropylene foams in melt compounding based rotational foam molding, J. Reinf. Plast. Comp. 21 (2002) 1079-1100.
[252] Pop-Iliev, R., Rizvi, G. M., Park, C. B., The importance of timely polymer sintering while processing polypropylene foams in rotational molding, Polym. Eng. Sci. 43 (2003) 40-54.
[253] Kumar, V., Weller, J. E., A model for the unfoamed skin on microcellular foams, Polym. Eng. Sci. 34 (1994) 169-173.
[254] Mazov, I., Burmistrov, I., Il'inykh, I., Stepashkin, A., Kuznetsov, D., Issi, J. P., Anisotropic thermal conductivity of polypropylene composites filled with carbon fibers and multiwall carbon nanotubes, Polym. Composite. 36 (2015) 1951-1957.
[255] Reza Barzegari, M., Rodrigue, D., Prediction of the shear modulus of polymer structural foams, J. Cell. Plast. 45 (2009) 555-576.

[256] Mejia, E. B., Mourad, A. H. I., Faqer, A. S. B., Halwish, D. F., Al Hefeiti, H. O., Al Kashadi, S. M., Cherupurakal, N., Mozumder, M. S., Impact on HDPE mechanical properties and morphology due to processing, Advances in Science and Engineering Technology International Conferences (2019) 1-5.
[257] Moscoso-Sánchez, F. J., Mendizábal, E., Jasso-Gastinel, C. F., Ortega-Gudiño, P., Robledo-Ortíz, J. R., González-Núñez, R., Rodrigue, D., Morphological and mechanical characterization of foamed polyethylene via biaxial rotational molding, J. Cell. Plast. 51 (2015) 489-503.
[258] Dou, Y., Rodrigue, D., Rotomolding of foamed and unfoamed GTR-LLDPE blends: Mechanical, morphological and physical properties, Cell. Polym. 37 (2018) 55-68.
[259] Abhilash, S. S., Singaravelu, D. L., Effect of fiber content on mechanical and morphological properties of bamboo fiber-reinforced linear low-density polyethylene processed by rotational molding, Trans. Indian. Inst. Met. 73 (2020) 1549-1554.
[260] Pop-Iliev, R., Park, C. B., Single-step rotational foam molding of skin-surrounded polyethylene foams, J. Cell. Plast. 39 (2003) 49-58.
[261] Pop-Iliev, R., Xu, D., Park, C. B., Manufacturability of fine-celled cellular structures in rotational foam molding, J. Cell. Plast. 40 (2004) 13-25.
[262] Perot, E., Maazouz, A., Study of polymer sintering during rotational molding, J. Polym. Eng. 27 (2007) 267-290.
[263] Perot, E., Lamnawar, K., Maazouz, A., Optimization and modelling of rotational molding process, Int. J. Mater. Form. 1 (2008) 783-786.
[264] Xu, D., Pop-Iliev, R., Park, C. B., Fenton, R. G., Fundamental study of CBA-blown bubble growth and collapse under atmospheric pressure, J. Cell. Plast. 41 (2005) 519-538.
[265] Pop-Iliev, R., Dong, N., Xu, D., Park, C. B., Visualization of the foaming mechanism of polyethylene blown by chemical blowing agents under ambient pressure, Adv. Polym. Tech. 26 (2007) 213-222.
[266] Emami, M., Takacs, E., Thompson, M. R., Vlachopoulos, J., Maziers, E., Visual studies of model foam development for rotational molding processes, Adv. Polym. Tech. 32 (2013) E809-E821.
[267] Liu, S. J., Tsai, C. H., An experimental study of foamed polyethylene in rotational molding, Polym. Eng. Sci. 39 (1999) 1776-1786.
[268] Archer, E., Harkin-Jones, E., Kearns, M. P., Fatnes, A. M., Processing characteristics and mechanical properties of metallocene catalyzed linear low-density polyethylene foams for rotational molding, Polym. Eng. Sci. 44 (2004) 638-647.
[269] Geyer, R., Jambeck, J. R., Law, K. L., Production, use, and fate of all plastics ever made, Sci. Adv. 3 (2017) e1700782.
[270] Maris, J., Bourdon, S., Brossard, J. M., Cauret, L., Fontaine, L., Montembault, V., Mechanical recycling: Compatibilization of mixed thermoplastic wastes, Polym. Degrad. Stab.147 (2018) 245-266.
[271] Adhikary, K. B., Pang, S., Staiger, M. P., Dimensional stability and mechanical behaviour of wood–plastic composites based on recycled and virgin high-density polyethylene (HDPE), Compos. Part B-Eng. 39 (2008) 807-815.
[272] Lu, N., Oza, S., Thermal stability and thermo-mechanical properties of hemp-high density polyethylene composites: effect of two different chemical modifications, Compos. Part B-Eng. 44 (2013) 484-490.
[273] Dvorak, M., Applicability of recycled HDPE for Rotational Molding, Degree Thesis, University of Helsinki, Finland, 2016.
[274] Chaisrichawla, S., Dangtungee, R., The usage of recycled material in rotational molding process for production of septic tank. Mater. Sci. Forum 936 (2018) 151-158.
[275] Tammaro, D., Di Maio, E., Early bubble coalescence in thermoplastic foaming, Mater. Lett. 228 (2018) 459-462.

[276] Hemmasi, A. H., Ghasemi, I., Bazyar, B., Samariha, A., Influence of nanoclay on the physical properties of recycled high-density polyethylene/bagasse nanocomposite, Middle-East. J. Sci. Res. 8 (2011) 648-651.
[277] Nourbakhsh, A., Ashori, A., Preparation and properties of wood plastic composites made of recycled high-density polyethylene, J. Compos. Mater. 43 (2009) 877-883.
[278] Yang, C., Navarro, M. E., Zhao, B., Leng, G., Xu, G., Wang, L., Jin, Y., Ding, Y., Thermal conductivity enhancement of recycled high density polyethylene as a storage media for latent heat thermal energy storage, Sol. Energy Mater. Sol. Cells. 152 (2016) 103-110.
[279] Bledzki, A. K., Faruk, O., Microcellular wood fiber reinforced PP composites: Cell morphology, surface roughness, impact, and odor properties, J. Cell. Plast. 41 (2005) 539-550.